Electromechanical Coupling of Distributed Piezoelectric Transducers for Passive Damping of Structural Vibrations: Comparison of Network Configurations

BY

Corrado Maurini

Thesis submitted to the Faculty of the
Virginia Polytechnic Institute and State University
in partial fulfillment of the requirements of the degree of

Master of Science
in
Engineering Science and Mechanics

Dr. Edmund G. Henneke

Dr. Francesco dell'Isola

Dr. Romesh G. Batra

Dr. Don H. Morris

February 15th, 2002

Blacksburg, Virginia

Keywords: Vibration Control, Electric Networks, Virtual Power Principle, Piezoelectric Transducers, Wave Propagation

Electromechanical Coupling of Distributed Piezoelectric Transducers for Passive Damping of Structural Vibrations: Comparison of Network Configurations

by

Corrado Maurini

(ABSTRACT)

In this work passive piezoelectric devices for vibration damping are studied. It is developed the basic idea of synthesizing electrical wave guides to obtain an optimal electro-mechanical energy exchange and therefore to dissipate the mechanical vibrational energy in the electric form. Modular PiezoElectroMechanical (PEM) structures are constituted by continuous elastic beams (or bars) coupled, by means of an array of PZT transducers, to lumped dissipative electric networks. Both refined and homogenized models of those periodic systems are derived by an energetic approach based on the principle of virtual powers. Weak and strong formulation of the dynamical problem are presented having in mind future studies involving the determination of numerical solutions.

In this framework the effectiveness of the proposed devices for the suppression of mechanical vibrations is investigated by a wave approach, considering both the extensional and flexural oscillations. The optimal values of the electric parameters for a fixed network topology are derived analytically by a pole placement technique. Their sensitivities on the dimensions of the basic cell of the periodic system and on the design frequency are studied. Moreover the dependence of damping performances on the frequency is analyzed. Comparing the performances of different network topological configurations, the advantages of controlling a mechanical structure with an electric analog are shown. As a consequence of those results, new interconnections of PZT transducers are proposed.

An experimental setup for the validation of the analytical and numerical results is proposed and tested. A classical experience on resonant shunted PZT is reproduced. Future experimental work is programmed.

Contents

List of Figures

List of Tables

Chapter 1

Introduction

1.1 Background and Motivations

The control of structural vibrations is one of the foremost issues of mechanical engineering. Vibrations are undesirable for reliability, comfort and functionality of mechanical devices. Indeed, they are a cause of material failure by fatigue, they generate noise that is disturbing for humans, they impose a limit to the achievable precision in machinery, their oscillations cause instability in aerodynamical systems, as happens for the wings of an airplane.

Traditional solutions to the problem are to utilize viscoelastic material to add damping to the structure or to design the mass and stiffness distribution to control its dynamical behavior. An alternative device for narrow band vibration damping is the Dynamical Vibration Absorber (DVA). It consists of a spring-mass-damper to be coupled to the system to obtain a resonant energy exchange and dissipation.

In the last decade many research efforts were devoted to study the applications to this field of the significant electromechanical coupling offered by the new generation of piezoelectric ceramics such as lead zirconate titanium (PZT). In this context active and passive techniques have been developed. Active controls use PZT materials as sensor and actuators to apply feedback control to the structure. These achieve good performances, but they present the disadvantages of an high power requirement, stability problems, and the need of a complex central unity for the implementation of the control law. Passive solutions suggest to utilize the two way piezoelectromechanical coupling to transfer mechanical energy in electrical form and dissipate it in resistances by the Joule effect. It has been show that resonant systems are more effective to this aim. In analogy to $DVAs$, piezoelectric transducers shunted on an inductance and a resistance can be bonded to a structure

to form a coupled highly dissipative system. Adjusting the electrical parameters, the RLC circuit[1] can be tuned on a given mechanical mode with replacing it with a pair of strongly damped electromechanical modes. The advantages of this solution are its constructive simplicity, its intrinsic stability and the total independence from the environment. Indeed, in principle passive devices not only do not require power to work, but they can even be used to produce small amounts of energy[2]. In practice the high inductor required to tune the mechanical system to the electric one are frequently synthesized with electronic circuit that require a small amount of power to work[3]. Resonant Shunted Piezoelectrics (RSP) are strongly preferable to the mechanical analog $DVAs$ because of their low cost, low weight, low space requirements and for their flexibility. Indeed, the electrical parameters can be easily adjusted to match the characteristics of the structural mode to be damped. Exploiting this aspect, semi-active systems in which the values of the electrical parameters are chosen by a real-time control unit have been proposed. Industrial applications of $RSPs$ are now available (see for example *www.acx.com* where smart skis and smart bikes are illustrated). The greatest disadvantage of these devices are that they are effective only in a narrow band of frequencies because of their one-degree-of-freedom resonant nature. To bypass this problem piezoelectric patches with multiple shunts, each one of which can be matched on a mechanical mode, have been proposed with good results.

An innovative idea presented by dell'Isola and Vidoli consists in establishing a distributed piezoelectric coupling between continuous mechanical and electric media to form a "smart structure"[4] capable to be adjusted for an optimal broadband damping. They proposed to think about controlling a continuous mechanical structure with its electrical analog to enhance a complete communication between the two systems. In the present work this idea is studied and implemented.

1.2 Literature Review

Hagood and Von Flotow [30] in 1991 presented the first complete analytical and experimental study on resonant and resistive shunted $PZTs$, proposing an optimization procedure analog to those adopted for Dynamic Vibrations Absorbers in classical texts on vibrations such as Timoshenko [10]. The subject has been developed also by Del Vescovo in [28], [29] presenting comparisons between

[1] The capacitance is given by the physical nature of PZT materials, that are dielectrics.

[2] Energy harvesting by PZT transducers is one of the most recent reaserch topics.

[3] Let us underline that this power consumption is related only to the particular actual realization of a passive device.

[4] Let us recall one of the most pertinent definitions of "smart structure":
A smart structure is a material systems with intelligence and life features integrated in the microstructure of the material system to reduce mass and energy and produce adaptive functionality.

experimental results and numerical prediction. Details about the optimal design are given in [32] and in [33] by Steffen and Inman, both for active and passive control techniques. They propose also the simultaneous use of $DVAs$ and $RSPs$. Multiple shunts are implemented by Hollkamp [39]. Lesieutre [31] presented an useful review on shunting circuits (inductive capacitive, resonant and switched) giving design indications for applications. Active controls using piezoelectric materials as sensors and actuators are proposed in [40] and [41], semi-active techniques in [42] and [43].

Models of piezoelectric materials as actuators in unidimensional structures have been developed by Crawley in [35] and [36]. On the other hand their behavior as sensor has been investigated by Shiroy and Chopra in [37]. A coupled PiezoElectroMechanical model is discussed in [34], where also a Finite Element implementation is presented. Emphasis on experimental testing is given in [38].

Dell'Isola and Vidoli proposed a distributed coupling between mechanical and electrical continua to dissipate mechanical energy in the electrical form. In [20] they present a continuum model of a piezoelectromechanical truss beam coupled with an electrical transmission line studying its application for the suppression of longitudinal and torsional vibrations while in [21] they look for solutions for the bending modes. The idea of the distributed passive control is then applied in [22] to study, by means of an homogenized model, the modal coupling between a beam and a second order electric transmission line.

1.3 Ideas and Research Objectives

The goal of the research project of which this work is an integrated part is to study and realize electromechanical systems for distributed passive control of vibrations in mechanical structures by piezoelectric transducers and electric networks, following and improving what has been done in [20], [21], [22]. In this context theoretical, numerical and experimental work is required.

The physical idea to be developed is to couple by means of PZT transducers a given mechanical continuum with an electric continuous medium possessing analogous characteristics, in order to realize an electromechanical energetic exchange for a wide range of frequencies. Indeed, if waves propagate in the same fashion in two media and if they have been tuned for a given wavelength, hence they are tuned for all. In this way one of the crucial issues of collocated passive control, the narrow band behavior, can be solved.

To implement this idea in engineering applications it is necessary to

1. find electrical *analogs* of mechanical systems

2. realize the *coupling* between the analogous electrical and mechanical systems

In finding the analog electrical *continuum* two difficulties are encountered:

1. the speed of propagation of energy in electrical continua is enormously different to that in mechanical media

2. the physics of electromagnetism and mechanics are not the same. There can be physical mechanical phenomena that have not an electric equivalent and vice-versa.

For these reasons it is required to *synthesize in an approximative fashion* the electric media by a lumped model. Then the coupling between the mechanical continuum and the electric lumped periodic system can be achieved by means of an array of piezoelectric transducers. With this idea we will focus our attention on periodic electromechanical systems similar to that whose basic cell is sketched in figure 1-1.

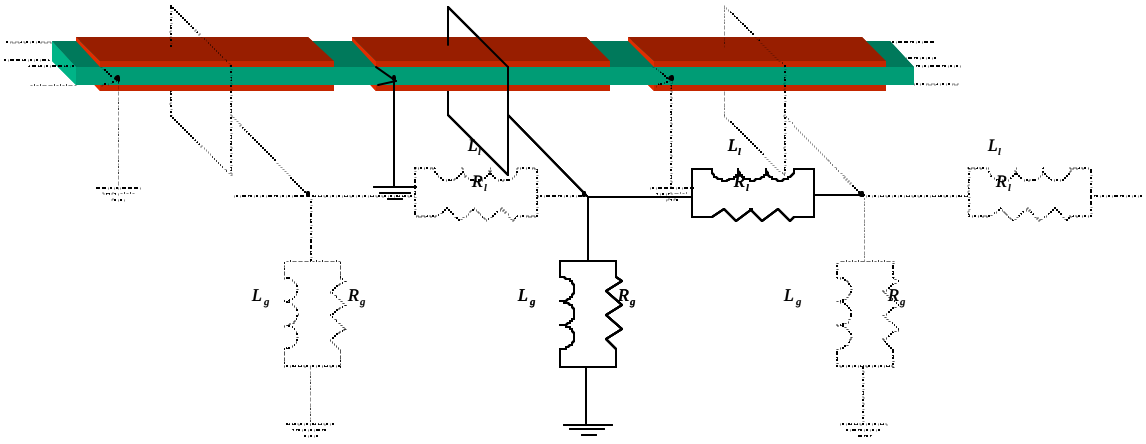

Figure 1-1: Periodic piezoelectromechancial beam

While a parallel study on electrical analogs of mechanical systems is carried on, the present work has the following main objectives:

1. *to establish both refined and homogenized models of the periodic electromechanical systems with distributed piezoelectric coupling.* Modular dissipative piezoelectromechanical systems composed by a mechanical continuum connected to a lumped electric network by means of an array of PZT transducers will be considered. It will be necessary to develop

   (a) a detailed model of the interaction between piezoelectric transducers and structures that underlines the two way electromechanical coupling, understanding how and by which hypotheses it can be simplified,

(b) develop a *refined model* of the modular piezoelectromechanical system,

(c) develop following [20], [22] *homogenized models*, identifying the constitutive relations by those found for the refined ones.

2. *to study and compare the qualitative features of different types of electric networks for the suppressions of mechanical extensional and flexural vibrations.* In particular, considering modular piezoelectromechanical media, we want to

   (a) optimize the value of the electric parameters in the networks for a series of different topologies to maximize the vibration damping,

   (b) perform a scale analysis, understanding the influence of the ratio between the length of the basic module and the characteristic wave lengths on the value of the optimal electric parameters and in the performances of the system for the vibration damping,

   (c) understand why and how optimized electrical systems with different topologies have different performances to damp mechanical vibrations.

3. *to realize and study experimentally the proposed piezoelectromechanical systems.* It will be necessary to

   (a) realize prototypes, facing the related technological problems

   (b) design and test an experimental set up and measurement procedure for their testing

   (c) verify experimentally the analytical and numerical results.

Constructive critical feedback between the experimental and modelling aspects will be crucial in this work. Indeed, in the research project the present is the first step toward an experimental realization of the proposed devices.

1.4 Outline

The present paper can be structured in three main parts. In each of them one of the three main objectives that have been outlined in the previous section will be treated.

In the first part composed by chapter 3,4,5 models of piezoelectromechanical systems will be developed. In particular, in chapter 3 the attention will be focused on electric systems presenting and modelling the electric networks that will be utilized for vibration damping. Some words on electromechanical analogies will be spent. In chapter 4 a refined unidimensional model of an elastic

beam on which PZT patches are bonded will be given. The system will be considered as a multilayer beam and its model will be deduced by the three-dimensional one imposing a given mechanical and electrical kinematics. The equations of motion will be furnished both in the strong and weak form, having mind future studies involving the determination of numerical solutions also for the refined model of the proposed smart structures. The hypotheses and the configurations for which the interactions between elastic and piezoelectric layers can be reduced to a simple model will be underlined. In chapter 5 the results achieved in chapter 3 and 4 will be applied to assemble the refined model of a periodic unidimensional piezoelectromechanical medium composed by an elastic beam coupled by means of a distributed array of PZT transducers to a lumped electric network. A continuous model of the periodic system will be derived by means of an homogenization procedure. Both the cases in which the electrical variables are coupled to the mechanical extensional and flexural behavior will be studied.

In the second part (chapter 6), the homogenized model previously deduced will be utilized to optimize the electrical networks for the vibration suppression and to infer important thumbnail informations about the characteristics of the system. A wave approach will be followed to perform a comparative analysis between different network connections. We will study the dependence of the optimal electric parameters on the dimensions of the basic cell of the periodic system, their sensitivity with respect to a change in the considered wavelength and the performance of the optimal systems for vibration damping.

In the third part (chapter 7) the problem of the experimental realization and testing of the proposed piezoelectromechanical system for the suppression of mechanical vibration will be addressed. The realized experimental apparatus and a tested measurement procedures will be described. The results of a classical experience on shunted $PZTs$, that has been reproduced to validate the experimental setup, will be presented. Finally future experiments will be designed.

In the following chapter the basic concept of continuum mechanics and piezoelectricity will be recalled. Moreover, referring to [3], the notation and the basic features of the Virtual Power Principle, whose modelling approach is adopted, will be presented.

Chapter 2

Preliminaries

In this chapter the basic concept of the kinematics of a continuum body will be recalled. Some words will be spent on the meaning and the formalism of the Virtual Power Principle that will be largely used in this work to derive the balance equations of dissipative electromechanical discrete and continuous systems. Finally the constitutive behavior of a piezoelectric material will be discussed furnishing applicative examples.

2.1 Continuum Kinematics

2.1.1 Body, References, Coordinates

A body can be identified with the closed region of the Euclidean space $\mathcal{E}$ that it occupies at a given instant in time. We will call this region the reference configuration $\mathcal{B}$ and the points $\mathbf{p} \in \mathcal{B}$ material points. Once a fixed Cartesian reference frame $\mathcal{C} = \{\mathbf{o}, \mathbf{e}_1, \mathbf{e}_2, \mathbf{e}_3\}$ is selected each point $\mathbf{p}$ can be associated with the oriented arrow $\overrightarrow{\mathbf{op}}$. Thus the space of points $\mathbf{p}$ can be structured as vector space $\mathcal{V}$ and each point can be represented also by the coordinate representation of $\overrightarrow{\mathbf{op}}$ in $\mathcal{C}$.

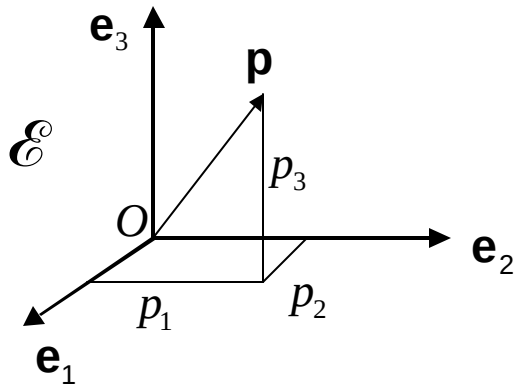

Reference frame

We will denote by

$$e = \{\mathbf{e}_1, \mathbf{e}_2, \mathbf{e}_3\} \tag{2.1}$$

the fixed basis for $\mathcal{V}$ and by

$$\mathbf{p} = \overrightarrow{\mathbf{op}} = p_1\mathbf{e}_1 + p_2\mathbf{e}_2 + p_3\mathbf{e}_3 = ep_e = e\begin{bmatrix} p_1 \\ p_2 \\ p_2 \end{bmatrix} \tag{2.2}$$

the vector $\mathbf{p} = \overrightarrow{\mathbf{op}}$ with coordinates p_e in the e basis.

We will introduce in $\mathcal{V}$ a scalar product " $\cdot$ " that is a bilinear, symmetric, positive definite application between pairs of elements of $\mathcal{V}$. If not otherwise specified, the scalar product is defined such that

$$e \cdot e := \begin{bmatrix} \mathbf{e}_1 \cdot \mathbf{e}_1 & \mathbf{e}_1 \cdot \mathbf{e}_2 & \mathbf{e}_1 \cdot \mathbf{e}_3 \\ \mathbf{e}_2 \cdot \mathbf{e}_1 & \mathbf{e}_2 \cdot \mathbf{e}_2 & \mathbf{e}_2 \cdot \mathbf{e}_3 \\ \mathbf{e}_3 \cdot \mathbf{e}_1 & \mathbf{e}_3 \cdot \mathbf{e}_2 & \mathbf{e}_3 \cdot \mathbf{e}_3 \end{bmatrix} = \mathbf{I} \tag{2.3}$$

where $\mathbf{I}$ is the third order identity matrix.

2.1.2 Deformations of Continuum Bodies

Definition 1 *A deformation of a body $\mathcal{B}$ is a mapping*

$$\begin{aligned} \mathbf{f} &: \mathcal{B} \mapsto \mathcal{E} \\ \mathbf{f} &: \mathbf{p} \mapsto \mathbf{x} := \mathbf{f}(\mathbf{p}) \end{aligned}$$

For the physical requirement of the impenetrability of the bodies and its continuity, $\mathbf{f}(\mathbf{p})$ must be a smooth 1-1 mapping from $\mathcal{B}$ to a bounded region of $\mathcal{E}$. An important role in the description of a deformation of a continuum body is played by the deformation gradient with respect to $\mathbf{p}$

$$\mathbf{F} : \mathbf{p} \to \mathbf{F}(\mathbf{p}) := \boldsymbol{\nabla}\mathbf{f}(\mathbf{p}) \tag{2.4}$$

whose determinant represents the local change in volume under $\mathbf{f}$. We must require $\det(\boldsymbol{\nabla}\mathbf{f}(\mathbf{p})) \neq 0$ *for each* $\mathbf{p} \in \mathcal{B}$. We will assume

$$\det(\boldsymbol{\nabla}\mathbf{f}(\mathbf{p})) > 0, \ \textit{for each } \mathbf{p} \in \mathcal{B}. \tag{2.5}$$

Definition 2 *Let $\mathcal{V}$ be the three dimensional vector space of translations of $\mathcal{B}$. The displacement field associated to the deformation* $\mathbf{f}$ *is a function*

$$\begin{aligned} \hat{\mathbf{u}} &: \mathcal{B} \mapsto \mathcal{V} \\ \hat{\mathbf{u}} &: \mathbf{p} \mapsto \mathbf{u} = \hat{\mathbf{u}}(\mathbf{p}) := \mathbf{f}(\mathbf{p}) - \mathbf{p} \end{aligned}$$

Remark 1 *The* displacement gradient *respect to* $\mathbf{p}$ *is*

$$\nabla\mathbf{u} = \boldsymbol{\nabla}(\mathbf{f}(\mathbf{p}) - \mathbf{p}) = \mathbf{F} - \mathbf{I}$$

$\mathbf{F}$,$\nabla\mathbf{u}$ are linear applications from $\mathcal{V}$ to $\mathcal{V}$ we say $\mathbf{F}$,$\nabla\mathbf{u} \in Lin(\mathcal{V})$. In particular $\mathbf{F} \in Lin^{+}(\mathcal{V})$

Definition 3 *A deformation* $\mathbf{f}$ *is called an* homogeneous deformation *if* $\mathbf{F}(\mathbf{p})$ *is constant for each* $\mathbf{p} \in \mathcal{B}$

Let us introduce in the vector space of oriented arrows the norm $\|\cdot\|$ induced by the ordinary scalar product. Thus it is possible to define the distance between two points $\mathbf{p}, \mathbf{q}$ by means of $\|\overrightarrow{\mathbf{pq}}\| = \|\mathbf{p} - \mathbf{q}\|$.

Definition 4 *A deformation* $\mathbf{f}$ *is a* rigid deformation *if it preserves distances between any pair of points of the body $\mathcal{B}$.*

It is possible to show that the deformation gradient of a rigid deformation is skew-symmetric.

Expanding a generic deformation in the neighborhood of a point $\mathbf{q} \in \mathcal{B}$ we can approximate its behavior as the superposition of a translation and an homogenous deformation

$$\mathbf{f}(\mathbf{p}) = \mathbf{f}(\mathbf{q}) + \mathbf{F}(\mathbf{q})(\mathbf{p} - \mathbf{q}) + o(\mathbf{p} - \mathbf{q}) \tag{2.6}$$

The deformation gradient $\mathbf{F}$ can be decomposed in its symmetric part $\mathbf{E}$ and skew symmetric part $\mathbf{W}$ as following

$$\mathbf{F} = \mathbf{D} + \mathbf{W} \tag{2.7}$$

where

$$\mathbf{D} = \frac{1}{2}\left(\mathbf{F}+\mathbf{F}^T\right) \tag{2.8}$$

$$\mathbf{W} = \frac{1}{2}\left(\mathbf{F}-\mathbf{F}^T\right) \tag{2.9}$$

In the same way the displacement gradient $\nabla\mathbf{u}$ can be decomposed as

$$\nabla\mathbf{u} = \mathbf{S}+\mathbf{W} \tag{2.10}$$

where

$$\mathbf{S} = \frac{1}{2}\left(\nabla\mathbf{u}+\nabla\mathbf{u}^T\right) \tag{2.11}$$

$$\mathbf{W} = \frac{1}{2}\left(\nabla\mathbf{u}-\nabla\mathbf{u}^T\right) \tag{2.12}$$

and $\mathbf{S}$ is called the *infinitesimal strain*

Thus each deformation can be locally decomposed in a rigid deformation and in a pure deformation as

$$\mathbf{f}(\mathbf{p}) = \mathbf{f}(\mathbf{q}) + \mathbf{D}(\mathbf{q})(\mathbf{p}-\mathbf{q}) + \mathbf{W}(\mathbf{q})(\mathbf{p}-\mathbf{q}) + o(\mathbf{p}-\mathbf{q}) \tag{2.13}$$

where

$$\mathbf{f}(\mathbf{q}) + \mathbf{W}(\mathbf{q})(\mathbf{p}-\mathbf{q}) \tag{2.14}$$

is the rigid component of $\mathbf{f}$ and

$$D(\mathbf{q})(\mathbf{p}-\mathbf{q}) \tag{2.15}$$

is the pure deformation. We denoted by $o(\mathbf{p}-\mathbf{q})$ higher order terms in the Taylor expansion of $\mathbf{f}(\mathbf{p})$ in a neighborhood of the point $\mathbf{q}$

If dynamical processes are considered, an appropriate terminology must be introduced.

Definition 5 *A motion of $\mathcal{B}$ is a smooth one parameter family of deformations $\mathbf{f}_t(\cdot)$ defined on $\mathcal{B}$*

for t in a given real interval $\mathcal{I}$. It can be represented by the function

$$\begin{aligned} \mathrm{x} \;&:\; \mathcal{B}\times\mathcal{I}\to\mathcal{E} \\ &:\; (\mathbf{p},t)\to\mathbf{x}=\mathrm{x}(\mathbf{p},t):=\mathbf{f}_t(\mathbf{p}) \end{aligned}$$

Definition 6 *The velocity field* $\mathrm{v}(\mathbf{p},t)$ *for a given motion* $\mathrm{x}(\mathbf{p},t)$ *is defined as*

$$\mathrm{v}(\mathbf{p},t):=\frac{\partial}{\partial t}\mathrm{x}(\mathbf{p},t)=:\dot{\mathrm{x}}(\mathbf{p},t)$$

Obviously the time derivatives of all the fields previously introduced can be defined.

Definition 7 *Let* $\mathbf{p}$ *and* $\mathbf{q}$ *be points of the euclidean space* $\mathcal{E}$*. A velocity field* $\mathrm{v}(\mathbf{p},t)$ *is a distributor if*

$$\mathrm{v}(\mathbf{p},t)=\mathrm{v}(\mathbf{q})+\quad(t)(\mathbf{p}-\mathbf{q})$$

where (t) *is a skew-symmetric linear transformation.*

The velocity field $\mathrm{v}(\mathbf{x},t)$ is one of a motion described by

$$\mathbf{x}=\mathbf{Q}(t)(\mathbf{p}-\mathbf{o})+\mathbf{c}(t) \tag{2.16}$$

with

$$\mathbf{Q}(t)\mathbf{Q}^T(t)=\mathbf{I} \tag{2.17}$$

and

$$(t)=\dot{\mathbf{Q}}(t)\mathbf{Q}^T(t) \tag{2.18}$$

Definition 8 *A tensor valued field in* $\mathcal{R}^3$ *is said to be objective if and only if its components transform tensorially with respect to (2.16).*

Let $\mathcal{C}$ be the linear space of the distributors C.

Remark 2 *Since each* $C\in\mathcal{C}$ *is the superposition of a translation and a rotation in the euclidean space* $\mathcal{E}$*, the dimension of* $\mathcal{C}$ *is* 6.

Definition 9 *A motion belonging to $\mathcal{C}$ is said to be rigidifying motion if $\mathcal{B}$ is a deformable continuum.*

2.1.3 Beam Kinematics

Let us consider in the Euclidean space $\mathcal{E}$ a straight line $\mathcal{A}$, called axis, a point $\mathbf{O}$ on it, called origin and a one parameter family of bounded plane regions $\mathcal{S}_x, x \in \mathcal{I} \subset \mathcal{R}$, called sections. It is now possible to fix a Cartesian reference frame $\mathcal{C} = \{\mathbf{O}, \mathbf{e_1}, \mathbf{e}_2, \mathbf{e}_3\}$, with origin $\mathbf{O}$ and the $\mathbf{e}_1 - axis$ parallel to $\mathcal{A}$.

A straight axis beam $\mathcal{B}$ can be geometrically described as the union of sections $\mathcal{S}_x$ for x in some closed interval $\mathcal{I}$ of $\mathcal{R}$. Formally

$$\mathcal{B} := \bigcup_{x \in \mathcal{I}} \mathcal{S}_x \tag{2.19}$$

The oriented arrow $\overrightarrow{OP}$ that is an element of the vector space $\mathcal{V}$ of translations in $\mathcal{E}$, can be associated at each point $\mathbf{p} \in \mathcal{B}$. In the reference $\mathcal{C}$

$$\overrightarrow{OP} = p_1\mathbf{e}_1 + p_2\mathbf{e}_2 + p_3\mathbf{e}_3 \tag{2.20}$$

and the set of three real numbers $\{p_1, p_2, p_3\}$ is the coordinate representation of $\overrightarrow{OP}$ in $\mathcal{C}$. $\overrightarrow{OP}$ can be partitioned in its orthogonal projection on the axis $\mathcal{A}$

$$\overrightarrow{OP_a} = p_1\mathbf{e}_1 \tag{2.21}$$

and its orthogonal projection on the section $\mathcal{S}_x$

$$\mathbf{s} := \overrightarrow{P_aP} = p_2\mathbf{e}_2 + p_3\mathbf{e}_3 \tag{2.22}$$

such that

$$\overrightarrow{OP} = \overrightarrow{OP_a} + \overrightarrow{P_aP} \tag{2.23}$$

where $\overrightarrow{OP_a}$ is an element of the three dimensional vector space $\mathcal{V}$ and $\mathbf{s} := \overrightarrow{P_aP}$ lies in the two dimensional vectorial space $\mathcal{W}$ of the translations in the plane.

Considering $\mathcal{B}$ the reference configuration of the beam, a motion can be mathematically de-

scribed by the smooth one parameter family of smooth maps

$$\mathbf{x}(\,\cdot\,,t) : \mathcal{B} \mapsto \mathcal{B}_t \tag{2.24}$$

such that each point $\mathbf{p}$ in the reference configuration $\mathcal{B}$ is mapped into its position $\mathbf{q}$ in the actual configuration $\mathcal{B}_t$ at time t by

$$\bar{\mathbf{x}} = \mathbf{x}(\mathbf{p},t) \tag{2.25}$$

The displacement vector field is naturally defined as follows

$$\mathbf{u}(\mathbf{p},t) = \bar{\mathbf{x}} - \mathbf{p} = \mathbf{x}(\mathbf{p},t) - \mathbf{p} \tag{2.26}$$

Remark 3 *In the basis* $e = \{\mathbf{e}_1, \mathbf{e}_2, \mathbf{e}_3\}$ $\mathbf{u}(\mathbf{p}_a, t)$ *can be written as*

$$\mathbf{u}(\mathbf{p},t) = u_1(p_1, p_2, p_3, t)\mathbf{e}_1 + u_2(p_1, p_2, p_3, t)\mathbf{e}_2 + u_3(p_1, p_2, p_3, t)\mathbf{e}_3$$

We will use the following notation

$$\mathbf{u}(\mathbf{p},t) = e\,(\mathbf{u}(\mathbf{p},t))_e = e \begin{bmatrix} u_1(p_1, p_2, p_3, t) \\ u_2(p_1, p_2, p_3, t) \\ u_3(p_1, p_2, p_3, t) \end{bmatrix}$$

where e *is the row vector* $\{\mathbf{e}_1, \mathbf{e}_2, \mathbf{e}_3\}$ *and the column vector* $(\mathbf{u}(\mathbf{p},t))_e$ *is the coordinate representation of* $\mathbf{u}(\mathbf{p},t)$ *in the basis* e*. In the same fashion*

$$\mathbf{x}(\mathbf{p},t) = e\,(\mathbf{x}(\mathbf{p},t))_e = e \begin{bmatrix} f_1(p_1, p_2, p_3, t) \\ f_2(p_1, p_2, p_3, t) \\ f_3(p_1, p_2, p_3, t) \end{bmatrix}$$

Moreover, given a function $g(p_1, p_2, p_3, t)$*, we will define*

$$g(p_1, t) := g(p_1, 0, 0, t)$$

The partition of $\overrightarrow{OP}$ induces the definition of the one parameter family of applications

$$\mathbf{G}_t(\mathbf{s}) := \mathbf{x}(\mathbf{p},t) - \mathbf{x}(\mathbf{p}_a, t) \tag{2.27}$$

such that

$$\mathbf{x}(\mathbf{p},t) = \mathbf{x}(\mathbf{p}_a, t) + \mathbf{G}_t(\mathbf{s}). \tag{2.28}$$

where

$$\mathbf{p}_a = \overrightarrow{OP_a} = e \begin{bmatrix} p_1 \\ 0 \\ 0 \end{bmatrix}, \mathbf{s} = \mathbf{p} - \mathbf{p}_a \tag{2.29}$$

The constraints imposed on $\mathbf{G}_t$ play a fundamental role in beam modelling. We will assume that the axis can move only in the $\mathbf{e}_2, \mathbf{e}_3 - plane$ and that $\mathbf{G}_t$ is the composition of a *in plane uniform deformation* $\mathbf{U}_t$ and a *rotation* $\mathbf{R}_t$ around the $\mathbf{e}_2 - axis$. Thus

$$\mathbf{G}_t(\mathbf{v}) = \mathbf{R}_t\left(\mathbf{U}_t(\mathbf{v})\right) \tag{2.30}$$

where $\mathbf{U} : \mathcal{W} \mapsto \mathcal{W}$ is linear and $\mathbf{R}_t \colon \mathcal{W} \mapsto \mathcal{V}$ has the following coordinate representation in the basis $e = \{\mathbf{e}_1, \mathbf{e}_2, \mathbf{e}_3\}$ for $\mathcal{V}$ and $e' = \{\mathbf{e}_2, \mathbf{e}_3\}$ for $\mathcal{W}$

$$(R_t)_e^{e'} = \begin{bmatrix} 0 & \sin(\theta) \\ 1 & 0 \\ 0 & \cos(\theta) \end{bmatrix} \tag{2.31}$$

Definition 10 *A beam has no shear deformation if the rotation* $\mathbf{R}_t$ *of the section* $\mathcal{S}_x$ *is such that in the actual configuration the angles between the sections and the axis remain the same those in the reference configuration.*

We will *linearize* the kinematics about the reference configuration and we will assume that the beam has *no shear deformability.*

Claim 1 *In the linearized kinematics the rotation* $\mathbf{R}_t$ *has the following coordinate representation in the* $e - e' - bases$

$$(R_t)_e^{e'} = \begin{bmatrix} 0 & \theta \\ 1 & 0 \\ 0 & 1 \end{bmatrix}$$

Claim 2 In the linearized kinematics of a beam with no shear deformation *the rotation angle of*

R_t *is*

$$\theta = -\frac{\partial x_3(p_1,t)}{\partial p_1} = -\frac{\partial u_3(p_1,t)}{\partial p_1}$$

Finally we can write the coordinate representation of the motion beam without shear deformation in the linear approximation

$$\begin{aligned}(\mathbf{x}(\mathbf{p},t))_e &= \begin{bmatrix} x_1(p_1,t) \\ 0 \\ x_3(p_1,t) \end{bmatrix} + \begin{bmatrix} 0 & -\frac{\partial x_3(p_1,t)}{\partial p_1} \\ 1 & 0 \\ 0 & 1 \end{bmatrix} \begin{bmatrix} U_{11} & U_{12} \\ U_{21} & U_{22} \end{bmatrix} \begin{bmatrix} p_2 \\ p_3 \end{bmatrix} \\ &= \begin{bmatrix} x_1(p_1,t) - \frac{\partial x_3(p_1,t)}{\partial p_1}(p_2U_{21} + p_3U_{22}) \\ p_2U_{11} + p_3U_{12} \\ x_3(p_1,t) + p_2U_{21} + p_3U_{22} \end{bmatrix}\end{aligned}$$

Remark 4 *In the hypotheses of rigid sections* $\mathbf{U} = \mathbf{I}$ *and*

$$\mathbf{x}(\mathbf{p},t) = e \begin{bmatrix} x_1(p_1,t) - \frac{\partial x_3(p_1,t)}{\partial p_1} p_3 \\ p_2 \\ x_3(p_1,t) + p_3 \end{bmatrix} \tag{2.32}$$

$$\mathbf{u}(\mathbf{p},t) = e \begin{bmatrix} u_1(p_1,t) - \frac{\partial u_3(p_1,t)}{\partial p_1} p_3 \\ 0 \\ u_3(p_1,t) \end{bmatrix} \tag{2.33}$$

2.2 Virtual Power Principle

2.2.1 Introduction

Our goal is to deduce homogenized and refined models of electromechanical dissipative systems. The variational principle of virtual power, that is an evolution of D'Alembert principle, leads us to a weak formulation of the problem that is general enough to consider the electromechanical coupling in dissipative processes. In this context the equilibrium is expressed by a balance of powers. The basic idea of this formulation is to describe forces not by their vectorial representation but by means of the power they exert for a given velocity field[1]. In other words once given the normed vector space $\mathcal{V}$ of virtual velocity fields v, the forces f acting on them are determined by the scalar values

[1] The terms velocity, kinematics and force are intented in a generalized meaning.

assumed by the linear functional

$$\begin{aligned} \mathcal{P} &: \mathcal{V} \to \mathcal{R} \\ &: \mathrm{v} \to \mathcal{P}(\mathrm{v}) = \langle \mathrm{f}, \mathrm{v} \rangle \end{aligned}$$

In this way the duality via a bilinear form $\langle \cdot, \cdot \rangle$ between the linear vector space of forces and virtual velocities is the way in which the forces are defined.

2.2.2 Definitions

State variables

Discrete and continuous systems are distinguished by the fact that at a given instant in time the configuration of a discrete system is given by a set of k *constants*

$$X = \{\mathbf{x}_1, ..., \mathbf{x}_k\} \tag{2.34}$$

while the configuration of a continuum body[2] $\mathcal{B}$ is given by a set of h *fields* defined on $\mathcal{B}$

$$U_0 = \{\mathbf{u}_1(\mathbf{p}), ..., \mathbf{u}_h(\mathbf{p})\} \tag{2.35}$$

and eventually by their spatial gradients

$$U_1, ..., U_n$$

where

$$U_i = \{\nabla^i \mathbf{u}_1(\mathbf{p}), ..., \nabla^i \mathbf{u}_m(\mathbf{p})\}, m \leq h, i = 1...n \tag{2.36}$$

The local state of a continuum body in the neighborhood of each point must be specified explicitly and its description will be as good as the greatest gradient order n considered (the concept of a Taylor expansion of each field $\mathbf{u}_i(\mathbf{p})$ should be kept in mind). The choice about which and how many spatial gradients to consider is a constitutive assumption. A theory which considers n spatial gradients is called $n - th$ gradient order theory.

On a continuum body a set of boundary conditions must be prescribed. In the approach we

[2] Here as before a continuum body is identified with the region $\mathcal{B}$ of the Euclidean space that it occupies at a fixed time instant t_0

are following only the boundary conditions prescribed directly on the elements of $U = U_0, ..., U_n$ (*essential boundary conditions*) must be explicitly considered. They will be in the form of n_{bc} equations (BC), in general non-homogeneous, that must be satisfied on a part of $\partial\mathcal{B}$ and they appear in the definition of the functional space in which the virtual velocities must lie.

We will focus our attention on a system $\mathcal{S}$ constituted by a continuum body $\mathcal{B}$ with a set of essential boundary conditions BC. The state of $\mathcal{S}$ at a fixed instant in time is given by the set

$$S = \{U_0, ..., U_n\}. \tag{2.37}$$

We will call S the set of the *state variables* of $\mathcal{S}$.

Example 1 *In a first order gradient theory the state of an electromechanical continuum in the quasi-electrostatic approximation can be described by*

$$S = \{\mathbf{u}(\mathbf{p}, t), \phi(\mathbf{p}, t), \nabla\mathbf{u}(\mathbf{p}, t), \nabla\phi(\mathbf{p}, t)\}, \mathbf{p} \in \mathcal{B} \tag{2.38}$$

where $\mathbf{u}(\mathbf{p}, t)$ *is the vectorial valued field describing the mechanical displacement from the reference configuration and* $\phi(\mathbf{p}, t)$ *is the scalar valued field of the time primitive of the electric potential.*

Actual and Virtual velocities

The elements of S are all functions of time and the set of their time derivatives

$$V = \{V_0, ..., V_n\} \tag{2.39}$$

where

$$V_i = \{\nabla^i\dot{\mathbf{u}}_1(\mathbf{p}), ..., \nabla^i\dot{\mathbf{u}}_m(\mathbf{p})\}, m \leq h, i = 1...n \tag{2.40}$$

are a velocity description of $\mathcal{S}$. Here we will distinguish between the velocity actually experienced during a motion (*actual velocities)* and the *virtual* velocities that will be denoted by a superscript "*". The virtual velocities do not need to satisfy the equation of motions, they are required only to be enough smooth and to satisfy the homogeneous version of the prescribed boundary conditions, otherwise they are arbitrary. We will denote by $\mathcal{V}$ the vector space of the virtual velocities.

On the actual and virtual velocities the same smoothness is required, but in general the functional spaces in which they lie are different because of the boundary conditions. In fact the actual velocities $\dot{\mathbf{u}}_i(\mathbf{p})$ must satisfy the prescribed essential boundary conditions while the virtual veloci-

ties are required to satisfy their homogeneous version. For numerical application it is useful to have the actual and virtual velocities in the same space. Thus if non-homogenous boundary conditions are present it is convenient to restate the problem converting them to an homogeneous form[3].

Focusing our attention on a first gradient order theory, let us denote the vector space of virtual velocities by

$$\mathcal{V} = \{v_i^*, \nabla v_i^*\}_{i=1...n} = \{\dot{s}_i, \nabla \dot{s}_i\}_{i=1...n} \tag{2.41}$$

The virtual velocities that are *objective* are called *objective virtual velocities*. Let's denote by $\mathcal{V}_{obj}$ the space spanned by them.

Example 2 *In an electromechanical continuum in the quasi-electrostatic approximation and for a first order-gradient theory the following set of virtual velocities can be chosen*

$$\mathcal{V} = \{\dot{\mathbf{u}}^*(\mathbf{p},t), \phi^*(\mathbf{p},t), \nabla\dot{\mathbf{u}}^*(\mathbf{p},t), \nabla\dot{\phi}^*(\mathbf{p},t)\} \tag{2.42}$$

Virtual Powers

The virtual powers are defined as a linear functional defined on the space $\mathcal{V}$ of the virtual velocities.

$$\mathcal{P} : \mathcal{V} \to \mathcal{R} \tag{2.43}$$

Thus the virtual powers are in the dual space of $\mathcal{V}$. The virtual velocities are *test* functions for the forces defined in the distributional sense by means of the corresponding powers.

Virtual Power of Internal Forces The virtual power of internal forces is characterized by the following

Axiom 1 *The virtual power of forces internal to a system $\mathcal{B}$ vanishes for all rigidifying motions of $\mathcal{B}$ considered at any time t.*

Proposition 1 *The virtual power $\mathcal{P}_{int}$ of the internal forces Φ exerted within a continuous medium that occupies, in the reference configuration, the region $\mathcal{B}$ of the euclidean space is expressed by a*

[3] A simple change of variables is required.

continuous linear functional on the normed[4] *linear space* $\mathcal{V}_{obj}$. *That is*

$$\mathcal{P}_{int}(\mathcal{B},\mathcal{V}) = \langle \Phi, v^* \rangle_{\mathcal{B}}\,, v^* \in \mathcal{V}_{obj}.$$

Thus to formulate an *a-priori* theory of a continuum it is necessary, after having chosen the space $\mathcal{V}$, to find $\mathcal{V}_{obj}$. In the present work we will specialize already existence theories in technical cases and we will write directly the expression of the internal power without facing the problem of finding $\mathcal{V}_{obj}$.

Example 3 *In an electromechanical continuum in the quasi-electrostatic approximation and for a first order-gradient theory the virtual velocity are (2.42) and*

$$\mathcal{V}_{obj} = \{\dot{\mathbf{S}}^*(\mathbf{p},t), \nabla\dot{\phi}^*(\mathbf{p},t)\} \tag{2.44}$$

where

$$\dot{\mathbf{S}}^*(\mathbf{p},t) = sym(\nabla\dot{\mathbf{u}}^*(\mathbf{p},t)) = \frac{1}{2}(\nabla\dot{\mathbf{u}}^*(\mathbf{p},t) + \nabla\dot{\mathbf{u}}^*(\mathbf{p},t)) \tag{2.45}$$

Hence the virtual power of the internal forces is

$$\begin{aligned} \mathcal{P}_{int}(\mathcal{B},\mathcal{V}) &= \mathcal{P}_{int,m}(\mathcal{B},\mathcal{V}) + \mathcal{P}_{int,e}(\mathcal{B},\mathcal{V}) && (2.46)\\ &= \left\langle \mathbf{T}, \dot{\mathbf{S}}^*(\mathbf{p},t) \right\rangle_{\mathcal{B}} + \left\langle \mathbf{J}, \nabla\dot{\phi}^*(\mathbf{p},t) \right\rangle_{\mathcal{B}} && (2.47) \end{aligned}$$

where the tensorial field $\mathbf{T}$ *and the vectorial field* $\mathbf{J}$ *are defined as the quantities on which* $\dot{\mathbf{S}}^*, \nabla\dot{\phi}^*$ *expend power. Physically* $\mathbf{T}$ *is the tensor that describes the tensional state of a continuum, while* $\mathbf{J}$ *can be interpreted as the time derivative of the electric displacement vector* $\mathbf{D}$*, that is a displacement current inside the dielectric body.*

Virtual Power of External Forces As the external forces are classified as at-distance, or volume, forces and contact forces, so are the respective powers.

Proposition 2 *The virtual power of distance, or volume, forces* $\mathbf{B}_d$ *exerted in a continuous medium occupying, in the reference configuration, the region* $\mathcal{B}$ *of the euclidean space* $\mathcal{E}$*, is a continuous*

[4] *The norm induced by the scalar product* $\langle \cdot, \cdot \rangle_{\mathcal{B}}$ *is considered.*

linear functional on $\mathcal{V}$.

$$\mathcal{P}_d(\mathcal{B}, \mathcal{V}) = \langle \Phi, v^* \rangle_{\mathcal{B}} := \int_{\mathcal{B}} \mathbf{B}_d \cdot v^*$$

Proposition 3 *The virtual power of contact forces* $\mathbf{B}_c$ *exerted in a continuous medium occupying, in the reference configuration, the region* $\mathcal{B}$ *of the euclidean space* $\mathcal{E}$*, is a continuous linear functional on* $\mathcal{V}$.

$$\mathcal{P}_c(\partial\mathcal{B}, \mathcal{V}) = \langle \Phi, v^* \rangle_{\partial\mathcal{B}} := \int_{\partial\mathcal{B}} \mathbf{B}_c \cdot v^*$$

The external forces can expend power in every type of virtual velocities, included the non objective ones. Often in applications only a few types of them are present.

Here we will considered the inertial forces as external forces despite that they are prescribed by something similar to a constitutive relation, while contact and volume forces are given by the environment in which the body is embedded.

Proposition 4 *The virtual power of inertial forces* $\mathcal{P}_a$ *experienced by a continuous medium occupying the domain* $\mathcal{B}$ *of the euclidean space* $\mathcal{E}$ *in the reference configuration is a continuous linear functional on the virtual velocities containing only time derivatives of the state fields and not their gradients.*

For example, in the purely mechanical case we will impose

$$\mathcal{P}_a(\mathcal{B}, v^*) = \int_{\mathcal{B}} -\rho \dot{v} \cdot v^* \tag{2.48}$$

where ρ is the mass density for unit volume in the medium. We underline that it is necessary to differentiate the notation between the actual velocities v and the virtual velocities v^*. The minus sign in the definition is due to the fact that they are considered as external forces.

The virtual power of all the external forces is given by the sum of the three contributions

$$\mathcal{P}_{ext}(\mathcal{B}, v^*) = \mathcal{P}_d(\mathcal{B}, v^*) + \mathcal{P}_c(\partial\mathcal{B}, v^*) + \mathcal{P}_a(\mathcal{B}, v^*) \tag{2.49}$$

Example 4 *Let* $\mathcal{B}$ *be an electromechanical dielectric in the quasi-electrostatic approximation. The virtual velocities are (2.42) and the virtual power of the external forces can be written as*

Power of distance forces

$$\begin{aligned} \mathcal{P}_d(\mathcal{B}, v^*) &= \mathcal{P}_{d,m}(\mathcal{B}, \dot{\mathbf{u}}^*(\mathbf{p},t)) && (2.50)\\ &= \langle \mathbf{b}, \dot{\mathbf{u}}^*(\mathbf{p},t)\rangle_{\mathcal{B}} && (2.51)\end{aligned}$$

Power of contact forces

$$\begin{aligned} \mathcal{P}_c(\partial\mathcal{B}, v^*) &= \mathcal{P}_{c,m}(\partial\mathcal{B}, \dot{\mathbf{u}}^*(\mathbf{p},t)) + \mathcal{P}_{c,e}(\partial\mathcal{B}, \dot{\phi}^*(\mathbf{p},t)) && (2.52)\\ &= \langle \mathbf{f}, \dot{\mathbf{u}}^*(\mathbf{p},t)\rangle_{\partial\mathcal{B}} + \left\langle \sigma, \dot{\boldsymbol{\phi}}^*(\mathbf{p},t)\right\rangle_{\partial\mathcal{B}} && (2.53)\end{aligned}$$

Power of inertial forces

$$\begin{aligned} \mathcal{P}_a(\partial\mathcal{B}, v^*) &= \mathcal{P}_{a,m}(\partial\mathcal{B}, \dot{\mathbf{u}}^*(\mathbf{p},t)) && (2.54)\\ &= \langle -\rho\ddot{\mathbf{u}}(\mathbf{p},t), \dot{\mathbf{u}}^*(\mathbf{p},t)\rangle_{\mathcal{B}} && (2.55)\end{aligned}$$

Hence the total power of the external forces is

$$\begin{aligned} \mathcal{P}_{ext}(\mathcal{B}, v^*) &= \mathcal{P}_d(\mathcal{B}, v^*) + \mathcal{P}_c(\partial\mathcal{B}, v^*) + \mathcal{P}_a(\mathcal{B}, v^*) && (2.56)\\ &= \left(\begin{array}{c} \mathcal{P}_{d,m}(\mathcal{B}, \dot{\mathbf{u}}^*(\mathbf{p},t)) + \mathcal{P}_{c,m}(\partial\mathcal{B}, \dot{\mathbf{u}}^*(\mathbf{p},t)) + \\ + \mathcal{P}_{c,e}(\partial\mathcal{B}, \dot{\phi}^*(\mathbf{p},t)) + \mathcal{P}_{a,m}(\partial\mathcal{B}, \dot{\mathbf{u}}^*(\mathbf{p},t)) \end{array} \right) \\ &= \left(\begin{array}{c} \int_{\mathcal{B}} \mathbf{b}\cdot\dot{\mathbf{u}}^*(\mathbf{p},t) + \int_{\partial\mathcal{B}} \mathbf{f}\cdot\dot{\mathbf{u}}^*(\mathbf{p},t) + \\ + \int_{\partial\mathcal{B}} \sigma\dot{\boldsymbol{\phi}}^*(\mathbf{p},t) + \int_{\mathcal{B}} -\rho\ddot{\mathbf{u}}(\mathbf{p},t)\cdot\dot{\mathbf{u}}^*(\mathbf{p},t) \end{array} \right) \end{aligned}$$

2.2.3 Statement

It's finally possible to enunciate the principle of virtual power.

Proposition 5 Principle of Virtual Power. *In a Galilean reference frame, and for an absolute Newtonian chronology, the virtual power of the internal forces of a system $\mathcal{B}$ balance the virtual power of external forces impressed on the system, for any smooth virtual velocity field satisfying the homogeneous version of the prescribed boundary conditions. Thus the following equality must hold for each smooth v^* satisfying the homogeneous version of the prescribed boundary conditions*

$$\mathcal{P}_{int}(\mathcal{B}, v^*) = \mathcal{P}_{ext}(\mathcal{B}, v^*) \tag{2.57}$$

Example 5 *Let $\mathcal{B}$ be an electromechanical dielectric in the quasi-electrostatic approximation. In a*

first order gradient theory the virtual velocities are (2.42), the virtual power of the internal forces is (2.46), the virtual power of the external forces is (2.56). Hence the power balance is expressed by

$$\begin{aligned} \mathcal{P}_{int,m} + \mathcal{P}_{int,e} &= \mathcal{P}_{d,m} + \mathcal{P}_{c,m} + \mathcal{P}_{c,e} + \mathcal{P}_{a,m} \\ \begin{pmatrix} \int_{\mathcal{B}} \mathbf{T} \cdot \dot{\mathbf{S}}^*(\mathbf{p},t) + \\ + \int_{\mathcal{B}} \mathbf{J} \cdot \nabla \dot{\phi}^*(\mathbf{p},t) \end{pmatrix} &= \begin{pmatrix} \int_{\mathcal{B}} \mathbf{b} \cdot \dot{\mathbf{u}}^*(\mathbf{p},t) + \int_{\partial\mathcal{B}} \sigma \dot{\phi}^*(\mathbf{p},t) + \\ + \int_{\partial\mathcal{B}} \mathbf{f} \cdot \dot{\mathbf{u}}^*(\mathbf{p},t) + \int_{\mathcal{B}} -\rho \ddot{\mathbf{u}}(\mathbf{p},t) \cdot \dot{\mathbf{u}}^*(\mathbf{p},t) \end{pmatrix} \end{aligned} \tag{2.58}$$

2.2.4 Considerations

From a kinematical description of the physical system by means of the principle of the virtual power, once considered the constitutive equations, a mathematical formulation of a boundary value problem can be obtained.

The formulation of a physical problem by means of the principle of the virtual power allows us to

1. Obtain a weak formulation of the problem. It is given by the statement of the principle power itself when the constitutive relations are considered.

2. Derive a Galerkin Formulation of the problem restating the principle of the virtual power performing a change of variables in order to have only essentially homogeneous boundary conditions.

3. Obtain numerical approximate solutions for the problem by means of a Galerkin Approximation. For example the Finite Element Method can be applied.

4. Derive the strong form of the balance equations rewriting the power balance with some integration by parts and considering that the virtual velocities are arbitrary. It must be underlined that, dealing with non-regular physical systems, a strong formulation of the equilibrium equations is not convenient because, while an analytical solution cannot be achieved, a numerical solution of the problem can be obtained directly as in 3.

5. Write the actual power balance for the system once the virtual velocities in (2.57) are substituted by the actual velocities.

6. Find a correspondence between the forces appparing in two different models of the same physical system once a kinematical map between them is given. It can be obtained imposing that corresponding forces expend the same power in corresponding virtual velocities. With this procedure constitutive equations of homogenized models of periodic systems can be evaluated from refined models. The latter possibility is central in this work.

2.3 Piezoelectric Materials

In a piezoelectric material mechanical phenomena are coupled with electrical ones by means of constitutive relations. Here we will recall the constitutive equations of Linear Piezoelectricity.

2.3.1 Linear Constitutive Relations

The state of a piezoelectric material is no longer determined only by the mechanical state variable. Electromechanical interactions are not negligible and it is necessary to introduce new fields to describe the electric state. We will consider the quasi-electrostatic case in which coupling between electrostatic and magnetic fields can be ignored and only the electrostatic state is included in the model. Different choices of the electrical state variable are possible (electric displacement vector $\mathbf{D}$, electric field vector $\mathbf{E}$, electric potential ϕ, ...).

The coupling between the electrical and mechanics fields is realized by means of the constitutive relations. The constitutive laws can be derived from a postulated expression of the Gibbs free energy and their explicit formulation depends upon the chosen mechanical and electrical state variables (see [7]). In the following we express the vectorial and tensorial quantities in a fixed orthonormal reference $\mathcal{C} = \{\mathbf{0}, e\}$ with the indicial notation (repeated indices are intended to be summed).

Claim 3 *The Gibbs free energy for a piezoelastic body is the scalar function*

$$G = -T_{ij}S_{ij} - D_h E_h$$

where the electric field vector E_h and the mechanical strain tensor S_{ij} are intensive state variables and the electric displacement vector and the mechanical stress tensor are extensive state variables.

Depending upon which state variables are chosen as independent the following four equivalent expressions of the constitutive relations can be derived[5]:

- $(\mathbf{S}, \mathbf{D})$-type (extensive type)

$$\begin{aligned} T_{ij} &= c^D_{ijkl}S_{kl} - h_{ijn}D_n \\ E_m &= -h_{mij}S_{ij} + \beta^S_{mn}D_n \end{aligned} \tag{2.59}$$

[5] One can easily derived by the the other by simply rearranging the system

where

$$\begin{aligned} c^D_{ijkl} &= \left[\frac{\partial G}{\partial S_{ij}\partial S_{kl}}\right]_D \quad h_{ijn} = \left[\frac{\partial G}{\partial S_{kl}\partial D_n}\right] \\ \beta^S_{mn} &= \left[\frac{\partial G}{\partial D_m \partial D_n}\right]_S \end{aligned} \tag{2.60}$$

- $(\mathbf{T}, \mathbf{E})$-type (intensive type)

$$\begin{aligned} S_{ij} &= s^E_{ijkl} T_{kl} + d_{ijn} E_n \\ D_m &= d_{mij} T_{ij} + \epsilon^T_{mn} E_n \end{aligned} \tag{2.61}$$

where

$$\begin{aligned} s^E_{ijkl} &= \left[\frac{\partial G}{\partial T_{ij}\partial T_{kl}}\right]_E \quad d_{ijn} = \left[\frac{\partial G}{\partial T_{kl}\partial E_n}\right] \\ \epsilon^S_{mn} &= \left[\frac{\partial G}{\partial E_m \partial E_n}\right]_S \end{aligned} \tag{2.62}$$

- $(\mathbf{T}, \mathbf{D})$-type (mixed type)

$$\begin{aligned} S_{ij} &= s^D_{ijkl} T_{kl} + g_{ijm} D_m \\ E_m &= -g_{ijm} T_{ij} + \beta^T_{mn} D_n \end{aligned} \tag{2.63}$$

where

$$\begin{aligned} s^D_{ijkl} &= \left[\frac{\partial G}{\partial T_{ij}\partial T_{kl}}\right]_D \quad g_{ijn} = \left[\frac{\partial G}{\partial T_{kl}\partial D_n}\right] \\ \beta^T_{mn} &= \left[\frac{\partial G}{\partial D_m \partial D_n}\right]_S \end{aligned} \tag{2.64}$$

- $(\mathbf{S}, \mathbf{E})$-type (mixed type)

$$\begin{aligned} T_{ij} &= c^E_{ijkl} S_{kl} - e_{ijm} E_m \\ D_m &= e_{ijm} S_{ij} + \epsilon^S_{mn} E_n \end{aligned} \tag{2.65}$$

where

$$\begin{aligned} c^E_{ijkl} &= \left[\frac{\partial G}{\partial S_{ij}\partial S_{kl}}\right]_E \quad e_{ijn} = \left[\frac{\partial G}{\partial S_{kl}\partial E_n}\right] \\ \epsilon^S_{mn} &= \left[\frac{\partial G}{\partial E_m \partial E_n}\right]_S \end{aligned} \tag{2.66}$$

Remark 5 *The state variables* $\mathbf{S}, \mathbf{T}, \mathbf{D}, \mathbf{E}$ *can be replaced by other physical quantities. In these the constitutive relations can be rewritten considering the expressions of the new variable in term of the old ones.*

Example 6 *If the time primitive ϕ of the electric potential is chosen as state variable, the constitutive equations should be expressed in term of the pair of electric variables $(\phi, \mathbf{J})$. Since*

$$E_m = \frac{\partial \dot{\phi}}{\partial x_m}, J_m = \dot{D}_m \tag{2.67}$$

the $(\mathbf{S}, \mathbf{E})$-type relations becomes

$$\begin{aligned} T_{ij} &= c^E_{ijkl} S_{kl} - e_{ijm} \frac{\partial}{\partial x_m} \dot{\phi} \\ J_m &= e_{ijm} \dot{S}_{ij} + \epsilon^S_{mn} \frac{\partial}{\partial x_n} \ddot{\phi} \end{aligned} \tag{2.68}$$

2.3.2 Voigt Notation

Piezoelectric materials present a particular symmetry: they are transversely isotropic with respect to an axis, called the polarization axis $\mathbf{P}$. If a reference system is oriented according to that symmetry, the parameters required to define the coordinate representation of the constitutive relations are drastically reduced[6]. Moreover adopting a particular notation, valid only in the fixed reference, the material characteristics can be given in a matrix form.

Let us orient a reference $C = \{\mathbf{O}, e\}$ such that the $\mathbf{e}_3 - axis$ will be parallel to the polarization direction $\mathbf{P}$ and let us denote with $1, 2, 3$ the directions associated to $\mathbf{e}_1, \mathbf{e}_2, \mathbf{e}_3$. If the following correspondence between each pair of indices ij of the tensorial notation and a index r of the so defined Voigt-Kelvin notation is introduced

$$\begin{array}{ccc} 11 \to 1 & 22 \to 2 & 33 \to 3 \\ 23 = 32 \to 4 & 13 = 31 \to 5 & 12 = 21 \to 6 \end{array} \tag{2.69}$$

the constitutive equations assume a simpler form and a matrix representation of them will be possible.

Remark 6 *The experimental data for the constitutive behavior of the piezoelectric material are given in the Voigt notation and in particular in the intrinsic $(\mathbf{S}, \mathbf{D})$-type or alternatively in the mixed $(\mathbf{S}, E)$-type.*

Example 7 *The constitutive equations of the $(\mathbf{S}, E) - type$ for a linear piezoelastic material, ex-*

[6] Because of the transverse isotropy the piezoelectric constitutive equation must be invariant under the group of rotations around the polarization axis.

pressed in the tensorial notation by (2.65), in the Voigt notation becomes

$$\begin{aligned} S &= s^E T + dE \\ D &= dT + \epsilon^T E \end{aligned} \tag{2.70}$$

where now S, T *are* $6x1$ *matrices,* E, D $3x1$ *matrices and* s^E, d, ϵ^T *are* $6x6, 6x3, 3x3$ *matrices expressed by*

$$S^E = \begin{bmatrix} s_{11}^E & s_{12}^E & s_{13}^E & 0 & 0 & 0 \\ s_{21}^E & s_{22}^E & s_{23}^E & 0 & 0 & 0 \\ s_{31}^E & s_{32}^E & s_{33}^E & 0 & 0 & 0 \\ 0 & 0 & 0 & s_{44}^E & 0 & 0 \\ 0 & 0 & 0 & 0 & s_{44}^E & 0 \\ 0 & 0 & 0 & 0 & 0 & 2(s_{11}^E - s_{12}^E) \end{bmatrix}$$

$$d = \begin{bmatrix} 0 & 0 & d_{31} \\ 0 & 0 & d_{31} \\ 0 & 0 & d_{33} \\ 0 & d_{15} & 0 \\ d_{15} & 0 & 0 \\ 0 & 0 & 0 \end{bmatrix}, \epsilon^T = \begin{bmatrix} \epsilon_{11}^T & 0 & 0 \\ 0 & \epsilon_{22}^T & 0 \\ 0 & 0 & \epsilon_{33}^T \end{bmatrix}$$

The zeros entries in the matrices are due only to the symmetries.

2.3.3 Uniaxial States

Frequently particular physical situations allow to neglect the influence of some secondary phenomena on the main aspects that one wants to model, consequently the number of variables needed to describe the state of the system can be reduced. Here we will give the definition of some of those situations and we will derive the corresponding constitutive equations, in order to use them in the following sections.

Definition 11 *A tensional state is called uniaxial along the* $i-axis$ *if all the stress components vanish except the one along the* $i-axis$*. Using the Voigt notation, a uniaxial tensional state in the* $1-direction$ *is characterized by*

$$T_2 = T_3 = T_4 = T_5 = T_6 = 0$$

Definition 12 *The electrostatic state is called uniaxial along the $i-axis$ if all field components not parallel to the $i-direction$ are zero. Using the Voigt notation, a uniaxial electrostatic state in the $3-direction$ is characterized by*

$$E_1 = E_2 = 0, D_1 = D_2 = 0$$

In the following we will focus our attention on the piezoelectric material with a uniaxial tensional state along the $1-direction$ and a uniaxial electrostatic state along the $3-direction$. We characterize this situation as follows:

Claim 4 *In a uniaxial stress state along the $1-direction$ and a uniaxial electrostatic state along the $3-direction$, equation (2.70) in the Voigt notation becomes*

$$\begin{bmatrix} S_1 \\ D_3 \end{bmatrix} = \begin{bmatrix} s_{11}^E & d_{31} \\ d_{31} & \epsilon_{33}^T \end{bmatrix} \begin{bmatrix} T_1 \\ E_3 \end{bmatrix} \tag{2.71}$$

Claim 5 *In a uniaxial stress state along the $1-direction$ and a uniaxial electrostatic state along the $3-direction$, equation (2.63) becomes*

$$\begin{bmatrix} S_1 \\ E_3 \end{bmatrix} = \begin{bmatrix} s_{11}^D & g_{31} \\ -g_{31} & \beta_{33}^T \end{bmatrix} \begin{bmatrix} T_1 \\ D_3 \end{bmatrix} \tag{2.72}$$

In following sections we will often use the inverse of the (2.72) that is

$$\begin{bmatrix} T_1 \\ D_3 \end{bmatrix} = \begin{bmatrix} c_{11}^E & -e_{31} \\ e_{31} & \epsilon_{33}^S \end{bmatrix} \begin{bmatrix} S_1 \\ E_3 \end{bmatrix} \tag{2.73}$$

where

$$\begin{aligned} c_{11}^E &= \frac{1}{s_{11}^E} \quad \epsilon_{33}^S = \frac{-d_{31}^2 + \epsilon_{33}^T s_{11}^E}{s_{11}^E} \\ e_{31} &= \frac{d_{31}}{s_{11}^E} \end{aligned} \tag{2.74}$$

2.3.4 PZT Transducers

In this work we will refer to a piezoelectric transducer as a specimen of *polarized* PZT material whose surfaces are plated in order to generate a electric field inside the body once a potential difference is applied between them. These conductive surfaces are called the *electrodes*. Depending upon the geometrical shape, the direction of polarization, and the direction along which the electric

field is applied, there are a great variety of PZT transducers able to couple the applied electric field with the mechanical shear or normal modes.

For applications to vibration control the most common configuration is the one in figure 2-1 where the transducer is constituted by a thin sheet of PZT material polarized along its thickness. Since the thickness t_p is usually $10-20$ times smaller than the transversal dimensions this type of transducer can be treated as an essentially two dimensional object. When a voltage difference is applied between the two electrodes an electric field is induced along the $3-direction$ and by the relations (2.65) a constant mechanical pre-stress along the 1 and 2 directions is generated. If no forces are applied on the lateral surfaces the result of the applied field is a uniform contraction or elongation in the $1-2$ plane.

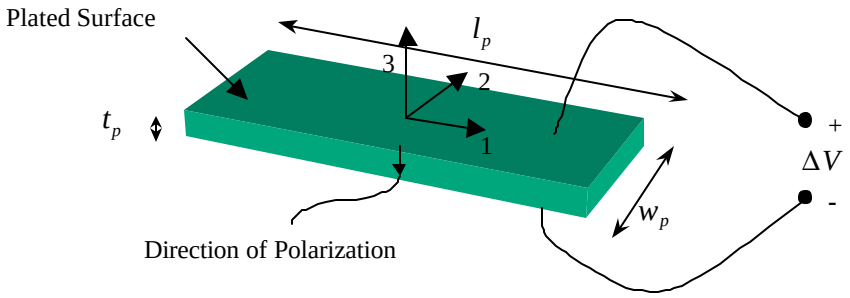

Figure 2-1: PZT sheet working by $3-1$ effect

When uniaxial stress states are considered the behavior of the PZT sheet is completely described by relations like (2.73). The manufacturers usually provide the performances of the PZT sheets giving the blocked force and the free elongation. These two quantities refer to a unidimensional model of the transducer. The blocked force is defined as the force exerted when the ends of the actuator are fixed and a given voltage is applied between the electrodes; the free elongation is the elongation experienced in the relevant direction for a given potential when no forces are applied. These characteristics can be derived also integrating equation (2.73) in order to get global constitutive relations of the type

$$\begin{bmatrix} F \\ Q \end{bmatrix} = \begin{bmatrix} k_{mm} & k_{me} \\ k_{em} & k_{ee} \end{bmatrix} \begin{bmatrix} \Delta L \\ V \end{bmatrix} \tag{2.75}$$

where ΔL is the total elongation, V, the applied voltage, F, the resultant force applied on the lateral surfaces and Q, the charge accumulated on the electrodes (see figure 2-2). Typical numerical values of the characteristics of a PZT transducer working by $3-1$ effect are given in figure 2-3.

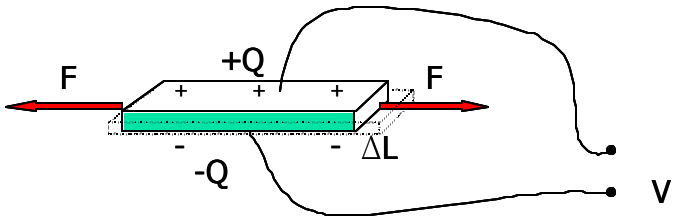

Figure 2-2: PZT sheet working by $3-1$ effect.

Transversal Dimensions	5 – 10 cm
Thickness	0.1 mm
Force	50-100 N
Displacement	1-10 μm
Voltage	10-100V
Resonance frequency	10.000Hz

Figure 2-3: Typical numerical values for the characteristics of a PZT transducer.

Chapter 3

Electrical Systems

The passive control of mechanical vibrations by means of PZT transducers is based on the piezoelectric coupling between a mechanical structure and an electric network. In this chapter the basic notions about electrical systems will be introduced focusing our attention on those aspects that will be useful in the following developments. After spending some words on electromechanical analogies, both a refined and homogenized model of a lumped electric transmission line will be developed by means of the Virtual Power Principle. In this fashion an example of the homogenization procedure that will be applied on more complex systems will be furnished.

3.1 Discrete Systems

We will consider a discrete electric system, or circuit, as a set of two-port networks, or components, with a specific interconnection.

A two-ports network is a physical device with two terminals that can be mathematically modelled as a binary relation between an intensive scalar variable through the terminals and an extensive scalar variable across the terminals. In the following the pairs of conjugate variables (ϕ, ι) and (v, χ) will be considered, where $v = \dot{\phi}$ is the electric potential difference across the network terminals and $\iota = \dot{\chi}$ is the electric current through the terminals. We will focus our attention to electric two-ports networks.

Remark 7 *ϕ, v are extensive state variables while ι, χ are intensive state variables and the products $\phi * \iota$, $v * \chi$ have the physical dimensions of a power.*

Axiom 2 *The virtual power for a two-ports network is given by*

$$\mathcal{P} = \iota * \dot{\phi}^*$$

if $\dot{\phi}^*$ is chosen as virtual velocity,

$$\mathcal{P} = v * \dot{\chi}^*$$

if $\dot{\chi}^*$ is chosen as virtual velocity.

We will consider the following basic passive linear components

Name	Resistor	Capacitor	Inductor
Diagram		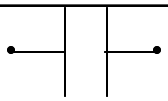	
Characteristic constant	$R\epsilon\mathcal{R}^+, (\ \ )$	$C\epsilon\mathcal{R}^+, (\mathrm{F})$	$L\epsilon\mathcal{R}^+, (\mathrm{H})$
Binary relation	$v = R\dot{\chi}$	$v = \frac{1}{C}\chi$	$v = L\ddot{\chi}$
Inverse binary relation	$\iota = \frac{1}{R}\dot{\phi}$	$\iota = C\ddot{\phi}$	$\iota = \frac{1}{L}\phi$

and the following basic active components

Name	Current generator	Voltage generator
Diagram	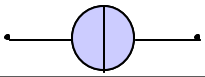	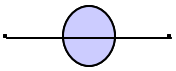
Binary relation	$\iota = I$, for each ϕ	$v = V$, for each χ

(3.1)

The definitions of the elementary interconnections between elements are

Definition 13 *Parallel connection. Two networks are connected in parallel if the same potential between their terminals is imposed.*

Definition 14 *Series connections. Two networks are e connected is series if the same current is imposed through their terminals.*

Remark 8 *The binary relation characterizing a component can be regarded as a* constitutive relation.

Remark 9 *Constitutive relations for a two-port network that is the composition of elementary components can be deduced by a power balance once a kinematic (connections between elements) is given.*

Proposition 6 *If ϕ is chosen as state variable the constitutive relation (or binary relation) for a parallel connection of an inductor L, a capacitor C and a resistor R is given by $\iota = C\ddot{\phi} + \frac{1}{L}\phi + \frac{1}{R}\dot{\phi}$.*

Proof. Denoting with the subscript the quantities relative to each component, the power

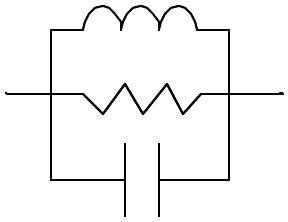

Figure 3-1: *RLC* parallel

balance can be written as

$$\iota\dot{\phi}^* = \iota_C\dot{\phi}^*_C + \iota_R\dot{\phi}^*_R + \iota_L\dot{\phi}^*_L \tag{3.2}$$

The parallel connection imposes that

$$\dot{\phi}^* = \dot{\phi}^*_R = \dot{\phi}^*_C = \dot{\phi}^*_L$$

thus (3.2) becomes

$$\iota\dot{\phi}^* = (\iota_C + \iota_R + \iota_L)\,\dot{\phi}^*$$

and for the arbitrariness of $\dot{\phi}^*$,

$$\iota = \iota_C + \iota_R + \iota_L = C\ddot{\phi} + \frac{1}{R}\dot{\phi} + \frac{1}{L}\phi$$

Proposition 7 *If χ is chosen as the state variable, the constitutive relation for a series connection of an inductor L, a capacitor C and a resistor R is given by*

$$v = L\ddot{\chi} + R\dot{\chi} + \frac{1}{C}\chi$$

Proof. The power balance is written as

$$v\dot{\chi}^* = v_L\dot{\chi}^*_L + v_R\dot{\chi}^*_R + v_C\dot{\chi}^*_C \tag{3.3}$$

The series connection imposes that

$$\dot{\chi}^* = \dot{\chi}_R^* = \dot{\chi}_C^* = \dot{\chi}_L^*$$

thus (3.3) becomes

$$v\dot{\chi}^* = (v_L + v_R + v_C)\,\dot{\chi}^*$$

and for the arbitrariness of $\dot{\chi}^*$,

$$v = v_L + v_R + v_C = L\ddot{\chi} + R\dot{\chi} + \frac{1}{C}\chi$$

3.2 Electromechanical Analogies

Electric and mechanical discrete systems with n degrees of freedom have the same mathematical model: a system of n second order ordinary differential equations. So that, once a mathematical model for a mechanical and for an electric system with the same number of degrees of freedom is given, it is possible to associate at each physical mechanical quantity the electrical one that plays the same role in the model. In this fashion electromechanical analogies for discrete systems are developed. The same procedure can be applied to continuous systems, as studied in ([23], [26]).

Example 8 *Let us consider the one degree of freedom mechanical system in figure 3-2. If we choose as the state variable the displacement u of the mass m, the following power balance must hold for each virtual velocity $\dot{u}^*$*

$$\begin{aligned} \mathcal{P}_{int} &= \mathcal{P}_{ext} + \mathcal{P}_a \\ F_{int}\dot{u}^* &= f\dot{u}\dot{u}^* + m\ddot{u}\dot{u}^* \\ (-ku - c\dot{u})\dot{u}^* &= f\dot{u}^* + m\ddot{u}\dot{u}^* \end{aligned}$$

By the arbitrariness of $\dot{u}^*$ the following equation must be satisfied

$$m\ddot{u} + c\dot{u} + ku = f \tag{3.4}$$

Example 9 *Let us consider the RLC series circuit in figure 3-3. If the electrical charge χ is chosen*

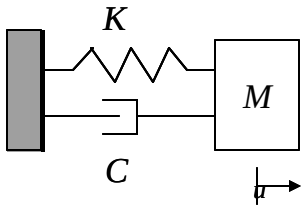

Figure 3-2: Spring-mass-damper system

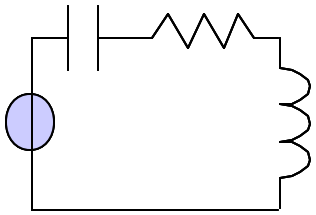

Figure 3-3: RLC series circuit

as the state variable, the following balance of power must hold for each virtual generalized velocity $\dot{\chi}^*$

$$\begin{aligned} \mathcal{P}_{int} &= \mathcal{P}_{ext} \\ v\dot{\chi}^* &= V\dot{\chi}^* \\ (R\dot{\chi} + \frac{1}{C}\chi + L\ddot{\chi})\dot{\chi}^* &= V\dot{\chi}^* \end{aligned}$$

By the arbitrariness of $\dot{\chi}^*$ *the following second order linear ordinary differential equation must be satisfied*

$$L\ddot{\chi} + R\dot{\chi} + L\ddot{\chi} = V \tag{3.5}$$

Example 10 *Let us consider the RLC parallel circuit in figure 3-4 If the time primitive of the*

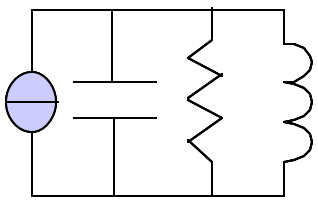

Figure 3-4: RLC parallel circuit

electrical potential ϕ is chosen as the state variable, the following balance of power must hold for each virtual generalized velocity $\dot{\phi}^*$

$$\begin{aligned} \mathcal{P}_{int} &= \mathcal{P}_{ext} \\ \iota\dot{\phi}^* &= I\dot{\phi}^* \\ (C\ddot{\phi} + \frac{1}{R}\dot{\phi} + \frac{1}{L}\phi)\dot{\phi}^* &= I\dot{\phi}^* \end{aligned}$$

By the arbitrariness of $\dot{\phi}^*$ the following second order linear ordinary differential equation must hold

$$C\ddot{\phi} + \frac{1}{R}\dot{\phi} + \frac{1}{L}\phi = V \tag{3.6}$$

Comparing the equation (3.4) with the equation (3.5) the *charge-displacement* electromechanical analogy can be deduced with the following identifications

$$\begin{aligned} u &\to \chi \quad f \to v \\ m &\to L \quad k \to C \\ c &\to R \end{aligned} \tag{3.7}$$

Comparing the equation (3.4) with the equation (3.6) the *voltage-velocity* electromechanical analogies can be deduced, with the following identifications

$$\begin{aligned} u &\to \phi \quad f \to \iota \\ m &\to C \quad k \to \tfrac{1}{L} \\ c &\to \tfrac{1}{R} \end{aligned} \tag{3.8}$$

3.3 Periodic Systems and Homogenized Models

3.3.1 Lumped Transmission Line

System Description

Let us consider a periodic one-dimensional electric lattice whose basic cell is composed by a parallel RLC element to ground G and a line element L as represented in figure 3-5.

Let be d the constant space interval between two cells, such that the $n-th$ cell is the position $x = nd$ and the $(n+1)-th$ cell is the position $x = (n+1)d$.

The resultant system is represented in figure 3-6 and it is a generalized lumped electric transmission line.

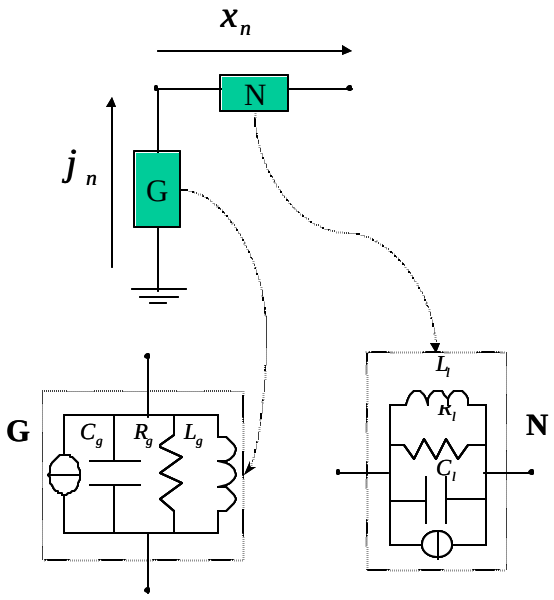

Figure 3-5: Transmission line: basic cell

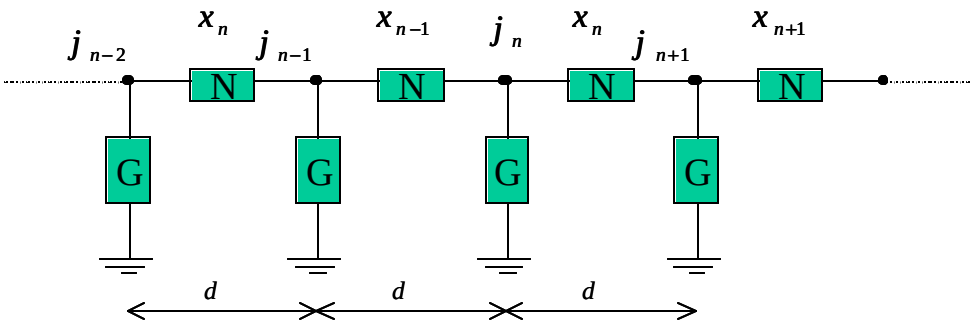

Figure 3-6: Generalized lumped trasmission line

Let us denote by ϕ_n the time primitive of the potential of the $n-th$ node, by ι_n the current to ground from the $n-th$ node, η_n the line current between the $n-th$ and the $(n+1)-th$ nodes. Since the basic cell is composed of a parallel RLC element to ground G and a parallel line RLC element N, the virtual powers spent in the virtual velocities $\dot{\phi}_n^*, \dot{\xi}_n^* = \left(\phi_{n+1}^* - \phi_n^*\right)$ are

- internal

$$\mathcal{P}_{int}^{(n)} = \iota_n \dot{\phi}_n^* + \eta_n \dot{\xi}_n^* \tag{3.9}$$

- external

$$\mathcal{P}_{ext}^{(n)} = I_n \dot{\phi}_n^* + Y_n \dot{\xi}_n^* \tag{3.10}$$

where I_n and Y_n denote the current exerted by the ground and line current generators, respectively.

The constitutive equations are

$$\begin{aligned} \iota_n &= G\phi_n \\ \eta_n &= N\xi_n \end{aligned} \tag{3.11}$$

where the linear differential operators

$$G = \left(C_g \frac{d^2}{dt^2} + \frac{1}{R_g}\frac{d}{dt} + \frac{1}{L_g} \right) \tag{3.12}$$

$$N = \left(C_l \frac{d^2}{dt^2} + \frac{1}{R_l}\frac{d}{dt} + \frac{1}{L_l} \right) \tag{3.13}$$

are defined[1].

Equations of Motion

Since in the expression of the power balance of the $n-th$ element, also the $(n+1)-th$ variable is involved, the variable ϕ_n is present only in the power expression of the $n-th$ and the $(n-1)-th$ cells. So that by the power balance

$$\sum \mathcal{P}_{int}^{(n)} = \sum \mathcal{P}_{ext}^{(n)} \tag{3.14}$$

and the arbitrariness of $\dot{\phi}_n^*$, collecting the term involving $\dot{\phi}_n^*$ in the expression

$$\begin{aligned} \mathcal{P}_{int}^{(n)} + \mathcal{P}_{int}^{(n-1)} &= \mathcal{P}_{ext}^{(n)} + \mathcal{P}_{ext}^{(n-1)} \\ \begin{pmatrix} \iota_n \dot{\phi}_n^* + \eta_n \left(\phi_{n+1}^* - \phi_n^*\right) + \\ \iota_{n-1} \dot{\phi}_{n-1}^* + \eta_{n-1} \left(\phi_n^* - \phi_{n-1}^*\right) \end{pmatrix} &= \begin{pmatrix} I_n \dot{\phi}_n^* + Y_n \left(\phi_{n+1}^* - \phi_n^*\right) + \\ I_{n-1} \dot{\phi}_{n-1}^* + Y_{n-1} \left(\phi_n^* - \phi_{n-1}^*\right) \end{pmatrix}, \end{aligned} \tag{3.15}$$

[1] The subscript "$_l$" indicates the line parameter, the subscript "$_g$" the parameters of the RLC element to ground

the following balance of currents must hold

$$\left(\iota_n - \eta_n + \eta_{n-1}\right) = \left(I_n - Y_n + Y_{n-1}\right) \tag{3.16}$$

Substituting the equations (3.11) into the previous expression we get

$$\begin{aligned} G\phi_n + N\left(-\phi_{n+1} + 2\phi_n - \phi_{n-1}\right) &= I_n - Y_n + Y_{n-1} & (3.17)\\ \left(G + 2N\right)\phi_n - N\phi_{n+1} - N\phi_{n-1} &= I_n - \left(Y_n - Y_{n-1}\right) & (3.18) \end{aligned}$$

that are the balance equations for the generic cell of the modular system. If the N, G are written explicitly they become

$$\begin{pmatrix} \left(C_g + 2C_l\right)\ddot{\phi}_n + \left(\frac{2}{L_l} + \frac{1}{L_g}\right)\phi_n + \left(\frac{2}{R_l} + \frac{1}{R_g}\right)\dot{\phi}_n \\ -C_l\left(\ddot{\phi}_{n+1} + \ddot{\phi}_{n-1}\right) - \frac{1}{L_l}\left(\phi_{n+1} + \phi_{n-1}\right) - \frac{1}{R_l}\left(\dot{\phi}_{n+1} + \dot{\phi}_{n-1}\right) \end{pmatrix} = I_n - \left(Y_n - Y_{n-1}\right) \tag{3.19}$$

If

$$\begin{aligned} R_g \to \infty \quad L_g \to \infty \\ \vec{\eta}_n \to 0 \quad C_l \to 0 \end{aligned}$$

then the equation of motion (3.19) reduces to

$$\begin{pmatrix} \left(C_g\right)\ddot{\phi}_n - \left(\frac{1}{L_l}\right)\left(\phi_{n+1} + \phi_{n-1} - 2\phi_n\right) \\ -\left(\frac{1}{R_l}\right)\left(\dot{\phi}_{n+1} + \dot{\phi}_{n-1} - 2\dot{\phi}_n\right) \end{pmatrix} = I_n - \left(Y_n - Y_{n-1}\right) \tag{3.20}$$

that is the equation of motion for the generic cell of a classic lumped electric line.

3.3.2 Homogenized Model

An homogenized model of the one-dimensional electric lattice presented in the previous section is a continuous electric transmission line. Once the virtual velocity fields for the continuous transmission line are chosen, the balance equations can be found by the power balance. On the other hand, the constitutive equations will be deduced giving a mapping between the kinematics of the homogenized and the lumped models and prescribing that the virtual powers spent in corresponding virtual velocities must be the same.

Kinematics

If we think of the transmission line as a physical continuous system, it occupies a *fixed* unidimensional region of the euclidean space. Let it be a straight line $\mathcal{T}$ and let us fix a curvilinear coordinate s on it.

If the time primitive of the electric potential[2] of a generic point of the line is chosen as the state variable, in a first order gradient theory the space of the virtual velocities is

$$\mathcal{V} = \{\dot{\phi}^*(s,t), \dot{\xi}^*(s,t)\} \tag{3.21}$$

where

$$\dot{\xi}^*(s,t) = \frac{d\dot{\phi}^*(s,t)}{ds} \tag{3.22}$$

Remark 10 *The $n-th$ elementary cell of the lattice model corresponds to the region $[nd,(n+1)d]$ of the continuous model.*

The continuous system can be identified with the lattice model only in an approximate fashion. In the lumped system the state of the $n-th$ cell at a given instant in time is determined only by two scalar quantities, ϕ_n and $\xi_n = \phi_{n+1} - \phi_n$, while in the continuous model it is given by smooth fields $\psi(s), \xi(s) = \frac{d\psi(s)}{ds}$ defined on the real interval $[nd,(n+1)d]$.

Considering the fields $\psi(s), \xi(s)$ constant in each cell the following kinematic mapping is assumed

$$\psi(s,t) = \phi_n(t) \tag{3.23}$$

$$\xi(s,t) = \frac{\xi_n(t)}{d} \tag{3.24}$$

for each $s \in [nd,(n+1)d]$.

Power Balance and Equilibrium Equations

The virtual powers for the continuous system can be written as

[2] All the potentials are referred to ground.

- internal virtual power

$$\begin{aligned}\mathcal{P}_{int}^{(H)} &= \int_{\mathcal{T}} \bar{\iota}\dot{\phi}^* + \int_{\mathcal{T}} \bar{\eta}\dot{\xi}^* \\ &= \int_{\mathcal{T}} \bar{\iota}\dot{\phi}^* + \int_{\mathcal{T}} \bar{\eta}\frac{d\dot{\phi}^*}{ds} \\ &= \int_{\mathcal{T}} \left(\bar{\iota}\dot{\phi}^* - \frac{d\bar{\eta}}{ds}\dot{\phi}^*\right) + [\bar{\eta}\dot{\phi}^*]_{\partial\mathcal{T}}\end{aligned} \tag{3.25}$$

- external virtual power

$$\begin{aligned}\mathcal{P}_{ext}^{(H)} &= \int_{\mathcal{T}} \left(\bar{I}\dot{\phi}^* + \bar{Y}\dot{\xi}^*\right) \\ &= \int_{\mathcal{T}} \left(\bar{I}\dot{\phi}^* - \frac{d\bar{Y}}{ds}\dot{\phi}^*\right) + [\bar{Y}\dot{\phi}^*]_{\partial\mathcal{T}}\end{aligned} \tag{3.26}$$

The power balance is expressed by

$$\mathcal{P}_{int}^{(H)} = \mathcal{P}_{ext}^{(H)} \tag{3.27}$$

Using (3.25) and (3.26), this can be rewritten as

$$\int_{\mathcal{T}} \left(\bar{\iota}\dot{\phi}^* - \frac{d\bar{\eta}}{ds}\dot{\phi}^*\right) + [\bar{\eta}\dot{\phi}^*]_{\partial\mathcal{T}} = \int_{\mathcal{T}} \left(\bar{I}\dot{\phi}^* - \frac{d\bar{Y}}{ds}\dot{\phi}^*\right) + [\bar{Y}\dot{\phi}^*]_{\partial\mathcal{T}} \tag{3.28}$$

Since this must hold for each regular $\dot{\phi}^*$ the following balance equation

$$\bar{\iota} + \frac{d\bar{\eta}}{ds} = \bar{I} + \frac{d\bar{Y}}{ds} \tag{3.29}$$

and constraints on the boundary conditions

$$[\bar{\eta}\dot{\phi}^*]_{\partial\mathcal{T}} = [\bar{Y}\dot{\phi}^*]_{\partial\mathcal{T}} \tag{3.30}$$

are derived

Constitutive Equations

The constitutive equations for the homogenized model of the lumped transmission line considered in the previous section will be derived considering the kinematic mapping (3.23) and imposing that in the elementary cell corresponding virtual velocities expend the same virtual power on corresponding generalized forces. In the elementary cell the virtual power of each virtual velocity

for the two models is

- homogenized model

Virtual velocity	$\mathcal{P}_{int}$	$\mathcal{P}_{ext}$
$\dot{\phi}^*$	$\int_{nd}^{(n+1)d} \bar{\iota}\dot{\phi}^* ds$	$\int_{nd}^{(n+1)d} \bar{I}\dot{\phi}^* ds$
$\dot{\xi}^*$	$\int_{nd}^{(n+1)d} \bar{\eta}\dot{\xi}^* ds$	$\int_{nd}^{(n+1)d} \bar{Y}\dot{\xi}^* ds$

- lumped model

Virtual velocity	$\mathcal{P}_{int}$	$\mathcal{P}_{ext}$
$\dot{\phi}_n^*$	$\iota_n\dot{\phi}_n^*$	$I_n\dot{\phi}_n^*$
$\dot{\xi}_n^*$	$\eta_n\dot{\xi}_n^*$	$Y_n\dot{\xi}_n^*$

For the prescribed equality of powers the following must hold

$$\begin{array}{ll} \int_{nd}^{(n+1)d} \bar{\iota}\dot{\phi}^* ds = \iota_n\dot{\phi}_n^* & \int_{nd}^{(n+1)d} \bar{I}\dot{\phi}^* ds = I_n\dot{\phi}_n^* \\ \int_{nd}^{(n+1)d} \bar{\eta}\dot{\xi}^* ds = \eta_n\dot{\xi}_n^* & \int_{nd}^{(n+1)d} \bar{Y}\dot{\xi}^* ds = Y_n\dot{\xi}_n^* \end{array} \tag{3.31}$$

Considering the kinematical map (3.23) and the constitutive equations (3.11) for the lumped model, $\dot{\phi}_n^*, \dot{\xi}_n^*$ can be replaced by the constants $\dot{\phi}^*, d\dot{\xi}^*$ and the previous relations imply that

$$\begin{array}{ll} \int_{nd}^{(n+1)d} \bar{\iota} ds = \iota_n & \int_{nd}^{(n+1)d} \bar{I} ds = I_n \\ \int_{nd}^{(n+1)d} \bar{\eta} ds = \eta_n d & \int_{nd}^{(n+1)d} \bar{Y} ds = Y_n d \end{array} \tag{3.32}$$

By the refined constitutive relations

$$\iota_n = G\phi = G\phi \tag{3.33}$$

$$\eta_n = N\xi = Nd\xi \tag{3.34}$$

hence, the mean values of the generalized forces $\bar{\iota}, \bar{\eta}, \bar{I}, \bar{Y}$ are given by

$$\begin{array}{ll} \bar{\iota} = \left(\frac{G}{d}\right)\phi & \bar{I} = \frac{I_n}{d} \\ \bar{\eta} = (Nd)\,\xi & \bar{Y} = Y_n d \end{array} \tag{3.35}$$

that are regarded as the constitutive relations for the continuous transmission line, homogenized model of the electrical lattice described in the previous section. Introducing the new operators

$$\bar{G} = \frac{G}{d} \tag{3.36}$$

$$= \left(\frac{C_g}{d}\frac{d^2}{dt^2} + \frac{1}{dR_g}\frac{d}{dt} + \frac{1}{dL_g}\right) \tag{3.37}$$

$$= \left(\bar{C}_g\frac{d^2}{dt^2} + \frac{1}{\bar{R}_g}\frac{d}{dt} + \frac{1}{\bar{L}_g\dot{\zeta}_g}\right) \tag{3.38}$$

and

$$\bar{N} = dN \tag{3.39}$$

$$= \left(dC_l\frac{d^2}{dt^2} + \frac{d}{R_l}\frac{d}{dt} + \frac{d}{L_l}\right) \tag{3.40}$$

$$= \left(\bar{C}_l\frac{d^2}{dt^2} + \frac{1}{\bar{R}_l}\frac{d}{dt} + \frac{1}{\bar{L}_l}\right) \tag{3.41}$$

the definitions of the distributed inductances, resistances and capacitances

$$\begin{array}{lll} \bar{C}_g = \frac{C_g}{d} & \bar{R}_g = dR_g & \bar{L}_g = dL_g \\ \bar{C}_l = dC_l & \bar{R}_l = \frac{R_l}{d} & \bar{L}_l = \frac{L_l}{d} \end{array} \tag{3.42}$$

is induced. Moreover let us define

$$\bar{I} = \frac{L_n}{d} \quad \bar{Y} = Y_n d \tag{3.43}$$

Equations of Motion

Substituting the constitutive equations (3.35) in the expression of the power balance (3.27) we get

$$\int_{\mathcal{T}} \left(\bar{G}\phi\dot{\phi}^* + \bar{N}\xi\dot{\xi}^*\right) = \int_{\mathcal{T}} \left(\bar{I}\dot{\phi}^* + \bar{Y}\dot{\xi}^*\right) \tag{3.44}$$

Considering that

$$\dot{\xi}^* = \frac{d\dot{\phi}^*}{ds} \tag{3.45}$$

and integrating by parts it becomes

$$\int_{\mathcal{T}} \left(\bar{G}\phi - \bar{N}\frac{d^2\phi}{ds^2}\right)\dot{\phi}^* = \int_{\mathcal{T}} \left(\bar{I} - \frac{d\bar{Y}}{ds}\right)\dot{\phi}^* \tag{3.46}$$

thus for the arbitrariness of $\dot{\phi}^*$

$$\bar{G}\phi - \bar{N}\frac{d^2\phi}{ds^2} = \bar{I} - \frac{d\bar{Y}}{ds} \tag{3.47}$$

The previous equations of motion for the continuous generalized transmission line can be rewritten in a explicit form substituting the expression of the operator $\bar{G}, \bar{N}$

$$\left(\bar{C}_g\frac{d^2\phi}{dt^2} + \frac{1}{\bar{R}_g}\frac{d\phi}{dt} + \frac{1}{\bar{L}_g}\phi\right) - \left(\bar{C}_l\frac{d^4\phi}{dt^2ds^2} + \frac{1}{\bar{R}_l}\frac{d^3\phi}{dtds^2} + \frac{1}{\bar{L}_l}\frac{d^2\phi}{ds^2}\right) = \bar{I} - \frac{d\bar{Y}}{ds} \tag{3.48}$$

Dimensionless Form The equations of motion can be rewritten in a dimensionless form introducing the dimensionless variables

$$\begin{array}{lll} \phi = \phi_0\psi & t = t_0\tau & s = x_0 x \\ \bar{I} = \bar{I}_0\bar{I}^a & \bar{Y} = \bar{Y}_0\bar{Y}^a & \end{array} \tag{3.49}$$

Defining the following dimensionless parameters

$$\begin{array}{lll} \beta_l = \frac{t_0}{x_0}\frac{1}{\sqrt{\bar{C}_g\bar{L}_l}} & \delta_l = \frac{1}{2\bar{R}_l x_0}\sqrt{\frac{\bar{L}_l}{\bar{C}_g}} & \kappa = \frac{\bar{C}_l}{x_0^2\bar{C}_g} \\ \beta_g = t_0\frac{1}{\sqrt{\bar{L}_g\bar{C}_g}} & \delta_g = \frac{1}{2\bar{R}_g}\sqrt{\frac{\bar{L}_a}{\bar{C}_g}} & \\ \chi_3 = \frac{t_0^2\bar{I}_0}{\bar{C}_g\phi_0} & \chi_4 = \frac{t_0^2\bar{Y}_0}{\bar{C}_g\phi_0 x_0} & \end{array} \tag{3.50}$$

the following equation is obtained

$$\psi + 2\delta_g\beta_g\dot{\psi} + \beta_g^2\psi - \kappa\ddot{\psi}'' + 2\delta_l\beta_l\dot{\psi}'' + \beta_l^2\psi'' = \chi_3\left(\bar{I}^a\right) - \chi_4\left(\bar{Y}^a\right)' \tag{3.51}$$

Example 11 *If*

$$\begin{array}{ll} \bar{R}_g \to \infty & \bar{L}_g \to \infty \\ \bar{R}_l \to \infty & \bar{C}_l \to 0 \end{array}$$

then

$$\begin{array}{ll} 2\delta_g\beta_g \to 0 & \beta_g^2 \to 0 \\ 2\delta_l\beta_l \to 0 & \kappa \to 0 \end{array}$$

and the (3.48) reduces to

$$\frac{d^2\phi}{dt^2} - \beta_l^2 \frac{d^2\phi}{ds^2} = \chi_3 \left(\bar{I}^a\right) - \chi_4 \left(\bar{Y}^a\right)' \tag{3.52}$$

that is known as telegraphist equation.

Example 12 *If*

$$\begin{aligned} \bar{L}_l, \bar{R}_l &\rightarrow \infty \\ \bar{C}_l &\rightarrow 0 \end{aligned}$$

then

$$\begin{aligned} &\beta_l^2 \rightarrow 0 \\ &2\delta_l\beta_l \rightarrow 0 \quad \kappa \rightarrow 0 \end{aligned}$$

and (3.48) reduces to

$$\left(\frac{d^2\phi}{dt^2} + 2\delta_g\beta_g\frac{d\phi}{dt} + \beta_g^2\phi\right) = \chi_3\bar{I}^a \tag{3.53}$$

that is an ordinary *linear second order differential equation in time. Since ϕ is a field defined on the real axis, the solution $\phi(s,t)$, recalling the dynamical system terminology, can be identified with the* flow *associated to the equation*

$$\left(\frac{d^2y}{dt^2} + 2\delta_g\beta_g\frac{dy}{dt} + \beta_g^2 y\right) = \chi_3\bar{I}^a$$

where y depends on t only. That is

$$\phi(s_0, t) = \phi(t; t_0, s_0)$$

where $\phi(t; t_0, s_0)$ is the unique *solution of the initial value problem*

$$\begin{aligned} \left(\frac{d^2y}{dt^2} + 2\delta_g\beta_g\frac{dy}{dt} + \beta_g^2 y\right) &= \chi_3\bar{I}^a \\ y(t_0) &= s_0 \end{aligned}$$

So that in this case the solution at a given point s depends only on the initial state at the point s, no matter what is the state of all other points of the continuum.

Chapter 4

Layered Composite PEM Beam

Our goal is to use piezoelectric materials to couple the vibrations of a mechanical structure with the dynamics of an electric network. In this chapter we will focus our attention on modelling the electromechanical interaction between a beam and a PZT transducer[1]. A convenient configuration of PZT sheets is the one presented in figure 4-1, known in literature as a *bimorph configuration*.

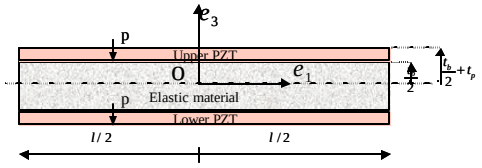

Figure 4-1: Laminated PiezoElectroMechanical (PEM) beam: lateral view

In this symmetric arrangement two thin PZT layers polarized over the thickness are bonded on a rectangular cross section elastic beam. The upper and lower surfaces of each layer are plated and play the role of electrodes. By the mechanical and material symmetries the flexural and extensional modes of the sandwiched beam are mechanically uncoupled. Depending upon the connections between the electrodes it is possible to have different types of electromechanical coupling:

[1] Here and in the following we will refer to a PZT transducer as a sheet of electroded PZT material as that presented in figure 2-1.

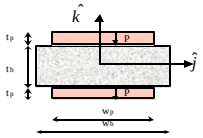

Figure 4-2: Laminated PiezoElectroMechanical (PEM) beam: cross section

- *extensional-electric* for the *in-phase* electric connection of the PZT sheets as in figure 4-3

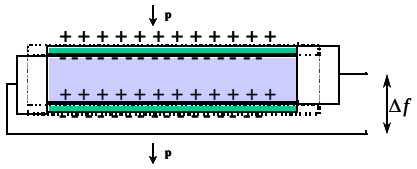

Figure 4-3: In-phase parallel connection of PZT layers for extensional coupling

- *flexural-electric* for the *out-of-phase* electric connection as in figure 4-4

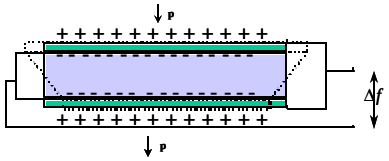

Figure 4-4: Out-of-phase parallel connection of PZT layers for flexural coupling

In the first section of this chapter we will derive an unidimensional model of the axially homogeneous beam in figure 4-1 treating it as a 3D piezoelastic continuum with an imposed kinematic. In order to follow an unified approach we will consider the general case without shortcuts between the electrodes. In this framework the configurations in figure 4-3, 4-4 will be understood as particular situations.

In the second section the power balance, the equations of motion and the constitutive relations for a simple elastic beam will be derived as a particular case. By dimensional analysis, the rotational inertia will be shown to be negligible for the numerical values relevant for applications and for the designed experimental setup.

Finally the possibility of deriving a weak formulation of the equations of motion for an axially non-homogeneous PiezoElectroMechanical (PEM) beam offered by the additivity of the virtual powers will be exploited considering an elastic beam with a pair of PZT transducers not covering all its axial length.

All the modelling procedure will be carried on keeping in mind the physical case of the piezoelectromechanical beam that has been realized experimentally as described in Chapter 7.

4.1 Continuous Layered Composite PEM Beam

An axially homogeneous three layered beam with a material and geometrical symmetry with respect to the beam central axis[2], such as that in figure 4-1, will be considered. Assuming the kinematics, the constitutive equations and the power balance of the system as a 3D piezoelastic continuum and a kinematical mapping between the 3D and the 1D representations, the power balance and the constitutive relations for the 1D model will be derived defining sectional stiffness, capacitance and coupling coefficients.

By the power balance a weak formulation of the balance equations will be directly deduced. A strong form of them will be obtained with the boundary conditions after integrations by parts. In this framework it will be shown[3] that for an axially homogeneous beam:

- the piezoelectric effect on the mechanical system reduces to a pair of equal and opposite forces applied on the ends of the PZT layers, with a module proportional to the applied voltage;
- the PZT transducer is electrically equivalent to a capacitance in parallel with a current generator with an imposed current proportional to the time derivative of the change in length of the PZT sheet.

The cases in which the upper and lower PZT layers are connected one to each other to couple the applied potential difference with the beam bending mode (out of phase connection, figure 4-4) and with the beam extensional mode (in phase connection, figure 4-3) will be treated separately, getting the respective coupling coefficients.

4.1.1 System Description

A composite 3-layer laminated piezoelectric beam with a geometrical and material symmetry with respect to a straight axis $\mathcal{A}$ (beam axis) will be modelled. The central layer is assumed to be an isotropic, linear elastic material with continuous boundaries. The upper and lower layers are assumed to be linear homogeneous piezoelastic materials, with the polarization axis oriented as in figures 4-1,4-2. Moreover the upper and lower surfaces of the piezoelectric layers are supposed to be plated and eventually subjected to a potential difference, while the lateral surfaces are bared[4].

[2] These symmetries are required to avoid a mechanical coupling between the beam extensional and flexural modes.

[3] The following results are frequently assumed in literature. The correspondence of the interaction between the structure and the PZT sheet is known as *Pin Forces Model*.

[4] This configuration is one of the PZT transducers that have been described in Chapter 1 and that have been utilized for the experimental realizations of the PEM beam (see Chapter 7).

The thickness of the central layer, t_b, is assumed much greater than that of the piezoelectric ones, t_p.

A description of the geometric configuration of the body is given specifying the regions of the euclidean space occupied in the reference configuration[5]. Define

- $\mathcal{B}_b = \mathcal{A} \times \mathcal{S}_b$ the elastic central layer, where $\mathcal{A}$ is the beam central axis and $\mathcal{S}_b$ is the part of the cross section occupied by the elastic material;
- $\mathcal{P}_u = \mathcal{A} \times \mathcal{S}_{pu}$ the upper PZT layer, where $\mathcal{A}$ is the beam central axis and $\mathcal{S}_{pu}$ is the part of the cross section occupied by the upper piezoelectric layer;
- $\mathcal{P}_l = \mathcal{A} \times \mathcal{S}_{pl}$ the lower PZT transducer, where $\mathcal{A}$ is the beam central axis and $\mathcal{S}_{pu}$ is the part of the cross section occupied by the lower piezoelectric layer;
- $\mathcal{B}_p = \mathcal{A} \times \mathcal{S}_p = \mathcal{P}_u \cup \mathcal{P}_l$ the total region occupied by PZT material, where

$$\mathcal{S}_p = \mathcal{S}_{pu} \cup \mathcal{S}_{pl} \tag{4.1}$$

- $\mathcal{B} = \mathcal{B}_b \cup \mathcal{B}_p$ the whole body.

Remark 11 *In the particular case of a beam with uniform and rectangular cross sections as represented in figures (4-1), (4-2), the regions cited above are*

$$\begin{aligned} \mathcal{A} &= [-\frac{l}{2}, \frac{l}{2}] \\ \mathcal{S}_{pu} &= [-w_p, w_p] \times [\frac{t_b}{2}, \frac{t_b}{2} + t_p] \\ \mathcal{S}_{pl} &= [-w_p, w_p] \times [-\frac{t_b}{2}, -\frac{t_b}{2} - t_p] \\ \mathcal{S}_b &= [-w_b, w_b] \times [-\frac{t_b}{2}, \frac{t_b}{2}] \end{aligned}$$

4.1.2 Kinematics

Hypotheses

In the application we will deal with[6] the following facts are verified:

[5] Considering a carthesian reference frame $\mathcal{C} = \{\mathbf{0}, \mathbf{e}_1, \mathbf{e}_2, \mathbf{e}_3\}$ the region of space

$$\mathcal{G} = \{\mathbf{p} = p_1\mathbf{e}_1 + p_2\mathbf{e}_2 + p_3\mathbf{e}_3 \in \mathcal{E} : p_1 \in [a_1, b_1], p_2 \in [a_2, b_2], p_3 \in [a_3, b_3]\}$$

will be denoted by

$$\mathcal{G} = [a_1, b_1] \times [a_2, b_2] \times [a_3, b_3]$$

[6] We refer to the physical situation of the experimental set up that has been realized (see Chapter 7).

- the thickness of the PZT layer is 10-20 times smaller than that of the elastic beam
- The thickness of the PZT transducers is negligible with respect to its transversal dimensions
- the upper and lower surfaces of each transducer are plated, thus equipotential, while the lateral surfaces are bare
- the piezoelectric material is polarized along its thickness

Hence, we will get the reduced kinematics of the beam in figure 4-1 under the following hypotheses:

1. the beam sections remain rigid;
2. small deformations and linearized kinematics;
3. no shear deformation;
4. perfect bonding between elastic and PZT layers;
5. constant electric field in the transducers;
6. uniform displacements along the thickness of the transducers equal to that of the surface in contact with the beam. This hypothesis is required for coherence once (5.) is assumed.

Remark 12 *These hypotheses are satisfied in physical situations if the beam thickness t_b, the beam length l_b, the transducer thickness t_p and the bonding layer thickness t_{bond} are such that*

$$t_{bond} \ll t_p \ll t_b \ll l_b \tag{4.2}$$

Kinematics of Composite Laminated Beam

Let us choose as state variables of the 3D model the mechanical displacement field $\mathbf{u}(\mathbf{p},t)$ and the electric potential $\phi(\mathbf{p})$. Since no electromechanical coupling is present in the elastic layer, the electric potential can be defined on the regions occupied by the piezoelectric layers whose upper and lower surfaces are plated and thus equipotential. We will denote by ϕ_{uu},ϕ_{ul} the electric potential of the upper and lower surfaces of the upper PZT layer, by ϕ_{lu}, ϕ_{ll} the ones of the lower PZT layer. In general $\phi_{uu} \neq \phi_{ul} \neq \phi_{lu} \neq \phi_{ll}$, but particular connections are often used to achieve specific goals. We will consider the following

1. *In-phase parallel connection* (see figure 4-3) for which

$$\phi_{uu} = \phi_{lu} = \phi_1 \tag{4.3}$$

$$\phi_{ul} = \phi_{ll} = \phi_2 \tag{4.4}$$

2. *Out–of-phase parallel connection* (see figure 4-4) for which

$$\phi_{uu} = \phi_{ll} = \phi_1 \tag{4.5}$$

$$\phi_{ul} = \phi_{lu} = \phi_2 \tag{4.6}$$

By the hypotheses 4,6 we can write (see also figure 4-5)

$$\mathbf{u}^u(p_1,t) = \mathbf{u}(p_1,0,\frac{t_b}{2},t), p_1 \in [a, a+l_a] \tag{4.7}$$

$$\mathbf{u}^l(p_1,t) = \mathbf{u}(p_1,0,-\frac{t_b}{2},t), p_1 \in [a, a+l_a] \tag{4.8}$$

where by $\mathbf{u}^u(p_1,t), \mathbf{u}^l(p_1,t), \mathbf{u}(p_1,p_2,p_3,t)$ are denoted the displacement fields of the upper layer, the lower layer and of the central layer respectively.

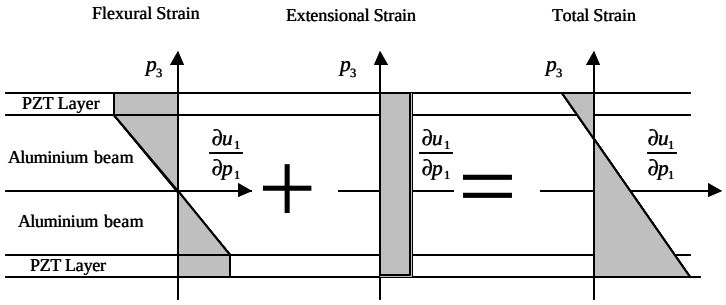

Figure 4-5: Assumed mechanical strain $\frac{\partial u_1}{\partial p_1}$ distribution along the thickness

Hence, considering the reduced kinematics for a beam with rigid sections and no shear deformation by the hypotheses about the distribution of the electric potential (see figure 4-6) we impose the following kinematical mapping[7]

[7] All the vectorial and tensorial quantitites are denoted with the Voigt notation once a reference $\mathcal{C} = \{\mathbf{o}, \mathbf{e}_1, \mathbf{e}_2, \mathbf{e}_3\}$ with $\mathbf{e}_1$ parallel to the central axis $\mathcal{A}$ and $\mathbf{e}_3$ parallel to the direction of polarization in the piezoelectric material is fixed, as in figure (4-1). The longitudinal and transverse components of the central axis displacement vector are denoted by u_1 and u_3 respectively.

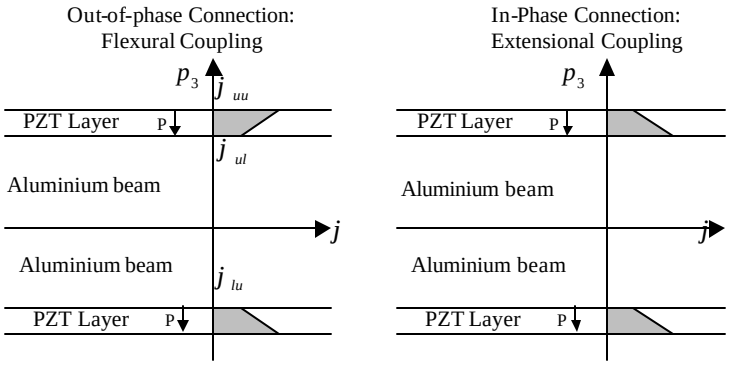

Figure 4-6: Assumed electric potential distribution along the thickness for in-phase and out-of-phase connections

- on $\mathcal{B}_b$

$$\begin{aligned} \dot{u}^*(\mathbf{p},t) &= \left[\begin{array}{ccc} \dot{u}_1^* - \frac{\partial \dot{u}_3^*}{\partial p_1} p_3 & 0 & \dot{u}_3^* \end{array} \right]^T \\ \dot{S}^*(\mathbf{p},t) &= \left[\begin{array}{cccccc} \frac{\partial \dot{u}_1^*}{\partial p_1} - \frac{\partial^2 \dot{u}_3^*}{\partial p_1^2} p_3 & 0 & 0 & 0 & 0 & 0 \end{array} \right]^T \end{aligned} \tag{4.9}$$

- on $\mathcal{B}_p$

  - on the upper layer $\mathcal{P}_u$

$$\begin{aligned} \dot{u}^*(\mathbf{p},t) &= \left[\begin{array}{ccc} \dot{u}_1^* - \frac{\partial \dot{u}_3^*}{\partial p_1} \frac{t_b}{2} & 0 & \dot{u}_3^* \end{array} \right]^T \\ \dot{S}^*(\mathbf{p},t) &= \left[\begin{array}{cccccc} \frac{\partial \dot{u}_1^*}{\partial p_1} - \frac{\partial^2 \dot{u}_3^*}{\partial p_1^2} \frac{t_b}{2} & 0 & 0 & 0 & 0 & 0 \end{array} \right]^T \\ \dot{\phi}^*(\mathbf{p},t) &= \dot{\phi}_{ul}^* + \frac{\left(\dot{\phi}_{uu}^* - \dot{\phi}_{ul}^*\right)}{t_p}(p_3 - \frac{t_b}{2}) \\ \nabla\dot{\phi}^*(\mathbf{p},t) &= \left[\begin{array}{ccc} 0 & 0 & \frac{\left(\dot{\phi}_{uu} - \dot{\phi}_{ul}\right)}{t_p} \end{array} \right]^T \end{aligned} \tag{4.10}$$

  - on the lower layer $\mathcal{P}_l$

$$\begin{aligned} \dot{u}^*(\mathbf{p},t) &= \left[\begin{array}{ccc} \dot{u}_1^* + \frac{\partial \dot{u}_3^*}{\partial p_1} \frac{t_b}{2} & 0 & \dot{u}_3^* \end{array} \right]^T \\ \dot{S}^*(\mathbf{p},t) &= \left[\begin{array}{cccccc} \frac{\partial \dot{u}_1^*}{\partial p_1} + \frac{\partial^2 \dot{u}_3^*}{\partial p_1^2} \frac{t_b}{2} & 0 & 0 & 0 & 0 & 0 \end{array} \right]^T \\ \dot{\phi}^*(\mathbf{p},t) &= \dot{\phi}_{lu}^* + \frac{\left(\dot{\phi}_{lu}^* - \dot{\phi}_{ll}^*\right)}{t_p}(p_3 + \frac{t_b}{2}) \\ \nabla\dot{\phi}^*(\mathbf{p},t) &= \left[\begin{array}{ccc} 0 & 0 & \frac{\left(\dot{\phi}_{lu}^* - \dot{\phi}_{ll}^*\right)}{t_p} \end{array} \right]^T \end{aligned} \tag{4.11}$$

4.1.3 Constitutive Relations

The body $\mathcal{B}$ is a composite material where the part $\mathcal{B}_b$ is as a linear elastic homogeneous solid, the part $\mathcal{B}_p$ a linear homogeneous piezoelastic continuum. Let us represent the constitutive laws by means of the Voigt notation once the reference in figure (4-1) is fixed. Since no forces are applied on the beam lateral surfaces an *uniaxial stress state* along the $1-direction$ is assumed both on the beam $\mathcal{B}_b$ and on the transducers $\mathcal{B}_p$. Moreover by the electric kinematic (4.10,4.11) an *uniaxial electric state* along the $3-direction$ is assumed. Thus the constitutive equations will be reduced to the form (2.73)

Linear Elastic Material

In the layer $\mathcal{B}_b$ the linear homogeneous elastic constitutive law for a uniaxial tension state is assumed in the form

$$T_1 = c_{11} S_1 \tag{4.12}$$

Example 13 *If an aluminium beam is considered the c_{11} constant is*

$$c_{11} = E_Y = 70GPa$$

Linear Piezoelastic Material

In the piezoelectric layers the linear piezoelastic constitutive equation for an uniaxial tension state and an uniaxial electric state, once the mechanical strain and the time primitive of the electric potential as state variables have been chosen, are assumed in the form

$$T_1 = c_{11}^E S_1 - e_{31} \frac{\partial \dot{\phi}}{\partial p_3} \tag{4.13}$$

$$J_3 = e_{31} \dot{S}_1 + \epsilon_{33}^S \frac{\partial \ddot{\phi}}{\partial p_3} \tag{4.14}$$

where the coefficients can be deduced by the material characteristics given in the technical data sheets by

$$\begin{array}{ll} c_{11}^E = \frac{1}{s_{11}^E} & \epsilon_{33}^S = \frac{-d_{31}^2 + \epsilon_{33}^T s_{11}^E}{s_{11}^E} \\ e_{31} = \frac{d_{31}}{s_{11}^E} & \end{array} \tag{4.15}$$

Example 14 *For the PZT material PSI-5H4E Ceramic used in the transducer of the company*

Piezo System[8] *the following material constants are given*

$$\begin{aligned} E_Y^E &= 6.2 * 10^{10} \frac{\mathrm{N}}{\mathrm{m}^2} \\ d_{31} &= -320 * 10^{-12} \frac{\mathrm{m}}{\mathrm{V}} \\ \epsilon_{33}^T &= 3800\epsilon_0 = 3.364\,6 \times 10^{-8} \frac{\mathrm{F}}{\mathrm{m}} \end{aligned}$$

and the following numerical values are found

$$c_{11}^E = E_Y^E = 6.2 * 10^{10} \tfrac{\mathrm{N}}{\mathrm{m}^2} \quad \epsilon_{33}^S = \tfrac{-d_{31}^2 + \epsilon_{33}^T s_{11}^E}{s_{11}^E} = 2.729\,7 \times 10^{-8} \tfrac{\mathrm{F}}{\mathrm{m}}$$
$$e_{31} = \tfrac{d_{31}}{s_{11}^E} = -19.84 \tfrac{\mathrm{N}}{\mathrm{m\,V}}$$

4.1.4 Power Balance

Let us consider the beam with the piezoelectric transducer as a body $\mathcal{B}$ composed by the two parts $\mathcal{B}_b$ and $\mathcal{B}_p$ as in 4.1.1, such that

$$\mathcal{B} = \mathcal{B}_b \cup \mathcal{B}_p \tag{4.16}$$

where $\mathcal{B}_b$ is an homogenous linear elastic medium and $\mathcal{B}_p$ a linear piezoelastic medium. Moreover let us denote by $\partial\mathcal{B}^u, \partial\mathcal{B}^f$ the parts of $\partial\mathcal{B} = \partial\mathcal{B}^u \cup \partial\mathcal{B}^f$ in which are imposed the displacements and the forces respectively and by $\partial\mathcal{B}^\phi, \partial\mathcal{B}^\sigma$ the parts of $\partial\mathcal{B} = \partial\mathcal{B}^\phi \cup \partial\mathcal{B}^\sigma$ on which are imposed the potential and the charge.

Recalling the expressions derived in the example (2.58) the balance of power for the system considered in figure (4-1) is expressed by

$$\begin{aligned} \mathcal{P}_{int,m} + \mathcal{P}_{int,e} &= \mathcal{P}_{d,m} + \mathcal{P}_{c,m} + \mathcal{P}_{c,e} + \mathcal{P}_{a,m} \\ \begin{pmatrix} \int_{\mathcal{B}} \mathbf{T} \cdot \dot{\mathbf{S}}^*(\mathbf{p},t) + \\ + \int_{\mathcal{B}_p} \mathbf{J} \cdot \nabla\dot{\phi}^*(\mathbf{p},t) \end{pmatrix} &= \begin{pmatrix} \int_{\mathcal{B}} \mathbf{b} \cdot \dot{\mathbf{u}}^*(\mathbf{p},t) + \int_{\partial\mathcal{B}^f} \mathbf{f} \cdot \dot{\mathbf{u}}^*(\mathbf{p},t) + \\ + \int_{\partial\mathcal{B}^\phi} \iota\dot{\boldsymbol{\phi}}^*(\mathbf{p},t) + \int_{\mathcal{B}} -\rho\ddot{\mathbf{u}}(\mathbf{p},t) \cdot \dot{\mathbf{u}}^*(\mathbf{p},t) \end{pmatrix} \end{aligned} \tag{4.17}$$

We will now rewrite each term of (4.17) taking into account the reduced kinematics derived in (4.9,4.10,4.11).

[8] *This is also the material that was utilized for the experimental set up described in Chapter 7.*

Mechanical Internal Power

The mechanical internal power $\mathcal{P}_{int,m}$ can be rewritten as

$$\begin{aligned}
\mathcal{P}_{int,m} &= \int_{\mathcal{B}} \mathbf{T}\cdot\dot{\mathbf{S}}^*(\mathbf{p},t) \\
&= \int_{\mathcal{B}_b} \mathbf{T}\cdot\dot{\mathbf{S}}^*(\mathbf{p},t) + \int_{\mathcal{P}_u} \mathbf{T}\cdot\dot{\mathbf{S}}^*(\mathbf{p},t) + \int_{\mathcal{P}_l} \mathbf{T}\cdot\dot{\mathbf{S}}^*(\mathbf{p},t) \\
&= \begin{pmatrix} \int_{\mathcal{A}} \left(\int_{\mathcal{S}_b} T_1\right) \frac{\partial \dot{u}_1{}^*}{\partial p_1} + \int_{\mathcal{A}} \left(\int_{\mathcal{S}_{pu}} T_1 + \int_{\mathcal{S}_{pl}} T_1\right) \frac{\partial \dot{u}_1{}^*}{\partial p_1} - \\ -\int_{\mathcal{A}} \left(\int_{\mathcal{S}_b} T_1 p_3\right) \frac{\partial^2 \dot{u}_3^*}{\partial p_1^2} - \int_{\mathcal{A}} \left(\int_{\mathcal{S}_{pu}} \frac{t_b}{2} T_1 - \int_{\mathcal{S}_{pl}} \frac{t_b}{2} T_1\right) \frac{\partial^2 \dot{u}_3^*}{\partial p_1^2} \end{pmatrix} \\
&= \int_{\mathcal{A}} \left(F \frac{\partial \dot{u}_1{}^*}{\partial p_1} + M \frac{\partial^2 \dot{u}_3^*}{\partial p_1^2} \right)
\end{aligned} \tag{4.18}$$

with the following definitions

$$F = F^{(b)} + F^{(p)} \quad M = M^{(b)} + M^{(p)}$$

where

$$\begin{aligned}
F^{(b)} &= \textstyle\int_{\mathcal{S}_b} T_1 & F^{(p)} &= \textstyle\int_{\mathcal{S}_{pu}} T_1 + \int_{\mathcal{S}_{pl}} T_1 \\
M^{(b)} &= -\textstyle\int_{\mathcal{S}_b} T_1 p_3 & M^{(p)} &= -\textstyle\int_{\mathcal{S}_{pu}} \frac{t_b}{2} T_1 + \int_{\mathcal{S}_{pl}} \frac{t_b}{2} T_1
\end{aligned}$$

Substituting into the previous expressions the constitutive laws

$$\begin{aligned}
T_1 &= c_{11} S_1 && on\ \mathcal{B}_b \\
T_1 &= c_{11}^E S_1 - e_{31} \frac{\partial \dot{\phi}}{\partial p_3} && on\ \mathcal{B}_p
\end{aligned} \tag{4.19}$$

we get

$$F^{(b)} = \left(\int_{\mathcal{S}_b} c_{11}\right) \frac{\partial u_1}{\partial p_1} - \left(\int_{\mathcal{S}_b} c_{11} p_3\right) \frac{\partial^2 u_3}{\partial p_1^2} \tag{4.20}$$

$$F^{(b)} = K_l^{(b)} \frac{\partial u_1}{\partial p_1} \tag{4.21}$$

and

$$F^{(p)} = \begin{pmatrix} \left(\int_{\mathcal{S}_{pu}\cup\mathcal{S}_{pl}} c_{11}^E\right) \frac{\partial u_1}{\partial p_1} - \\ -\left(\int_{\mathcal{S}_{pu}} c_{11}^E \frac{t_b}{2} - \int_{\mathcal{S}_{pl}} c_{11}^E \frac{t_b}{2}\right) \frac{\partial^2 u_3}{\partial p_1^2} - \\ -\left(\int_{\mathcal{S}_{pu}} \frac{e_{31}}{t_p}\right) \left(\dot{\phi}_{uu} - \dot{\phi}_{ul}\right) - \left(\int_{\mathcal{S}_{pL}} \frac{e_{31}}{t_p}\right) \left(\dot{\phi}_{lu} - \dot{\phi}_{ll}\right) \end{pmatrix} \tag{4.22}$$

$$F^{(p)} = K_l^{(p)} \frac{\partial u_1}{\partial p_1} - G_l \left(\dot{\phi}_{uu} - \dot{\phi}_{ul} + \dot{\phi}_{lu} - \dot{\phi}_{ll}\right) \tag{4.23}$$

where

$$\begin{array}{ll} K_l^{(b)} = \int_{\mathcal{S}_b} c_{11} & K_l^{(p)} = \int_{\mathcal{S}_{pu}} c_{11}^E + \int_{\mathcal{S}_{pl}} c_{11}^E \\ G_l = \frac{1}{t_p} \int_{\mathcal{S}_{pu}} e_{31} = \frac{1}{t_p} \int_{\mathcal{S}_{pL}} e_{31} & \end{array} \tag{4.24}$$

Moreover

$$M^{(b)} = -\left(\int_{\mathcal{S}_b} c_{11} p_3\right) \frac{\partial u_1}{\partial p_1} + \left(\int_{\mathcal{S}_b} c_{11} p_3^2\right) \frac{\partial^2 u_3}{\partial p_1^2} \tag{4.25}$$

$$M^{(b)} = K_f^{(b)} \frac{\partial^2 u_3}{\partial p_1^2} \tag{4.26}$$

and

$$M^{(p)} = \left(\begin{array}{c} -\left(\int_{\mathcal{S}_{pu}} \frac{t_b}{2} c_{11}^E - \int_{\mathcal{S}_{pl}} \frac{t_b}{2} c_{11}^E\right) \frac{\partial u_1}{\partial p_1} + \\ + \left(\int_{\mathcal{S}_{pu}} c_{11}^E \left(\frac{t_b}{2}\right)^2 + \int_{\mathcal{S}_{pl}} c_{11}^E \left(\frac{t_b}{2}\right)^2\right) \frac{\partial^2 u_3}{\partial p_1^2} + \\ + \left(\int_{\mathcal{S}_{pu}} \frac{t_b e_{31}}{2t_p}\right) \left(\dot{\phi}_{uu} - \dot{\phi}_{ul}\right) - \left(\int_{\mathcal{S}_{pu}} \frac{t_b e_{31}}{2t_p}\right) \left(\dot{\phi}_{lu} - \dot{\phi}_{ll}\right) \end{array} \right) \tag{4.27}$$

$$M^{(p)} = K_f^{(p)} \frac{\partial^2 u_3}{\partial p_1^2} + G_f \left(\dot{\phi}_{uu} - \dot{\phi}_{ul} - \dot{\phi}_{lu} + \dot{\phi}_{ll}\right) \tag{4.28}$$

where

$$K_f^{(b)} = \int_{\mathcal{S}_b} c_{11} p_3^2 \tag{4.29}$$

$$K_f^{(p)} = \left(\frac{t_b}{2}\right)^2 \int_{\mathcal{S}_{pu}} c_{11}^E + \left(\frac{t_b}{2}\right)^2 \int_{\mathcal{S}_{pl}} c_{11}^E \tag{4.30}$$

$$G_f = \frac{t_b}{2t_p} \int_{\mathcal{S}_{pu}} e_{31} = \frac{t_b}{2t_p} \int_{\mathcal{S}_{pl}} e_{31} \tag{4.31}$$

In the previous calculations we considered that, for the geometrical and material symmetries respect to the chosen reference

$$\int_{\mathcal{S}_{pu}} \frac{t_b}{2} c_{11}^E - \int_{\mathcal{S}_{pl}} \frac{t_b}{2} c_{11}^E = 0 \tag{4.32}$$

$$\int_{\mathcal{S}_b} c_{11} p_3 = 0 \tag{4.33}$$

Hence we can finally rewrite the internal mechanical power in the unidimensional model as

$$\begin{aligned}
\mathcal{P}_{int,m} &= \int_{\mathcal{A}} \left(F \frac{\partial \dot{u_1}^*}{\partial p_1} + M \frac{\partial^2 \dot{u}_3^*}{\partial p_1^2} \right) && (4.34) \\
&= \int_{\mathcal{A}} \left(K_l \frac{\partial u_1}{\partial p_1} - G_l \left(\dot{\phi}_{uu} - \dot{\phi}_{ul} + \dot{\phi}_{lu} - \dot{\phi}_{ll} \right) \right) \frac{\partial \dot{u_1}^*}{\partial p_1} + && (4.35) \\
&\quad + \int_{\mathcal{A}} K_f \frac{\partial^2 u_3}{\partial p_1^2} + G_f \left(\dot{\phi}_{uu} - \dot{\phi}_{ul} - \dot{\phi}_{lu} + \dot{\phi}_{ll} \right) \frac{\partial^2 \dot{u}_3^*}{\partial p_1^2}
\end{aligned}$$

where

$$\begin{aligned}
K_f &= K_f^{(b)} + K_f^{(p)} && (4.36) \\
K_l &= K_l^{(b)} + K_l^{(p)}
\end{aligned}$$

are the beam extensional and flexural stiffness, G_l and G_f are the homogenized extensional-electric and flexural-electric coupling coefficients homogenized over a section.

Internal Electric Power

The internal electric power $\mathcal{P}_{int,e}$ becomes

$$\begin{aligned}
\mathcal{P}_{int,e} &= \int_{\mathcal{B}_p} \mathbf{J} \cdot \nabla \dot{\phi}^*(\mathbf{p},t) && (4.37) \\
&= \int_{\mathcal{A}} \int_{\mathcal{S}_p} \left(J_3 \frac{\partial \dot{\phi}^*}{\partial p_3} \right) \\
&= \int_{\mathcal{A}} \left(\left(\int_{\mathcal{S}_{pu}} \frac{J_3}{t_p} \right) \left(\dot{\phi}_{uu} - \dot{\phi}_{ul} \right) + \left(\int_{\mathcal{S}_{pl}} \frac{J_3}{t_p} \right) \left(\dot{\phi}_{lu} - \dot{\phi}_{ll} \right) \right) \\
&= \left(I^{(u)} \left(\dot{\phi}_{uu} - \dot{\phi}_{ul} \right) + I^{(l)} \left(\dot{\phi}_{lu} - \dot{\phi}_{ll} \right) \right)
\end{aligned}$$

with the following definitions

$$\begin{aligned}
I^{(u)} &= \int_{\mathcal{A}_p} \int_{\mathcal{S}_{pu}} \frac{J_3}{t_p} && (4.38) \\
I^{(l)} &= \int_{\mathcal{A}_p} \int_{\mathcal{S}_{pl}} \frac{J_3}{t_p} && (4.39)
\end{aligned}$$

Substituting into the previous expressions the constitutive law

$$J_3 = e_{31} \dot{S}_1 + \epsilon_{33}^S \frac{\partial \ddot{\phi}}{\partial p_3}, \ on \ \mathcal{B}_p \qquad (4.40)$$

we get

$$
\begin{aligned}
I^{(u)} &= \left(\int_{\mathcal{A}}\left(\frac{1}{t_p}\int_{\mathcal{S}_{pu}} e_{31}\right)\frac{\partial \dot{u}_1}{\partial p_1}\right) - \int_{\mathcal{A}}\left(\frac{t_b}{2t_p}\left(\int_{\mathcal{S}_{pu}} e_{31}\right)\frac{\partial^2 \dot{u}_3}{\partial p_1^2}\right) + \left(\frac{1}{t_p^2}\int_{\mathcal{A}}\int_{\mathcal{S}_{pu}} \epsilon_{33}^S\right)\left(\ddot{\phi}_{uu} - \ddot{\phi}_{ul}\right) \\
I^{(u)} &= \int_{\mathcal{A}}\left(G_l\frac{\partial \dot{u}_1}{\partial p_1}\right) - \int_{\mathcal{A}}\left(G_f\frac{\partial^2 \dot{u}_3}{\partial p_1^2}\right) + \left(\ddot{\phi}_{uu} - \ddot{\phi}_{ul}\right)\int_{\mathcal{A}} H^{(u)}
\end{aligned}
$$

for the upper transducer and

$$
\begin{aligned}
I^{(l)} &= \left(\int_{\mathcal{A}}\left(\frac{1}{t_p}\int_{\mathcal{S}_l} e_{31}\right)\frac{\partial \dot{u}_1}{\partial p_1}\right) + \left(\int_{\mathcal{A}}\left(\frac{t_b}{2t_p}\int_{\mathcal{S}_{pl}} e_{31}\right)\frac{\partial^2 \dot{u}_3}{\partial p_1^2}\right) + \left(\frac{1}{t_p^2}\int_{\mathcal{A}}\int_{\mathcal{S}_{pl}} \epsilon_{33}^S\right)\left(\ddot{\phi}_{lu} - \ddot{\phi}_{ll}\right) \\
I^{(l)} &= \int_{\mathcal{A}}\left(G_l\frac{\partial \dot{u}_1}{\partial p_1}\right) + \int_{\mathcal{A}}\left(G_f\frac{\partial^2 \dot{u}_3}{\partial p_1^2}\right) + \left(\ddot{\phi}_{lu} - \ddot{\phi}_{ll}\right)\int_{\mathcal{A}} H^{(l)}
\end{aligned}
$$

for the lower one, with the further definition of the capacitance per unit of length

$$
H = \frac{1}{t_p^2}\int_{\mathcal{S}_{pu}} \epsilon_{33}^S = H^{(u)} = H^{(l)} \tag{4.41}
$$

Hence the internal electric power can be expressed by

$$
\begin{aligned}
\mathcal{P}_{int,e} &= \left(I^{(u)}\left(\dot{\phi}_{uu}^* - \dot{\phi}_{ul}^*\right) + I^{(l)}\left(\dot{\phi}_{lu}^* - \dot{\phi}_{ll}^*\right)\right) \\
&= \left(\int_{\mathcal{A}}\left(G_l\frac{\partial \dot{u}_1}{\partial p_1}\right) - \int_{\mathcal{A}}\left(G_f\frac{\partial^2 \dot{u}_3}{\partial p_1^2}\right) + \int_{\mathcal{A}} H\left(\ddot{\phi}_{uu} - \ddot{\phi}_{ul}\right)\right)\left(\dot{\phi}_{uu}^* - \dot{\phi}_{ul}^*\right) \\
&\quad + \left(\int_{\mathcal{A}}\left(G_l\frac{\partial \dot{u}_1}{\partial p_1}\right) + \int_{\mathcal{A}}\left(G_f\frac{\partial^2 \dot{u}_3}{\partial p_1^2}\right) + \left(\ddot{\phi}_{lu} - \ddot{\phi}_{ll}\right)\int_{\mathcal{A}} H\right)\left(\dot{\phi}_{lu}^* - \dot{\phi}_{ll}^*\right)
\end{aligned}
$$

Mechanical External Power of the Distance Forces

The mechanical external power $\mathcal{P}_{d,m}$ of the distance forces can be rewritten as

$$
\begin{aligned}
\mathcal{P}_{d,m} &= \int_{\mathcal{B}} \mathbf{b}\cdot\dot{\mathbf{u}}^*(\mathbf{p},t) = \\
&= \begin{pmatrix} \int_{\mathcal{A}}\int_{\mathcal{S}_b}\left(\dot{u}_1^* - \frac{\partial \dot{u}_3^*}{\partial p_1}p_3\right) + \int_{\mathcal{A}}\int_{\mathcal{S}_{pu}} b_1\left(\dot{u}_1^* - \frac{\partial \dot{u}_3^*}{\partial p_1}\frac{t_b}{2}\right) + \\ + \int_{\mathcal{A}}\int_{\mathcal{S}_{pl}} b_1\left(\dot{u}_1^* + \frac{\partial \dot{u}_3^*}{\partial p_1}\frac{t_b}{2}\right) + \int_{\mathcal{A}}\int_{\mathcal{S}_p} b_3\dot{u}_3^* + \int_{\mathcal{A}}\int_{\mathcal{S}_b} b_3\dot{u}_3^* \end{pmatrix} \\
&= \begin{pmatrix} \int_{\mathcal{A}}\left(\left(\int_{\mathcal{S}_b} b_1\right)\dot{u}_1^* - \left(\int_{\mathcal{S}} p_3 b_1\right)\frac{\partial \dot{u}_3^*}{\partial p_1}\right) + \\ + \int_{\mathcal{A}}\left(\left(\int_{\mathcal{S}_p} b_1\right)\dot{u}_1^* - \left(\frac{t_b}{2}\left(\int_{\mathcal{S}_{pu}} b_1 - \int_{\mathcal{S}_{pl}} b_1\right)\right)\frac{\partial \dot{u}_3^*}{\partial p_1}\right) + \\ \int_{\mathcal{A}}\int_{\mathcal{S}_p} b_3\dot{u}_3^* + \int_{\mathcal{A}}\int_{\mathcal{S}_b} b_3\dot{u}_3^* \end{pmatrix} \\
&= \int_{\mathcal{A}}\left(B_1\dot{u}_1^* - B_\theta\frac{\partial \dot{u}_3^*}{\partial p_1} + B_3\dot{u}_3^*\right)
\end{aligned} \tag{4.42}
$$

with the definitions

$$\begin{aligned} B_1 &= B_1^{(b)} + B_1^{(p)} = \left(\int_{\mathcal{S}_p} b_1\right) + \left(\int_{\mathcal{S}_p} b_1\right) \\ B_3 &= B_3^{(b)} + B_3^{(p)} = \left(\int_{\mathcal{S}_b} b_3\right) + \left(\int_{\mathcal{S}_p} b_3\right) \\ B_\theta &= B_\theta^{(b)} + B_\theta^{(p)} = \int_{\mathcal{S}_b} p_3 b_1 + \tfrac{t_b}{2}\left(\int_{\mathcal{S}_{pu}} b_1 - \int_{\mathcal{S}_{pl}} b_1\right) \end{aligned} \tag{4.43}$$

Mechanical External Power of Contact Forces

The mechanical power $\mathcal{P}_{c,m}$ of external contact forces becomes

$$\begin{aligned} \mathcal{P}_{c,m} &= \int_{\partial\mathcal{B}} \mathbf{f}\cdot\dot{\mathbf{u}}^*(\mathbf{p},t) \\ &= \int_{\mathcal{A}}\int_{\partial\mathcal{S}} \left(f_1\dot{u}_1^* - f_1\frac{\partial \dot{u}_3^*}{\partial p_1}p_3 + f_3\dot{u}_3^*\right) \\ &= \int_{\mathcal{A}} \left(P_1\dot{u}_1^* - P_\theta\frac{\partial \dot{u}_3^*}{\partial p_1} + P_3\dot{u}_3^*\right) \end{aligned} \tag{4.44}$$

with the definitions

$$\begin{aligned} &P_1 = \textstyle\int_{\partial\mathcal{S}} f_1 \quad P_\theta = \int_{\partial\mathcal{S}} f_1 p_3 \\ &P_3 = \textstyle\int_{\partial\mathcal{S}} f_3 \end{aligned} \tag{4.45}$$

Electrical External Power

Let us denote by $\mathcal{F}_{uu}, \mathcal{F}_{ul}, \mathcal{F}_{lu}, \mathcal{F}_{ll}$ the upper and lower surfaces of the upper and lower transducers.

Since only the upper and lower surfaces of the transducers are plated, the electric external power $\mathcal{P}_{c,e}$ becomes

$$\mathcal{P}_{c,e} = \iota_u\left(\dot{\phi}_{uu}^* - \dot{\phi}_{ul}^*\right) + \iota_l\left(\dot{\phi}_{lu}^* - \dot{\phi}_{ll}^*\right) \tag{4.46}$$

where the $\iota's$ physically represent the currents flowing through the transducers.

Mechanical Power of Inertial Forces

The power $\mathcal{P}_{a,m}$ of the inertial forces acting on the structure can be rewritten as

$$\begin{aligned} \mathcal{P}_{a,m} &= \int_{\mathcal{B}} -\rho\ddot{\mathbf{u}}(\mathbf{p},t)\cdot\dot{\mathbf{u}}^*(\mathbf{p},t) \\ &= \left(-\int_{\mathcal{A}}\left(\lambda\left(\ddot{u}_1\dot{u}_1{}^* + \ddot{u}_3\dot{u}_3^*\right) + \alpha\frac{\partial\ddot{u}_3}{\partial p_1}\frac{\partial\dot{u}_3^*}{\partial p_1}\right)\right) \end{aligned} \tag{4.47}$$

with the definitions

$$\lambda = \lambda^{(b)} + \lambda^{(p)} \tag{4.48}$$

$$\alpha = \alpha^{(b)} + \alpha^{(p)} \tag{4.49}$$

$$\begin{array}{ll} \lambda^{(b)} = \left(\int_{\mathcal{S}_b} \rho\right) & \alpha^{(b)} = \left(\int_{\mathcal{S}_b} \rho p_3^2\right) \\ \lambda^{(p)} = \left(\int_{\mathcal{S}_p} \rho\right) & \alpha^{(p)} = \left(\frac{t_b^2}{4}\int_{\mathcal{S}_{pu}} \rho + \frac{t_b^2}{4}\int_{\mathcal{S}_{pl}} \rho\right) \end{array} \tag{4.50}$$

and considering that for the assumed symmetry

$$\left(\int_{\mathcal{S}_b} \rho p_3\right) = 0 = \left(\int_{\mathcal{S}_{pu}} \rho\right) - \left(\int_{\mathcal{S}_{pl}} \rho\right) \tag{4.51}$$

Statement

The balance (4.17) can be written explicitly as

$$\left(\begin{array}{c} \int_{\mathcal{A}_b}\left(F\frac{\partial \dot{u}_1^*}{\partial p_1} + M\frac{\partial^2 \dot{u}_3^*}{\partial p_1^2}\right) + \\ I^{(u)}\left(\dot{\phi}_{uu}^* - \dot{\phi}_{ul}^*\right) + \\ + I^{(l)}\left(\dot{\phi}_{lu}^* - \dot{\phi}_{ll}^*\right) \end{array}\right) = \left(\begin{array}{c} \int_{\mathcal{A}}\left(B_1 + P_1 - \lambda\ddot{u}_1\right)\dot{u}_1{}^* \\ -\int_{\mathcal{A}}\left(B_\theta + P_\theta + \alpha\frac{\partial \ddot{u}_3}{\partial p_1}\right)\frac{\partial \dot{u}_3^*}{\partial p_1} + \\ + \int_{\mathcal{A}}\left(B_3 + P_3 - \lambda\ddot{u}_3\right)\dot{u}_3^* + \\ + \iota_u\left(\dot{\phi}_{uu}^* - \dot{\phi}_{ul}^*\right) + \iota_l\left(\dot{\phi}_{lu}^* - \dot{\phi}_{ll}^*\right) \end{array}\right) \tag{4.52}$$

or equivalently as

$$\int_{\mathcal{A}}\left(F\frac{\partial \dot{u}_1^*}{\partial p_1} + M\frac{\partial^2 \dot{u}_3^*}{\partial p_1^2}\right) = \left(\begin{array}{c} \int_{\mathcal{A}}\left(\left(R_1 - \lambda\ddot{u}_1\right)\dot{u}_1{}^* - \left(R_\theta + \alpha\frac{\partial \ddot{u}_3}{\partial p_1}\right)\frac{\partial \dot{u}_3^*}{\partial p_1} + \left(R_3 - \lambda\ddot{u}_3\right)\dot{u}_3^*\right) + \\ \left(\iota_u - I^{(u)}\right)\left(\dot{\phi}_{uu}^* - \dot{\phi}_{ul}^*\right) + \left(\iota_l - I^{(l)}\right)\left(\dot{\phi}_{lu}^* - \dot{\phi}_{ll}^*\right) \end{array}\right) \tag{4.53}$$

if the definitions

$$\begin{aligned} R_1 &= B_1 + P_1 \\ R_3 &= B_3 + P_3 \\ R_\theta &= B_\theta + P_\theta \end{aligned} \tag{4.54}$$

are introduced.

4.1.5 Balance Equations

Generic Case

The following integrals by part hold

$$\begin{aligned}
\int_{-\frac{l}{2}}^{\frac{l}{2}} F\frac{\partial \dot{u}_1^*}{\partial p_1}dp_1 &= [F\dot{u}_1^*]_0^l - \int_{-\frac{l}{2}}^{\frac{l}{2}} \frac{\partial F}{\partial p_1}\dot{u}_1^* dp_1 \\
\int_{-\frac{l}{2}}^{\frac{l}{2}} M\frac{\partial^2 \dot{u}_3^*}{\partial p_1^2}dp_1 &= \left[M\frac{\partial \dot{u}_3^*}{\partial p_1}\right]_0^l - \left[\frac{\partial M}{\partial p_1}\dot{u}_3^*\right]_0^l + \int_{-\frac{l}{2}}^{\frac{l}{2}} \frac{\partial^2 M}{\partial p_1^2}\dot{u}_3^* dp_1 \\
\int_{-\frac{l}{2}}^{\frac{l}{2}} R_\theta\frac{\partial \dot{u}_3^*}{\partial p_1}dp_1 &= [R_\theta \dot{u}_3^*]_0^l - \int_{-\frac{l}{2}}^{\frac{l}{2}} \frac{\partial R_\theta}{\partial p_1}\dot{u}_3^* dp_1
\end{aligned} \tag{4.55}$$

thus the power balance (4.53) can be written as

$$\begin{pmatrix} [F\dot{u}_1^*]_0^l + \\ + \left[M\frac{\partial \dot{u}_3^*}{\partial p_1}\right]_0^l + \\ + \left[\left(-\frac{\partial M}{\partial p_1} + R_\theta + \alpha\frac{\partial \ddot{u}_3}{\partial p_1}\right)\dot{u}_3^*\right]_0^l \end{pmatrix} = \begin{pmatrix} \int_{-\frac{l}{2}}^{\frac{l}{2}} \left(R_1 - \lambda\ddot{u}_1 + \frac{\partial F}{\partial p_1}\right)\dot{u}_1{}^* dp_1 + \\ \int_{-\frac{l}{2}}^{\frac{l}{2}} \begin{pmatrix} \frac{\partial R_\theta}{\partial p_1} + \frac{\partial}{\partial p_1}\left(\alpha\frac{\partial \ddot{u}_3}{\partial p_1}\right) + \\ -\frac{\partial^2 M}{\partial p_1^2} + R_3 - \lambda\ddot{u}_3 \end{pmatrix}\dot{u}_3^* dp_1 + \\ \left(\iota_u - I^{(u)}\right)\left(\dot{\phi}_{uu}^* - \dot{\phi}_{ul}^*\right) + \\ + \left(\iota_l - I^{(l)}\right)\left(\dot{\phi}_{lu}^* - \dot{\phi}_{ll}^*\right) \end{pmatrix} \tag{4.56}$$

Since the virtual velocities can be chosen arbitrarily, providing that they are smooth enough and that they satisfy the homogeneous version of the prescribed essential boundary conditions, equation (4.56) is verified if and only if

$$R_1 - \lambda\ddot{u}_1 + \frac{\partial F}{\partial p_1} = 0 \tag{4.57}$$

$$\frac{\partial R_\theta}{\partial p_1} + \frac{\partial}{\partial p_1}\left(\alpha\frac{\partial \ddot{u}_3}{\partial p_1}\right) - \frac{\partial^2 M}{\partial p_1^2} - \lambda\ddot{u}_3 + R_3 = 0 \tag{4.58}$$

$$\left(\iota_u - I^{(u)}\right)\left(\dot{\phi}_{uu}^* - \dot{\phi}_{ul}^*\right) + \left(\iota_l - I^{(l)}\right)\left(\dot{\phi}_{lu}^* - \dot{\phi}_{ll}^*\right) = 0 \tag{4.59}$$

on $\mathcal{B}$ and

$$[F\dot{u}_1^*]_0^l = 0 \tag{4.60}$$

$$\left[M\frac{\partial \dot{u}_3^*}{\partial p_1}\right]_0^l = 0 \tag{4.61}$$

$$\left[\left(-\frac{\partial M}{\partial p_1} + R_\theta + \alpha\frac{\partial \ddot{u}_3}{\partial p_1}\right)\dot{u}_3^*\right]_0^l = 0 \tag{4.62}$$

on $\partial\mathcal{B}$.

The first three equations are the balance equations for the beam (extensional, bending, electrical), the latter three are the conditions that must be satisfied at the boundaries. Here the axial continuity is required but not also its homogeneity.

Considering the following constitutive relations for the unidimensional model that have been derived by homogenizing over a section those of the 3D model with the imposed kinematics

$$F = K_l \frac{\partial u_1}{\partial p_1} - G_l \left(\dot{\phi}_{uu} - \dot{\phi}_{ul} + \dot{\phi}_{lu} - \dot{\phi}_{ll} \right) \tag{4.63}$$

$$M = K_f \frac{\partial^2 u_3}{\partial p_1^2} + G_f \left(\dot{\phi}_{uu} - \dot{\phi}_{ul} - \dot{\phi}_{lu} + \dot{\phi}_{ll} \right) \tag{4.64}$$

$$I^{(u)} = \int_{\mathcal{A}} \left(G_l \frac{\partial \dot{u}_1}{\partial p_1} \right) - \int_{\mathcal{A}} \left(G_f \frac{\partial^2 \dot{u}_3}{\partial p_1^2} \right) + \left(\ddot{\phi}_{uu} - \ddot{\phi}_{ul} \right) \int_{\mathcal{A}} H \tag{4.65}$$

$$I^{(l)} = \int_{\mathcal{A}} \left(G_l \frac{\partial \dot{u}_1}{\partial p_1} \right) + \int_{\mathcal{A}} \left(G_f \frac{\partial^2 \dot{u}_3}{\partial p_1^2} \right) + \left(\ddot{\phi}_{lu} - \ddot{\phi}_{ll} \right) \int_{\mathcal{A}} H \tag{4.66}$$

the following equations are deduced

$$-\frac{\partial}{\partial p_1} \left(K_l \frac{\partial u_1}{\partial p_1} \right) + \lambda \ddot{u}_1 = R_1 \tag{4.67}$$

$$\frac{\partial^2}{\partial p_1^2} \left(K_f \frac{\partial^2 u_3}{\partial p_1^2} \right) - \frac{\partial}{\partial p_1} \left(\alpha \frac{\partial \ddot{u}_3}{\partial p_1} \right) + \lambda \ddot{u}_3 = \frac{\partial R_\theta}{\partial p_1} + R_3 \tag{4.68}$$

$$\left(\iota_u - I^{(u)} \right) \left(\dot{\phi}^*_{uu} - \dot{\phi}^*_{ul} \right) + \left(\iota_l - I^{(l)} \right) \left(\dot{\phi}^*_{lu} - \dot{\phi}^*_{ll} \right) = 0 \tag{4.69}$$

together with the boundary conditions

$$\left[\left(K_l \frac{\partial u_1}{\partial p_1} - G_l \left(\dot{\phi}_{uu} - \dot{\phi}_{ul} + \dot{\phi}_{lu} - \dot{\phi}_{ll} \right) \right) u_1^* \right]_{-\frac{l}{2}}^{\frac{l}{2}} = 0 \tag{4.70}$$

$$\left[\left(K_f \frac{\partial^2 u_3}{\partial p_1^2} + G_f \left(\dot{\phi}_{uu} - \dot{\phi}_{ul} - \dot{\phi}_{lu} + \dot{\phi}_{ll} \right) \right) \frac{\partial \dot{u}_3^*}{\partial p_1} \right]_{-\frac{l}{2}}^{\frac{l}{2}} = 0 \tag{4.71}$$

$$\left[\left(\frac{\partial}{\partial p_1} \left(K_f \frac{\partial^2 u_3}{\partial p_1^2} \right) + R_\theta + \alpha \frac{\partial \ddot{u}_3}{\partial p_1} \right) \dot{u}_3^* \right]_{-\frac{l}{2}}^{\frac{l}{2}} = 0 \tag{4.72}$$

These are the equations of motion and the boundary conditions for the laminated piezoelectromechanical, axially continuous, symmetric beam.

Remark 13 *The influence of the electrical quantity on the mechanical equations is exerted only by the boundary conditions.*

Remark 14 *The extensional equation is uncoupled from the bending and electric ones if*

$$\dot{\phi}_{uu} - \dot{\phi}_{ul} + \dot{\phi}_{lu} - \dot{\phi}_{ll} = 0$$

A particular case is the out-of-phase parallel connections between the two piezoelectric layers in which

$$\dot{\phi}_{uu} = \dot{\phi}_{ll} \quad \dot{\phi}_{ul} = \dot{\phi}_{lu}$$

Remark 15 *The bending equation is uncoupled from the extensional and electric ones if*

$$\dot{\phi}_{uu} - \dot{\phi}_{ul} - \dot{\phi}_{lu} + \dot{\phi}_{ll} = 0$$

A particular case is the in-phase parallel connections between the two piezoelectric layers in which

$$\dot{\phi}_{ul} = \dot{\phi}_{ll} \quad \dot{\phi}_{uu} = \dot{\phi}_{lu}$$

By the remarks above we can study separately the *flexural-electric coupling for the out-of-phase connection and the extensional-electric coupling for the in-phase connection.*

In-Phase Connection: Extensional-Electric Coupling

In the case of an electric connection between the piezoelectric layers as in figure 4-7 the equations

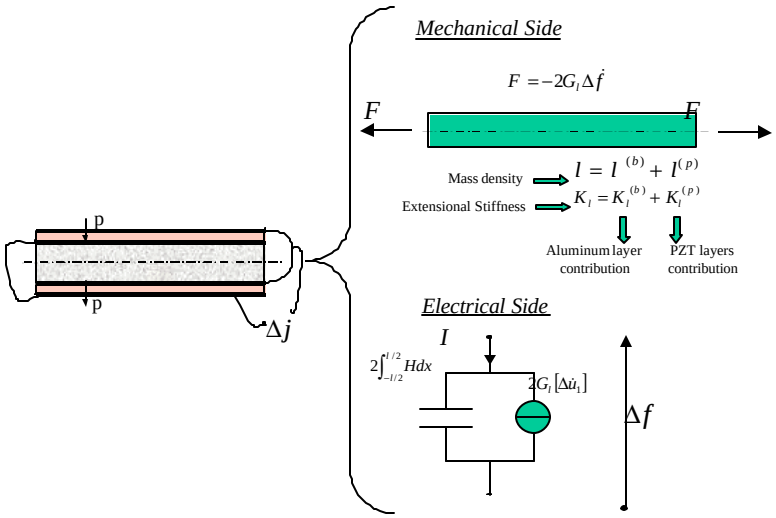

Figure 4-7: Mechanical and electrical equivalents of axially homogeneous PEM with in-phase connected PZT sheets

of motion become

$$\begin{aligned} -\frac{\partial}{\partial p_1}\left(K_l\frac{\partial u_1}{\partial p_1}\right)+\lambda\ddot{u}_1 &= R_1 \\ \frac{\partial^2}{\partial p_1^2}\left(K_f\frac{\partial^2 u_3}{\partial p_1^2}\right)-\frac{\partial}{\partial p_1}\left(\alpha\frac{\partial\ddot{u}_3}{\partial p_1}\right)+\lambda\ddot{u}_3 &= \frac{\partial R_\theta}{\partial p_1}+R_3 \\ 2\int_{\mathcal{A}}\left(G_l\frac{\partial\dot{u}_1}{\partial p_1}\right)dp_1+2\Delta\ddot{\phi}\int_{\mathcal{A}}H &= \iota \end{aligned} \tag{4.73}$$

plus the boundary conditions

$$\begin{aligned} \left[\left(K_l\frac{\partial u_1}{\partial p_1}-2G_l\Delta\dot{\phi}\right)u_1^*\right]_{-\frac{l}{2}}^{\frac{l}{2}} &= 0 \\ \left[\left(K_f\frac{\partial^2 u_3}{\partial p_1^2}\right)\frac{\partial\dot{u}_3^*}{\partial p_1}\right]_{-\frac{l}{2}}^{\frac{l}{2}} &= 0 \\ \left[\left(\frac{\partial}{\partial p_1}\left(K_f\frac{\partial^2 u_3}{\partial p_1^2}\right)+R_\theta+\alpha\frac{\partial\ddot{u}_3}{\partial p_1}\right)\dot{u}_3^*\right]_{-\frac{l}{2}}^{\frac{l}{2}} &= 0 \end{aligned} \tag{4.74}$$

where

$$\Delta\phi=\phi_{uu}-\phi_{ll}\quad \iota=\iota_u+\iota_l \tag{4.75}$$

Remark 16 *With this symmetric configuration in which a in-phase voltage is applied to the two PZTs, the piezoelectric effect couples the extensional behavior of the beam with the applied electric potential. As a consequence of the applied voltage a longitudinal deformation*

$$\frac{\partial u_1}{\partial p_1}=\frac{2G_l}{K_l}\Delta\dot{\phi}$$

is imposed on the boundary of the beam. Hence its effect corresponds to two equal and opposite forces

$$F=2G_l\Delta\dot{\phi}$$

applied on the boundaries.

Remark 17 *The piezoelectric effect causes a current in the electric terminal given by*

$$\iota_p=2\int_{\mathcal{A}}\left(G_l\frac{\partial\dot{u}_1}{\partial p_1}\right)dp_1$$

proportional to the beam curvature. If the piezoelectric layers are materially and geometrically homogeneous G_l is constant and the current generated by the mechanical deformation becomes

$$\iota_p = 2G_l \int_{\mathcal{A}} \left(\frac{\partial \dot{u}_1}{\partial p_1} \right) dp_1 = 2G_l \left[\dot{u}_1 \right]_{-\frac{l}{2}}^{\frac{l}{2}}$$

Hence it is proportional to the time rate of the total elongation of the PZT layers.

Out-of-phase Connection: Flexural-Electric Coupling

If the *PZT* layers are connected in parallel and in opposition of phase as in figure 4-8 the equations

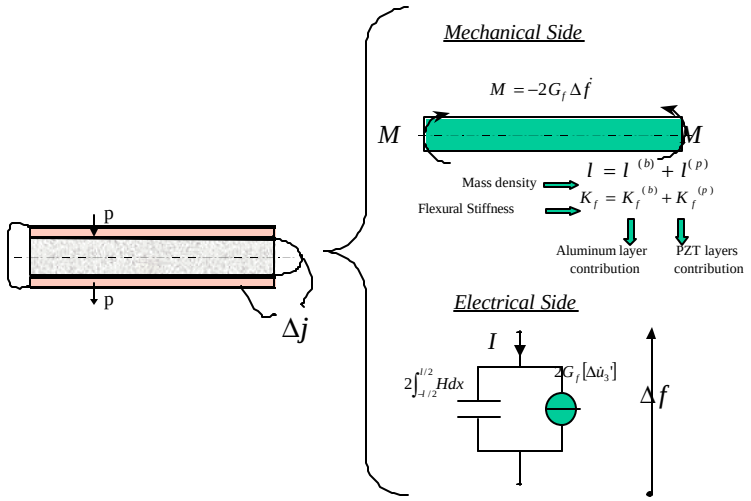

Figure 4-8: Mechanical and electrical equivalents of axially homogeneous PEM with out-of-phase connected PZT sheets

of motion become

$$\begin{aligned} -\frac{\partial}{\partial p_1}\left(K_l \frac{\partial u_1}{\partial p_1} \right) + \lambda \ddot{u}_1 &= R_1 \\ \frac{\partial^2}{\partial p_1^2}\left(K_f \frac{\partial^2 u_3}{\partial p_1^2} \right) - \frac{\partial}{\partial p_1}\left(\alpha \frac{\partial \ddot{u}_3}{\partial p_1} \right) + \lambda \ddot{u} &= \frac{\partial R_\theta}{\partial p_1} + R_3 \\ 2\int_{-\frac{l}{2}}^{\frac{l}{2}} \left(G_f \frac{\partial^2 \dot{u}_3}{\partial p_1^2} \right) dp_1 + 2\int_{-\frac{l}{2}}^{\frac{l}{2}} H \Delta \ddot{\phi} &= \iota \end{aligned} \tag{4.76}$$

plus the boundary conditions

$$\left[\left(K_l\frac{\partial u_1}{\partial p_1}\right)u_1^*\right]_{-\frac{l}{2}}^{\frac{l}{2}} = 0 \tag{4.77}$$

$$\left[\left(K_f\frac{\partial^2 u_3}{\partial p_1^2}+G_f\left(2\Delta\dot{\phi}\right)\right)\frac{\partial \dot{u}_3^*}{\partial p_1}\right]_{-\frac{l}{2}}^{\frac{l}{2}} = 0$$

$$\left[\left(\frac{\partial}{\partial p_1}\left(K_f\frac{\partial^2 u_3}{\partial p_1^2}\right)+R_\theta+\alpha\frac{\partial \ddot{u}_3}{\partial p_1}\right)\dot{u}_3^*\right]_{-\frac{l}{2}}^{\frac{l}{2}} = 0$$

where

$$\Delta\phi=\dot{\phi}_{uu}-\dot{\phi}_{ul}\quad \iota=\iota_u-\iota_l \tag{4.78}$$

Remark 18 *In this skew − symmetric configuration in which the potential difference between the PZT layers is applied with a relative phase difference of* 180°*, the beam bending mode is coupled with the electrical variable by means of the boundary conditions. The piezoelectric effect on the laminated beam imposes a curvature on the boundary given by*

$$\frac{\partial^2 u_3}{\partial p_1^2}=-\frac{2G_f}{K_f}\Delta\dot{\phi}$$

Hence its effect its equivalent to a two equal and opposite moments applied to the boundary, with a modulus

$$M=-\left(2G_f\right)\Delta\dot{\phi}$$

Remark 19 *The piezoelectric effect causes a current in the electric terminals given by*

$$\iota_p=2\int_{-\frac{l}{2}}^{\frac{l}{2}}\left(G_f\frac{\partial^2 \dot{u}_3}{\partial p_1^2}\right)dp_1$$

If the piezoelectric layers are homogeneous and with constant cross section, G_f *is constant and the current generated by the mechanical deformation becomes*

$$\iota_p=2G_f\int_{-\frac{l}{2}}^{\frac{l}{2}}\left(\frac{\partial^2 \dot{u}_3}{\partial p_1^2}\right)dp_1=2G_f\left[\frac{\partial \dot{u}_3}{\partial p_1}\right]_{-\frac{l}{2}}^{\frac{l}{2}}$$

Hence it is proportional to the time rate of difference of the central axis slope at the two ends, that is the beam spatially averaged curvature time rate.

4.1.6 Weak Formulation

The weak formulation for the dynamical problem of a continuous piezoelectromechanical layered beam can be derived directly by the expression of the power balance (4.52) substituting in it the constitutive equations.

Since we are treating continuous systems the virtual velocities must be elements of an opportune functional space. In particular, as underlined in the statement of the virtual power principle, they are required to

1. be smooth enough to evaluate the integrals involved in the virtual power principle.

2. satisfy the homogeneous version of the prescribed essential boundary conditions.

The spatial distribution of the electric variable ϕ in the continuous body was prescribed in function of its value at the boundaries such that it satisfies the requirement 1., 2. for each value of $\dot{\phi}^*_{uu}, \dot{\phi}^*_{ul}, \dot{\phi}^*_{lu}, \dot{\phi}^*_{ll}$. Thus no further specification is necessary on it. For the mechanical virtual velocities, a distinction must be made between the vertical and the horizontal components $\dot{u}^*_3, \dot{u}^*_1$ because in the problem statement the spatial derivative up to the second order for $\dot{u}^*_3$ and up to the first for $\dot{u}^*_1$ are present. Let us denote by

- H^1_0 the space of functions having square integrable[9] derivatives up to the first order and satisfying the homogeneous version of the boundary conditions prescribed directly on them (essential boundary conditions for u_1).

- H^2_0 the space of functions having square integrable derivatives up to the second order and satisfying the homogeneous version of the boundary conditions prescribed on them and on their spatial derivatives up to first order (essential boundary conditions for u_3)

Also the weak formulation will be given separately for the flexural-electric and extensional-electric cases.

Extensional-Electric Coupling

If the electrical connections between the PZT layers are such that

$$\phi_{uu} = \phi_{lu} \quad \phi_{ul} = \phi_{ll} \tag{4.79}$$

[9] In the Lebesgue sense.

the piezoelectric coupling is symmetric and the mechanical displacements due to bending are electrically filtered out since they are skew-symmetric.

Defining

$$\Delta\phi = \phi_{uu} - \phi_{ll} \quad \iota = \iota_u + \iota_l \tag{4.80}$$

the constitutive equations can be written in the form[10]

$$\begin{aligned} F &= F^{(b)} + F^{(p)} = K_l \frac{\partial u_1}{\partial p_1} - 2G_l \Delta\dot{\phi} \\ M &= M^{(b)} + M^{(p)} = K_f \frac{\partial^2 u_3}{\partial p_1^2} \\ I &= 2\int_{-\frac{l}{2}}^{\frac{l}{2}} \left(G_l \frac{\partial \dot{u}_1}{\partial p_1} \right) dp_1 + 2\Delta\ddot{\phi} \int_{-\frac{l}{2}}^{\frac{l}{2}} H \end{aligned} \tag{4.81}$$

Hence the power balance (4.52), mechanically limited to extensional behavior, becomes

$$\begin{pmatrix} \int_{-\frac{l}{2}}^{\frac{l}{2}} K_l \frac{\partial u_1}{\partial p_1} \frac{\partial \dot{u}_1^*}{\partial p_1} dp_1 - 2\Delta\dot{\phi} \int_{-\frac{l}{2}}^{\frac{l}{2}} G_l \frac{\partial \dot{u}_1^*}{\partial p_1} dp_1 + \\ +2\Delta\dot{\phi}^* \int_{-\frac{l}{2}}^{\frac{l}{2}} \left(G_l \frac{\partial \dot{u}_1}{\partial p_1} \right) dp_1 + 2\Delta\ddot{\phi}\Delta\dot{\phi}^* \int_{-\frac{l}{2}}^{\frac{l}{2}} H \end{pmatrix} = \begin{pmatrix} \int_{-\frac{l}{2}}^{\frac{l}{2}} (R_1 - \lambda\ddot{u}_1)\, \dot{u}_1^* dp_1 \\ +\iota\Delta\dot{\phi}^* \end{pmatrix} \tag{4.82}$$

The weak formulation is:

- The equation (4.82) must hold

$$for\ each\ \dot{u}_1^* \in H_0^1, \Delta\dot{\phi}^* \in \mathcal{R}$$

  This is also a Galerkin formulation in the case in which the prescribed essential boundary conditions are homogeneous, otherwise it will be easily obtained with a simple change of variable.

Remark 20 *If the layered beam is axially homogeneous, the quantities*

$$G_l, K_l, \lambda$$

will be constant and the power balance (4.82) will assume the simplified expression

$$\begin{pmatrix} K_l \int_{-\frac{l}{2}}^{\frac{l}{2}} \frac{\partial u_1}{\partial p_1} \frac{\partial \dot{u}_1^*}{\partial p_1} dp_1 - 2G_l \Delta\dot{\phi} \left[\dot{u}_1^*\right]_{-\frac{l}{2}}^{\frac{l}{2}} + \\ +2G_l \left[\dot{u}_1\right]_{-\frac{l}{2}}^{\frac{l}{2}} \Delta\dot{\phi}^* + 2Hl\Delta\ddot{\phi}\Delta\dot{\phi}^* \end{pmatrix} = \begin{pmatrix} \int_{-\frac{l}{2}}^{\frac{l}{2}} R_1 \dot{u}_1^* dp_1 \\ -\lambda \int_{-\frac{l}{2}}^{\frac{l}{2}} \ddot{u}_1 dp_1 + \iota\Delta\dot{\phi}^* \end{pmatrix}$$

[10] The flexural behaviour is neglected since it is uncoupled from the extensional-electric modes

Flexural-Electric Coupling

To obtain a coupling between the electric and flexural beam modes the following electric conditions must be imposed

$$\phi_{uu} = \phi_{ll} \quad \phi_{ul} = \phi_{lu} \tag{4.83}$$

Thus introducing the definitions

$$\Delta\dot{\phi} = \dot{\phi}_{uu} - \dot{\phi}_{ul} \quad I = I^{(u)} - I^{(l)} \quad \iota = \iota_u - \iota_l \tag{4.84}$$

the constitutive equations can be rewritten[11] as

$$\begin{aligned} M &= M^{(b)} + M^{(p)} = K_f \frac{\partial^2 u_3}{\partial p_1^2} + 2G_f \left(\Delta\dot{\phi}\right) \\ I &= -2\int_{-\frac{1}{2}}^{\frac{1}{2}} \left(G_f \frac{\partial^2 \dot{u}_3}{\partial p_1^2}\right) dp_1 + 2\Delta\ddot{\phi}\int_{-\frac{1}{2}}^{\frac{1}{2}} H \end{aligned} \tag{4.85}$$

So that the power balance for this specific case becomes

$$\begin{pmatrix} \int_{-\frac{1}{2}}^{\frac{1}{2}} K_f \frac{\partial^2 u_3}{\partial p_1^2}\frac{\partial^2 \dot{u}_3^*}{\partial p_1^2} dp_1 + 2\Delta\dot{\phi}\int_{-\frac{1}{2}}^{\frac{1}{2}} G_f \frac{\partial^2 \dot{u}_3^*}{\partial p_1^2} dp_1 + \\ -2\Delta\dot{\phi}^* \int_{-\frac{1}{2}}^{\frac{1}{2}} \left(G_f \frac{\partial^2 \dot{u}_3}{\partial p_1^2}\right) dp_1 + 2\Delta\ddot{\phi}\Delta\dot{\phi}^* \int_{-\frac{1}{2}}^{\frac{1}{2}} H \end{pmatrix} = \begin{pmatrix} -\int_{-\frac{1}{2}}^{\frac{1}{2}} \left(R_\theta + \alpha\frac{\partial \ddot{u}_3}{\partial p_1}\right)\frac{\partial \dot{u}_3^*}{\partial p_1} dp_1 + \\ +\int_{-\frac{1}{2}}^{\frac{1}{2}} \left(R_3 - \lambda\ddot{u}_3\right)\dot{u}_3^* dp_1 + \\ +\iota\Delta\dot{\phi}^* \end{pmatrix} \tag{4.86}$$

The weak formulation of the problem is obtained imposing that equation (4.86) must hold

$$for\ each\ \dot{u}_3^* \in H_0^2, \Delta\dot{\phi}^* \in \mathcal{R} \tag{4.87}$$

If the boundary conditions that are prescribed on $\dot{u}_3^*, \frac{\partial \dot{u}_3^*}{\partial p_1}$ are homogeneous this is also a Galerkin formulation that can be directly used to obtain a numerical solution by means of a Galerkin approximation. Otherwise a simple change of variable is required to convert the problem to a new one with homogeneous essential boundary conditions.

Remark 21 *If the layered beam is axially homogeneous the quantities*

$$K_f, G_f, \alpha, \lambda$$

[11] The extensional behaviour is neglected since it is uncoupled from the flexural-electric modes

will be constant and the power balance (4.86) can be rewritten in the simplified form

$$\begin{pmatrix} K_f \int_{-\frac{l}{2}}^{\frac{l}{2}} \frac{\partial^2 u_3}{\partial p_1^2} \frac{\partial^2 \dot{u}_3^*}{\partial p_1^2} dp_1 + 2G_f \Delta\dot{\phi} \left[\frac{\partial \dot{u}_3^*}{\partial p_1}\right]_{-\frac{l}{2}}^{\frac{l}{2}} + \\ -2G_f \left[\frac{\partial \dot{u}_3}{\partial p_1}\right]_{-\frac{l}{2}}^{\frac{l}{2}} \Delta\dot{\phi}^* + 2Hl\Delta\ddot{\phi}\Delta\dot{\phi}^* \end{pmatrix} = \begin{pmatrix} -\int_{-\frac{l}{2}}^{\frac{l}{2}} R_\theta \frac{\partial \dot{u}_3^*}{\partial p_1} dp_1 - \alpha \int_{-\frac{l}{2}}^{\frac{l}{2}} \frac{\partial \ddot{u}_3}{\partial p_1} dp_1 + \\ + \int_{-\frac{l}{2}}^{\frac{l}{2}} R_3 \dot{u}_3^* dp_1 - \lambda \int_{-\frac{l}{2}}^{\frac{l}{2}} \ddot{u}_3 \dot{u}_3^* dp_1 + \\ + \iota \Delta\dot{\phi}^* \end{pmatrix}$$

4.2 Elastic Beam

The governing equations for a continuous, isotropic, linear elastic beam can be derived from the case of the layered piezoelastic beam by simply letting vanish the thickness of the piezoelectric layers. Here the equilibrium equations in the strong and weak form, following what has been done in the previous section, are reported.

4.2.1 Equilibrium Equations

The equilibrium equations for a linear elastic isotropic beam are

$$\begin{aligned} -\frac{\partial}{\partial p_1}\left(K_l \frac{\partial u_1}{\partial p_1}\right) + \lambda \ddot{u}_1 &= R_1 \\ \frac{\partial^2}{\partial p_1^2}\left(K_f \frac{\partial^2 u_3}{\partial p_1^2}\right) - \frac{\partial}{\partial p_1}\left(\alpha \frac{\partial \ddot{u}_3}{\partial p_1}\right) + \lambda \ddot{u}_3 &= \frac{\partial R_\theta}{\partial p_1} + R_3 \end{aligned} \tag{4.88}$$

plus the boundary conditions

$$\begin{aligned} \left[\left(K_l \frac{\partial u_1}{\partial p_1}\right) u_1^*\right]_{-\frac{l}{2}}^{\frac{l}{2}} &= 0 \\ \left[\left(K_f \frac{\partial^2 u_3}{\partial p_1^2} + G_f\left(2\Delta\dot{\phi}\right)\right) \frac{\partial \dot{u}_3^*}{\partial p_1}\right]_{-\frac{l}{2}}^{\frac{l}{2}} &= 0 \\ \left[\left(\frac{\partial}{\partial p_1}\left(K_f \frac{\partial^2 u_3}{\partial p_1^2}\right) + R_\theta + \alpha \frac{\partial \ddot{u}_3}{\partial p_1}\right) \dot{u}_3^*\right]_{-\frac{l}{2}}^{\frac{l}{2}} &= 0 \end{aligned} \tag{4.89}$$

4.2.2 Weak Formulation

For each

$$\dot{u}_1^* \in H_0^1, \dot{u}_3^* \in H_0^2 \tag{4.90}$$

the following power balance must hold

$$\left(\begin{array}{c} \int_{-\frac{l}{2}}^{\frac{l}{2}} K_f \frac{\partial^2 u_3}{\partial p_1^2}\frac{\partial^2 \dot{u}_3^*}{\partial p_1^2} dp_1 + \\ + \int_{-\frac{l}{2}}^{\frac{l}{2}} K_l \frac{\partial u_1}{\partial p_1}\frac{\partial \dot{u}_1^*}{\partial p_1} dp_1 \end{array}\right) = \left(\begin{array}{c} -\int_{-\frac{l}{2}}^{\frac{l}{2}} \left(R_\theta + \alpha \frac{\partial \ddot{u}_3}{\partial p_1}\right)\frac{\partial \dot{u}_3^*}{\partial p_1} dp_1 + \\ + \int_{-\frac{l}{2}}^{\frac{l}{2}} \left(R_3 - \lambda \ddot{u}_3\right)\dot{u}_3^* dp_1 + \\ + \int_{-\frac{l}{2}}^{\frac{l}{2}} \left(R_1 - \lambda \ddot{u}_1\right)\dot{u}_1^* dp_1 \end{array}\right) \tag{4.91}$$

4.2.3 Dimensional Analysis and Approximations

Introducing the dimensionless variables

$$\begin{array}{cccc} p_1' = \frac{p_1}{l_0} & u_3' = \frac{u_3}{l_3} & t' = \frac{t}{t_0} & \alpha' = \frac{\alpha}{\alpha_0} \\ K_f' = \frac{K_f}{k_0} & R_\theta' = \frac{R_\theta}{m_0} & R_3' = \frac{R_3}{f_0} & \end{array} \tag{4.92}$$

the equilibrium equations (4.88) become

$$\frac{k_0 l_3}{l_0^4}\frac{\partial^2}{\partial p_1'^2}\left(K_f'\frac{\partial^2 u_3'}{\partial p_1'^2}\right) - \frac{l_3\alpha_0}{l_0^2 t_0^2}\frac{\partial}{\partial p_1'}\left(\alpha'\frac{\partial u_3}{\partial p_1' \partial t'^2}\right) + \frac{\lambda l_3}{t_0^2}\frac{\partial u_3'}{\partial t'^2} = \frac{m_0}{l_0}\frac{\partial R_\theta'}{\partial p_1'} + f_0 R_3' \tag{4.93}$$

$$\frac{\partial^2}{\partial p_1'^2}\left(K_f'\frac{\partial^2 u_3'}{\partial p_1'^2}\right) - \eta\frac{\partial}{\partial p_1'}\left(\alpha'\frac{\partial u_3}{\partial p_1' \partial t'^2}\right) + \gamma\frac{\partial u_3'}{\partial t'^2} = \nu\frac{\partial R_\theta'}{\partial p_1'} + \mu R_3' \tag{4.94}$$

with

$$\begin{array}{cc} \eta = \frac{l_0^2\alpha_0}{k_0 t_0^2} & \gamma = \frac{\lambda l_0^4}{k_0 t_0^2} \\ \nu = \frac{m_0 l_0^3}{k_0 l_3} & \mu = \frac{l_0^4 f_0}{k_0 l_3} \end{array} \tag{4.95}$$

Let us choose t_0 such that $\gamma = 1$, thus

$$t_0 = l_0^2\sqrt{\frac{\lambda}{k_0}} \tag{4.96}$$

and

$$\eta = \frac{\alpha_0}{\lambda l_0^2} \quad \gamma = 1 \tag{4.97}$$

In application is frequently verified that

$$\eta = \frac{\alpha_0}{\lambda l_0^2} \ll 1 \tag{4.98}$$

consequently the term

$$\eta \frac{\partial}{\partial p_1'} \left(\alpha' \frac{\partial u_3}{\partial p_1' \partial t'^2} \right) \tag{4.99}$$

in(4.94), physically representing the rotational inertia of the beam, can be neglected and (4.94) becomes

$$\frac{\partial^2}{\partial p_1'^2} \left(K_f' \frac{\partial^2 u_3'}{\partial p_1'^2} \right) + \gamma \frac{\partial u_3'}{\partial t'^2} = \nu \frac{\partial R_\theta'}{\partial p_1'} + \mu R_3' \tag{4.100}$$

which is the Euler equation for an elastic beam. A numerical example is discussed

Example 15 *Let us consider a rectangular cross section aluminum beam with*[12]

$$t_b = 4\,\text{mm} \qquad w_b = 40\,\text{mm}$$
$$l_b = 510\,\text{mm}$$

Consequently

$$\eta = \frac{\alpha_0}{\lambda l_0^2} = \frac{1}{12} \left(\frac{t_b}{l_b} \right)^2 = 5.126\,2 \times 10^{-6}$$

and (4.98) is well satisfied

In the following we will assume that (4.98) is verified and the term (4.99) will be neglected.

4.3 Beam with PZT Transducers

Let us consider a beam with a PZT transducer, as represented in figure 4-9, 4-10. The two PZT

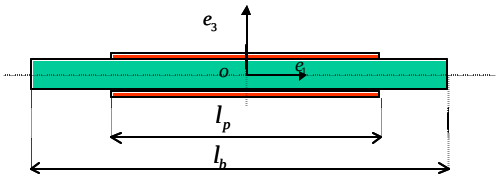

Figure 4-9: Bimorph PZT transducer on a elastic beam: lateral view

layers are considered to be connected in parallel and out of phase to realize a coupling between the

[12] *The numerical values refer to those of the experimental set up described in Chapter 7.*

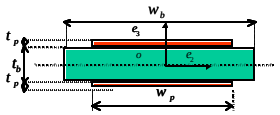

Figure 4-10: Bimorph PZT transducer on a beam: cross section

electric variables and the flexural mode of the beam. All the kinematical hypotheses previously used will be tacitly assumed.

The whole body $\mathcal{B}$ can be partitioned in

$$\mathcal{B} = \mathcal{B}_r + \mathcal{B}_c + \mathcal{B}_l \tag{4.101}$$

where

- $\mathcal{B}_l$ is the left part composed only by an homogeneous elastic beam
- $\mathcal{B}_c$ is the central part composed by a $3 - layers$ piezoelastic beam
- $\mathcal{B}_r$ is the right part composed only by an homogeneous elastic beam

By the additivity of the virtual powers

$$\mathcal{P}(\mathcal{B}) = \mathcal{P}(\mathcal{B}_l \cup \mathcal{B}_c \cup \mathcal{B}_r) = \mathcal{P}(\mathcal{B}_l) + \mathcal{P}(\mathcal{B}_c) + \mathcal{P}(\mathcal{B}_r) \tag{4.102}$$

Hence the expressions of the external and internal virtual powers can be easily assembled since those of each part are known from the previous sections. Since only the bending mode of the beam will be considered, the following virtual velocities can be chosen

$$\begin{aligned} \mathcal{V} &= \{\mathcal{V}_m, \mathcal{V}_e\} \\ \mathcal{V}_m &= \{\dot{u}_3^*, \tfrac{\partial \dot{u}_3^*}{\partial p_1}, \tfrac{\partial^2 \dot{u}_3^*}{\partial p_1^2}\} \quad \mathcal{V}_e = \{\dot{\Delta\phi}^*\} \end{aligned} \tag{4.103}$$

where $\dot{\Delta\phi}$ is the potential difference across the two parallel connected PZT layers.

4.3.1 Internal Powers

We can write

$$\mathcal{P}_{int}(\mathcal{B}, \mathcal{V}) = \mathcal{P}_{int,m}(\mathcal{B}, \mathcal{V}_m) + \mathcal{P}_{int,e}(\mathcal{B}, \mathcal{V}_e) \tag{4.104}$$

where with $\mathcal{P}(\mathcal{B},\mathcal{V})$ is denoted the power expended on the virtual velocity $\mathcal{V}$ in the part $\mathcal{B}$. Considering the reference in figure 4-9 the internal powers are given by

$$\begin{aligned}
\mathcal{P}_{int}(\mathcal{B},\mathcal{V}_e) &= \left(-2G_f\left[\frac{\partial \dot{u}_3}{\partial p_1}\right]_{-\frac{l_p}{2}}^{\frac{l_p}{2}} + 2\Delta\ddot{\phi}\int_{-\frac{l_p}{2}}^{+\frac{l_p}{2}} H\right)\Delta\dot{\phi}^* \qquad (4.105)\\
\mathcal{P}_{int}(\mathcal{B},\mathcal{V}_m) &= \mathcal{P}_{int}(\mathcal{B}_r,\mathcal{V}_m)+\mathcal{P}_{int}(\mathcal{B}_c,\mathcal{V}_m)+\mathcal{P}_{int}(\mathcal{B}_d,\mathcal{V}_m)\\
&= K_f^{(b)}\int_{-\frac{l_b}{2}}^{-\frac{l_p}{2}}\frac{\partial^2 u_3}{\partial p_1^2}\frac{\partial^2 \dot{u}_3^*}{\partial p_1^2}dp_1 +\\
&\quad \left(K_f^{(b)}+K_f^{(p)}\right)\int_{-\frac{l_p}{2}}^{+\frac{l_p}{2}}\frac{\partial^2 u_3}{\partial p_1^2}\frac{\partial^2 \dot{u}_3^*}{\partial p_1^2}dp_1 + 2G_f\Delta\dot{\phi}_i\left[\frac{\partial \dot{u}_3^*}{\partial p_1}\right]_{-\frac{l_p}{2}}^{\frac{l_p}{2}} +\\
&\quad K_f^{(b)}\int_{\frac{l_b}{2}}^{\frac{l_p}{2}}\frac{\partial^2 u_3}{\partial p_1^2}\frac{\partial^2 \dot{u}_3^*}{\partial p_1^2}dp_1\\
&= K_f^{(b)}\int_{-\frac{l_b}{2}}^{\frac{l_b}{2}}\frac{\partial^2 u_3}{\partial p_1^2}\frac{\partial^2 \dot{u}_3^*}{\partial p_1^2}dp_1 + K_f^{(p)}\int_{-\frac{l_p}{2}}^{+\frac{l_p}{2}}\frac{\partial^2 u_3}{\partial p_1^2}\frac{\partial^2 \dot{u}_3^*}{\partial p_1^2}dp_1\\
&\quad +2G_f\Delta\dot{\phi}_i\left[\frac{\partial \dot{u}_3^*}{\partial p_1}\right]_{-\frac{l_p}{2}}^{\frac{l_p}{2}}
\end{aligned}$$

where $K_f, K_f^{(b)}, G_f$, H are given in *Appendix B*.

4.3.2 External Powers

If the external actions are

1. a mechanical vertical force per unit length R_3
2. a mechanical moment per unit length R_θ
3. a electric current generator $\bar{\imath}$

the external powers are

$$
\begin{aligned}
\mathcal{P}_{ext}(\mathcal{B},\mathcal{V}_e) &= \bar{\iota}\Delta\dot{\phi}^* \qquad (4.106)\\
\mathcal{P}_{ext}(\mathcal{B},\mathcal{V}_m) &= \mathcal{P}_{ext}(\mathcal{B}_r,\mathcal{V}_m)+\mathcal{P}_{ext}(\mathcal{B}_c,\mathcal{V}_m)+\mathcal{P}_{ext}(\mathcal{B}_d,\mathcal{V}_m)\\
&= \int_{-\frac{l_b}{2}}^{-\frac{l_p}{2}}\left(-\left(R_\theta+\alpha^{(b)}\frac{\partial\ddot{u}_3}{\partial p_1}\right)\frac{\partial\dot{u}_3^*}{\partial p_1}+\left(R_3-\lambda^{(b)}\ddot{u}_3\right)\dot{u}_3^*\right)dp_1+\\
&\quad \int_{-\frac{l_p}{2}}^{\frac{l_p}{2}}\left(\begin{array}{c}-\left(R_\theta+\left(\alpha^{(p)}+\alpha^{(b)}\right)\frac{\partial\ddot{u}_3}{\partial p_1}\right)\frac{\partial\dot{u}_3^*}{\partial p_1}\\ +\left(R_3-\left(\lambda^{(p)}+\lambda^{(b)}\right)\ddot{u}_3\right)\dot{u}_3^*\end{array}\right)dp_1\\
&\quad \int_{\frac{l_p}{2}}^{\frac{l_b}{2}}\left(-\left(R_\theta+\alpha^{(b)}\frac{\partial\ddot{u}_3}{\partial p_1}\right)\frac{\partial\dot{u}_3^*}{\partial p_1}+\left(R_3-\lambda^{(b)}\ddot{u}_3\right)\dot{u}_3^*\right)dp_1\\
&= \int_{-\frac{l_b}{2}}^{\frac{l_b}{2}}\left(-\left(R_\theta+\alpha^{(b)}\frac{\partial\ddot{u}_3}{\partial p_1}\right)\frac{\partial\dot{u}_3^*}{\partial p_1}+\left(R_3-\lambda^{(b)}\ddot{u}_3\right)\dot{u}_3^*\right)dp_1\\
&\quad \int_{-\frac{l_p}{2}}^{\frac{l_p}{2}}\left(-\alpha^{(p)}\frac{\partial\ddot{u}_3}{\partial p_1}\frac{\partial\dot{u}_3^*}{\partial p_1}+\lambda^{(p)}\ddot{u}_3\dot{u}_3^*\right)dp_1
\end{aligned}
$$

where the explicit expressions of $\alpha=\alpha^{(b)}+\alpha^{(p)}, \lambda=\lambda^{(b)}+\lambda^{(p)}, R_3, R_\theta$ are given in *Appendix B*.

4.3.3 Power Balance

The balance of power

$$
\begin{aligned}
\mathcal{P}_{int}(\mathcal{B},\mathcal{V}_m)+\mathcal{P}_{int}(\mathcal{B},\mathcal{V}_e) &= \mathcal{P}_{ext}(\mathcal{B},\mathcal{V}_m)+\mathcal{P}_{ext}(\mathcal{B},\mathcal{V}_e) \qquad (4.107)\\
\left(\begin{array}{c}K_f^{(b)}\int_{-\frac{l_b}{2}}^{\frac{l_b}{2}}\frac{\partial^2 u_3}{\partial p_1^2}\frac{\partial^2\dot{u}_3^*}{\partial p_1^2}dp_1+\\ +K_f^{(p)}\int_{-\frac{l_p}{2}}^{+\frac{l_p}{2}}\frac{\partial^2 u_3}{\partial p_1^2}\frac{\partial^2\dot{u}_3^*}{\partial p_1^2}dp_1+\\ +2G_f\dot{\Delta\phi}_i\left[\frac{\partial\dot{u}_3^*}{\partial p_1}\right]_{-\frac{l_p}{2}}^{\frac{l_p}{2}}\\ -2G_f\left[\frac{\partial\dot{u}_3}{\partial p_1}\right]_{-\frac{l_p}{2}}^{\frac{l_p}{2}}\Delta\dot{\phi}^*\\ +2\left(\int_{-\frac{l_p}{2}}^{+\frac{l_p}{2}}H\right)\Delta\ddot{\phi}\Delta\dot{\phi}^*\end{array}\right) &= \left(\begin{array}{c}\int_{-\frac{l_b}{2}}^{\frac{l_b}{2}}\left(\begin{array}{c}-\left(R_\theta+\alpha^{(b)}\frac{\partial\ddot{u}_3}{\partial p_1}\right)\frac{\partial\dot{u}_3^*}{\partial p_1}+\\ \left(R_3-\lambda^{(b)}\ddot{u}_3\right)\dot{u}_3^*\end{array}\right)dp_1\\ -\int_{-\frac{l_p}{2}}^{\frac{l_p}{2}}\left(\begin{array}{c}\alpha^{(p)}\frac{\partial\ddot{u}_3}{\partial p_1}\frac{\partial\dot{u}_3^*}{\partial p_1}\\ +\lambda^{(p)}\ddot{u}_3\dot{u}_3^*\end{array}\right)dp_1\\ +\bar{\iota}\Delta\dot{\phi}^*\end{array}\right)
\end{aligned}
$$

must hold for each $\Delta\dot{\phi}^*\in\mathcal{R}$ and for each $u_3\in H_0^2\left([-\frac{l_b}{2},\frac{l_b}{2}]\right)$. This is also a weak formulation of the problem. It can be fruitfully applied to obtain numerical solution of the dynamical problem by means of a Galerkin Approximation.

4.4 Results Review

In this chapter a model of a PEM layered beam has been derived imposing a prescribed kinematics on a 3D Cauchy Continuum model. The following hypotheses have been assumed:

1. The beam sections remain rigid
2. Small deformations and linearized kinematics
3. No shear deformation
4. Perfect bonding between elastic and PZT layers
5. Constant electric field in the transducers
6. Uniform displacements along the thickness of the transducers equal to that of the surface in contact with the beam.

The following kinematical descriptors of the state of unidimensional electromechanical beam have been chosen

- the beam central axis transversal deflection $u_3(p_1, t)$
- the beam section attitude $\gamma = \frac{\partial u_3(p_1,t)}{\partial p_1}$
- the beam central axis longitudinal displacement $u_1(p_1, t)$
- the time primitive of the potential difference applied between the electrodes[13] $\Delta\phi(t)$

By means of the virtual power principle we have found

1. the weak and strong formulation of the equations of motion for
   (a) the *three layered PEM beam* in figure 4-3 with *in-phase* connected PZT sheets. They are given equations (4.82) and $(4.73 - 4.74)$ respectively;
   (b) the *three layered PEM beam* in figure 4-4 with *out-of-phase* connected PZT sheets. They are given equations (4.86) and $(4.76 - 4.77)$ respectively.

[13] Let us underline that the $\Delta\phi(t)$ does not depend on the spatial variable. This is beacause the surfaces of the PZT sheets are electroded, thus equipotential. This fact allows us to describe, by means of an imposed kinematics, the electric state of the transducer only by a scalar variable, defining as dual quantity the electric current I flowing throw the electric terminals. In this way the pair of PZT transducers can be electrically regarded as a two port network.

(c) an *elastic beam*. They are given by equations (4.91) and $(4.88-4.89)$, respectively. The negligibility of the rotational inertia has been discussed by means of a dimensional analysis

2. the constitutive relations for an unidimensional model of

(a) the *three layered PEM beam* in figure 4-3 with *in-phase* connected PZT sheets. They are given by

$$\begin{aligned} F &= \left(K_l^{(p)} + K_l^{(b)}\right) \frac{\partial u_1}{\partial p_1} - 2G_l \Delta \dot{\phi} \\ M &= \left(K_f^{(p)} + K_f^{(b)}\right) \frac{\partial^2 u_3}{\partial p_1^2} \\ I &= 2\int_{-\frac{l}{2}}^{\frac{l}{2}} \left(G_l \frac{\partial \dot{u}_1}{\partial p_1}\right) dp_1 + 2\Delta \ddot{\phi} \int_{-\frac{l}{2}}^{\frac{l}{2}} H \end{aligned} \tag{4.108}$$

(b) the *three layered PEM beam* in figure 4-4 with *out-of-phase* connected PZT sheets. They are given by

$$\begin{aligned} F &= \left(K_l^{(p)} + K_l^{(b)}\right) \frac{\partial u_1}{\partial p_1} \\ M &= \left(K_f^{(p)} + K_f^{(b)}\right) \frac{\partial^2 u_3}{\partial p_1^2} + 2G_f \left(\Delta \dot{\phi}\right) \\ I &= -2\int_{-\frac{l}{2}}^{\frac{l}{2}} \left(G_f \frac{\partial^2 \dot{u}_3}{\partial p_1^2}\right) dp_1 + 2\Delta \ddot{\phi} \int_{-\frac{l}{2}}^{\frac{l}{2}} H \end{aligned} \tag{4.109}$$

where F, M are the axial force and moment acting representing the contact actions in the unidimensional model of the beam, and I is the current flowing through the electric terminals of the PZT sheets. The expressions and the physical dimensions of all the quantities introduced are reported in *Appendix B*

3. how and by which hypotheses the interaction between the structure and the PZT patches can be reduced to the simple model that is represented in figure 4-8 for the flexural coupling and in figure 4-7 for the extensional coupling.

Hence we have understood the physical behavior of a beam with bonded PZT transducers studying the equations of motions and the boundary conditions derived for some meaningful situations. As outlined with an example in the last section of this chapter the power expressions for the simple cases that have been considered explicitly will *allow us to derive the model of a complex system by means of the virtual power principle following an assembling procedure*. The last

point will be crucial in the following chapters and, in general, to obtain numerical solution for the dynamical problem of complex PEM systems. .

Chapter 5

Periodic PEM Structures and Homogenized Models

The main idea of this work is to design and analyze electromechanical systems with distributed piezoelectric coupling for the suppression of mechanical vibrations. An unidimensional periodic PiezoElectroMechanical structure with distributed coupling can be physically realized interconnecting an array of PZT transducers bonded on an elastic beam with a lumped electric transmission line, as sketched in figure 5-1. In the present chapter both a refined and an homogenized model of that periodic system will be developed. The refined model will be deduced gathering the representations of its parts that have been derived in the previous chapters[1]. In this context we will make use of the additivity of the virtual powers. The constitutive equations of the homogenized model will be derived by those of the refined one by means of a kinematical mapping.

The homogenized model provide a rough description of the system valid only to analyze perturbations with a characteristic wave length greater than the dimensions of the basic cell. However it allows us to infer important qualitative thumbnail information (see the following chapter) about the behavior of the PEM structure. Indeed its mathematical model will be reduced[2] to two coupled Partial Differential Equations (PDE) whose dimensionless form will be provided.

Both the cases of *longitudinal-electric* coupling and *flexural-electric* coupling will be treated.

[1] See Chapter 3 for the transmission line, and Chapter 4 for the beam with PZT transducers.

[2] The refined model is mathematically represented by a system of a partial differential equation coupled with N ordinary differential equations, where N is the number of cells composing the modular system.

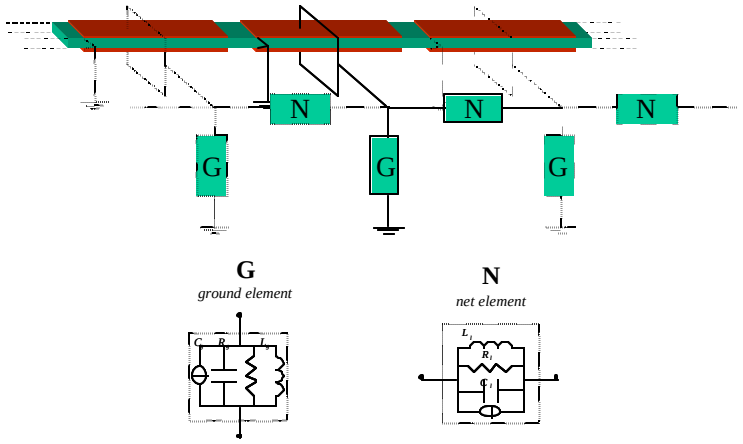

Figure 5-1: Basic cell of the periodic PEM structure

5.1 Bending Coupling

Let us derive both the refined and the homogenized model of a periodic piezoelectromechanical system whose basic cell is represented in figure 5-1.

5.1.1 Refined Model of the Basic Cell

The generic cell of the system is represented in figure 5-1. Let us denote it by $\mathcal{S}_i$. It can be thought as the union of

1. a piezoelastic beam $\mathcal{B}_i$ whose model has been derived as studied in Chapter 4;
2. a RLC parallel element to ground $\mathcal{G}_i$ whose model has been derived in Chapter 3;
3. a line RLC parallel element $\mathcal{L}_i$ whose model has been derived in Chapter 3.

Thus

$$\mathcal{S}_i = \mathcal{B}_i \cup \mathcal{G}_i \cup \mathcal{L}_i \tag{5.1}$$

where the parts $\mathcal{B}_i, \mathcal{G}_i, \mathcal{L}_i$ have been studied in the previous chapters and an expression for their powers has been already given. In the reference fixed in figure 5-1 the beam central axis is the set

$$\mathcal{A}_i \equiv \{\mathbf{p} = p_1 \mathbf{e}_1 : p_1 \in [-\frac{l_e}{2}, \frac{l_e}{2}]\} \tag{5.2}$$

We will focus our attention on the flexural behavior of the beam and we will not describe the extensional mode. Indeed because of the assumed electric connections and the symmetry the

extensional mode is uncoupled from the flexural-electric mode. Assuming all the hypotheses $(1-6)$ introduced in 4.1.2, the state of $\mathcal{S}_i$ can be described by the set of virtual velocities

$$\mathcal{V} = \mathcal{V}_m \cup \mathcal{V}_e \tag{5.3}$$

with

$$\mathcal{V}_m = \{\dot{u}_r^*, \frac{\partial \dot{u}_r^*}{\partial p_1}, \frac{\partial^2 \dot{u}_r^*}{\partial p_1^2}\} \quad \mathcal{V}_e = \{\dot{\phi}_r^*, \dot{\xi}_r^*\} \tag{5.4}$$

where

- $u_r = \hat{u}_r(p_1)$ is the vertical displacement of the beam central axis and is defined on $\mathcal{A}_i$,
- ϕ_r is the time primitive of the electric potential difference across the PZT layers and the RLC element to ground $\mathcal{G}_i$,
- ξ_r is the time primitive of the potential difference across the line RLC element $\mathcal{L}_i$.

The power for the generic cell $\mathcal{S}_i$ can be easily derived by assembling the expressions that have been found in the previous chapters. Indeed for the additivity of the powers we can write

$$\mathcal{P}(\mathcal{S}_i) = \mathcal{P}(\mathcal{B}_i) + \mathcal{P}(\mathcal{G}_i) + \mathcal{P}(\mathcal{L}_i)$$

Notation 6 *In the following we will denote by*

$$\mathcal{P}(\mathcal{B}, v^*) \tag{5.5}$$

the virtual power expended on the virtual velocity v^* in the part $\mathcal{B}$. When v^* is omitted all the virtual velocities are implicitly considered. Moreover we will indicate by a subscript $_{int}$ the virtual power of the internal forces, and by $_{ext}$ the virtual power of the external forces.

Internal Power By the expressions of the previous chapters

$$\begin{aligned} \mathcal{P}_{int}(\mathcal{B}_i) &= \mathcal{P}_{int}(\mathcal{B}_i, \frac{\partial^2 \dot{u}_r^*}{\partial p_1^2}) + \mathcal{P}_{int}(\mathcal{B}_i, \dot{\phi}_r^*) \\ \mathcal{P}_{int}(\mathcal{G}_i) &= \mathcal{P}_{int}(\mathcal{G}_i, \dot{\phi}_r^*) \\ \mathcal{P}_{int}(\mathcal{L}_i) &= \mathcal{P}_{int}(\mathcal{L}_i, \dot{\xi}_r^*) \end{aligned} \tag{5.6}$$

where

$$\begin{aligned}
\mathcal{P}_{int}(\mathcal{B}_i, \frac{\partial^2 \dot{u}_r^*}{\partial p_1^2}) &= \int_{-\frac{l_b}{2}}^{\frac{l_b}{2}} K_f^{(b)} \frac{\partial^2 u_r}{\partial p_1^2} \frac{\partial^2 \dot{u}_r^*}{\partial p_1^2} dp_1 + \int_{-\frac{l_p}{2}}^{+\frac{l_p}{2}} K_f^{(p)} \frac{\partial^2 u_r}{\partial p_1^2} \frac{\partial^2 \dot{u}_r^*}{\partial p_1^2} dp_1 \qquad (5.7)\\
&\quad + 2\dot{\phi}_r \int_{-\frac{l_p}{2}}^{+\frac{l_p}{2}} G_f \frac{\partial^2 \dot{u}_r^*}{\partial p_1^2} dp_1 \\
\mathcal{P}_{int}(\mathcal{B}_i, \dot{\phi}_r^*) &= -2\dot{\phi}_r^* \int_{-\frac{l_p}{2}}^{+\frac{l_p}{2}} G_f \frac{\partial^2 \dot{u}_r}{\partial p_1^2} dp_1 + 2 \int_{-\frac{l_p}{2}}^{+\frac{l_p}{2}} H \ddot{\phi}_r \dot{\phi}_r^* \qquad (5.8)\\
\mathcal{P}_{int}(\mathcal{G}_r, \dot{\phi}_r^*) &= \eta_r \dot{\phi}_r^* \qquad (5.9)\\
&= C_g \frac{d^2 \phi_r}{dt^2} \dot{\phi}_r^* + \frac{1}{R_g} \frac{d\phi_r}{dt} \dot{\phi}_r^* + \frac{1}{L_g} \phi_r \dot{\phi}_r^* \\
\mathcal{P}_{int}(\mathcal{L}_i, \dot{\xi}_i^*) &= \iota_r \dot{\xi}_r^* \qquad (5.10)\\
&= C_l \frac{d^2 \xi_r}{dt^2} \dot{\xi}_r^* + \frac{1}{R_g} \frac{d\xi_r}{dt} \dot{\xi}_r^* + \frac{1}{L_g} \xi_r \dot{\xi}_r^*
\end{aligned}$$

External Power By the expressions deduced in the previous chapters

$$\begin{aligned}
\mathcal{P}_{ext}(\mathcal{B}_i) &= \mathcal{P}_{ext}(\mathcal{B}_i, \dot{u}_r^*) + \mathcal{P}_{ext}(\mathcal{B}_i, \frac{\partial \dot{u}_r^*}{\partial p_1}) \\
\mathcal{P}_{ext}(\mathcal{G}_i) &= \mathcal{P}_{ext}(\mathcal{G}_i, \dot{\phi}_r^*) \\
\mathcal{P}_{ext}(\mathcal{L}_i) &= \mathcal{P}_{ext}(\mathcal{L}_i, \dot{\xi}_r^*)
\end{aligned}$$

where

$$\begin{aligned}
\mathcal{P}_{ext}(\mathcal{B}_i, \dot{u}_r^*) &= \int_{-\frac{l_b}{2}}^{\frac{l_b}{2}} \left(R_3 - \lambda^{(b)} \ddot{u}_r \right) \dot{u}_r^* dp_1 - \int_{-\frac{l_p}{2}}^{\frac{l_p}{2}} \lambda^{(p)} \ddot{u}_r \dot{u}_r^* dp_1 \qquad (5.11)\\
\mathcal{P}_{ext}(\mathcal{B}_i, \frac{\partial \dot{u}_r^*}{\partial p_1}) &= -\int_{-\frac{l_b}{2}}^{\frac{l_b}{2}} \left(R_\theta + \alpha^{(b)} \frac{\partial \ddot{u}_r}{\partial p_1} \right) \frac{\partial \dot{u}_r^*}{\partial p_1} dp_1 - \int_{-\frac{l_p}{2}}^{\frac{l_p}{2}} \alpha^{(p)} \frac{\partial \ddot{u}_r}{\partial p_1} \frac{\partial \dot{u}_r^*}{\partial p_1} dp_1 \qquad (5.12)\\
\mathcal{P}_{ext}(\mathcal{G}_i, \dot{\phi}_r^*) &= I_r \dot{\phi}_r^* \qquad (5.13)\\
\mathcal{P}_{ext}(\mathcal{L}_i, \dot{\xi}_r^*) &= Y_r \dot{\xi}_r^* \qquad (5.14)
\end{aligned}$$

Power Balance The power balance for the basic cell of the periodic system can be easily written imposing the equality between the internal and external powers. Moreover a weak formulation for a modular system can be derived by writing its internal and external powers as a sum of those of its cells and equating them.

5.1.2 Homogenized Continuous Model

Let us define an electromechanical straight axis beam as the unidimensional continuum whose configuration is described by the three scalar valued fields

$$\{u, \gamma, \phi\} \tag{5.15}$$

defined on the unidimensional domain

$$\mathcal{A} = \{\mathbf{p} \in \mathcal{E} : \mathbf{p} = p_1 \mathbf{e}_1\} \tag{5.16}$$

where $\mathcal{C} = \{\mathbf{o}, \mathbf{e}_1, \mathbf{e}_2, \mathbf{e}_3\}$ is an opportunely chosen Cartesian reference and u, γ, ϕ represent respectively the vertical displacement of the beam axis, the rotation of the beam sections and the electrical potential referred to ground. Here it is assumed that the beam is constrained to move in the $\mathbf{e}_1 - \mathbf{e}_3$ plane. With a first order gradient theory in all the variables the following set of virtual velocities can be chosen

$$\mathcal{V} = \{\dot{u}^*, \frac{\partial \dot{u}^*}{\partial p_1}, \dot{\gamma}^*, \frac{\partial \dot{\gamma}^*}{\partial p_1}, \dot{\phi}^*, \frac{\partial \dot{\phi}^*}{\partial p_1}\} \tag{5.17}$$

We will assume a linear theory and that the beam is not shear deformable, thus

$$\dot{\gamma}^* = \frac{\partial \dot{u}^*}{\partial p_1} \tag{5.18}$$

and the set of virtual velocities can be reduced to

$$\mathcal{V} = \{\dot{u}^*, \frac{\partial \dot{u}^*}{\partial p_1}, \frac{\partial^2 \dot{u}^*}{\partial p_1^2}, \dot{\phi}^*, \frac{\partial \dot{\phi}^*}{\partial p_1}\} \tag{5.19}$$

Virtual Powers

The virtual powers are written as a linear functional on the virtual velocities. As usual we will distinguish between internal and external virtual powers.

Internal Virtual Powers Let us split the internal power in the sum of the contributions relative to each objective element of (5.19)

$$\mathcal{P}_{int}(\mathcal{A}) = \mathcal{P}_{int}(\mathcal{A}, \frac{\partial^2 \dot{u}^*}{\partial p_1^2}) + \mathcal{P}_{int}(\mathcal{A}, \dot{\phi}^*) + \mathcal{P}_{int}(\mathcal{A}, \frac{\partial \dot{\phi}^*}{\partial p_1}) \tag{5.20}$$

Thus the following internal actions are identified

$$\begin{array}{ll} \mathcal{P}_{int}(\mathcal{A}, \frac{\partial^2 \dot{u}^*}{\partial p_1^2}) = \int_{\mathcal{A}} M \frac{\partial^2 \dot{u}^*}{\partial p_1^2} & \mathcal{P}_{int}(\mathcal{A}, \dot{\phi}^*) = \int_{\mathcal{A}} \eta \dot{\phi}^* \\ \mathcal{P}_{int}(\mathcal{A}, \frac{\partial \dot{\phi}^*}{\partial p_1}) = \int_{\mathcal{A}} \iota \frac{\partial \dot{\phi}^*}{\partial p_1} & \end{array} \tag{5.21}$$

External Virtual Powers The external powers are

$$\mathcal{P}_{ext}(\mathcal{A}) = \mathcal{P}_{ext}(\mathcal{A}, \dot{u}^*) + \mathcal{P}_{ext}(\mathcal{A}, \frac{\partial \dot{u}^*}{\partial p_1}) + \mathcal{P}_{ext}(\mathcal{A}, \dot{\phi}^*) + \mathcal{P}_{ext}(\mathcal{A}, \frac{\partial \dot{\phi}^*}{\partial p_1}) \tag{5.22}$$

and the following external actions are identified

$$\begin{array}{ll} \mathcal{P}_{ext}(\mathcal{A}, \dot{u}^*) = \int_{\mathcal{A}} F_3 \dot{u}^* & \mathcal{P}_{ext}(\mathcal{A}, \frac{\partial \dot{u}^*}{\partial p_1}) = \int_{\mathcal{A}} F_\theta \frac{\partial \dot{u}^*}{\partial p_1} \\ \mathcal{P}_{ext}(\mathcal{A}, \dot{\phi}^*) = \int_{\mathcal{A}} \bar{I} \dot{\phi}^* & \mathcal{P}_{ext}(\mathcal{A}, \frac{\partial \dot{\phi}^*}{\partial p_1}) = \int_{\mathcal{A}} \bar{Y} \frac{\partial \dot{\phi}^*}{\partial p_1} \end{array} \tag{5.23}$$

Power Balance

By the principle of the Virtual Power the following power balance must hold for each regular virtual velocity ($\mathcal{P}_{int}(\mathcal{A}) = \mathcal{P}_{ext}(\mathcal{A})$)

$$\int_{\mathcal{A}} M \frac{\partial^2 \dot{u}^*}{\partial p_1^2} + \int_{\mathcal{A}} \eta \dot{\phi}^* + \int_{\mathcal{A}} \iota \frac{\partial \dot{\phi}^*}{\partial p_1} = \left(\begin{array}{c} \int_{\mathcal{A}} F_3 \dot{u}^* + \int_{\mathcal{A}} F_\theta \frac{\partial \dot{u}^*}{\partial p_1} + \\ + \int_{\mathcal{A}} \bar{I} \dot{\phi}^* + \int_{\mathcal{A}} \bar{Y} \frac{\partial \dot{\phi}^*}{\partial p_1} \end{array} \right) \tag{5.24}$$

Equilibrium Equations

Integrating by parts the terms of (5.24) containing the spatial derivatives of $\dot{u}^*$ and of $\dot{\phi}^*$ we obtain

$$\begin{array}{rcl} \int_{\mathcal{A}} M \frac{\partial^2 \dot{u}^*}{\partial p_1^2} + \int_{\mathcal{A}} \eta \dot{\phi}^* + \int_{\mathcal{A}} \iota \frac{\partial \dot{\phi}^*}{\partial p_1} & = & \left(\begin{array}{c} \int_{\mathcal{A}} F_3 \dot{u}^* + \int_{\mathcal{A}} F_\theta \frac{\partial \dot{u}^*}{\partial p_1} \\ + \int_{\mathcal{A}} \bar{I} \dot{\phi}^* + \int_{\mathcal{A}} \bar{Y} \frac{\partial \dot{\phi}^*}{\partial p_1} \end{array} \right) \\ \left(\begin{array}{c} \left[M \frac{\partial \dot{u}^*}{\partial p_1} \right]_{\partial \mathcal{A}} - \left[\frac{\partial M}{\partial p_1} \dot{u}^* \right]_{\partial \mathcal{A}} + \int_{\mathcal{A}} \frac{\partial^2 M}{\partial p_1^2} \dot{u}^* + \\ \int_{\mathcal{A}} \eta \dot{\phi}^* + \left[\iota \dot{\phi}^* \right]_{\partial \mathcal{A}} - \int_{\mathcal{A}} \frac{\partial \iota}{\partial p_1} \dot{\phi}^* \end{array} \right) & = & \left(\begin{array}{c} \int_{\mathcal{A}} F_3 \dot{u}^* + [F_\theta \dot{u}^*]_{\partial \mathcal{A}} - \int_{\mathcal{A}} \frac{\partial F_\theta}{\partial p_1} \dot{u}^* + \\ \int_{\mathcal{A}} \bar{I} \dot{\phi}^* + \left[\bar{Y} \dot{\phi}^* \right]_{\partial \mathcal{A}} - \int_{\mathcal{A}} \frac{\partial \bar{Y}}{\partial p_1} \dot{\phi}^* \end{array} \right) \\ \left(\begin{array}{c} \left[M \frac{\partial \dot{u}^*}{\partial p_1} \right]_{\partial \mathcal{A}} - \left[\frac{\partial M}{\partial p_1} \dot{u}^* \right]_{\partial \mathcal{A}} + \left[\iota \dot{\phi}^* \right]_{\partial \mathcal{A}} + \\ \int_{\mathcal{A}} \left(\frac{\partial^2 M}{\partial p_1^2} - F_3 + \frac{\partial F_\theta}{\partial p_1} \right) \dot{u}^* \end{array} \right) & = & \left(\begin{array}{c} [F_\theta \dot{u}^*]_{\partial \mathcal{A}} + \left[\bar{Y} \dot{\phi}^* \right]_{\partial \mathcal{A}} - \\ \int_{\mathcal{A}} \left(\eta - \frac{\partial \iota}{\partial p_1} - \bar{I} + \frac{\partial \bar{Y}}{\partial p_1} \right) \dot{\phi}^* \end{array} \right) \end{array} \tag{5.25}$$

Since the virtual velocities are arbitrary the following equilibrium equations are derived

$$\frac{\partial^2 M}{\partial p_1^2} = F_3 - \frac{\partial F_\theta}{\partial p_1} \tag{5.26}$$

$$\eta - \frac{\partial \iota}{\partial p_1} = \bar{I} - \frac{\partial \bar{Y}}{\partial p_1} \tag{5.27}$$

if the boundary conditions are such that

$$[-F_\theta \dot{u}^*]_{\partial\mathcal{A}} + \left[M\frac{\partial \dot{u}^*}{\partial p_1}\right]_{\partial\mathcal{A}} - \left[\frac{\partial M}{\partial p_1}\dot{u}^*\right]_{\partial\mathcal{A}} + \left[\left(\iota - \bar{Y}\right)\dot{\phi}^*\right]_{\partial\mathcal{A}} = 0 \tag{5.28}$$

Remark 22 *Equation (5.28) is a constraint imposed on the boundary condition by the adopted formulation with the virtual power principle. We say that boundary conditions that satisfy (5.28) are* ideal. *In the following we will assume that (5.28) is verified.*

Constitutive Equations

Kinematical Map If dynamical phenomena with a wave length $\lambda_w \gg l_e$, where l_e is the dimension of the basic cell of the periodic system are considered, the continuous fields can be approximated on each cell by a constant.

With this idea we impose the following kinematical mapping between the descriptors of the refined and homogenized models [3]

$$\begin{array}{lll} u_r \to u & u_r' \to u' & u_r'' \to u'' \\ \phi_r \to \phi & & \frac{\xi_r}{d} \to \phi' \end{array} \tag{5.29}$$

Power Balance

Notation 7 *The homogenized material constants will be denoted by the same letters of the refined ones adding a "$^-$". In general they will not have the same physical dimensions.*

Imposing the balance of the powers expended in corresponding (by 5.29) virtual velocities and considering the mapping 5.29, by the arbitrariness of the virtual velocities, the following constitutive equations for the homogenized model have been found[4]

$$\begin{array}{c} M = \bar{K}_f u'' + \bar{G}_f \dot{\phi} \\ \eta = -\bar{G}_f \dot{u}'' + \frac{1}{\bar{L}_g}\phi + \frac{1}{\bar{R}_g}\dot{\phi} + \bar{C}_g \ddot{\phi} \quad \iota = \frac{1}{\bar{L}_l}\phi' + \frac{1}{\bar{R}_l}\dot{\phi}' + \bar{C}_l \ddot{\phi}' \end{array} \tag{5.30}$$

[3] The quantities relative to the refined model are denoted by a subscripted "$_r$"

[4] These have been obtained by means of a Mathematica code.

where

$$\begin{array}{cc} \bar{K}_f = \frac{1}{l_e}\left(\int_{-\frac{l_e}{2}}^{\frac{l_e}{2}} K_f^{(b)} dp_1 + \int_{-\frac{l_p}{2}}^{\frac{l_p}{2}} K_f^{(p)} dp_1\right) & \bar{C}_l = C_l l_e \\ \bar{G}_f = \frac{2}{l_e}\int_{-\frac{l_p}{2}}^{\frac{l_p}{2}} G_f^{(p)} dp_1 & \bar{C}_g = \frac{C_g + 2l_p H}{l_e} \\ \bar{L}_l = \frac{L_l}{l_e} & \bar{R}_l = \frac{R_l}{l_e} \\ \bar{L}_g = L_g l_e & \bar{R}_g = R_g l_e \end{array} \tag{5.31}$$

The external actions in the homogenized model are given by

$$\begin{array}{cc} F_3 = R_3 - \bar{\lambda}\ddot{u} & F_\theta = R_\theta + \bar{\alpha}\ddot{u}' \\ \bar{I} = I_r & \bar{Y} = \frac{Y_r}{l_e} \end{array} \tag{5.32}$$

where

$$\bar{\lambda} = \frac{1}{l_e}\left(\int_{-\frac{l_e}{2}}^{\frac{l_e}{2}} \lambda^{(b)} dp_1 + \int_{-\frac{l_p}{2}}^{\frac{l_p}{2}} \lambda^{(p)} dp_1\right) \tag{5.33}$$

$$\bar{\alpha} = \frac{1}{l_e}\left(\int_{-\frac{l_e}{2}}^{\frac{l_e}{2}} \alpha^{(b)} dp_1 + \int_{-\frac{l_p}{2}}^{\frac{l_p}{2}} \alpha^{(p)} dp_1\right) \tag{5.34}$$

Equations of motion Substituting the constitutive relations in the equilibrium equations (5.26) we get the homogenized equations of motion for the coupled electromechanical continuum in a strong form

$$\left(\bar{K}_f u''\right)'' + \left(\bar{G}_f \dot{\phi}\right)'' + \bar{\lambda}\ddot{u} + \left(\bar{\alpha}\ddot{u}'\right)' = F_3 - F_\theta' \tag{5.35}$$

$$\frac{1}{\bar{L}_g}\phi + \frac{1}{\bar{R}_g}\dot{\phi} + \bar{C}_g\ddot{\phi} - \left(\frac{1}{\bar{L}_l}\phi'\right)' - \left(\frac{1}{\bar{R}_l}\dot{\phi}'\right)' - \left(\bar{C}_l\ddot{\phi}'\right)' - \bar{G}_f\dot{u}'' = \bar{I} - \bar{Y}' \tag{5.36}$$

Since we consider systems that are constituted by an array of identical cells, the homogenized material characteristics are constant in space. Thus we can rewrite the equation of motion as

$$\bar{K}_f u'''' + \bar{G}_f\dot{\phi}'' + \bar{\lambda}\ddot{u} + \bar{\alpha}\ddot{u}'' = F_3 - F_\theta' \tag{5.37}$$

$$\frac{1}{\bar{L}_g}\phi + \frac{1}{\bar{R}_g}\dot{\phi} + \bar{C}_g\ddot{\phi} - \frac{1}{\bar{L}_l}\phi'' - \frac{1}{\bar{R}_l}\dot{\phi}'' - \bar{C}_l\ddot{\phi}'' - \bar{G}_f\dot{u}'' = \bar{I} - \bar{Y}' \tag{5.38}$$

The electrical $(\bar{I}, -\bar{Y}')$ and mechanical $(F_3, -F_\theta')$ forcing terms can vanish and the homogeneous system corresponding to (5.37) is easily obtained.

Dimensionless From The equations can be conveniently rewritten in dimensionless form introducing new dimensionless variables such that

$$\begin{array}{cccc} u = u_0 v & t = t_0 \tau & p_1 = x_0 x & \phi = \phi_0 \psi \\ F_3 = F_{30} P_3 & F_\theta = F_{\theta 0} P_\theta & \bar{I} = \bar{I}_0 \bar{I}^a & \bar{Y} = \bar{Y}_0 \bar{Y}^a \end{array} \tag{5.39}$$

They becomes

$$\left(\begin{array}{c} \frac{\bar{K}_f u_0}{x_0^4} \frac{\partial^4 v}{\partial x^4} + \frac{\bar{G}_f \phi_0}{x_0^2 t_0} \frac{\partial^3 \psi}{\partial x^2 \partial \tau} \\ + \frac{\bar{\lambda} u_0}{t_0^2} \frac{\partial^2 v}{\partial \tau^2} + \frac{\bar{\alpha} u_0}{x_0^2 t_0^2} \frac{\partial^4 v}{\partial x^2 \partial \tau^2} \end{array} \right) = F_{30} P_3 - \frac{F_{\theta 0}}{x_0} \frac{\partial P_\theta}{\partial x} \tag{5.40}$$

$$\left(\begin{array}{c} \frac{\phi_0}{\bar{L}_g} \psi + \frac{\phi_0}{\bar{R}_g t_0} \frac{\partial \psi}{\partial \tau} + \frac{\bar{C}_g \phi_0}{t_0^2} \frac{\partial^2 \psi}{\partial \tau^2} - \frac{\phi_0}{\bar{L}_l x_0^2} \frac{\partial^2 \psi}{\partial x^2} \\ - \frac{\phi_0}{\bar{R}_l x_0^2 t_0} \frac{\partial^3 \psi}{\partial x^2 \partial \tau} - \frac{\bar{C}_l \phi_0}{x_0^2 t_0^2} \frac{\partial^4 \psi}{\partial x^2 \partial \tau^2} - \frac{\bar{G}_f u_0}{x_0^2 t_0} \frac{\partial^3 v}{\partial x^2 \partial \tau} \end{array} \right) = \bar{I}_0 \bar{I}^a - \frac{\bar{Y}_0}{x_0} \frac{\partial \bar{Y}^a}{\partial x} \tag{5.41}$$

or, equivalently,

$$\left(\begin{array}{c} \frac{\partial^2 v}{\partial \tau^2} + \frac{t_0^2 \bar{K}_f}{\bar{\lambda} x_0^4} \frac{\partial^4 v}{\partial x^4} + \\ + \frac{t_0^2 \bar{G}_f \phi_0}{\bar{\lambda} u_0 x_0^2 t_0} \frac{\partial^3 \psi}{\partial x^2 \partial \tau} + \frac{\bar{\alpha}}{\bar{\lambda} x_0^2} \frac{\partial^4 v}{\partial x^2 \partial \tau^2} \end{array} \right) = \frac{t_0^2 F_{30}}{\bar{\lambda} u_0} P_3 - \frac{t_0^2 F_{\theta 0}}{\bar{\lambda} u_0 x_0} \frac{\partial P_\theta}{\partial x} \tag{5.42}$$

$$\left(\begin{array}{c} \frac{\partial^2 \psi}{\partial \tau^2} + \frac{t_0^2}{\bar{C}_g \bar{L}_g} \psi + \frac{t_0}{\bar{C}_g \bar{R}_g} \frac{\partial \psi}{\partial \tau} - \frac{t_0^2}{\bar{C}_g \bar{L}_l x_0^2} \frac{\partial^2 \psi}{\partial x^2} \\ - \frac{t_0}{\bar{C}_g \bar{R}_l x_0^2} \frac{\partial^3 \psi}{\partial x^2 \partial \tau} - \frac{\bar{C}_l}{\bar{C}_g x_0^2} \frac{\partial^4 \psi}{\partial x^2 \partial \tau^2} - \frac{\bar{G}_f t_0 u_0}{\bar{C}_g x_0^2 \phi_0} \frac{\partial^3 v}{\partial x^2 \partial \tau} \end{array} \right) = \frac{t_0^2 \bar{I}_0}{\bar{C}_g \phi_0} \bar{I}^a - \frac{t_0^2 \bar{Y}_0}{\bar{C}_g \phi_0 x_0} \frac{\partial \bar{Y}^a}{\partial x} \tag{5.43}$$

Defining the dimensionless coefficients

$$\begin{array}{cccc} \alpha = \frac{t_0^2 \bar{K}_f}{\bar{\lambda} x_0^4} & \gamma_1 = \frac{\bar{G}_f t_0 \phi_0}{\bar{\lambda} u_0 x_0^2} & \gamma_2 = \frac{\bar{G}_f t_0 u_0}{\bar{C}_g x_0^2 \phi_0} & \\ \beta_l^2 = \frac{t_0^2}{\bar{C}_g \bar{L}_l x_0^2} & 2\delta_l = \frac{t_0}{\bar{C}_g \bar{R}_l x_0^2} & \rho = \frac{\bar{\alpha}}{\bar{\lambda} x_0^2} & \\ \beta_g^2 = \frac{t_0^2}{\bar{C}_g \bar{L}_g} & 2\delta_g = \frac{t_0}{\bar{C}_g \bar{R}_g} & \kappa = \frac{\bar{C}_l}{\bar{C}_g x_0^2} & \\ \chi_1 = \frac{t_0^2 F_{30}}{\bar{\lambda} u_0} & \chi_2 = \frac{t_0^2 F_{\theta 0}}{\bar{\lambda} u_0 x_0} & \chi_3 = \frac{t_0^2 \bar{I}_0}{\bar{C}_g \phi_0} & \chi_4 = \frac{t_0^2 \bar{Y}_0}{\bar{C}_g \phi_0 x_0} \end{array} \tag{5.44}$$

and choosing the dimensionless time t_0 and the dimensionless electric variable ϕ_0 such that

$$t_0 = \sqrt{\frac{\bar{\lambda}}{\bar{K}_f}} x_0^2 \quad \phi_0 = \sqrt{\frac{\bar{\lambda}}{\bar{C}_g}} u_0 \tag{5.45}$$

the dimensionless parameters

$$\begin{array}{cccc} \alpha = 1 & \gamma_1 = \gamma & \gamma_2 = \gamma & \gamma = \frac{\bar{G}_f}{\sqrt{\bar{C}_g \bar{K}_f}} \\ \beta_l = \sqrt{\frac{\bar{\lambda}}{\bar{K}_f \bar{C}_g L_l}} x_0 & \delta_l = \frac{1}{2\bar{C}_g \bar{R}_l x_0^2} \sqrt{\frac{\bar{\lambda}}{\bar{K}_f}} x_0^2 & \rho = \frac{\bar{\alpha}}{\bar{\lambda} x_0^2} & \\ \beta_g = \sqrt{\frac{\bar{\lambda}}{\bar{K}_f \bar{C}_g \bar{L}_g}} x_0^2 & \delta_g = \frac{1}{2\bar{C}_g \bar{R}_g} \sqrt{\frac{\bar{\lambda}}{\bar{K}_f}} x_0^2 & \kappa = \frac{\bar{C}_l}{\bar{C}_g x_0^2} & \\ \chi_1 = \frac{x_0^4 F_{30}}{u_0 \bar{K}_f} & \chi_2 = \frac{x_0^3 F_{\theta 0}}{u_0 \bar{K}_f} & \chi_3 = \sqrt{\frac{\bar{\lambda}}{\bar{C}_g}} \frac{x_0^4 \bar{I}_0 u_0}{\bar{K}_f} & \chi_4 = \sqrt{\frac{\bar{\lambda}}{\bar{C}_g}} \frac{x_0^3 u_0 \bar{Y}_0}{\bar{K}_f} \end{array} \tag{5.46}$$

are found and the equations (5.42) can be rewritten as

$$v'''' + \rho \ddot{v}'' + \gamma \dot{\psi}'' + \ddot{v} = \chi_1 P_3 - \chi_2 P_g' \tag{5.47}$$

$$-\kappa \ddot{\psi}'' - 2\delta_l \dot{\psi}'' - \gamma \dot{v}'' - \beta_l^2 \psi'' + \ddot{\psi} + 2\delta_g \dot{\psi} + \beta_g^2 \psi = \chi_3 \bar{I}^a - \chi_4 \bar{Y}' \tag{5.48}$$

where the symbols $\dot{}$ and $'$ are redefined as the *dimensionless* temporal and spatial partial derivatives.

For sake of simplicity in the following we will consider particular cases in which some of the electrical elements of the basic cell vanish or tend to infinity. Since, as it has been shown in the previous chapter, the dimensionless parameter ρ in the common applications is very small, we will pose $\rho = 0$

Vanishing Ground Element Let us consider the case in which

$$\begin{array}{cc} L_g \to \infty & R_g \to \infty \\ C_l \to 0 & \rho \to 0 \end{array} \Longrightarrow \begin{array}{cc} \beta_g \to 0 & \beta_g \delta_g \to 0 \\ \kappa \to 0 & \rho \to 0 \end{array} \tag{5.49}$$

Hence the equations (5.37) simplify to

$$v'''' + \gamma \dot{\psi}'' + \ddot{v} = \chi_1 P_3 - \chi_2 P_g' \tag{5.50}$$

$$-2\delta_l \dot{\psi}'' - \gamma \dot{v}'' - \beta_l^2 \psi'' + \ddot{\psi} = \chi_3 \bar{I}^a - \chi_4 \left(\bar{Y}^a\right)' \tag{5.51}$$

If also the line resistance is absent ($R_l \to \infty$, since parallel connected) then the system is conservative[5] and since $\delta_l \to 0$ the equations of motion reduce to

$$\begin{aligned} v'''' + \gamma \dot{\psi}'' + \ddot{v} &= \chi_1 P_3 - \chi_2 P_g' \\ -\gamma \dot{v}'' - \beta_l^2 \psi'' + \ddot{\psi} &= \chi_3 \bar{I}^a - \chi_4 \left(\bar{Y}^a\right)' \end{aligned} \tag{5.52}$$

[5] In this definition we have not considered the external forces.

Vanishing Line Element If

$$\left\{ \begin{array}{lll} L_l \to \infty & R_l \to \infty & \\ C_l \to 0 & \bar{Y}^a \to 0 & \rho \to 0 \end{array} \right. \Longrightarrow \left\{ \begin{array}{ll} \beta_l \to 0 & \delta_l \to 0 \\ \kappa \to 0 & \end{array} \right. \tag{5.53}$$

then the following equations are obtained

$$v'''' + \gamma \dot{\psi}'' + \ddot{v} = \chi_1 P_3 - \chi_2 P_g' \tag{5.54}$$

$$-\gamma \dot{v}'' + \ddot{\psi} + 2\delta_g \dot{\psi} + \beta_g^2 \psi = \chi_3 \bar{I}^a \tag{5.55}$$

The correspondent conservative case is obtained with $R_g \to \infty$

$$v'''' + \gamma \dot{\psi}'' + \ddot{v} = \chi_1 P_3 - \chi_2 P_g' \tag{5.56}$$

$$-\gamma \dot{v}'' + \ddot{\psi} + \beta_g^2 \psi = \chi_3 \bar{I}^a - \chi_4 \left(\bar{Y}^a \right)' \tag{5.57}$$

5.2 Extensional Coupling

If the PZT layers of each module are electrically connected in phase as in figure 4-4, then the state variable in the electric network is coupled with the extensional mode of the mechanical beam. As has been underlined before, the bending mode of the beam is uncoupled from the extensional one because of the geometric and materials symmetries. Hence focusing our attention on the electromechanical coupling, we will consider only the extensional-electric modes of the beam. The model procedure followed in the previous section we will quickly repeat for the new case, to derive equations analogous to (5.47) for the extensional coupling.

5.2.1 Refined Model of the Basic Cell

Kinematics

The following set of virtual velocities can be chosen

$$\mathcal{V}_m = \{\dot{u}_r^*, \tfrac{\partial \dot{u}_r^*}{\partial p_1}\} \quad \mathcal{V}_e = \{\dot{\phi}_r^*, \dot{\xi}_r^*\} \tag{5.58}$$

$$\mathcal{V} = \mathcal{V}_m \cup \mathcal{V}_e \tag{5.59}$$

where

- $u_r = \hat{u}_r(p_1, t)$ is the *axial* displacement of the beam central axis and is defined on $\mathcal{A}_i$,
- ϕ_r is the time primitive of the electric potential difference across the PZT layers and the *RLC* element to ground $\mathcal{G}_i$,
- ξ_r is the time primitive of the potential difference across the line *RLC* element $\mathcal{L}_i$.

Virtual Powers

With the same notation adopted for the bending coupling, the expressions of the virtual powers will be split up in

$$\mathcal{P}(\mathcal{S}_i) = \mathcal{P}(\mathcal{B}_i) + \mathcal{P}(\mathcal{G}_i) + \mathcal{P}(\mathcal{L}_i) \tag{5.60}$$

Internal Power By the expressions that have been derived in the previous chapters

$$\begin{aligned}
\mathcal{P}_{int}(\mathcal{B}_i) &= \mathcal{P}_{int}(\mathcal{B}_i, \frac{\partial \dot{u}_r^*}{\partial p_1}) + \mathcal{P}_{int}(\mathcal{B}_i, \dot{\phi}_r^*) && (5.61)\\
\mathcal{P}_{int}(\mathcal{G}_i) &= \mathcal{P}_{int}(\mathcal{G}_i, \dot{\phi}_r^*) && (5.62)\\
\mathcal{P}_{int}(\mathcal{L}_i) &= \mathcal{P}_{int}(\mathcal{L}_i, \dot{\xi}_r^*) && (5.63)
\end{aligned}$$

where

$$\begin{aligned}
\mathcal{P}_{int}(\mathcal{B}_i, \frac{\partial \dot{u}_r^*}{\partial p_1}) &= \int_{-\frac{l_b}{2}}^{\frac{l_b}{2}} K_l^{(b)} \frac{\partial u_r}{\partial p_1} \frac{\partial \dot{u}_r^*}{\partial p_1} dp_1 + \int_{-\frac{l_p}{2}}^{+\frac{l_p}{2}} K_l^{(p)} \frac{\partial u_r}{\partial p_1} \frac{\partial \dot{u}_r^*}{\partial p_1} dp_1 \\
&\quad + 2\dot{\phi}_r \int_{-\frac{l_p}{2}}^{+\frac{l_p}{2}} G_l \frac{\partial \dot{u}_r^*}{\partial p_1} dp_1 && (5.64)\\
\mathcal{P}_{int}(\mathcal{B}_i, \dot{\phi}_r^*) &= -2\dot{\phi}_r^* \int_{-\frac{l_p}{2}}^{+\frac{l_p}{2}} G_l \frac{\partial \dot{u}_r^*}{\partial p_1} dp_1 + 2 \int_{-\frac{l_p}{2}}^{+\frac{l_p}{2}} H \ddot{\phi}_r \dot{\phi}_r^* && (5.65)\\
\mathcal{P}_{int}(\mathcal{G}_r, \dot{\phi}_r^*) &= \eta_r \dot{\phi}_r^* && (5.66)\\
&= C_g \frac{d^2\phi_r}{dt^2} \dot{\phi}_r^* + \frac{1}{R_g} \frac{d\phi_r}{dt} \dot{\phi}_r^* + \frac{1}{L_g} \phi_r \dot{\phi}_r^* \\
\mathcal{P}_{int}(\mathcal{L}_i, \dot{\xi}_i^*) &= \iota_r \dot{\xi}_r^* && (5.67)\\
&= C_l \frac{d^2\xi_r}{dt^2} \dot{\xi}_r^* + \frac{1}{R_g} \frac{d\xi_r}{dt} \dot{\xi}_r^* + \frac{1}{L_g} \xi_r \dot{\xi}_r^*
\end{aligned}$$

External Power By the expressions that have been deduced in the previous chapters

$$\mathcal{P}_{ext}(\mathcal{B}_i) = \mathcal{P}_{ext}(\mathcal{B}_i, \dot{u}_r^*) \tag{5.68}$$

$$\mathcal{P}_{ext}(\mathcal{G}_i) = \mathcal{P}_{ext}(\mathcal{G}_i, \dot{\phi}_r^*) \tag{5.69}$$

$$\mathcal{P}_{ext}(\mathcal{L}_i) = \mathcal{P}_{ext}(\mathcal{L}_i, \dot{\xi}_r^*) \tag{5.70}$$

where

$$\mathcal{P}_{ext}(\mathcal{B}_i, \dot{u}_r^*) = \int_{-\frac{l_b}{2}}^{\frac{l_b}{2}} \left(R_1 - \lambda^{(b)}\ddot{u}_r\right) \dot{u}_r^* dp_1 \tag{5.71}$$

$$\mathcal{P}_{ext}(\mathcal{G}_i, \dot{\phi}_r^*) = I_r \dot{\phi}_r^* \tag{5.72}$$

$$\mathcal{P}_{ext}(\mathcal{L}_i, \dot{\xi}_r^*) = Y_r \dot{\xi}_r^* \tag{5.73}$$

5.2.2 Homogenized Continuous Model

Kinematics

To study the extensional behavior of an electromechanical beam we can describe its state by the set of scalar valued fields $\{u, \phi\}$ defined on the unidimensional domain

$$\mathcal{A} = \{\mathbf{p} \in \mathcal{E} : \mathbf{p} = p_1 \mathbf{e}_1, p_1 \in \mathcal{I} \subset \mathcal{R}\} \tag{5.74}$$

where $\mathcal{C} = \{\mathbf{o}, \mathbf{e}_1, \mathbf{e}_2, \mathbf{e}_3\}$ is an opportunely chosen Cartesian reference and u, ϕ represent respectively the *axial* displacement of the beam axis and the electrical potential referred to ground. With a first order gradient theory in all the variables the following set of virtual velocities can be chosen

$$\mathcal{V} = \{\dot{u}^*, \frac{\partial \dot{u}^*}{\partial p_1}, \dot{\phi}^*, \frac{\partial \dot{\phi}^*}{\partial p_1}\} \tag{5.75}$$

Virtual Powers

The internal and external powers are written as a linear functional on the corresponding virtual velocities and the internal and external actions are consequently identified.

Internal Virtual Powers We can divide the internal power in the electrical and mechanical contributions

$$\mathcal{P}_{int}(\mathcal{A}) = \mathcal{P}_{int}(\mathcal{A}, \frac{\partial \dot{u}^*}{\partial p_1}) + \mathcal{P}_{int}(\mathcal{A}, \dot{\phi}^*) + \mathcal{P}_{int}(\mathcal{A}, \frac{\partial \dot{\phi}^*}{\partial p_1}) \tag{5.76}$$

where

$$\mathcal{P}_{int}(\mathcal{A}, \frac{\partial \dot{u}^*}{\partial p_1}) = \int_{\mathcal{A}} N \frac{\partial \dot{u}^*}{\partial p_1} \tag{5.77}$$

$$\mathcal{P}_{int}(\mathcal{A}, \dot{\phi}^*) = \int_{\mathcal{A}} \eta \dot{\phi}^* \tag{5.78}$$

$$\mathcal{P}_{int}(\mathcal{A}, \frac{\partial \dot{\phi}^*}{\partial p_1}) = \int_{\mathcal{A}} \iota \frac{\partial \dot{\phi}^*}{\partial p_1} \tag{5.79}$$

External Virtual Powers Also the external power can be divided into the mechanical and external contributions. The mechanical and electrical external actions are consequently identified. We have

$$\mathcal{P}_{ext}(\mathcal{A}) = \mathcal{P}_{ext}(\mathcal{A}, \dot{u}^*) + \mathcal{P}_{ext}(\mathcal{A}, \dot{\phi}^*) + \mathcal{P}_{ext}(\mathcal{A}, \frac{\partial \dot{\phi}^*}{\partial p_1}) \tag{5.80}$$

where

$$\mathcal{P}_{ext}(\mathcal{A}, \dot{u}^*) = \int_{\mathcal{A}} F_1 \dot{u}^* \tag{5.81}$$

$$\mathcal{P}_{ext}(\mathcal{A}, \dot{\phi}^*) = \int_{\mathcal{A}} \bar{I} \dot{\phi}^* \tag{5.82}$$

$$\mathcal{P}_{ext}(\mathcal{A}, \frac{\partial \dot{\phi}^*}{\partial p_1}) = \int_{\mathcal{A}} \bar{Y} \frac{\partial \dot{\phi}^*}{\partial p_1} \tag{5.83}$$

Power Balance

The power balance prescribes that for each regular virtual velocity field, that satisfy the homogeneous version of the prescribed essential boundary conditions, the following equality must hold $(\mathcal{P}_{int}(\mathcal{A}) = \mathcal{P}_{ext}(\mathcal{A}))$

$$\int_{\mathcal{A}} N \frac{\partial \dot{u}^*}{\partial p_1} + \int_{\mathcal{A}} \eta \dot{\phi}^* + \int_{\mathcal{A}} \iota \frac{\partial \dot{\phi}^*}{\partial p_1} = \int_{\mathcal{A}} F_1 \dot{u}^* + + \int_{\mathcal{A}} \bar{I} \dot{\phi}^* + \int_{\mathcal{A}} \bar{Y} \frac{\partial \dot{\phi}^*}{\partial p_1} \tag{5.84a}$$

Equilibrium Equations

Integrating by parts the terms of (5.84a) involving the spatial derivatives of $\dot{u}^*$ and $\dot{\phi}^*$ we obtain

$$[N \dot{u}^*]_{\partial \mathcal{A}} - \int_{\mathcal{A}} \left(\frac{\partial N}{\partial p_1} + F_1 \right) \dot{u}^* = \int_{\mathcal{A}} \left(\bar{I} - \frac{\partial \bar{Y}}{\partial p_1} + \frac{\partial \iota}{\partial p_1} - \eta \right) \dot{\phi}^* + \left[\left(\bar{Y} - \iota \right) \dot{\phi}^* \right]_{\partial \mathcal{A}}$$

Since the previous expressions must hold for each virtual velocity the following equilibrium equations must be satisfied

$$-\frac{\partial N}{\partial p_1} = F_1 \tag{5.85a}$$

$$\eta - \frac{\partial \iota}{\partial p_1} = \bar{I} - \frac{\partial \bar{Y}}{\partial p_1} \tag{5.85b}$$

Moreover the following conditions must be verified on the boundary

$$[N\dot{u}^*]_{\partial\mathcal{A}} - \left[\left(\bar{Y} - \iota\right)\dot{\phi}^*\right]_{\partial\mathcal{A}} = 0 \tag{5.86}$$

Constitutive Equations

Assuming the same hypotheses and adopting the same procedure as with the bending coupling, the following homogenized constitutive equations have been derived

$$N = \bar{K}_l u' + \bar{G}_l \dot{\phi} \tag{5.87}$$

$$\eta = \bar{G}_l \dot{u}' + \frac{1}{\bar{L}_g}\phi + \frac{1}{\bar{R}_g}\dot{\phi} + \bar{C}_g \ddot{\phi} \tag{5.88}$$

$$\iota = \frac{1}{\bar{L}_l}\phi' + \frac{1}{\bar{R}_l}\dot{\phi}' + \bar{C}_l \ddot{\phi}' \tag{5.89}$$

where

$$\begin{array}{cc} \bar{K}_l = \frac{1}{l_e}\left(\int_{-\frac{l_e}{2}}^{\frac{l_e}{2}} K_l^{(b)} dp_1 + \int_{-\frac{l_p}{2}}^{\frac{l_p}{2}} K_l^{(p)} dp_1\right) & \bar{C}_l = C_l l_e \\ \bar{G}_l = \frac{2}{l_e}\int_{-\frac{l_p}{2}}^{\frac{l_p}{2}} G_l^{(p)} dp_1 & \bar{C}_g = \frac{C_g + 2 l_p H}{l_e} \\ \bar{L}_l = \frac{L_l}{l_e} & \bar{R}_l = \frac{R_l}{l_e} \\ \bar{L}_g = L_g l_e & \bar{R}_g = R_g l_e \end{array} \tag{5.90}$$

The external actions in the homogenized model are given by

$$\begin{array}{cc} F_1 = R_1 - \bar{\lambda}\ddot{u} & \\ \bar{I} = I_r & \bar{Y} = \frac{Y_r}{l_e} \end{array} \tag{5.91}$$

where

$$\bar{\lambda} = \frac{1}{l_e}\left(\int_{-\frac{l_e}{2}}^{\frac{l_e}{2}} \lambda^{(b)} dp_1 + \int_{-\frac{l_p}{2}}^{\frac{l_p}{2}} \lambda^{(p)} dp_1\right) \tag{5.92}$$

$$\bar{\alpha} = \frac{1}{l_e}\left(\int_{-\frac{l_e}{2}}^{\frac{l_e}{2}} \alpha^{(b)} dp_1 + \int_{-\frac{l_p}{2}}^{\frac{l_p}{2}} \alpha^{(p)} dp_1\right) \tag{5.93}$$

Equations of Motion Substituting the constitutive relations in the equilibrium equations we get the homogenized equations of motion for the coupled electromechanical continuum in a strong form

$$-\left(\bar{K}_l u'\right)' - \left(\bar{G}_l \dot{\phi}\right)' + \bar{\lambda}\ddot{u} = F_1 \tag{5.94}$$

$$\frac{1}{\bar{L}_g}\phi + \frac{1}{\bar{R}_g}\dot{\phi} + \bar{C}_g\ddot{\phi} - \left(\frac{1}{\bar{L}_l}\phi'\right)' - \left(\frac{1}{\bar{R}_l}\dot{\phi}'\right)' - \left(\bar{C}_l\ddot{\phi}'\right)' + \bar{G}_l\dot{u}' = \bar{I} - \bar{Y}' \tag{5.95}$$

If periodic PEM beams are considered, the homogenized material characteristics are constant and the previous equations become

$$-\bar{K}_f u'' - \bar{G}_l\dot{\phi}' + \bar{\lambda}\ddot{u} = F_1 \tag{5.96}$$

$$\frac{1}{\bar{L}_g}\phi + \frac{1}{\bar{R}_g}\dot{\phi} + \bar{C}_g\ddot{\phi} - \frac{1}{\bar{L}_l}\phi'' - \frac{1}{\bar{R}_l}\dot{\phi}'' - \bar{C}_l\ddot{\phi}'' + \bar{G}_l\dot{u}' = \bar{I} - \bar{Y}' \tag{5.97}$$

Dimensionless Form Introducing the dimensionless variables

$$\begin{array}{lll} u = u_0 v & t = t_0\tau & p_1 = x_0 x \quad \phi = \phi_0\psi \\ F_1 = F_{10}P_1 & & \bar{I} = \bar{I}_0\bar{I}^a \quad \bar{Y} = \bar{Y}_0\bar{Y}^a \end{array} \tag{5.98}$$

the equations (5.96) become

$$-\frac{\bar{K}_l u_0}{x_0^2}\frac{\partial^2 v}{\partial x^2} - \frac{\bar{G}_l\phi_0}{x_0 t_0}\frac{\partial^2\psi}{\partial x\partial\tau} + \frac{\bar{\lambda}u_0}{t_0^2}\frac{\partial^2 v}{\partial\tau^2} = F_{10}P_1 \tag{5.99}$$

$$\begin{pmatrix} \frac{\phi_0}{\bar{L}_g}\psi + \frac{\phi_0}{\bar{R}_g t_0}\frac{\partial\psi}{\partial\tau} + \frac{\bar{C}_g\phi_0}{t_0^2}\frac{\partial^2\psi}{\partial\tau^2} - \frac{\phi_0}{\bar{L}_l x_0^2}\frac{\partial^2\psi}{\partial x^2} \\ -\frac{\phi_0}{\bar{R}_l x_0^2 t_0}\frac{\partial^3\psi}{\partial x^2\partial\tau} - \frac{\bar{C}_l\phi_0}{x_0^2 t_0^2}\frac{\partial^4\psi}{\partial x^2\partial\tau^2} + \frac{\bar{G}_l u_0}{x_0 t_0}\frac{\partial^2 v}{\partial x\partial\tau} \end{pmatrix} = \bar{I}_0\bar{I}^a - \frac{\bar{Y}_0}{x_0}\frac{\partial\bar{Y}^a}{\partial x} \tag{5.100}$$

Dividing each equation by the coefficient of the term with only two time derivatives, we obtain

$$\frac{\partial^2 v}{\partial\tau^2} + \frac{t_0^2\bar{K}_l}{\bar{\lambda}x_0^2}\frac{\partial^2 v}{\partial x^2} - \frac{t_0^2\bar{G}_l\phi_0}{\bar{\lambda}u_0 x_0 t_0}\frac{\partial^2\psi}{\partial x\partial\tau} = \frac{t_0^2 F_{10}}{\bar{\lambda}u_0}P_1 \tag{5.101}$$

$$\begin{pmatrix} \frac{\partial^2\psi}{\partial\tau^2} + \frac{t_0^2}{\bar{C}_g\bar{L}_g}\psi + \frac{t_0}{\bar{C}_g\bar{R}_g}\frac{\partial\psi}{\partial\tau} - \frac{t_0^2}{\bar{C}_g\bar{L}_l x_0^2}\frac{\partial^2\psi}{\partial x^2} \\ -\frac{t_0}{\bar{C}_g\bar{R}_l x_0^2}\frac{\partial^3\psi}{\partial x^2\partial\tau} - \frac{\bar{C}_l}{\bar{C}_g x_0^2}\frac{\partial^4\psi}{\partial x^2\partial\tau^2} + \frac{\bar{G}_l t_0 u_0}{\bar{C}_g x_0\phi_0}\frac{\partial^2 v}{\partial x\partial\tau} \end{pmatrix} = \frac{t_0^2\bar{I}_0}{\bar{C}_g\phi_0}\bar{I}^a - \frac{t_0^2\bar{Y}_0}{\bar{C}_g\phi_0 x_0}\frac{\partial\bar{Y}^a}{\partial x} \tag{5.102}$$

Defining the dimensionless coefficients

$$\begin{array}{ccc} \alpha = \frac{t_0^2 \bar{K}_l}{\bar{\lambda} x_0^2} & \gamma = \frac{\bar{G}_l t_0 \phi_0}{\bar{\lambda} u_0 x_0} & \gamma = \frac{\bar{G}_l t_0 u_0}{\bar{C}_g x_0 \phi_0} \\ \beta_l^2 = \frac{t_0^2}{\bar{C}_g \bar{L}_l x_0^2} & 2\delta_l = \frac{t_0}{\bar{C}_g \bar{R}_l x_0^2} & \\ \beta_g^2 = \frac{t_0^2}{\bar{C}_g \bar{L}_g} & 2\delta_g = \frac{t_0}{\bar{C}_g \bar{R}_g} & \kappa = \frac{\bar{C}_l}{\bar{C}_g x_0^2} \\ \chi_1 = \frac{t_0^2 F_{10}}{\bar{\lambda} u_0} & \chi_3 = \frac{t_0^2 \bar{I}_0}{\bar{C}_g \phi_0} & \chi_4 = \frac{t_0^2 \bar{Y}_0}{\bar{C}_g \phi_0 x_0} \end{array} \tag{5.103}$$

and choosing the dimensionless time t_0 and the dimensionless electric variable ϕ_0 such that

$$t_0 = \sqrt{\frac{\bar{\lambda}}{\bar{K}_l}} x_0 \quad \phi_0 = \sqrt{\frac{\bar{\lambda}}{\bar{C}_g}} u_0 \tag{5.104}$$

the dimensionless parameters

$$\begin{array}{ccc} \alpha = 1 & \gamma_1 = \gamma & \gamma_2 = \gamma \\ \beta_l = \sqrt{\frac{\bar{\lambda}}{\bar{C}_g \bar{L}_l \bar{K}_l}} & \delta_l = \frac{1}{2\bar{C}_g \bar{R}_l x_0^2} \sqrt{\frac{\bar{\lambda}}{\bar{K}_l}} x_0 & \gamma = \frac{\bar{G}_l}{\sqrt{\bar{C}_g \bar{K}_l}} \\ \beta_g = \sqrt{\frac{\bar{\lambda}}{\bar{K}_l \bar{C}_g \bar{L}_g}} x_0 & \delta_g = \frac{1}{2\bar{C}_g \bar{R}_g} \sqrt{\frac{\bar{\lambda}}{\bar{K}_l}} x_0 & \kappa = \frac{\bar{C}_l}{\bar{C}_g x_0^2} \\ \chi_1 = \frac{F_{10}}{u_0 \bar{K}_l} x_0^2 & \chi_3 = \frac{\bar{I}_0}{u_0 \bar{K}_l} \sqrt{\frac{\bar{\lambda}}{\bar{C}_g}} x_0^2 & \chi_4 = \frac{\bar{Y}_0}{u_0 \bar{K}_l} \sqrt{\frac{\bar{\lambda}}{\bar{C}_g}} x_0 \end{array} \tag{5.105}$$

are found and the equations (5.96) can be rewritten as

$$\begin{aligned} -\upsilon'' - \gamma \dot{\psi}' + \ddot{v} &= \chi_1 P_1 \\ -\kappa \ddot{\psi}'' - 2\delta_l \dot{\psi}'' - \beta_l^2 \psi'' + \gamma \dot{\upsilon}' + \ddot{\psi} + 2\delta_g \dot{\psi} + \beta_g^2 \psi &= \chi_3 \bar{I}^a - \chi_4 \bar{Y}^{a\prime} \end{aligned} \tag{5.106}$$

where the symbols $\dot{}$ and $'$ have been redefined as the *dimensionless* temporal and spatial partial derivatives respectively.

As for the bending vibrations, we will treat particular cases of (5.106).

Vanishing Ground Element Let us consider the case in which

$$\left\{ \begin{array}{cc} L_g \to \infty & R_g \to \infty \\ C_l \to 0 & \rho \to 0 \end{array} \right. \Longrightarrow \left\{ \begin{array}{cc} \beta_g \to 0 & \delta_g \to 0 \\ \kappa \to 0 & \end{array} \right. \tag{5.107}$$

Hence the equations (5.106) simplify to

$$-\upsilon'' - \gamma \dot{\psi}' + \ddot{v} = \chi_1 P_1 \tag{5.108}$$

$$-2\delta_l \dot{\psi}'' - \beta_l^2 \psi'' + \ddot{\psi} + \gamma \dot{\upsilon}' = \chi_3 \bar{I}^a - \chi_4 \bar{Y}^{a\prime} \tag{5.109}$$

If also the line resistance is absent ($R_l \to \infty$, since parallel connected) then the system is conservative[6] and since $\delta_l \to 0$ the equations of motion reduce to

$$-v'' - \gamma\dot{\psi}' + \ddot{v} = \chi_1 P_1 \tag{5.110}$$

$$-\beta_l^2\psi'' + \ddot{\psi} + \gamma\dot{v}' = \chi_3\bar{I}^a - \chi_4\bar{Y}^{a\prime} \tag{5.111}$$

Vanishing Line Element If

$$\left\{\begin{array}{ll} L_l \to \infty & R_l \to \infty \\ C_l \to 0 & \bar{Y}^a \to 0 \end{array}\right. \Longrightarrow \left\{\begin{array}{ll} \beta_l \to 0 & \delta_l \to 0 \\ \kappa \to 0 & \rho \to 0 \end{array}\right. \tag{5.112}$$

then the following equations are obtained

$$-v'' - \gamma\dot{\psi}' + \ddot{v} = \chi_1 P_3 \tag{5.113}$$

$$\ddot{\psi} + 2\delta_g\dot{\psi} + \beta_g^2\psi + \gamma\dot{v}' = \chi_3\bar{I}^a \tag{5.114}$$

The corresponding conservative case is obtained with $R_g \to \infty$

$$-v'' - \gamma\dot{\psi}' + \ddot{v} = \chi_1 P_3 - \chi_2 P_g' \tag{5.115}$$

$$\ddot{\psi} + \beta_g^2\psi + \gamma\dot{v}' = \chi_3\bar{I}^a \tag{5.116}$$

[6] In this definition we have not considered the external forces.

Chapter 6

Comparison of Optimal Network Configurations

In the previous chapter periodic physical systems in which a distributed piezoelectromechanical coupling between a beam (or bar) and an electric network is realized has been presented following [22]. An homogenized model for it has been derived. Here we want to analyze the applications of that concept to the control of the mechanical vibrations of a structure. To this end we will study how the proprieties of a monochromatic wave propagating in the electromechanical infinite media depend on its wave number and on the electric circuit parameters. The optimal values of the electrical parameters will be found (Minimizing the decay time of the propagative wave) for *three different network topological configurations* with a single inductor and resistor per module. A comparative analysis of the obtained results will be performed. We will discuss

1. the performances in the mechanical vibration damping;
2. the dependence of the optimal electric parameters on the number of modules of the periodic system that are spanned by the chosen wavelength;
3. the sensitivities of the optimal parameters on the assumed wave number;
4. the behavior of PEM beams designed for a wave number k_0 when wave numbers different from k_0 are considered.

Both the cases of the *longitudinal-electric* and *transversal-electric* coupling will be examined.

The wave analysis on an infinite medium may be useful also when *finite structures* must be studied. Indeed, the vibration modes of a simply supported mechanical beam can be interpreted

as stationary monochromatic waves with a wave length given in function of the beam length and the mode number considered.

Numerical results for the PEM beams which has been experimentally realized, as it will described in Chapter 7, will be furnished.

6.1 Wave Form Solutions

Let us consider a mono-dimensional infinite media the state of which is determined by a $n-th$ dimensional vector field $\mathbf{v}$, defined on the cartesian product of a spatial and a temporal domain. Let us assume that its dynamics is governed by a system of n $PDEs$ in the form

$$\frac{d^2\mathbf{v}}{dt^2} + \mathcal{D}_1\frac{d\mathbf{v}}{dt} + \mathcal{D}_0\mathbf{v} = 0 \tag{6.1}$$

where $\mathcal{D}_1, \mathcal{D}_0$ are space differential operators. If a Fourier method on the spatial variable is applied to (6.1), its general solution can be written as superposition of *waves* of the type

$$\mathbf{v} = \hat{\mathbf{v}}_k \cos(kx) \tag{6.2}$$

where k is a dimensionless wave number and $\hat{\mathbf{v}}$ is a vector function of time only. Hence by the study of the properties of the solutions in the form (6.2) as function of the wave number it is possible to get a deeper insight into the dynamical proprieties of the PEM we are dealing with.

The fact that the media is mono-dimensional simplifies the discussion since k and x are scalars. In the following we will consider k as a fixed *real, positive* parameter[1]. Substituting (6.2) into (6.1) the generic spatial derivative can be easily evaluated and $\mathcal{D}_1, \mathcal{D}_0$ transform into two real algebraic operators $\mathbf{D}_{1,k}, \mathbf{D}_{0,k}$. Then (6.1) transforms in the following system of Ordinary Differential Equations for the temporal evolution of a solution of (6.1) in the form (6.2) for a given k

$$\frac{d^2\hat{\mathbf{v}}_k}{dt^2} + \mathbf{D}_{1,k}\frac{d\hat{\mathbf{v}}_k}{dt} + \mathbf{D}_{0,k}\hat{\mathbf{v}}_k = 0 \tag{6.3}$$

This system can be rewritten in the normal form of a system of the first order in $\mathcal{R}^{2n}$

$$\frac{d\hat{\mathbf{y}}}{dt} = \mathbf{A}_k\hat{\mathbf{y}} \tag{6.4}$$

[1] Physically it corresponds to study of the propagation of waves with a given, fixed wavelegth λ (Let's recall that $\lambda = \frac{2\pi}{k}$)

with

$$\hat{\mathbf{y}} = \begin{bmatrix} \hat{\mathbf{v}}_k \\ \frac{d\hat{\mathbf{v}}_k}{dt} \end{bmatrix}, \mathbf{A}_k = \begin{bmatrix} \mathbf{0}_n & \mathbf{I}_n \\ -\mathbf{D}_{0,k} & -\mathbf{D}_{1,k} \end{bmatrix}$$

where we denoted by $\mathbf{0}_n$ and $\mathbf{I}_n$ the null and identity operators on $\mathcal{R}^n$. Hence the theory of linear first order systems of autonomous homogeneous $ODEs$ can be fruitfully applied to study the qualitative properties of the temporal evolution of solutions in the form (6.2).

The differential problem (6.4) is posed in the vector space $\mathcal{V} = \mathcal{R}^{2n}$, and $\mathbf{A}_k$, for each k, is a linear operator mapping $\mathcal{V}$ into itself ($\mathbf{A}_k \in L(\mathcal{V}, \mathcal{V})$). It is well known that its general solution starting from the initial data $\hat{\mathbf{y}}_0$ at $t = 0$ is given by (see [15])

$$\hat{\mathbf{y}} = e^{\mathbf{A}_k t}\hat{\mathbf{y}}_0 \tag{6.5}$$

However, in order to study the qualitative properties of this type of solutions, it is opportune to get a deeper insight into (6.5). To this end it should be necessary to describe explicitly how to write the exponential of a real operator $\mathbf{A}_k$ in the general case. Here we will only report in a convenient form the fundamental results of the theory of the system of linear autonomous, homogeneous ODE, referring to [14-17] for a complete treatment.

First of all, let us note that since $\mathbf{A}_k$ is real, its eigenvalues must appear in complex conjugate pairs. Without loss of generality, let us split the set Σ of the distinct eigenvalues of $\mathbf{A}_k$ into

- a set $\{\lambda_i\}_{i=1...p}$ of p distinct real eigenvalues, each one characterized by an algebraic multiplicity a_i
- a set $\{\omega_i, \omega_i^*\}_{i=p+1...p+q}$ of q distinct conjugate pairs of complex (with non vanishing imaginary part) eigenvalues, each one characterized by an algebraic Each λ_i will be associated with a generalized eigenspace $\mathcal{N}_i^\Lambda$, with $\dim(\mathcal{N}_i^\Lambda) \leq a_i$, while to each pair $\{\omega_i, \omega_i^*\}$ will correspond the pair of generalized eigenspaces $\{\mathcal{N}_i^\omega, \mathcal{N}_i^{\omega^*}\}$ with $\dim(\mathcal{N}_i^\omega) = \dim(\mathcal{N}_i^{\omega^*}) \leq a_i$. However, since $\mathbf{A}_k$ is real, if $\{\mathbf{e}_1^i, ..., \mathbf{e}_{a_i}^i\}$ is a basis of $\mathcal{N}_i^\omega$, it is convenient to not distinguish between the *complex* $\mathcal{N}_i^\omega$ and $\mathcal{N}_i^{\omega^*}$, and to associate to each pair $\{\omega_i, \omega_i^*\}$ the *real* generalized eigenspace $\mathcal{N}_i$ defined as

$$\mathcal{N}_i = \mathcal{R} - Span\{\mathrm{Re}(\mathbf{e}_1^i), -\mathrm{Im}(\mathbf{e}_{a_i}^i), ..., \mathrm{Re}(\mathbf{e}_{a_i}^i), -\mathrm{Im}(\mathbf{e}_{a_i}^i)\} \tag{6.6}$$

Hence let us define the set $\{\mathcal{N}_i\}_{i=1,...,p+q}$, where

$$\mathcal{N}_i = \begin{cases} \mathcal{N}_i^{\Lambda} & for \qquad i = 1, ..., p \\ \mathcal{N}_i & for \quad i = p+1, ..., p+q \end{cases} \tag{6.7}$$

It is possible to show that the vector space $\mathcal{V}$ can be decomposed into a direct sum of the $\mathcal{N}_i$, that is,

$$\mathcal{V} = \oplus_{i=1..p+q} \mathcal{N}^i \tag{6.8}$$

Moreover, each $\mathcal{N}^i$ is invariant under $\mathbf{A}_k$. As a consequence the operator $\mathbf{A}_k$ can be decomposed as the sum

$$\mathbf{A}_k = \oplus_{i=1..p+q} \mathbf{A}_k^{(i)} \tag{6.9}$$

where each $\mathbf{A}_k^{(i)}$ is the restriction of $\mathbf{A}_k$ on $\mathcal{N}^i$. So that the differential problem (6.4) can be decomposed into $p+q$ sub-problems in the $p+q$ generalized eigenspaces $\{\mathcal{N}^i\}_{i=1,...,p+q}$. Let us denote by

$$\hat{\mathbf{y}}^i = e^{\mathbf{A}_k t} \hat{\mathbf{y}}_0^i \in \mathcal{N}^i \tag{6.10}$$

the solution of (6.4) starting from initial data $\hat{\mathbf{y}}_0^i \in \mathcal{N}^i$. Hence it is meaningful to introduce the following definition

Definition 15 (Wave Mode) *We define as the $i-th$ wave mode the generalized eigenspace $\mathcal{N}^i \subset \mathcal{V}$ of the differential operator $\mathbf{A}_k$ defined by (6.7). Each wave mode is invariant under the flow of (6.4).*

At this point we can fruitfully consider the consequences of the following theorem (see [16] of for a complete proof [17]).

Theorem 8 *Each coordinate of the solution $\hat{\mathbf{y}}^i \in \mathcal{N}^i$ of (6.4) with $\hat{\mathbf{y}}_0 = \hat{\mathbf{y}}_0^i \in \mathcal{N}^i$ is a linear combination of functions of the form*

$$t^k e^{\lambda_i^R t} \tag{6.11}$$

for $i = 1, ..., p$ *and of*

$$t^k e^{\omega_i^R t} \cos(\omega_i^I t) \quad or \quad t^k e^{\omega_i^R t} \sin(\omega_i^I t) \tag{6.12}$$

for $i = p+1, ..., p+q$, *where* $\omega_i^R = \mathrm{Re}(\omega_i), \omega_i^I = \mathrm{Im}(\omega_i)$ *and* $k \leq a_i$. *In particular, if the algebraic multiplicity* a_i *of an eigenvalue is the same of its geometrical multiplicity, then* $k = 0$.

Thus it is possible to distinguish between $p+q$ different wave modes $\{\mathbf{y}^{(i)}\}_{i=1,..,p+q}$, each one characterized by a temporal evolution expressed by a linear combination of terms of the form (6.11) or (6.12) and by the fact of lying in the generalized eigenspace $\mathcal{N}^i$.

Remark 23 (Dispersion Relations) *The functions giving the real and imaginary part of the eigenvalues as a function of the wavenumber can be interpreted as the dispersion relations of the media. The imaginary part* $\omega_i^I(k)$ *of each complex eigenvalue furnishes the wave frequency corresponding to a wave with a given wavenumber* k, *while its real part, if negative, will characterize the damping properties of each wave mode. If real eigenvalues are concerned, the corresponding contribution to the temporal evolution of (6.2) will not be oscillatory, but a simple exponential decay.*

In the following we will focus our attention only on systems having eigenvalues with a negative real part (dissipative systems). In particular we are interested in estimating in a simple way the damping proprieties of a given system in the form (6.4)

Lemma 1 *Let* $k, a, r > 0$ *and let us consider the functions*

$$f(t) = t^k e^{-at}, g(t) = t^k e^{-at} \cos(rt) \tag{6.13}$$

Then there exist two real, positive constants $M > 0$ *and* $0 < c < a$ *such that, for each* $t > 0$

$$f(t) < M e^{-ct} \quad g(t) < M e^{-ct} \tag{6.14}$$

Moreover if we denote by C *the set of real positive numbers* c *such that* $0 < c < a$ *and (6.14) holds, then*

$$\sup_{c \in C}(c) = a \tag{6.15}$$

Proof. *Let us show the result for* $g(t)$, *since the same reasoning is valid also for* $f(t)$. *The function* $t^k \cos(rt) e^{-(a-c)t}$ *is bounded for* $t > 0$ *and* $c < a$. *Then there exists a constant* $M > 0$ *such*

that

$$t^k \cos(rt) e^{-at} < M e^{-ct} \tag{6.16}$$

For each $0 < c < a$ *such that (6.14) holds, it is possible to define* $\delta \in \mathcal{R}^+$ *such that*

$$c = a - \delta \tag{6.17}$$

Hence

$$\sup(c) = \sup(a - \delta) = a - \inf(\delta) = a \tag{6.18}$$

■

Remark 24 *The temporal evolution of a solution of the type (6.2) in the generalized eigenspace* $\mathcal{N}^i$ *is a linear combination of* $n_i \leq a_i$ *terms of the form (6.11) or (6.12). Let us denote by* $f_h(t)$ *the generic one. Hence, by the previous lemma, there exist two constants* $c_h, M_h > 0$ *such that* $f_h(t) < M_h e^{-c_h t}$ *for each* $t > 0$. *Denoting by* $M = \max_{h=1,...n_i} M_h$ *and by* $c = \min_{h=1,...n_i} c_h$, *we can write*

$$f_h(t) < M e^{-ct} \tag{6.19}$$

for each $h = 1, ..., n_i$ *and for each* $t > 0$. *Moreover* $\sup_{c \in C}(c) = -\omega_i^R$

We can introduce the following definitions that will be useful to state an optimization problem for the control of the vibrations of the PEM beams the dynamics of which we would like to study.

Definition 16 (Modal Decay Rate) *For each generalized eigenspace* $\mathcal{N}^i$ *we can define the characteristic* damping rate *of the* $i-th$ *wave mode as the constant*

$$\alpha_i = -\frac{2\pi}{\omega_i^R} \tag{6.20}$$

This characterizes the exponential decay rate of the contribution to the general solution of (6.1) due to the $i-th$ *wave mode.*

Definition 17 (Modal Decay Time) *For each generalized eigenspace* $\mathcal{N}^i$ *we can define the characteristic* damping time *of the* $i-th$ *wave mode as the constant*

$$\theta^{(i)} := \frac{2\pi}{-\omega_i^R} \tag{6.21}$$

This furnishes the characteristic damping time of the contribution to the general solution of (6.1) due to the $i-th$ wave mode.

Definition 18 (Modal Damping Ratio) *Defining the modal period as*

$$T^{(i)} = \frac{2\pi}{\left|\omega_h^I\right|} \tag{6.22}$$

and denoting by n_p^i the number of modal periods after which the amplitude of $e^{\omega_i^R t}$ is reduced to $\frac{1}{e^{2\pi}}$ of its initial value, we define the damping ratio of the $i-th$ mode as

$$\zeta_i := \frac{1}{n_p^i} \tag{6.23}$$

It is given by

$$\zeta_i = \frac{T^{(i)}}{\theta^{(i)}} = \left|\frac{\omega_i^R}{\omega_i^I}\right| \tag{6.24}$$

Obviously ζ_i depends on the wave number k since ω_i does.

We can now extend the previous definitions to the whole system, attributing to it the proprieties of the worst (for the vibration damping) wave mode as follows.

Definition 19 (System Decaying Rate) *We define the system decay rate as*

$$= \min_i \left|\omega_i^R\right| \tag{6.25}$$

This characterizes the exponential decay rate of the general solution of (6.1).

Definition 20 (System Decaying Time) *We define the system decay time Θ as*

$$\Theta := \max_i(\theta^{(i)}) = \underline{1} \tag{6.26}$$

Let us denote by m one of the indexes for which $\theta^{(m)} = \Theta$. Both Θ and m depend on the wave number k since each $\theta^{(i)}$ does.

Definition 21 (System Damping Ratio) *Let us define the system damping ratio as*

$$Z := \frac{T^{(m)}}{\Theta} \tag{6.27}$$

where m is one of the indexes for which $\theta^{(m)} = \Theta$. We have also

$$Z = \frac{}{|\omega_m^I|} = \left|\frac{\omega_m^R}{\omega_m^I}\right|$$

Let us underline that

$$Z \neq \min_i \left(\zeta^{(i)}\right) \tag{6.28}$$

Obviously Z and m depend on the wave number k since each $\theta^{(i)}$ does.

The *phase velocity* of the $i-th$ wave mode is given by

$$v_i^p = \hat{v}_i^p(k) = \frac{\omega_i^I(k)}{k} \tag{6.29}$$

while the *group velocity* is defined as

$$v_i^g = \hat{v}_i^g(k) := \frac{d\omega_i^I(k)}{dk} \tag{6.30}$$

If the relation $\omega_i(k)$ is linear, then $v^p = v^g$ otherwise $v^p \neq v^g$ and the medium is said to be *dispersive.*

Let us recall the relationships between the wave number k and the wave length λ,

$$k = \frac{2\pi}{\lambda} \tag{6.31}$$

and the wave frequency ν and pulsation ω,

$$\omega = 2\pi\nu \tag{6.32}$$

The temporal period of the wave is given by $T = \frac{2\pi}{\omega} = \frac{1}{\nu}$

Remark 25 (Dimensionless Wave Number) *Let λ_{w_0} be the characteristic wave length of the physical phenomena considered. Thus we can set the dimensionless length*

$$x_0 = \lambda_{w_0} \tag{6.33}$$

Consequently the dimensionless wave number relative to a wave length λ_w will be

$$k = 2\pi \frac{x_0}{\lambda_w} = \frac{2\pi}{\lambda_w/\lambda_{w0}} \tag{6.34}$$

If $\lambda_w = \lambda_{w0}$ then $k = 2\pi$.

6.2 Waves in PiezoElectroMechanical Beams

In the previous chapter we introduced PEM beams for the damping of the structural vibrations by means of PZT transducers and electric networks. We derived an homogenized model for

1. a *bar* coupled with an *electric transmission line* by means of an array of PZT transducers in bimorph configuration with *in-phase* electric connections
2. a *beam* coupled with an *electric transmission line* by means of an array of PZT transducers in bimorph configuration with *out-of-phase* electric connections

Let us study the properties of solution of type (6.2) in those systems, the dimensionless equations of which are given by (5.47),(5.106), assuming that

- the rotational inertia is negligible, thus $\rho \to 0$
- the line capacitance C_l is zero, thus $\kappa \to 0$
- the capacitance to ground is given only by the PZT patch and C_g vanishes[2].

These systems of PDE's can be in general written in the form of

$$\frac{d^2\mathbf{v}}{dt^2} + \mathcal{D}_1 \frac{d\mathbf{v}}{dt} + \mathcal{D}_0 \mathbf{v} = 0 \tag{6.35}$$

where

$$\mathcal{D}_1 = \begin{pmatrix} \mathcal{D}_1^{mm} & \mathcal{D}_1^{me} \\ -\mathcal{D}_1^{me} & \mathcal{D}_1^{ee} \end{pmatrix} \quad \mathcal{D}_0 = \begin{pmatrix} \mathcal{D}_0^{mm} & \mathcal{D}_0^{me} \\ -\mathcal{D}_0^{me} & \mathcal{D}_0^{ee} \end{pmatrix}$$

are two by two matrices of differential operators and

$$\mathbf{v} = u\mathbf{e}_m + \phi\mathbf{e}_e$$

[2] As we will show an additional capacitance to ground C_g has a negative influence on the performances in the vibration suppresion.

is the vector defining the configuration of the electromechanical system. Here we denote by u the mechanical variable, by ϕ the electrical variable, by $\{\mathbf{e}_m, \mathbf{e}_e\}$ the basis corresponding to a pure mechanical and electrical vector respectively. Obviously this system is a particular case of the one studied in a previous section for $n = 2$

Let us start studying the general case of a PEM beam with a network topological connection as that in figure 6-1. Then we will focalize our attention on particular cases.

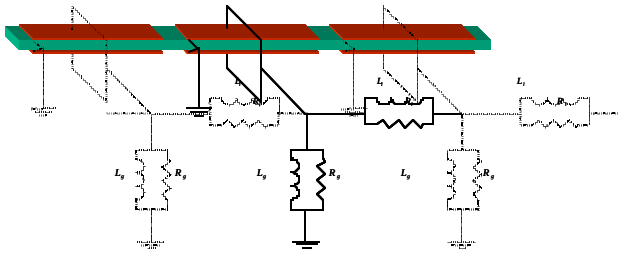

Figure 6-1: Basic Cell: Electric Connections

We will consider the two cases of the coupling between transversal and electric waves realized with out-of-phase connected PZT sheets and longitudinal-electric waves realized with in-phase connected $PZTs$. In what follows we will write the equations in coordinates assuming the basis $\{\mathbf{e}_m, \mathbf{e}_e\}$

6.2.1 Transversal-Electric Coupling

The system of $PDEs$ in this case is

$$\begin{aligned} v'''' + \gamma\dot{\psi}'' + \ddot{v} &= 0 \\ \ddot{\psi} + 2\delta_l\dot{\psi}'' + 2\delta_g\dot{\psi} - \gamma\dot{v}'' - \beta_l^2\psi'' + \beta_g^2\psi &= 0 \end{aligned} \tag{6.36}$$

Assuming a wave form solution with a wave number k we can find

$$D_1 = \begin{pmatrix} 0 & -\gamma k^2 \\ \gamma k^2 & -2\delta_l k^2 + 2\delta_g \end{pmatrix} \quad D_0 = \begin{pmatrix} k^4 & 0 \\ 0 & \beta_g^2 + k^2\beta_l^2 \end{pmatrix}$$

Hence the coordinate representation of the corresponding operator $\mathbf{A}_k$ is

$$A_k = \begin{bmatrix} 0 & 0 & 1 & 0 \\ 0 & 0 & 0 & 1 \\ -k^4 & 0 & 0 & \gamma k^2 \\ 0 & -\beta_g^2 - k^2\beta_l^2 & -\gamma k^2 & 2\delta_l k^2 - 2\delta_g \end{bmatrix} \tag{6.37}$$

$$A_k = \begin{bmatrix} 0 & 0 & 1 & 0 \\ 0 & 0 & 0 & 1 \\ -k^4 & 0 & 0 & \gamma k^2 \\ 0 & -\beta_g^2 - k^2\beta_l^2 & -\gamma k^2 & 2\delta_l k^2 - 2\delta_g \end{bmatrix} \tag{6.38}$$

Its eigenvalues can be found as roots of the following forth order characteristic polynomial

$$\begin{aligned} p(\omega) &= \omega^4 + \left(-2\delta_l k^2 + 2\delta_g\right)\omega^3 + \left(\beta_g^2 + k^4 + k^2\beta_l^2 + \gamma^2 k^4\right)\omega^2 \\ &\quad + \left(2k^4\delta_g - 2k^6\delta_l\right)\omega + k^4\beta_g^2 + k^6\beta_l^2 \end{aligned} \tag{6.39}$$

6.2.2 Longitudinal-Electric Coupling

The system of $PDEs$ is

$$\begin{aligned} -v'' + \gamma\dot{\psi}' + \ddot{v} &= 0 \\ \ddot{\psi} + 2\delta_l\dot{\psi}'' + 2\delta_g\dot{\psi} - \gamma\dot{v}' - \beta_l^2\psi'' + \beta_g^2\psi &= 0 \end{aligned} \tag{6.40}$$

Assuming a wave form solution with a wave number k we can find

$$D_1 = \begin{pmatrix} 0 & i\gamma k \\ -i\gamma k^2 & -2\delta_l k^2 + 2\delta_g \end{pmatrix} \quad D_0 = \begin{pmatrix} k^2 & 0 \\ 0 & \beta_g^2 + k^2\beta_l^2 \end{pmatrix}$$

Hence the coordinate representation of the corresponding operator $\mathbf{A}_k$ is

$$A_k = \begin{bmatrix} 0 & 0 & 1 & 0 \\ 0 & 0 & 0 & 1 \\ -k^2 & 0 & 0 & -i\gamma k \\ 0 & -\beta_g^2 - k^2\beta_l^2 & i\gamma k & 2\delta_l k^2 - 2\delta_g \end{bmatrix} \tag{6.41}$$

Its eigenvalues can be found as roots of the following forth order characteristics polynomial with real coefficients

$$\begin{aligned} p(\omega) &= \omega^4 + \left(-2\delta_l k^2 + 2\delta_g\right)\omega^3 + \left(\beta_g^2 + k^2(1 + \beta_l^2 - \gamma^2)\right)\omega^2 && (6.42) \\ &\quad + \left(2k^2\delta_g - 2k^4\delta_l\right)\omega + k^2\beta_g^2 + k^4\beta_l^2 && (6.43) \end{aligned}$$

Notation 9 *The parameters of the systems with the longitudinal and the transversal coupling are denoted by the same letters, however in each case they must be defined by (5.46), (5.105) respectively.*

Remark 26 (Parameters range) *To maintain a physical meaning all the parameters are constrained to be real and positive. Moreover we will consider*

$$0 < \gamma < 1 \tag{6.44}$$

6.3 Optimization for Vibrations Suppression

Our aim is to study the applications to the suppression of mechanical vibrations of the PiezoElectroMechanical system that have been introduced in the previous chapter. An optimal design of the electric networks to maximize the energy dissipation is required. Thus we need to

1. define a performance index to be maximized (or a cost function to be minimized) related to the damping properties of the system
2. define the electric parameters to be optimized specifying the functional dependence of the performance index on them
3. maximize the performance index with respect to the electric parameters determining their optimal values. In this phase it is necessary to choose an optimization method.

In the following sections we will focus our attention only on the optimization problem related to the vibration control of the systems (6.36,6.40) in which only two electric parameters are left free. They will be in the form of

1. a dimensionless tuning parameter β to be chosen between the β_g, β_l in equations (6.36,6.40), that is associated to the value of an inductor

2. a dimensionless damping parameter δ to be chosen between the δ_g, δ_l in equations (6.36,6.40) that is associated with the value of a resistor

6.3.1 Performance Index

The performance index of a control technique can be chosen in different ways depending on the application that is considered. The principal goals in the vibrations control are the reduction of the forced and free response of the system. Here we consider the problem of the optimization of the electrical parameters in the electromechanical systems (6.36,6.40) in order to let the free oscillations characterized by a given wavelength decay as fast as possible. To this aim we will analyze the damping properties of solutions of the type (6.2) in an infinite media. In this framework, as it has been pointed out in a previous section, the temporal evolution resulting from to arbitrarily given initial data can be characterized by the *decay time* of each wave mode, thus by the real part of the corresponding eigenvalue. Moreover the damping properties of the whole system for a fixed wavenumber can be controlled by referring to the following performance index

$$P = \quad = \frac{1}{\Theta} \tag{6.45}$$

where Θ and have been defined by (6.26) and (6.25). The optimization problem related to the maximization of P is completely equivalent to the minimization of the cost function $C = \frac{1}{P} = \Theta$ that has a direct physical interpretation since Θ has been defined as the greatest modal decay time.

In order to formalize the optimization problem it is opportune to underline the functional dependence of P on the relevant parameters. Let us recall that P is a function of the eigenvalues of the system (6.4) governing the evolution of a wave with a fixed wave number. Since the characteristic polynomials (6.39,6.42) depend on the tuning parameters β, on the damping parameter δ and on the wave number k, for which the system is analyzed, it will be

$$P = \hat{P}(k, \beta, \delta) \tag{6.46}$$

Hence, aiming to optimally damp the waves with a given wavenumber k_0, we can state the following optimization problem

Problem 10 (Optimization for a given wave number k_0) *Given a wave number k_0, find the*

optimal tuning and damping electric parameters

$$\beta_{opt} = \hat{\beta}_{opt}(k_0) \geq 0 \quad \delta_{opt} = \hat{\delta}_{opt}(k_0) \geq 0$$

such that for each $\beta \geq 0, \delta \geq 0$

$$\hat{P}(k_0, \beta, \delta) \leq \hat{P}(k_0, \hat{\beta}_{opt}(k_0), \hat{\delta}_{opt}(k_0))$$

Once the relations $\hat{\beta}_{opt}(k_0), \hat{\delta}_{opt}(k_0)$, giving the optimal electric parameters in function of the given wavenumber, are found, it is particularly meaningful to study the behavior of

$$\tilde{P}(k, k_0) = \hat{P}(k, \hat{\beta}_{opt}(k_0), \hat{\delta}_{opt}(k_0)) \tag{6.47}$$

as a function of k. Indeed it describes the damping properties for waves with wavenumber k in a system optimized for a wavenumber k_0, and it will furnish us a criterion to compare the properties of systems characterized by different network topologies.

Remark 27 (Resonant Structures) *The present approach, that is based on the analysis of infinite PEM beams, is meaningful and convenient also for* finite structures*. Indeed, considering for example the free vibrations of a simply supported mechanical beam of length* l*, its* $n-th$ *vibration mode can be interpreted as a stationary wave with a wave length* $\lambda = \frac{2l}{n}$ *and a wave number* $k = \frac{n}{4\pi l}$*. Hence its temporal evolution is given by a solution of the form (6.2)*

6.3.2 Optimization Method

The evaluation of the performance index (6.45) requires us to find the roots of a fourth order polynomial as a function of the parameters β, δ and the wave number k. Although analytical formulas for these are available, they have a complex expression and the analytical maximization of the performance index is not trivial. We assume the following useful reasonable results frequently used in *pole placement* optimization techniques[3], that can be checked numerically in each case by plotting the root loci of the characteristic polynomial as function of the electric parameters.

Claim 11 (Optimal Pole Placement) *For the systems (6.36,6.40) the performance index (6.45) is maximized when the roots of the characteristic polynomial appear in the form of two complex conjugate pairs of coincident roots. Hence the systems we are considering are optimized when their*

[3] See for example [30] or [28]

characteristic polynomials can be factorized as

$$(\omega - \bar{\omega})^2(\omega - \bar{\omega}^*)^2 = 0 \tag{6.48}$$

This assumption can be checked numerically in each specific case.

With this assumption it is possible to find analytical expressions for the relations giving the optimal electric tuning and damping electric parameters as a function of the wavenumber k_0. Indeed, imposing that the characteristic polynomial of the system, whose coefficients are functions of β, δ can be factorized as (6.48), a nonlinear system of four equations in the four unknowns

$$\beta, \delta, \mathrm{Re}(\omega), \mathrm{Im}(\omega) \tag{6.49}$$

is found. The corresponding solution will furnish the values of β_{opt}, δ_{opt} and of the corresponding performance index (that is trivially given by $\mathrm{Re}(\omega)$) as function of k_0. In other words it is possible to find the following functions

$$\hat{\beta}_{opt}(k_0), \hat{\delta}_{opt}(k_0), \hat{P}(k_0, \hat{\beta}_{opt}(k_0), \hat{\delta}_{opt}(k_0)) \tag{6.50}$$

Once the relations (6.50) are known, it is possible to analyze also the sensitivity of the optimal parameters with respect to the wave number for which the system has been optimized, that are defined as follows:

Definition 22 (Parameter Sensitivity) *We define the* sensitivity *of the optimal values of the parameters with respect to a change of the wave number k the two quantities*

$$\hat{\sigma}_\beta(k) = \frac{\frac{d\hat{\beta}_{opt}(k)}{dk}}{\hat{\beta}_{opt}(k)} \quad \hat{\sigma}_\delta(k) = \frac{\frac{d\hat{\delta}_{opt}(k)}{dk}}{\hat{\delta}_{opt}(k)} \tag{6.51}$$

If these are evaluated for $k = 2\pi$, they will represent the sensitivity of the optimal parameters for a change of the wave number about that one relative to the characteristic wave length x_0.

In the following we will apply explicitly the outlined method to the cases on which we are interested.

6.4 Transversal-Electric Waves

In this case the linear operator that defines the system of *ODEs* governing the temporal evolution of electromechanical waves with a wavenumber k_0 is (6.37) and its characteristic polynomial is (6.39). We will find the optimal parameters for the following network configurations, particular cases of that in figure 6-1:

1. *Isolated Resonant Shunts* (figure 6-2). Only the ground inductance and resistance L_g, R_g are present. This case can be obtained from the general one by letting $L_l, R_l \to \infty$ (Thus $\beta_l \to 0, \delta_l \to 0$)

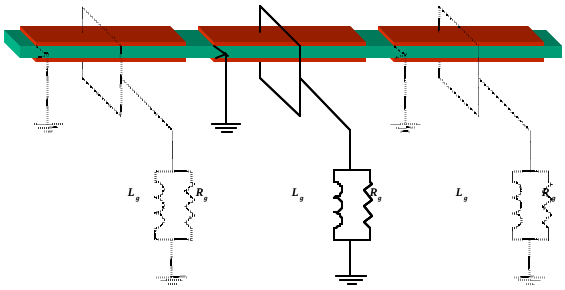

Figure 6-2: Isolated Resonant Shunts (*IRS*): Basic Cell

2. *Transmission Line with Line Resistance and Inductance* (figure 6-3).Only the line inductance and resistance L_l, R_l are present. This case can be obtained from the general one by letting $L_g, R_g \to \infty$ (Thus $\beta_g \to 0, \delta_g \to 0$)

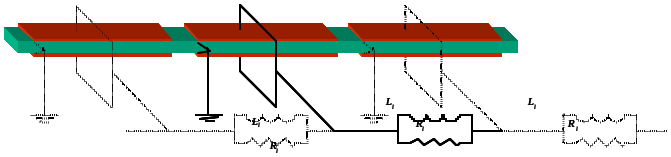

Figure 6-3: Trasmission Line with Line Resistance and Inductance (*TL*-R_l-L_l): Basic Cell

3. *Transmission Line with Line Inductance and Ground Resistance* (figure 6-4). In this case the line element reduces to an inductance L_l,while the element to ground reduces to a resistance R_g. The correspondent equations can be derived by letting $L_l, R_l \to \infty$.

In each case the PZT pairs of each element are electrically connected out-of-phase to realize a bending coupling. Hence we reduced the problem in finding the optimal resistance and inductance

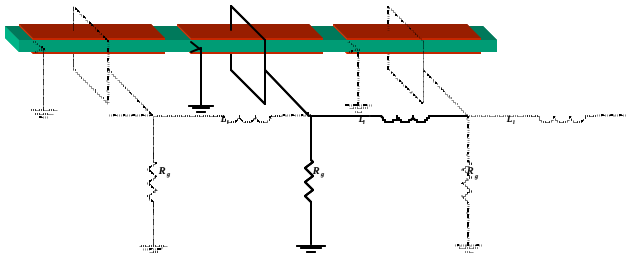

Figure 6-4: Trasmission Line with Line Inductance and Ground Resistance (TL-R_g-L_l): Basic Cell

for the three network configurations above in each case of which *only two electrical parameters are left free*. Thus the optimal parameters can be found with the procedure outlined in the previous section.

For the following developments let us recall the expressions of the dimensionless parameters

$$\begin{aligned} \beta_l &= \sqrt{\frac{\bar{\lambda}}{\bar{K}_f \bar{C}_g \bar{L}_l}}\, x_0 \quad \delta_l = \frac{1}{2x_0 \bar{R}_l \bar{C}_g}\sqrt{\frac{\bar{\lambda}}{\bar{K}_f}}\, x_0 \quad \gamma = \frac{\bar{G}_f}{\sqrt{\bar{K}_f \bar{C}_g}} \\ \beta_g &= \sqrt{\frac{\bar{\lambda}}{\bar{K}_f \bar{C}_g \bar{L}_g}}\, x_0^2 \quad \delta_g = \frac{1}{2\bar{R}_g \bar{C}_g}\sqrt{\frac{\bar{\lambda}}{\bar{K}_f}}\, x_0^2 \end{aligned} \tag{6.52}$$

and the relations between the homogenized and actual electrical quantities

$$\begin{aligned} \bar{L}_l &= \frac{L_l}{l_e} = L_l \frac{n_e}{x_0} \qquad \bar{R}_l = \frac{R_l}{l_e} = R_l \frac{n_e}{x_0} \qquad \bar{C}_g = \frac{C_g}{l_e} + 2f_l H = C_g \frac{n_e}{x_0} + 2f_l H \\ \bar{L}_g &= L_g l_e = L_g \frac{x_0}{n_e} \quad \bar{R}_g = R_g l_e = R_g \frac{x_0}{n_e} \end{aligned} \tag{6.53}$$

that have been rewritten in a convenient form by introducing the number n_e of elements in the characteristic length, such that

$$l_e = \frac{x_0}{n_e} \tag{6.54}$$

and the ratio

$$f_l = \frac{l_p}{l_e} \tag{6.55}$$

between the length of the PZT patch and that of the whole element.

The numerical values relative to the example presented in Appendix C will be considered[4]. For that case it has been found

$$\begin{array}{ll} \beta_l = \sqrt{\frac{\bar{\lambda}}{\bar{K}_f \bar{C}_g \bar{L}_l}} x_0 = 73.1\sqrt{\frac{x_0^3}{L_l n_e}} & \delta_l = \frac{1}{2R_l C_g}\sqrt{\frac{\bar{\lambda}}{\bar{K}_f}} = 1.56\times 10^4 \frac{x_0}{R_l n_e} \\ \beta_g = \sqrt{\frac{\bar{\lambda}}{\bar{K}_f \bar{C}_g \bar{L}_g}} x_0^2 = 73.1\sqrt{\frac{n_e x_0^3}{L_g}} & \delta_g = \frac{x_0^2}{2R_g C_g}\sqrt{\frac{\bar{\lambda}}{\bar{K}_f}} = 1.56\times 10^4 \sqrt{n_e^3 x_0}\frac{1}{R_g} \\ \gamma = \frac{\bar{G}_f}{\sqrt{\bar{K}_f \bar{C}_g}} = 0.212 & \kappa = \frac{\bar{C}_l}{\bar{C}_g x_0^2} = 1.82\times 10^5 \frac{C_l}{n_e x_0} \end{array} \tag{6.56}$$

6.4.1 Isolated Resonant Shunts (IRS)

The characteristic polynomial can be derived from the general case by posing $\beta_l = 0, \delta_l = 0$. It becomes

$$\omega^4 + 2\delta_g \omega^3 + \left(\beta_g^2 + k^4 + \gamma^2 k^4\right)\omega^2 + 2k^4 \delta_g \omega + k^4 \beta_g^2 = 0 \tag{6.57}$$

The values of the dimensionless parameters β_g, δ_g for which the two pairs of complex conjugate roots coalesce in a single pair are

$$\beta_{opt} = k^4 \quad \delta_{opt} = \gamma k^2$$

The real and imaginary parts of the roots corresponding to the optimal solution are given by

$$\omega^R = k^2 \frac{\gamma}{2} \quad \omega^I = k^2 \sqrt{1 - \left(\frac{\gamma}{2}\right)^2} \tag{6.58}$$

Hence the optimal values of the inductor and the resistor in each module are[5]

$$L_g^{opt} = \frac{\bar{\lambda} x_0^3}{2\bar{K}_f f_l H}\frac{n_e}{k^4} \quad R_g^{opt} = \frac{x_0}{2\bar{G}_f}\sqrt{\frac{\bar{\lambda}}{2f_l H}}\frac{n_e}{k^2} \tag{6.59}$$

The sensitivities $\sigma_L^{(1)}, \sigma_R^{(1)}$ of the optimal parameters respect to the wave number k are given by

$$\sigma_L^{(1)} = \left[\frac{d\frac{1}{k^4}}{dk} \Big/ \frac{1}{k^4}\right]_{k=2\pi} = -\frac{2}{\pi} \approx -63.6\% \quad \sigma_R^{(1)} = \left[\frac{d\frac{1}{k^2}}{dk} \Big/ \frac{1}{k^2}\right]_{k=2\pi} = -\frac{1}{\pi} \approx -31.8\% \tag{6.60}$$

[4] They are relative to the geometrical and material characteristics of the PEM beam that was experimentally realized, as it is described in Chapter 7.

[5] It has been posed

$$C_g = 0$$

Indeed an additional capacitance to ground has a negative effect on the damping ratio.

In the numerical case considered in Appendix C

$$L_g^{opt} = 3.43 n_e x_0^3 \frac{\mathrm{H}}{\mathrm{m}^3} \quad R_g^{opt} = 1.87 \times 10^3 . n_e x_0 \frac{}{\mathrm{m}} \tag{6.61}$$

For a wave length corresponding to the first mode of a simply supported beam[6] with a length $l_b = 0.51\,\mathrm{m}$, we can set $x_0 = 2l_b = 1.02\,\mathrm{m}$, consequently

$$L_g^{opt} = 3.64 n_e\,\mathrm{H} \quad R_g^{opt} = 1.90 \times 10^3 n_e \tag{6.62}$$

For $n_e = 10$,

$$L_g^{opt} = 36.4\,\mathrm{H} \quad R_g^{opt} = 19.0 \times 10^3 \tag{6.63}$$

6.4.2 Transmission Line with Line Resistance and Inductance(TL-R_l-L_l)

The characteristic polynomial can be derived from the general case by posing $\beta_g = 0$, $\delta_g = 0$. It is

$$\omega^4 - 2\delta_l k^2 \omega^3 + \left(k^4 + k^2\beta_l^2 + \gamma^2 k^4\right)\omega^2 - 2k^6\delta_l\omega + k^6\beta_l^2 = 0 \tag{6.64}$$

The values of the dimensionless parameters β_l, δ_l for which the two pairs of complex conjugate roots coalesce in a single pair are

$$\beta_{opt} = k^2 \quad \delta_{opt} = \gamma \tag{6.65}$$

The real and imaginary parts of the roots corresponding to the optimal solution are given by

$$\omega^R = k^2\frac{\gamma}{2} \quad \omega^I = k^2\sqrt{1 - \left(\frac{\gamma}{2}\right)^2} \tag{6.66}$$

Hence the optimal line inductance and resistance in each module are ($C_g = 0$)

$$L_l^{opt} = \frac{\bar{\lambda}x_0^3}{\bar{K}_f(2f_l H)}\frac{1}{n_e k^2} \quad R_l^{opt} = \frac{x_0}{2\bar{G}_f}\sqrt{\frac{\bar{\lambda}}{2f_l H}}\frac{1}{n_e} \tag{6.67}$$

and the corresponding sensitivities with respect to k are

$$\sigma_L^{(2)} = \left[\frac{d\frac{1}{k^2}}{dk}\Big/\frac{1}{k^2}\right]_{k=2\pi} = -\frac{1}{\pi} \approx -31.831\% \quad \sigma_R^{(2)} = 0 \tag{6.68}$$

[6] Again, the geometrical dimensions and boundary conditions refer to the *PEM* that was experimentally realized as described in Chapter 7.

In the numerical case considered in Appendix C

$$L_l^{opt} = 1.35 \times 10^2 \frac{x_0^3}{n_e} \frac{\mathrm{H}}{\mathrm{m}^3} \quad R_l^{opt} = 73.5 \times 10^3 \frac{x_0}{n_e} . \frac{-}{\mathrm{m}} \tag{6.69}$$

For a wave length corresponding to the first mode of a pinned-pinned beam with a length[7] $l_b = 0.51\,\mathrm{m}$, we can set $x_0 = 2l_b = 1.02\,\mathrm{m}$, consequently

$$L_l^{opt} = \frac{1.44}{n_e} \times 10^2\,\mathrm{H} \quad R_l^{opt} = \frac{75.0}{n_e} \times 10^3 \tag{6.70}$$

For $n_e = 10$,

$$L_l^{opt} = 14.4\,\mathrm{H} \quad R_l^{opt} = 7.50 \times 10^3 \tag{6.71}$$

6.4.3 Transmission Line with Line Inductance and Ground Resistance(TL-$\mathbf{R}_g$-$\mathbf{L}_l$)

This case can be obtained from the general one by letting $L_g, R_l \to \infty$. Since with these positions $\beta_g \to 0, \delta_l \to 0$, the characteristic polynomial becomes

$$\omega^4 + 2\delta_g\omega^3 + \left(k^4 + k^2\beta_l^2 + \gamma^2 k^4\right)\omega^2 + 2k^4\delta_g\omega + k^6\beta_l^2 = 0 \tag{6.72}$$

The values of the electrical parameters for which the four roots of the characteristic polynomial coalesce in a single pair are

$$\beta_l^{opt} = k^2 \quad \delta_g^{opt} = \gamma k^2 \tag{6.73}$$

The real and imaginary parts of the roots corresponding to the optimal solution are given by

$$\omega_i = k^2\frac{\gamma}{2} \quad \omega_r = k^2\sqrt{1 - \left(\frac{\gamma}{2}\right)^2} \tag{6.74}$$

Hence the optimal inductor and resistor in each module are

$$L_l^{opt} = \frac{\bar{\lambda}x_0^3}{\bar{K}_f(2f_lH)} \frac{1}{n_e k^2} \quad R_g^{opt} = \frac{x_0}{2\bar{G}_f}\sqrt{\frac{\bar{\lambda}}{2f_lH}}\frac{n_e}{k^2} \tag{6.75}$$

[7] Again, the geometrical dimensions and boundary conditions refer to the *PEM* that was experimentally realized as described in Chapter 7.

Table 6.1: Transverse-Electric waves: optimal values and sensitivities with respect to the wave number of the electric parameters for different network configurations

Network\Parameter	L_{opt}	σ_L	R_{opt}	σ_R
IRS	$c_L \frac{n_e}{k^4}$	$-\frac{2}{\pi}$	$c_R \frac{n_e}{k^2}$	$-\frac{1}{\pi}$
(TL-R_l-L_l)	$c_L \frac{1}{n_e k^2}$	$-\frac{1}{\pi}$	$c_R \frac{1}{n_e}$	0
(TL-R_g-L_l)	$c_L \frac{1}{n_e k^2}$	$-\frac{1}{\pi}$	$c_R \frac{n_e}{k^2}$	$-\frac{1}{\pi}$

The sensitivities with respect to k are

$$\sigma_L^{(3)} = \left[\frac{d\frac{1}{k^2}}{dk} / \frac{1}{k^2}\right]_{k=2\pi} = -\frac{1}{\pi} \approx -31.8\% \quad \sigma_R^{(3)} = \left[\frac{d\frac{1}{k^2}}{dk} / \frac{1}{k^2}\right]_{k=2\pi} = -\frac{1}{\pi} \approx -31.8\% \tag{6.76}$$

In the numerical case considered in Appendix C

$$L_l^{opt} = 1.35 \times 10^2 \frac{x_0^3}{n_e} \frac{\mathrm{H}}{\mathrm{m}^3} \quad R_g^{opt} = 1.87 \times 10^3 x_0 n_e . \frac{}{\mathrm{m}} \tag{6.77}$$

For a wave length corresponding to the first mode of a pinned-pinned beam with a length[8] $l_b = 0.51\,\mathrm{m}$, we can set $x_0 = 2l_b = 1.02\,\mathrm{m}$, consequently

$$L_l^{opt} = \frac{1.44}{n_e} \times 10^2\,\mathrm{H} \quad R_l^{opt} = 1.90 n_e \times 10^3 \tag{6.78}$$

For $n_e = 10$

$$L_l^{opt} = 14.4\,\mathrm{H} \quad R_l^{opt} = 19.0 \times 10^3 \tag{6.79}$$

6.4.4 Comparison of Network Configurations

Optimal Electric Parameters

The results that have been deduced for the optimal inductor and resistor for the three network configurations proposed are summarized in table 6.1, where the constants

$$c_L = \frac{\bar{\lambda} x_0^3}{2\bar{K}_f f_l H} \quad c_R = \frac{x_0}{2\bar{G}_f} \sqrt{\frac{\bar{\lambda}}{2 f_l H}} \tag{6.80}$$

are introduced. In table 6.2 the numerical values of those expressions are given for the numerical case previously introduced, where n_e is left as a parameter.

Let us underline the following important results:

[8] Again, the geometrical dimensions and boundary conditions refer to the *PEM* that was experimentally realized as described in Chapter 7.

Table 6.2: Transverse-Electric waves: optimal values of the electric dimensionless parameters for different network configurations

Network\Parameter	L_{opt} (H)	R_{opt} (k)
IRS	$3.64 n_e$	$1.90 n_e$
(TL-R_l-L_l)	$143.6 \frac{1}{n_e}$	$74.98 \frac{1}{n_e}$
(TL-R_g-L_l)	$143.6 \frac{1}{n_e}$	$1.90 n_e$

1. about the dependence of the optimal values on n_e:

   (a) The value of $L_{opt} = c_L \frac{1}{n_e k^2}$ is the same for both the network configurations with a line inductor (*TL-R_g-L_l* and *TL-R_l-L_l*)

   (b) The value of $R_{opt} = c_R \frac{n_e}{k^2}$ is the same for both network configurations with a ground resistor (*IRS* and *TL-R_g-L_l*)

   (c) For different network configurations the optimal inductor in each element of the periodic system has an opposite dependence on the number of elements n_e in a wave length: L_{opt} is proportional to n_e for the *IRS* configuration with a ground inductor, proportional to $\frac{1}{n_e}$ for the networks with a line inductor (*TL-R_l-L_l*, *TL-R_g-L_l*). Thus

   $$\frac{L_{opt}^{line}}{L_{opt}^{ground}} = \frac{1}{n_e^2}$$

   (d) The optimal resistor in each element as a function of n_e has the same behavior as the optimal inductor: R_{opt} is proportional to n_e when it is connected to ground (*IRS* and *TL-R_g-L_l* networks), it is proportional to $\frac{1}{n_e}$ when it is a line resistor (*TL-R_l-L_l* configuration)

2. about the sensitivity of the optimal parameters respect to k:

   (a) In the networks with a line inductor (*TL-R_l-L_l*, *TL-R_g-L_l*) σ_L is half of that in the configuration with a ground inductor (*IRS*)

   $$\frac{\sigma_L^{line}}{\sigma_L^{ground}} = \frac{1}{2}$$

   (b) In the network *TL-R_l-L_l* with a line resistor, σ_R is zero.

Decaying Time

Referring to the definitions (6.26),(6.27) it is interesting to compare the values of the decay time and of the damping ratio for the optimal values of the electric parameters.

We can note that in an optimal system, the characteristic decay time is the same for all three networks configurations examined. It is given by

$$\Theta = \frac{1}{\omega^R} = \frac{2}{\gamma k^2} \tag{6.81}$$

while the corresponding frequency is

$$\omega^I = k^2 \sqrt{1 - \left(\frac{\gamma}{2}\right)^2} \tag{6.82}$$

Thus the optimal damping ratio becomes

$$Z = \frac{\omega^R}{\omega^I} = \frac{\gamma}{\sqrt{4 - \gamma^2}} \tag{6.83}$$

such that, considering the expressions of γ and of $\bar{C}_g$, can be rewritten as

$$Z = \frac{1}{\sqrt{\frac{8\bar{K}_f \bar{C}_g}{\bar{G}_f^2} - 1}} = \frac{1}{\sqrt{\frac{4\bar{K}_f \left(\frac{C_g}{x_0} n_e + 2 f_l H\right)}{\bar{G}_f^2} - 1}} \tag{6.84}$$

Hence it is evident that *an additional capacitance* C_g, in parallel to the PZT one, *has a negative effect*. So that it is convenient to pose $C_g = 0$. In that case

$$Z = \frac{1}{\sqrt{\frac{8\bar{K}_f f_l H}{\bar{G}_f^2} - 1}} \tag{6.85}$$

With the numerical values that have been considered

$$Z = .106 = 10.6\% \tag{6.86}$$

We can also associate to the system the characteristic number of periods, n_{per}

$$n_{per} = \frac{1}{Z} = 9.40 \tag{6.87}$$

We can conclude that once the electric parameters are set to the optimal values, *the damping ratio*

and the decay time are independent of the network topology.

Waves in Optimal Systems: Damping by Varying the Wave Number

If waves with a fixed wave number k_0 are considered, it is possible to fix the corresponding optimal electric parameters to minimize the decay time of the propagating waves. However it is interesting to study the behavior of the systems optimized for k_0 when wave numbers $k \neq k_0$ are considered. To this end the solution of the characteristic equations for the optimal electric parameters as a function of k give important information. In figure 6-5 the real and the imaginary parts of the two complex conjugate pairs,

$$\omega_{1,2}(k/k_0) = \omega_1^R \pm i\omega_1^I \quad \omega_{3,4}(k/k_0) = \omega_2^R \pm i\omega_2^I \tag{6.88}$$

representing the roots of the secular equation, are reported for the three network configurations. The colors represent the mechanical (dark), electrical (bright) or coupled (mixed) characteristic of the wave mode[9].

[9] The color is given as a function of the ratio between the mechanical and electrical amplitude of each wave mode.

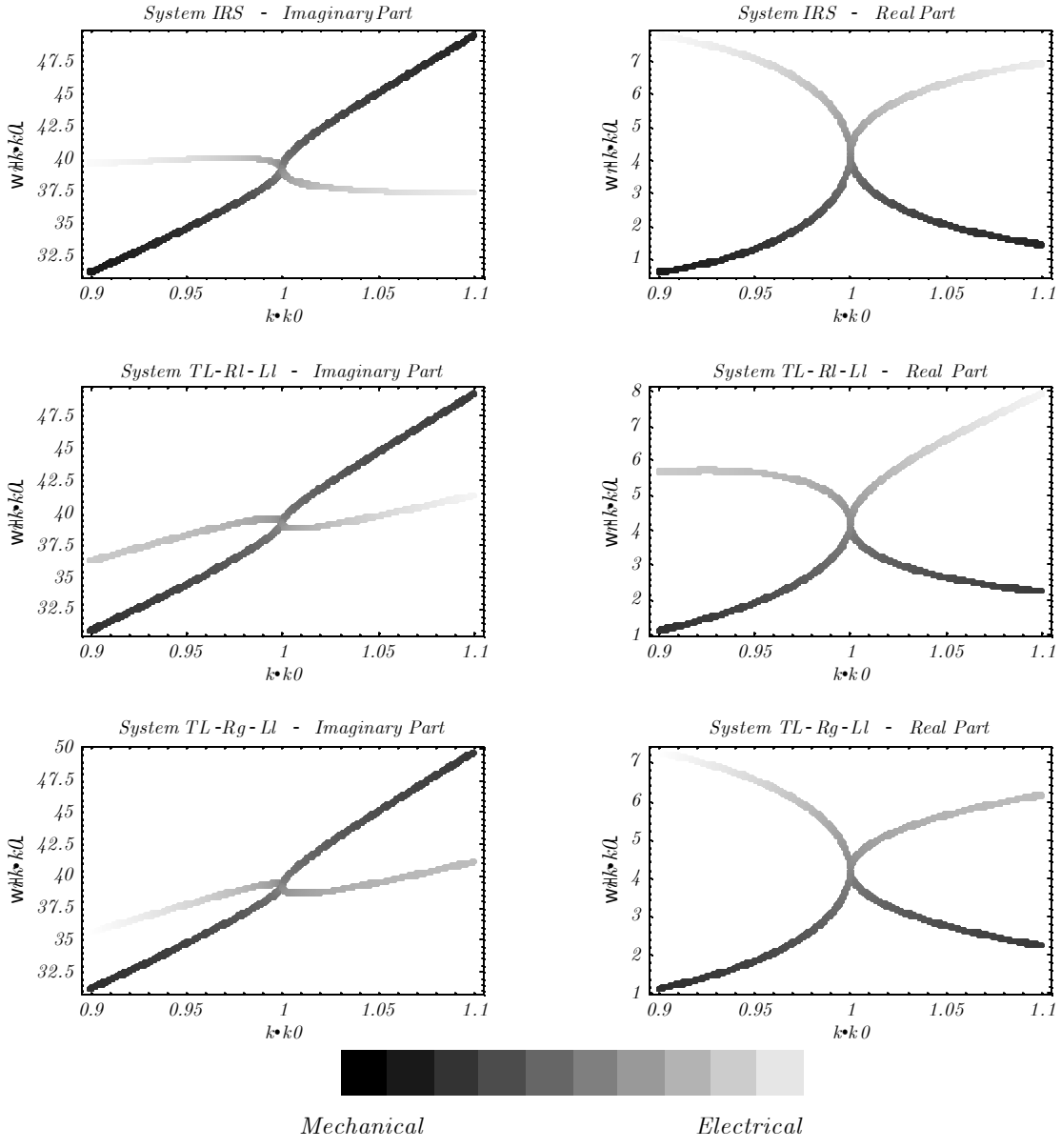

Figure 6-5: Real and imaginary parts of $\omega(k)$, solution of the characteristic polynomial in the optimal system for trasverse-electric waves: comparison of network configurations

A direct comparison between the damping performances of the three network configurations can be achieved by plotting the function

$$\breve{P}(x) := \hat{P}(xk_0, \hat{\beta}_{opt}(k_0), \hat{\delta}_{opt}(k_0)) \tag{6.89}$$

or equivalently the reciprocal $\breve{C}(x) = \frac{1}{\breve{P}(x)}$ representing the characteristic damping time for waves with wavenumber $k = xk_0$ in a system optimized for waves with wavenumber k_0. The function $\breve{C}(x)$ for the three network configurations that have been analyzed is reported in figure 6-6.

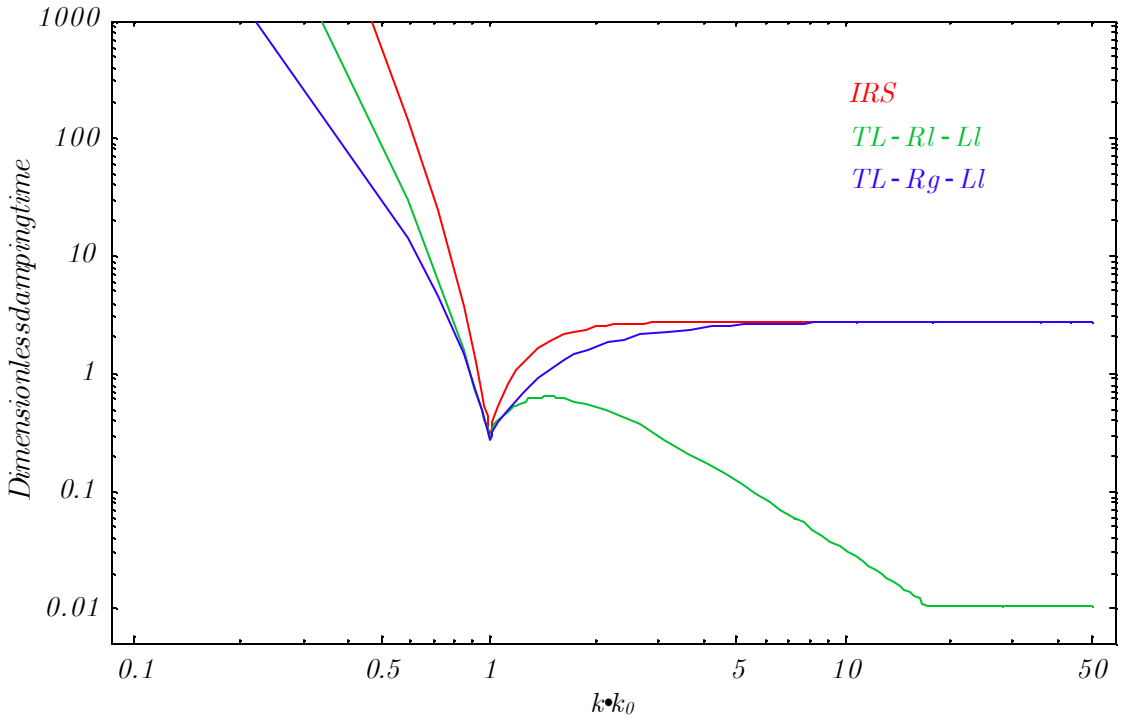

Figure 6-6: Dimensionless damping time as function of k/k_0

Looking at this plot , the fact that the green system $(TL - R_l - L_g)$ is decaying faster for wave numbers k greater than that one for which it has been optimized, can appear as a contradiction. However, also the dependence of the optimal decay time on the wave number must be taken into account (see relations(6.58,6.66,6.74)). Hence, to make the discussion clearer, we report in a plot (figure 6-7) the function

$$\breve{C}_{ratio}(x) = \frac{\breve{C}(x)}{\breve{C}_{opt}(x)} \tag{6.90}$$

where

$$\breve{C}_{opt}(x) := \frac{1}{\breve{P}(x, \hat{\beta}_{opt}(x), \hat{\delta}_{opt}(x))} \tag{6.91}$$

expressing, for each system, the ratio between the actual damping time $\breve{C}(\frac{k}{k_0})$ and that one obtainable in a system optimized each time for the actual wave number k.

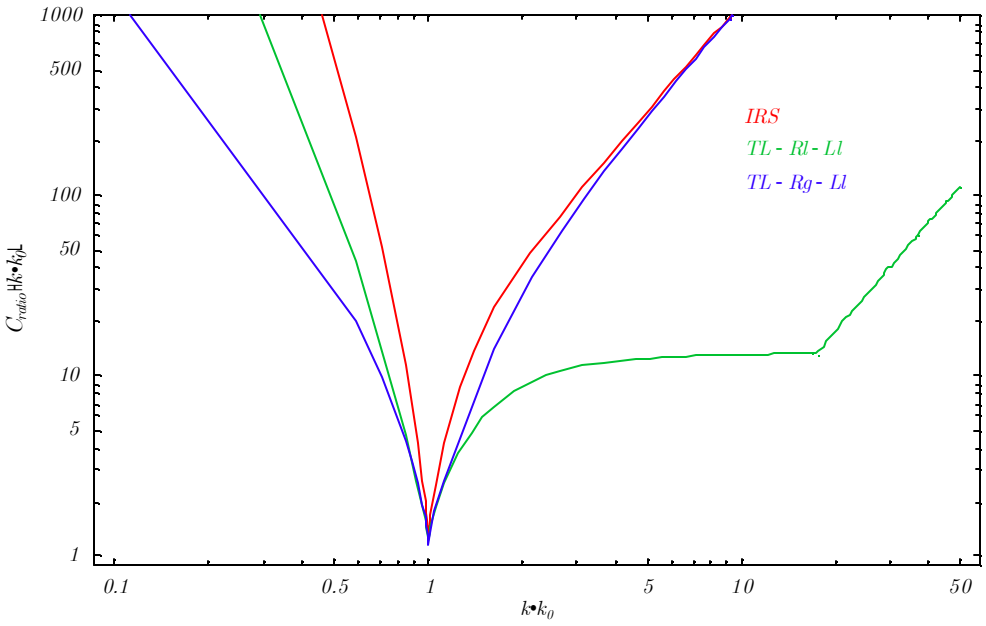

Figure 6-7: Ratio between the actual damping time and that one achievable in optimal conditions as a function of k/k_0

Looking at the presented plots we can check numerically the previously assumed circumstances:

1. For all the network configurations considered the four complex roots of the secular equations can be collected in two pairs of the form 6.88 (see figure 6-5).

2. In the relevant parameter range the performance index $\breve{P}(k)$ is maximized when the two pairs of roots of the secular equation coalesce in a single one (see figure 6-5 and 6-7).

These important facts were used to find *analytical relations* for the optimal values of the electric parameters and the performance of the optimal systems.

We can also note that in correspondence of the value k_0 of k for which the systems have been optimized, there is an effective coupling between the mechanical and electric components of the propagating waves (see colors in figure 6-5).

The most important result can be deduced by figure 6-7. As it has been previously noted, the performances of the three network configurations are the same for the value of the wave length $k = k_0$ for which they have been designed. *However the networks TL-R_l-L_l with a line inductance realizing second order electric transmission lines present better performances for values of k greater than k_0.* In particular the system *TL-R_l-L_l* realizes a damping time less than ten times greater than the optimal one for $1 \leq \frac{k}{k_0} \leq 20$. For applications this fact is very important since it shows that, with an opportune network connection, it is possible to significantly damp waves with a wide range of wavenumbers. For instance, considering a simply supported PEM beam, if one optimizes the system for the wavelength relative to the first bending mode, one can strongly damp also the second, third and fourth mode.

In order to emphasize this fact, in figure 6-8 the modal mechanical energies of the first six bending modes of a PEM with different network connections optimized for the first mode are presented.

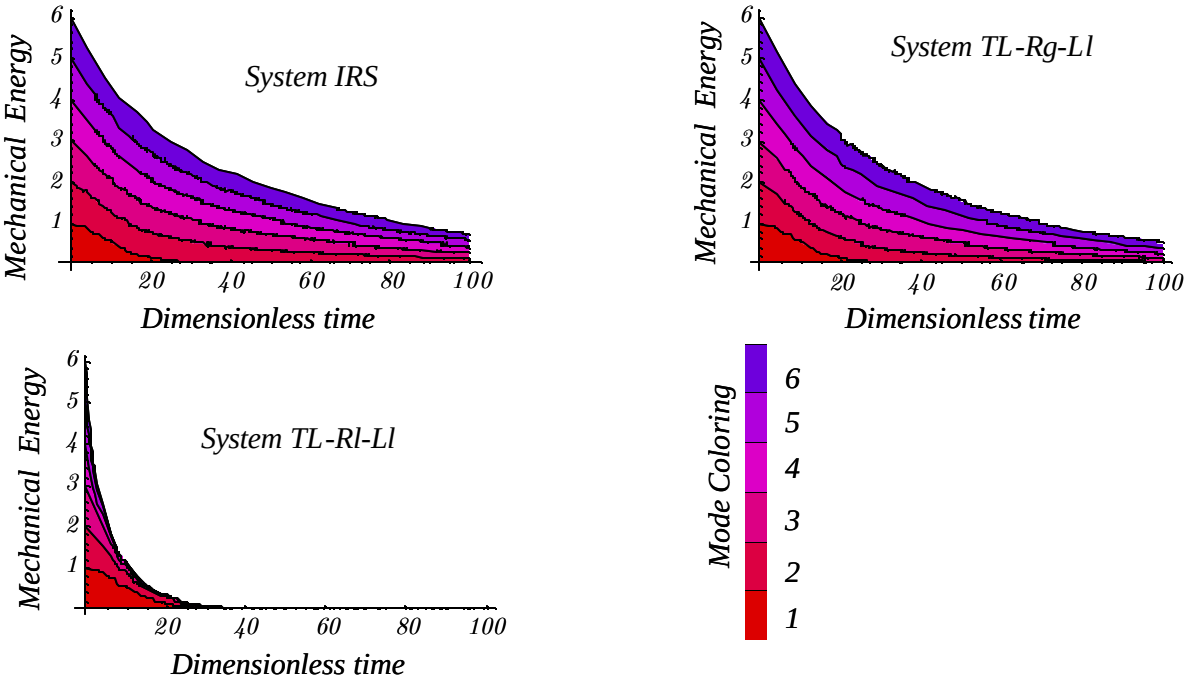

Figure 6-8: Modal mechanical energies as a fuction of time for a simply supported PEM beam with different network topologies optimized for the first bending mode.

6.5 Longitudinal-Electric Waves

For the longitudinal case we will follow the same procedure adopted for the transverse-electric waves.

6.5.1 Isolated Resonant Shunts (IRS)

The characteristic polynomial can be derived from the general case by posing $\beta_l = 0, \delta_l = 0$. It becomes

$$\omega^4 + 2\delta_g\omega^3 + \left(\beta_g^2 + k^2\left(1-\gamma^2\right)\right)\omega^2 + 2k^2\delta_g\omega + k^2\beta_g^2 = 0 \tag{6.92}$$

The values of the dimensionless parameters β_g, δ_g for which the two pairs of complex conjugate roots coalesce in a single pair, are

$$\beta_{opt} = k \quad \delta_{opt} = \gamma k \tag{6.93}$$

The real and imaginary parts of the roots corresponding to the optimal solution are given by

$$\omega^R = k\frac{\gamma}{2} \quad \omega^I = k\sqrt{1-\left(\frac{\gamma}{2}\right)^2} \tag{6.94}$$

Hence the optimal values of the inductor and the resistor in each module are[10]

$$L_g^{opt} = \frac{\bar{\lambda}x_0^3}{2\bar{K}_l f_l H}\frac{n_e}{k^2} \quad R_g^{opt} = \frac{x_0}{2\bar{G}_l}\sqrt{\frac{\bar{\lambda}}{2f_l H}}\frac{n_e}{k} \tag{6.95}$$

The sensitivities $\sigma_L^{(1)}, \sigma_R^{(1)}$ of the optimal parameters with respect to the wave number k are given by

$$\sigma_L^{(1)} = \left[\frac{d\frac{1}{k^2}}{dk}\Big/\frac{1}{k^2}\right]_{k=2\pi} = -\frac{1}{\pi} \approx -31.8\% \quad \sigma_R^{(1)} = \left[\frac{d\frac{1}{k}}{dk}\Big/\frac{1}{k}\right]_{k=2\pi} = -\frac{1}{2\pi} \approx -15.9\% \tag{6.96}$$

In the numerical case considered in Appendix C

$$L_g^{opt} = 207 n_e x_0^3 \times 10^{-6}\frac{\mathrm{H}}{\mathrm{m}^3} \quad R_g^{opt} = 23.44 n_e x_0 \frac{}{\mathrm{m}} \tag{6.97}$$

[10] It has been posed

$$C_g = 0$$

Indeed an additional capacitance to ground has a negative effect on the damping ratio.

For a wave length corresponding to the first mode of a simply supported beam with a length[11] $l_b = 0.51\,\mathrm{m}$, we can set $x_0 = 2l_b = 1.02\,\mathrm{m}$, consequently

$$L_g^{opt} = 219.7 \times 10^{-6} n_e\,\mathrm{H} \quad R_g^{opt} = 23.\,9 n_e \tag{6.98}$$

For $n_e = 10$

$$L_g^{opt} = 219.7 \times 10^{-5}\,\mathrm{H} \quad R_g^{opt} = 239 \tag{6.99}$$

6.5.2 Transmission Line with Line Resistance and Inductance(TL-R_l-L_l)

The characteristic polynomial can be derived from the general case by posing $\beta_g = 0$, $\delta_g = 0$. It is

$$\omega^4 - 2\delta_l k^2 \omega^3 + k^2\left(1 + \beta_l^2 - \gamma^2\right)\omega^2 - 2k^4\delta_l\omega + k^4\beta_l^2 = 0 \tag{6.100}$$

The values of the dimensionless parameters β_l, δ_l for which the two pairs of complex conjugate roots coalesce in a single pair, are

$$\beta_{opt} = 1 \quad \delta_{opt} = \gamma/k \tag{6.101}$$

The real and imaginary parts of the roots corresponding to the optimal solution are given by

$$\omega^R = k\frac{\gamma}{2} \quad \omega^I = k\sqrt{1 - \left(\frac{\gamma}{2}\right)^2} \tag{6.102}$$

Hence the optimal line inductance and resistance in each module are ($C_g = 0$)

$$L_l^{opt} = \frac{\bar{\lambda} x_0^3}{\bar{K}_l (2 f_l H)} \frac{1}{n_e} \quad R_l^{opt} = \frac{x_0}{2\bar{G}_l}\sqrt{\frac{\bar{\lambda}}{2 f_l H}}\frac{k}{n_e} \tag{6.103}$$

and the corresponding sensitivities with respect to k are

$$\sigma_L^{(2)} = 0 \quad \sigma_R^{(2)} = \left[\frac{dk}{dk}/k\right]_{k=2\pi} = \frac{1}{2\pi} \approx 15.9\% \tag{6.104}$$

In the numerical case considered in Appendix C

$$L_l^{opt} = 8.179 \times 10^{-3}\frac{x_0^3}{n_e}\frac{\mathrm{H}}{\mathrm{m}\,3} \quad R_l^{opt} = 925.2\frac{x_0}{n_e}\frac{}{\mathrm{m}} \tag{6.105}$$

[11] Again, the geometrical dimensions and boundary conditions refer to the *PEM* that has been experimentally realized as described in Chapter 7.

For a wave length corresponding to the first mode of a pinned-pinned beam with a length[12] $l_b = 0.51\,\mathrm{m}$ we can set $x_0 = 2l_b = 1.02\,\mathrm{m}$, consequently

$$L_l^{opt} = 8.68 \times 10^{-3} \frac{1}{n_e}\,\mathrm{H} \quad R_l^{opt} = \frac{943.7}{n_e} \tag{6.106}$$

For $n_e = 10$

$$L_l^{opt} = 8.68 \times 10^{-4}\,\mathrm{H} \quad R_l^{opt} = 94.37 \tag{6.107}$$

6.5.3 Transmission Line with Line Inductance and Ground Resistance(TL-R_g-L_l)

This case can be obtained from the general one by letting $L_g, R_l \to \infty$. Since with these conditions $\beta_g = 0, \delta_l = 0$ the characteristic polynomial becomes

$$\omega^4 + 2\delta_g\omega^3 + k^2\left(1 + \beta_l^2 - \gamma^2\right)\omega^2 + 2k^2\delta_g\omega + k^4\beta_l^2 = 0 \tag{6.108}$$

The values of the electrical parameters for which the roots of the characteristic polynomial coalesce in a single pair are

$$\beta_l^{opt} = 1 \quad \delta_g^{opt} = \gamma k \tag{6.109}$$

The real and imaginary parts of the roots corresponding to the optimal solution are given by

$$\omega^R = k\frac{\gamma}{2} \quad \omega^I = k\sqrt{1 - \left(\frac{\gamma}{2}\right)^2} \tag{6.110}$$

Hence the optimal inductor and resistor in each module are

$$L_l^{opt} = \frac{\bar{\lambda}x_0^3}{\bar{K}_l(2f_lH)}\frac{1}{n_e} \quad R_g^{opt} = \frac{x_0}{2\bar{G}_l}\sqrt{\frac{\bar{\lambda}}{2f_lH}}\frac{n_e}{k} \tag{6.111}$$

The sensitivities with respect to k are

$$\sigma_L^{(3)} = 0 \quad \sigma_R^{(3)} = \left[\frac{d\frac{1}{k}}{dk}\Big/\frac{1}{k}\right]_{k=2\pi} = -\frac{1}{2\pi} \approx -15.9\% \tag{6.112}$$

[12] Again, the geometrical dimensions and boundary conditions refer to the *PEM* that has been experimentally realized as described in Chapter 7.

Table 6.3: Longitudinal-Electric waves: optimal values and sensitivities respect to the wave number of the electric parameters for different network configurations

Network\Parameter	L_{opt}	σ_L	R_{opt}	σ_R
IRS	$c_L \frac{n_e}{k^2}$	$-\frac{1}{\pi}$	$c_R \frac{n_e}{k}$	$-\frac{1}{2\pi}$
(TL-R_l-L_l)	$c_L \frac{1}{n_e}$	0	$c_R \frac{k}{n_e}$	$\frac{1}{2\pi}$
(TL-R_g-L_l)	$c_L \frac{1}{n_e}$	0	$c_R \frac{n_e}{k}$	$-\frac{1}{2\pi}$

In the numerical case considered in Appendix C

$$L_l^{opt} = 8.179 \times 10^{-3} \frac{x_0^3}{n_e} \frac{\mathrm{H}}{\mathrm{m3}} \quad R_g^{opt} = 23.44 n_e x_0 \frac{}{\mathrm{m}} \tag{6.113}$$

For a wave length corresponding to the first mode of a pinned-pinned beam with a length[13] $l_b = 0.51\,\mathrm{m}$ we can set $x_0 = 2l_b = 1.02\,\mathrm{m}$, consequently

$$L_l^{opt} = 8.68 \times 10^{-3} \frac{1}{n_e}\,\mathrm{H} \quad R_g^{opt} = 23.9 n_e \tag{6.114}$$

For $n_e = 10$

$$L_l^{opt} = 8.68 \times 10^{-4}\,\mathrm{H} \quad R_g^{opt} = 239 \tag{6.115}$$

6.5.4 Comparison of Network Configurations

Optimal Electric Parameters

The results obtained for the optimal inductor and resistor for the three network configurations proposed are summarized in table 6.3, where the constants

$$c_L = \frac{\bar{\lambda} x_0^3}{2\bar{K}_l f_l H} \quad c_R = \frac{x_0}{2\bar{G}_l} \sqrt{\frac{\bar{\lambda}}{2 f_l H}}$$

are introduced. In table 6.4 the numerical values of those expressions are given for the numerical case previously introduced, where n_e is left as a parameter.

The results obtained are qualitatively analogous to those for the transverse waves. In this case we can note that for the network topologies with a line inductor (*TL-R_l-L_l*, *TL-R_g-L_l*) the optimal inductor is independent of the wavenumber. So that, with those configurations it is possible to tune the electrical and mechanical systems for all frequencies. This is a direct consequence of the fact

[13] Again, the geometrical dimensions and boundary conditions refer to the *PEM* that has been experimentally realized as described in Chapter 7.

Table 6.4: Longitudinal-Electric waves: optimal values of the electric dimensionless parameters for different network configurations

Network\Parameter	L_{opt} (H)	R_{opt} (k)
IRS	$219.7 \times 10^{-6} n_e$	$23.9 n_e$
(TL-R_l-L_l)	$8.68 \times 10^{-3} \frac{1}{n_e}$	$\frac{943.7}{n_e}$
(TL-R_g-L_l)	$8.68 \times 10^{-3} \frac{1}{n_e}$	$23.9 n_e$

that the differential equations governing the evolutions of the mechanical and electrical systems are, for this cases, of the same order. However for all the network configurations that have been analyzed, the optimal resistor in each module depends on the wavenumber. Hence, despite of being possible to realize an optimal energy exchange between the mechanical and electrical systems for all the wavenumbers, it is not possible to realize also an optimal damping for all wavenumbers.

Decay Time

In the three cases that have been examined the characteristic number of periods to damp the waves in optimal conditions is the same, given by

$$n_p = \frac{\sqrt{4-\gamma^2}}{\gamma} = \sqrt{\frac{4}{\gamma^2} - 1} = \sqrt{\frac{8\bar{K}_l f_l H}{\bar{G}_l^2} - 1}$$

corresponding to a damping ratio

$$Z = \frac{1}{n_p} = \frac{1}{\sqrt{\frac{8\bar{K}_l f_l H}{\bar{G}_l^2} - 1}} \tag{6.116}$$

Hence once the electric parameters are set to the optimal values *the damping ratio and the decay time are independent of the network* considered.

Waves in Optimal Systems: Damping Varying the Wave Number

For the coupling between the extensional and electrical waves in PEM beams let us report only the fundamental results that are summarized in figures 6-9, 6-10. In the first one the dimensionless decay time $\breve{C}(k/k_0)$ as a function of the ratio k/k_0 in systems optimized for a wavenumber k_0 is plotted, while figure 6-10 shows the behavior of the function $\breve{C}_{ratio}(k/k_0)$, defined by (6.90), for the three network configurations that have been analyzed.

Looking at the previous plots we can deduce conclusions similar to those derived for the transverse waves. In particular we can note that with the network topologies TL-L_l-R_l and TL-L_l-R_g

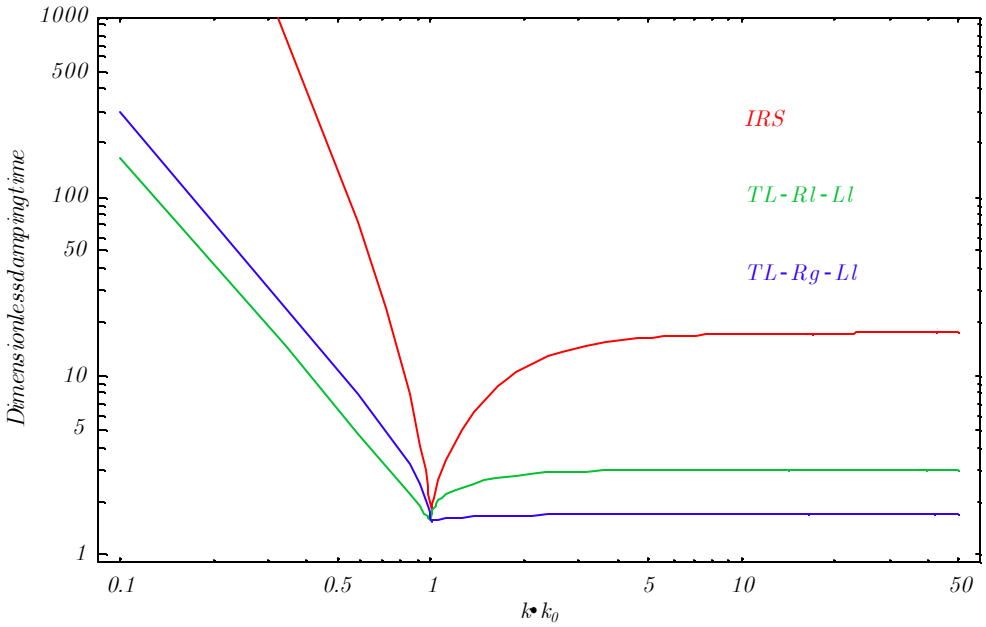

Figure 6-9: Dimensionless damping time as a function of k/k_0 in systems that have been optimized for a wavenumber k_0

it is possible to realize a better damping than with *IRS*. The first one is better for $\frac{k}{k_0} < 1$ while the second for $\frac{k}{k_0} > 1$. However, since the optimal resistor depends on the wavenumber, despite the fact that damping time is independent of the wavenumber for $\frac{k}{k_0} > 1$ (see blue line in figure 6-9), the systems cannot be optimized for all wavenumbers (see figure 6-10)

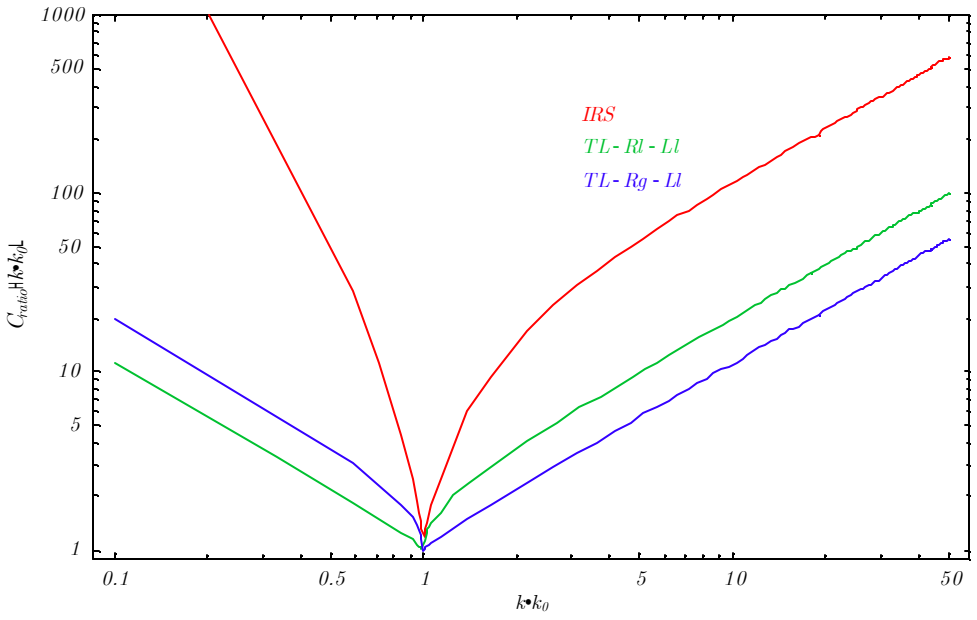

Figure 6-10: Ratio between the actual damping time and that one achievable in optimal conditions as a function of k/k_0

Chapter 7

Experiments

The problem of the experimental realization of a PEM beam to be used for the validation of the analytical and numerical results has been addressed. An experimental setup for the modal analysis of mechanical and electrical systems has been tested and an identification procedure to extrapolate their modal characteristics from the experimental frequency response has been developed. The electronic devices[1] needed to assemble the electrical networks presented in the previous chapters have been realized and tested. Finally a classical experiment for resonant shunted PZTs has been reproduced to check the whole experimental apparatus.

7.1 Goals

The main goal of the experimental project of which this work is the starting point is the validation of the numerical and analytical results obtained about the effectiveness of a distributed piezoelectric coupling between a structure and an electric network for the broadband passive control of mechanical vibrations. The final ambition is to realize prototypes to experimentally compare the performances of the following systems:

1. a beam coupled with a resonant RLC circuit by means of a PZT transducer;
2. a beam coupled with n separated RLC circuits by means of a periodic array of PZT transducers (see figure 6-2);
3. a beam coupled with the lumped version of a second order transmission line by means of a periodic array of PZT transducers (see figures 6-3 and 6-4).

[1] In principle the proposed electrical networks are composed only of resistors and inductors. However the characteristics required by the latter induce us to synthetize them by electronic devices.

The present work is the first step of this program. Its objectives are

1. to test technological solutions for the experimental use of PZT materials;
2. to develop and test both an experimental setup and an identification procedure for the extraction of the modal parameters of electromechanical systems;
3. to realize and characterize a pinned-pinned beam with five pairs of PZT transducers in bimorph configuration to be used in a series of future experiments;
4. to realize and characterize the electronic devices needed to assemble the electrical networks;
5. to test the objects at points 3 and 4 by reproducing a classical experiment for a resonant shunted PZT.

7.2 System Design and Realization

The experimental apparatus has been designed to facilitate the measurements and to emphasize the relevant physical aspects utilizing materials and geometrical parameters frequently faced in engineering applications. The original idea carried on in this project is the realization of a distributed piezoelectric coupling between a mechanical and an electrical continuum for vibration damping. As a matter of fact only a lumped version of an electrical continuum effectively coupled with a mechanical structure can be actualized[2]. Hence a modular PEM beam has been set up.

Two critical technological problems that have been faced:

1. bonding the PZT transducers on the beam leaving an electrical access to the electrodes
2. realizing large value adjustable inductors with low parasite resistances.

7.2.1 Beam with PZT Transducers

The simply supported beam with five pairs of PZT transducers in bimorph configuration in figure 7-1 has been realized. The beam was made from aluminum (Young modulus $E_Y = 70 \times 10^9\,\mathrm{Pa}$, mass density $\rho_b = 2700\frac{\mathrm{kg}}{\mathrm{m}^3}$).

The geometrical dimensions of the beam

$$\text{lenght } l_b = 51\,\mathrm{mm}$$
$$\text{width } w_b = 40\,\mathrm{mm}$$
$$\text{thickness } t_b = 4\,\mathrm{mm}$$

[2] See the Introduction for more datails about the problem.

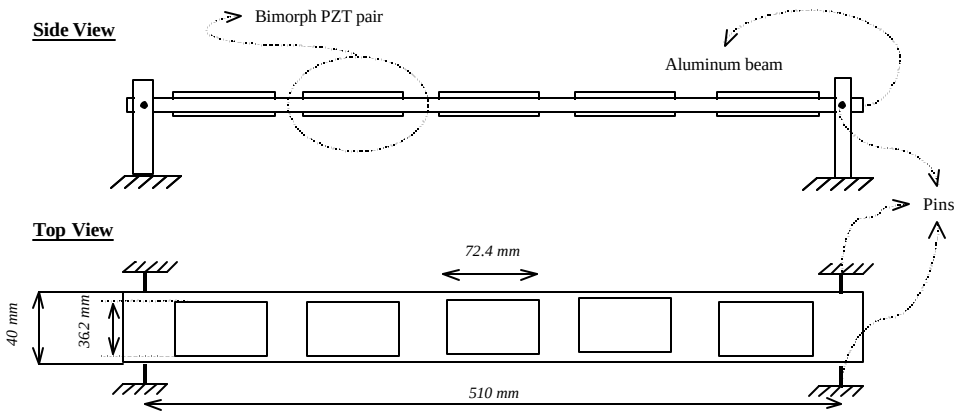

Figure 7-1: Pinned-pinned beam with five bimorph PZT pairs

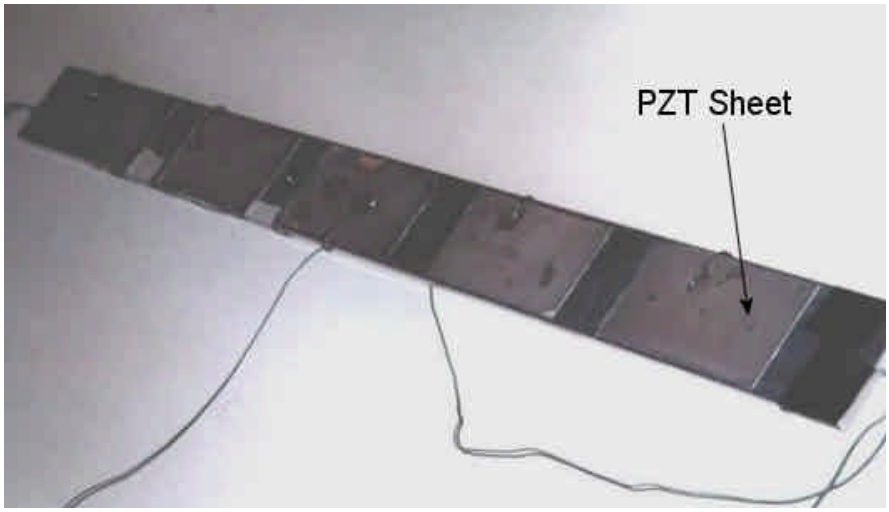

Figure 7-2: Realized beam with PZT transducers

have been chosen to maintain the first natural frequency above 30 Hz to avoid difficulties for dynamical measurements.

The system can be interpreted as the assembly of five modules as evident in figure 7-1. The number of basic cells has been chosen to realize a modular system that, in the frequency range of interest, can be approximated sufficiently well by an homogenized continuous model. Here we focused our attention on the first mechanical spatial mode of the simply supported beam.

Piezoelectric Transducers

The *Piezo System T110-H4E-602* transducers were used. They are composed of a single sheet of PZT *PSI-5H4E Ceramic* material with nickel electroded upper and lower surfaces. The charac-

teristics of the PZT material are reported in figure 7-4. Each item is sold as a parallelepiped of dimensions $74.2 \times 74.2 \times 0.267\,\text{mm}$.

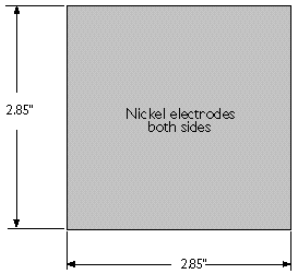

Figure 7-3: Single sheet piezoelectric transducer

The sheet was cut using a diamond edge into two equal parts with

$$\text{lenght } l_p = 74.2\,\text{mm}$$
$$\text{width } w_p = 36.1\,\text{mm}$$
$$\text{thickness } t_p = 0.267\,\text{mm}$$

The transverse dimensions have been chosen in agreement with those of the beam. The transducers

PIEZOELECTRIC			
Composition		Lead Zirconate Titanate	
Material Designation		PSI-5H-S4-ENH (Industry Type 5H, Navy Type VI)	
Relative Dielectric Constant (@ 1 kHz)	K^T_3	3800	
Piezoelectric Strain Coefficient	d_{33}	650×10^{-12}	meters/Volt
	d_{31}	-328×10^{-12}	meters/Volt
Piezoelectric Voltage Coefficient	g_{33}	19.0×10^{-3}	Volt meters/Newton
	g_{31}	-8.5×10^{-3}	Volt meters/Newton
Coupling Coefficient	k_{33}	0.75	
	k_{31}	0.44	
Polarization Field	Ep	1.5×10^6	Volts/meter
Initial Depolarization Field	Ec	3.0×10^6	Volts/meter
MECHANICAL			
Density		7800	kg/meter^3
Mechanical Q		80	
Elastic Modulus	Y^E_3	5.0×10^{10}	Newtons/meter^2
	Y^E_1	6.2×10^{10}	Newtons/meter^2
THERMAL			
Thermal Expansion Coefficient		-3×10^{-6}	meters/meter °C
Curie Temperature		350	°C

Figure 7-4: Characteristics of used PZT material.

have been designed with two contrasting goals: to have a high electromechanical coupling and to limit the voltage across the two electrodes. Indeed, realizing electronic devices for high voltage applications is a technological problem, especially when operational amplifiers are adopted (see

7.2.2).

The choice of this type of transducers was motivated by

1. the possibility of cutting a transducer in a desired shape
2. its constructive simplicity that allows a good understanding of its behavior
3. the good characteristic of the PZT material
4. the high price/quality ratio

Each bimorph pair of PZTs has been realized as reported in figure 7-5. The two sheets were connected in *parallel* and *out-of-phase* to obtain a flexural-electric coupling. The electric connections to the electrodes have been realized using a 60/40 solder alloy and a specific flux for nickel electrodes. The PZT sheets were bonded to the aluminum beam using an electrically conductive silver-loaded epoxy resin. In this way the lower electrode of the PZT was electrically accessible by means of the conductive beam that was grounded. The connections were optimized to reduce the number of wires number and lengths to limit induced noise.

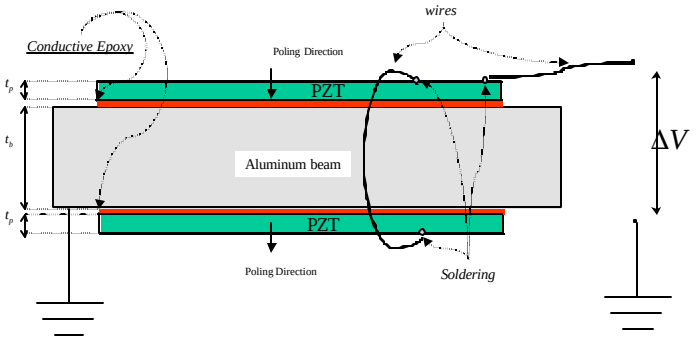

Figure 7-5: PZT pair in bimorph configuration: detailed constructive scheme.

7.2.2 Electric Networks

In principle the needed electric networks are composed only of elementary components, as resistors, capacitors and inductors. However, as has been found by theoretical analysis, vary large value adjustable inductors with low parasite resistances are required. Completely passive components with these characteristics are not convenient. Here synthetic inductors have been used.

Synthetic Inductors

The synthetic inductors that have been used are electronic circuits composed of resistors, capacitors and operational amplifiers. The problem of synthesizing analog circuits presenting a desired input impedance has been widely studied in electronics. These circuits are known as General Impedance Converters (GIC). Here an alternative modification of Antoniou's GIC, presented in [27], has been used. The circuit diagram is reported in figure 7-6.

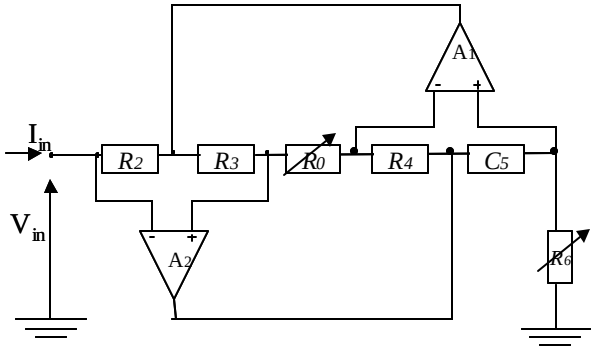

Figure 7-6: Synthetic inductor: an alternative modification of Antoniou's GIC

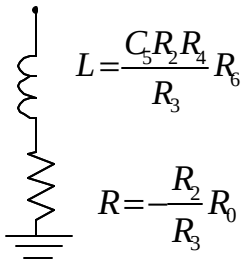

Figure 7-7: Synthetic Inductor: ideal equivalent impedance

The ideal input impedance of this circuit (see figure 7-7) is the same as a series connection between an inductor and a negative resistor with values

$$\begin{aligned} L &= \frac{C_5 R_2 R_4}{R_3} R_6 \\ R &= -\frac{R_2}{R_3} R_0 \end{aligned} \tag{7.1}$$

In this way the desired equivalent inductance and resistance can be obtained by simply adjusting the values of the two trimmers R_6 and R_0 respectively, on which they are linearly dependent. To have good behavior in the desired range of the equivalent parameters the following values of the

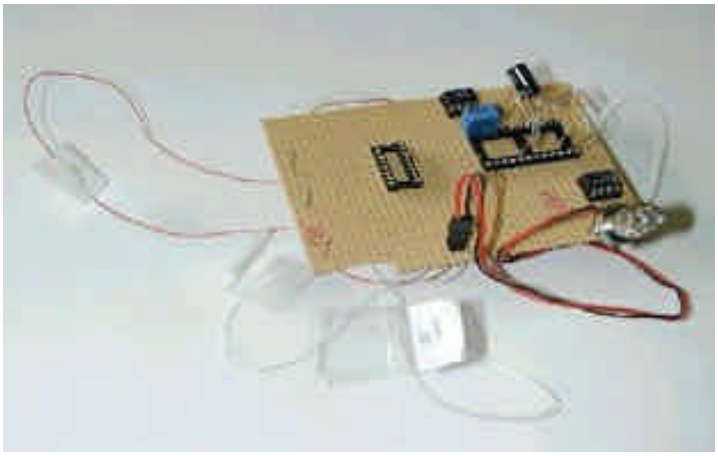

Figure 7-8: Synthetic Inductor

components were chosen

$$R_2 = 3\,\mathrm{k} \qquad R_3 = 1\,\mathrm{k}$$
$$R_4 = 1\,\mathrm{k} \qquad C_5 = 10\,\mu\mathrm{F}$$

The opportunity of having a negative series resistance is useful because it allows the cancellation of parasite resistances that can have a negative effect on vibration damping.

The actual behavior of the synthetic inductor has been investigated experimentally by measuring the frequency response of the RLC circuit composed when a series connection with a known capacitance is realized, as in figure 7-9. In figure 7-18 the experimental values of the equivalent

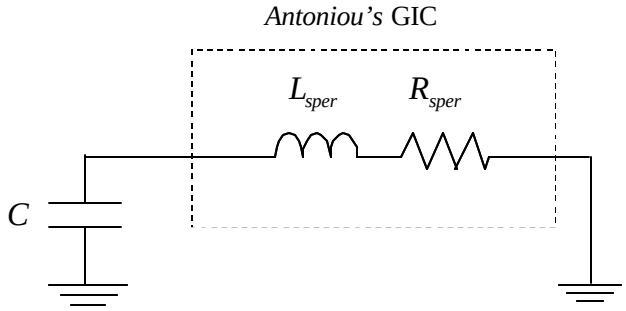

Figure 7-9: RLC resonant circuit for experimental testing of the Antoniou's GIC by frequency response measurements.

resistance are reported as a function of R_6 comparing them with those from (7.1). In figure 7-19 the total actual parasite resistance of the GIC is plotted as a function of the values of $R_{0.}$ In both the cases a linear interpolation of the experimental data is also added with the respective coefficient

of correlation R^2.

The circuit in figure 7-6 must have one terminal connected to ground. However floating synthetic inductors can be obtained in a similar way. For more information see [23].

A negative aspect of this solution is that operational amplifiers need a dual DC power supply to work. Thus despite of the components of the electric networks are theoretically passive, its actual realization requires an external power supply. However the power absorbed by the Op-Amp is very low and it is not comparable with that required in active control techniques. The operational amplifiers $TL-081$ have been used with DC voltage supply at $\pm 12V$, furnished by two batteries connected as in figure 7-10.

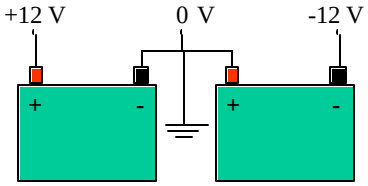

Figure 7-10: Batteries for alimentation of Op-Amps

7.3 Experimental Modal Analysis

Mechanical and electrical dynamical measures were taken in a frequency range from 10 to 800 Hz following the standard modal analysis techniques. The modal characteristics of the mechanical and the electrical systems were extrapolated from their frequency response by means of an identification procedure. Here the peculiarities of the experimental apparatus and of the measurement procedure will be emphasized, referring to [13], [12] for generalities about the subject.

7.3.1 Instrumentation

Hardware

For the dynamical measurements the following instrumental hardware has been used

1. Piezoelectric accelerometer *Bruel&Kier* 4393 with charge amplifier *Bruel&Kier* 2635
2. Force transducer *Bruel&Kier* 8200 with charge amplifier *Bruel&Kier* 2635
3. Electromagnetic shaker *Bruel&Kier* 4809 with power amplifier *Bruel&Kier* 2700
4. Scanning laser vibrometer *Polytec* $OF055$ with controller *Polytec* $OFV\ 30001S$

5. Analogical two channels oscilloscope *Hameg* $203-5$

6. Personal Computer, processor *AMD-K6* 266 MHz, 64 *Mb* Ram memory, equipped with

   (a) A/D converter National Instruments $PCI-4452$ (Basic technical data in figure 7-11, for more informations see *www.ni.com*)

   (b) A/D and D/A converter National Instruments $AT-MIO-16E-10$ (Basic technical data in figure 7-11, for more informations see *www.ni.com*)

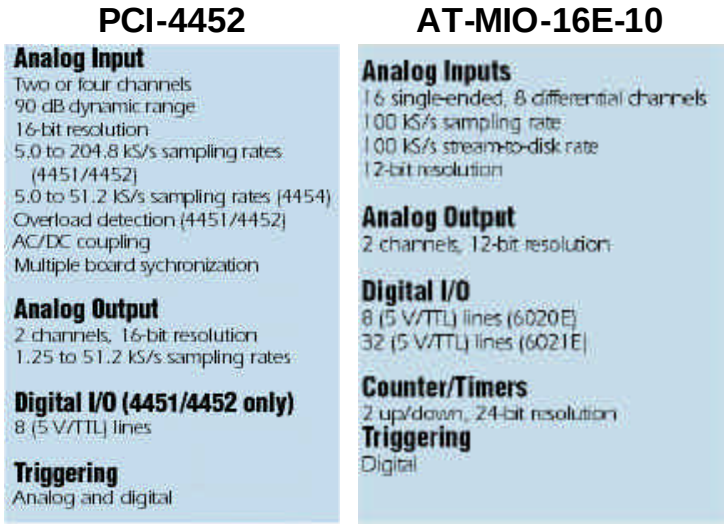

Figure 7-11: Acquisition and generation boards technical datasheets.

Software

A personal computer has been utilized for the management of the digital input and output and signal processing. In an unique LabView code the following Virtual Instruments were gathered

1. sweep[3] generator

2. anti-leakage windowing on the input and output signals

3. spectrum analyzer

4. frequency response analyzer

[3] A sweep is a sinuosodal signal with a frequency linearly dependent on time. Its time representation is of the type

$$f(t) = f_0 \sin\left(\frac{\omega_2-\omega_1}{T}t^2 + \omega_1 t\right)$$

It spans linearly the frequencies from ω_1 to ω_2 for t between 0 and T. It is a transient excitation signal frequently used in Experimental Modal Analysis to investigate the behavior of the system in an assigned frequency range.

7.3.2 Experimental Setup for Mechanical and Electrical FRF Measures

The main measurements regarded the mechanical frequency response of the simply supported beam in figure 7-1 and the electrical frequency response of a RLC resonant circuit with the GIC in figure 7-6. To obtain the frequency response of a physical system between an input and an output terminal we followed the procedure represented in figure 7-12. Three fundamental logical phases can be distinguished

1. excitation (input)
2. measurements of the given input and the consequent output
3. signal processing

The third is identical for mechanical and electrical systems, the other two are different. Indeed, if a mechanical system is considered the electrical quantities must be transduced to mechanical ones for the excitation and vice-versa for the measurements[4].

The signal generation and processing have been implemented by means of a personal computer with a LabView code. A transient excitation method has been adopted generating a digital *sweep* signal.The outputs of each measurement were the digital time signals, their FFTs, and the system FRF. Only the FFTs have been stored to extract from them the modal parameters by an identification procedure.

Let us describe the details of the mechanical and electrical experimental setups separately.

Mechanical Experimental Set up

The chain of measurement in figure 7-13 has been utilized to obtain the frequency response of a mechanical or electromechanical beam[5] relative to a force input and an acceleration output. The structure has been excited by means of a shaker (1) (the numbers refer to those in figure 7-13), that is controlled through an amplifier by a digital input given with the electronic calculator (7). For the Digital/Analog conversions the board $AT-MIO-16E-10$ (8) has been utilized. The shaker has been attached to the structure through a support to limit the rotational stiffening in correspondence to the attachment point. The force effectively transmitted to the structure has been measured with a force transducer (2). The output was measured by means of a piezoelectric accelerometer (4)

[4] The signals are intended to be electrical. All the physical quantities to be measured must be transduced to electric signals (if they are not) in order to process them..

[5] Indeed the same set up can be used when the beam is coupled or not to an electric network by means of PZTs transducers.

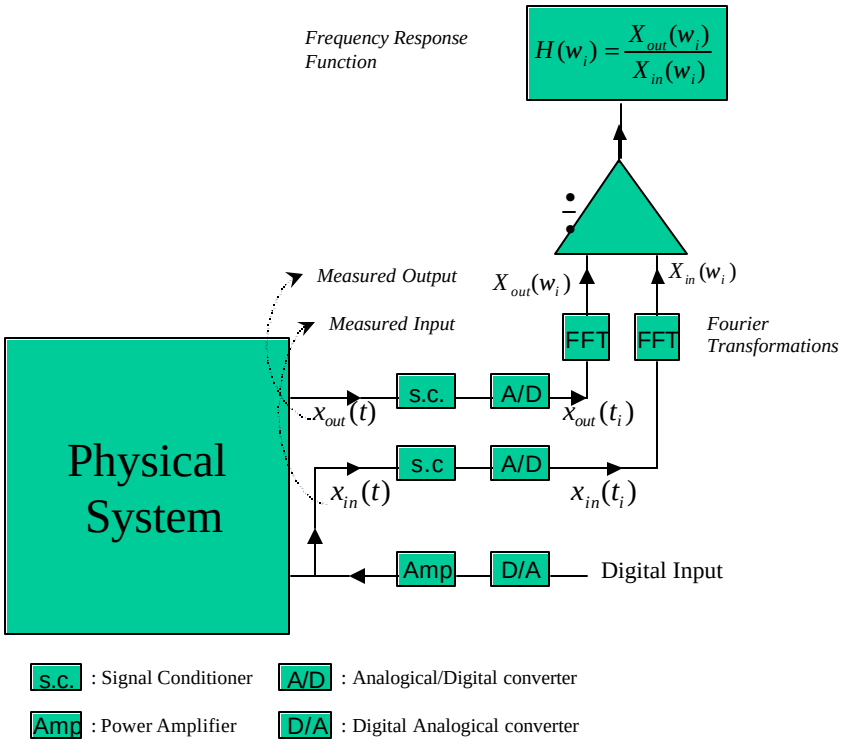

Figure 7-12: Logical scheme for Frequency Response measurements

attached with a thin layer of wax. The locations of the excitation and the response have been optimized to

1. give the best results for the first mode of the simply supported beam, compatibly with the presence of the PZT patches. Indeed, if one considers the spatial shape of the first mode, the force transducer has been placed where the rotation is the smallest, the accelerometer where the deflection is the greatest[6].

2. avoid particular positions for which some fundamental modes are automatically filtered out.

The two measured analog signals have been amplified and conditioned by two charge amplifiers (3,5). Then they were sampled using the board $PCI-4452$ in which both analog and real-time digital anti-aliasing filters were incorporated.

[6] Obeying those criteria, the central position should be chosen. Unfortunately it is occupied by the PZT layers.

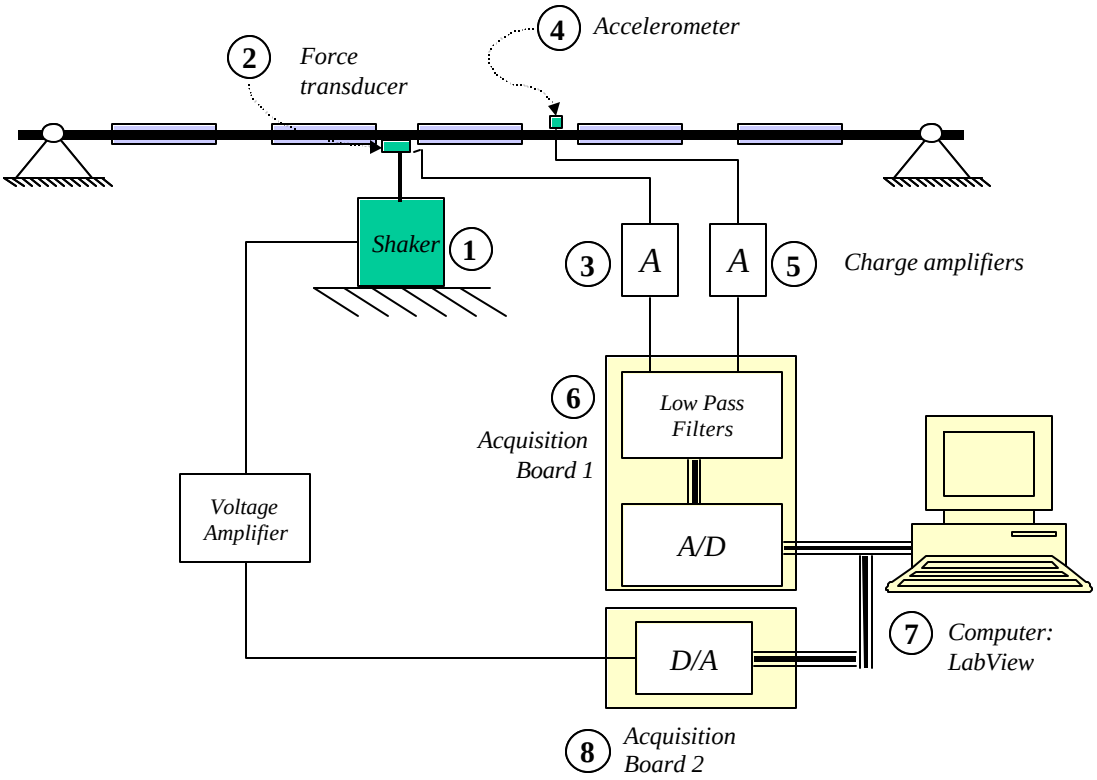

Figure 7-13: Experimental set up for mechanical FRF measurements

Electrical Experimental set up

The experimental set up for the electrical measurements differs from the previous one only because no transducers are needed since the physical quantities to be measured and to be imposed are voltages. The frequency response of a *RLC* series circuit has been found as sketched in figure 7-14.

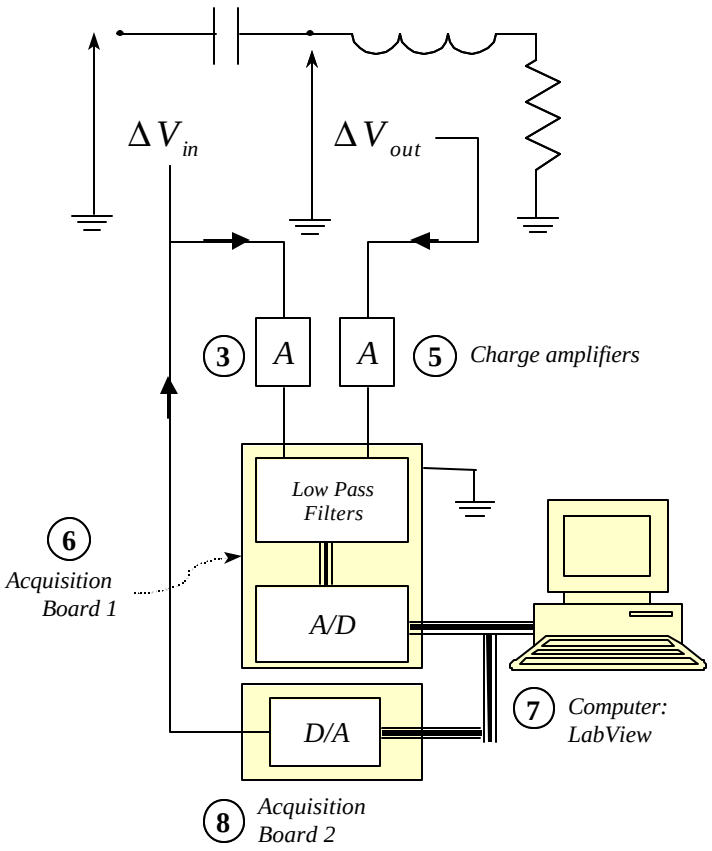

Figure 7-14: Experimental set up for electrical FRF measurements

7.3.3 Identification Procedure

From the frequency response, given as a complex scalar function defined on the frequency domain, the modal characteristics of the measured systems has been extracted. The averaged resonant frequencies and damping ratios were deduced with the respective confidence intervals from a series of N measures taken in the same conditions and for the same values of the acquisition parameters. The procedure followed is outlined in figure 7-15. Three main phases can be distinguished

1. *Synchronization and Statistical Analysis* of the input and output frequency domain data as result of a set of N experiments taken in the same conditions. These have been averaged calculating the empirical variances and input-output covariances. A foregoing synchronization is required to eliminate a residual phase shift between the measures. This is realized minimizing the weighted phase differences of the complex amplitudes in the frequency domain by introducing a delay. In figure 7-17 an example of the statistical analysis on the FRF experimental data for a simply supported beam is reported.

2. *Frequency Domain Identification* of each set of data and extraction of the resonant frequencies and damping ratios. This step has been implemented utilizing a MatLab Toolbox. It requires as input the frequency domain data with an estimation of the variances and input-output covariances and the number of poles and zeros to be assumed for a Laplace domain form of the model in which the system must be identified. As outputs the estimated poles and zeros are given. The real and imaginary parts of each complex conjugate pair of poles can be easily converted to the corresponding natural frequency and damping ratio. This procedure has been repeated for the N sets of measures. An example of the output of the MatLab code is given in figure 7-15.

3. *Statistical Analysis of the Modal Parameters* resulting from the N identifications. From the N sets of the extracted resonant frequencies and damping ratios the mean values of the modal parameters have been derived with the respective confidence intervals.

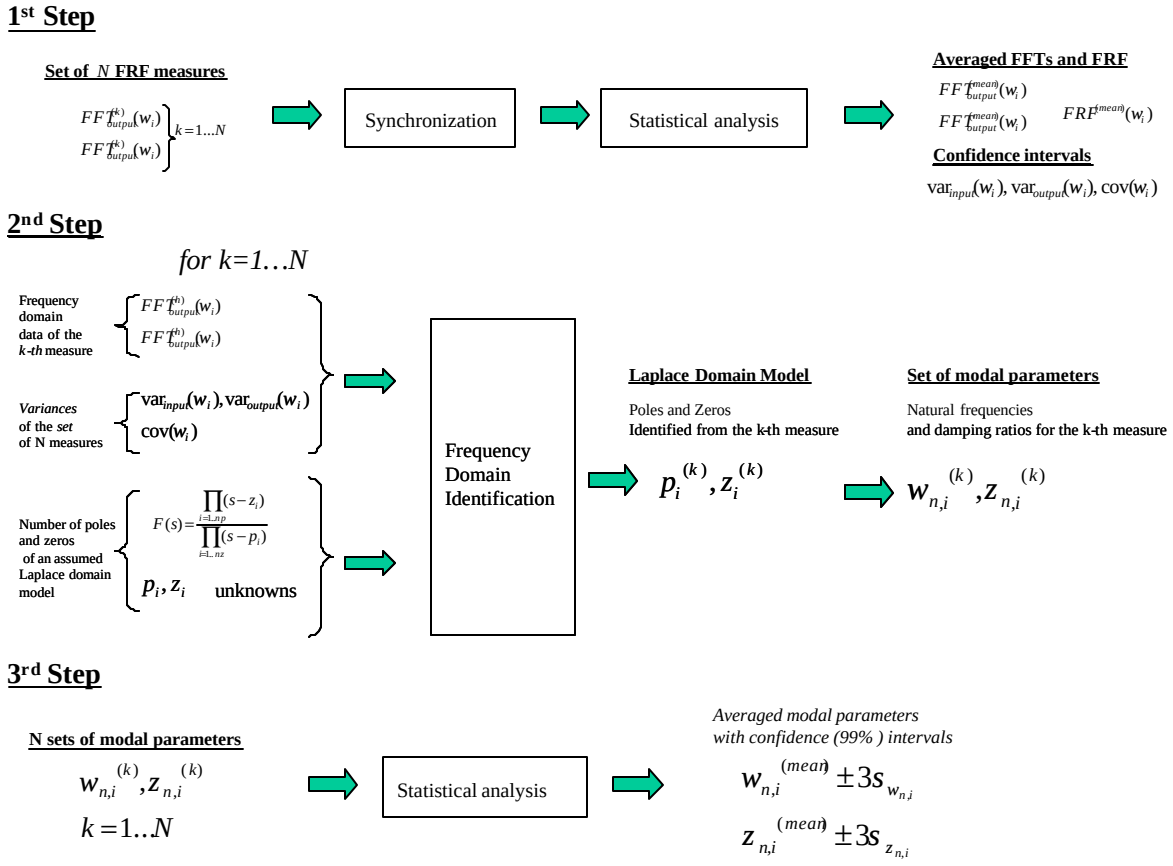

Figure 7-15: Identification procedure

7.4 Results

7.4.1 Beam Modal Parameters

The natural frequencies and damping ratios of the first three modes of the beam in figure 7-1 without the PZT transducers have been found experimentally following the procedure outlined in the previous sections. In particular the experimental setup in figure 7-13 and the identification procedure in figure 7-15 have been adopted. The following results have been found

Mode	Natural Frequency (Hz)		Damping Ratio	
	Mean Value	99% C.I.	Mean Value	99% C.I.
1st	34.95	$\pm 2.2 \times 10^{-2}$	0.10%	$\pm 7.5 \times 10^{-3}$%
2nd	137.2	$\pm 2.9 \times 10^{-3}$	0.26%	$\pm 1.3 \times 10^{-3}$%
3rd	304.5	$\pm 3.2 \times 10^{-3}$	0.24%	$\pm 1.46 \times 10^{-3}$%

We can note that the confidence intervals are very narrow, thus the measurements are good. This is a validation of the experimental setup and of the quality of the utilized instruments. However let us underline that the statistical analysis has been performed on a set of measures taken with the same experimental conditions. In particular small values of the damping ratio are strongly influenced by the environment and must be considered only as an indication of their order of magnitude. An example of the identification of experimental frequency response for one of the N measures in the range from 10 to 400 Hz is presented is figure 7-16 together with the extracted poles and zeros and the phase error between the measured data and the identified FRF.

7.4.2 Synthetic Inductors Characterization

The values of the equivalent resistance and inductance of the synthetic inductor in figure 7-6 have been extrapolated by frequency response measurements of the resonant circuit assembled once a series connection with a known capacitance is realized (see figure 7-9). The measures have been taken as in figure 7-14. The resonant frequency and damping ratio have been deduced with the same procedure followed for the mechanical beam. The equivalent inductance and resistance as a function of the variable resistors R_6 and R_0 are reported in figures 7-18 and 7-19 respectively. A linear interpolation of the experimental data is presented (see also 7.2.2).

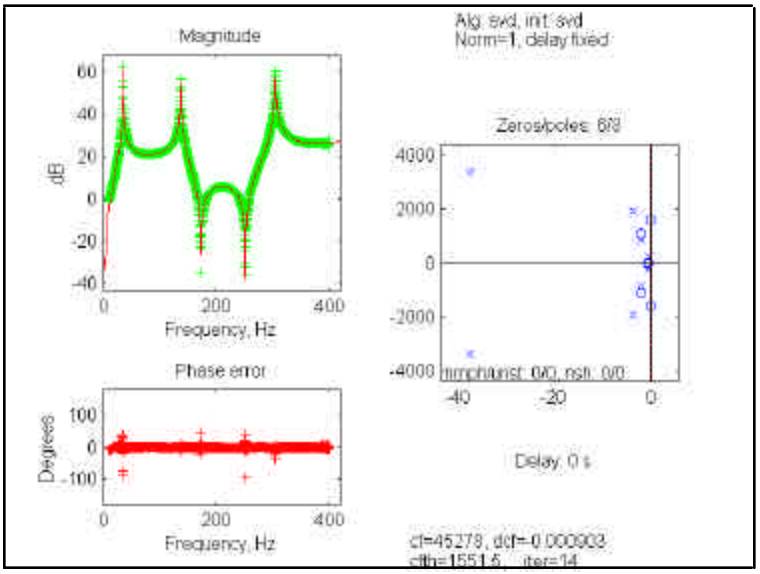

Figure 7-16: Results of the identification of the first three modes of the simply supported aluminum beam

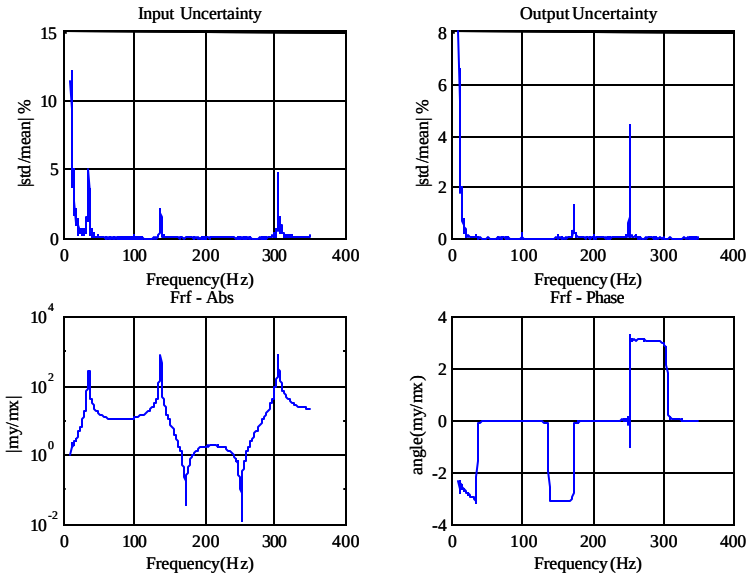

Figure 7-17: Statistical analysis on a set of 15 measures of the beam FRF: mean values and uncertainties

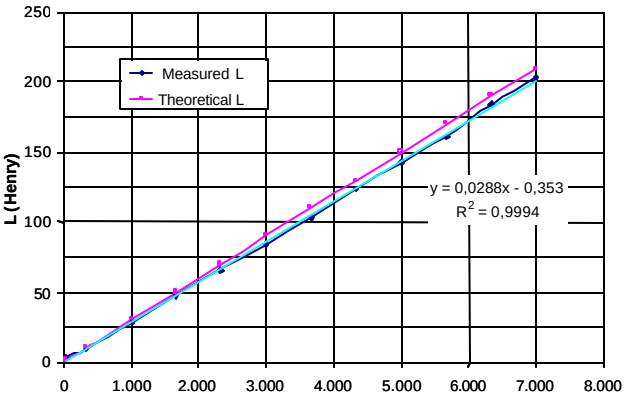

Figure 7-18: Synthetic inductor: experimental and theoretical equivalent inductance L vs resistance R_6

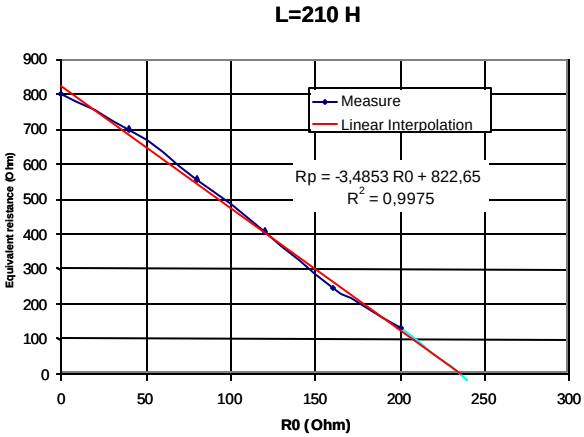

Figure 7-19: Effect of R_0 on the parasite resistance for a fixed equivalent inductance $L = 210\,\mathrm{H}$.

7.4.3 Beam with Resonant Shunted PZT

To validate the experimental apparatus set up for future investigations (see 7.5), a basic experiment on shunted PZT has been replicated using the simply supported beam with the bonded piezoelectric sheets and the tested synthetic inductor. The main idea of coupling the first mode of the beam with the dynamics of a dissipative RLC circuit utilizing the piezoelectric transducer has been developed. Only the central PZT pair has been used, shunting it with a series connection of a resistor and a synthetic inductor. The other transducers have been short-circuited as in figure 7-20. We will

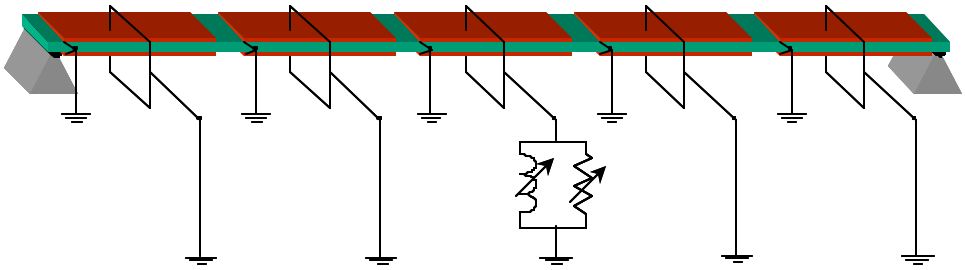

Figure 7-20: Configuration for the resonant shunted PZT experiment

present quickly only the obtained result skipping the details about the experiment since the case has been widely studied in literature (see for example [30] or [29]). The values of the resistor and of the inductor for an optimal damping of the first mode of the beam have been evaluated by measurement of the first beam natural frequency for open-circuited and short-circuited PZT. The FRF has been found with the experimental set up in figure 7-13. Then the modal parameters have been extracted with the identification procedure in figure 7-15. We found

$$\begin{aligned} L_{opt} &= 36 \text{ H} \\ R_{opt} &= 2.1 \text{ k} \end{aligned}$$

In figure 7-21 the experimental frequency response of the beam for electric parameter values close to the optimal ones are compared with those for open and short-circuit conditions. The corresponding poles found by means of the frequency domain identification are plotted in the complex plane in figure 7-22. As can be noted a relevant reduction of the forced response is obtained and the damping ratio is significantly increased. However the reduction of the frequency response is achieved only for a narrow band centered on the resonance frequency. The issue of developing a broadband damping should be solved by the distributed coupling, as we hope to verify with future experiments.

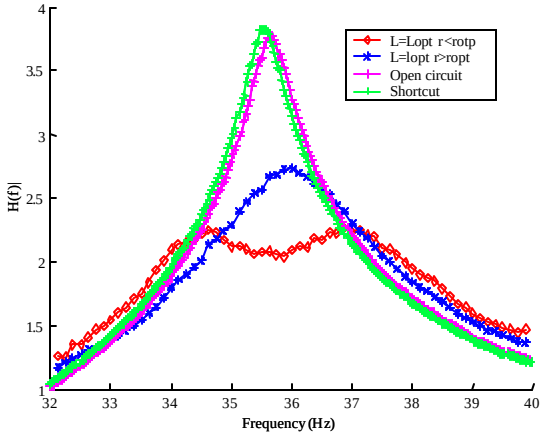

Figure 7-21: Frequency responce reduction for tuned resonant shunted PZT

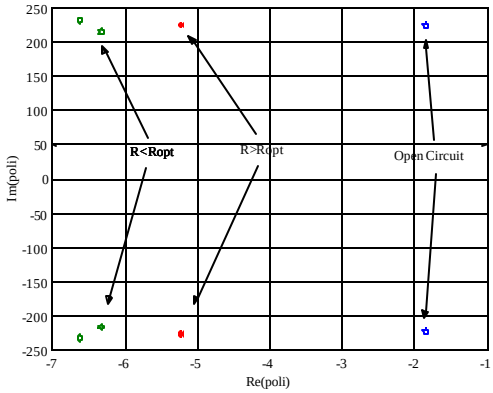

Figure 7-22: Poles of the coupled system varying the electric parameters

7.5 Next Steps

To achieve the goals of the experimental project of which this work was the starting point the following systems[7] must be assembled utilizing the simply supported beam and the synthetic inductors that have been realized:

1. a beam coupled with 5 resonant RLC circuits

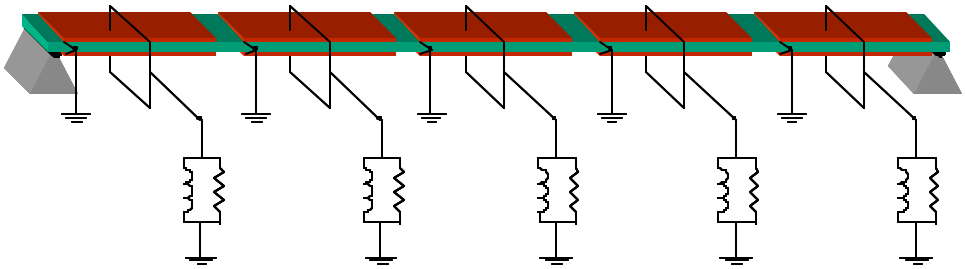

2. a beam coupled with the lumped version of an electric transmission line with line resistances and inductances

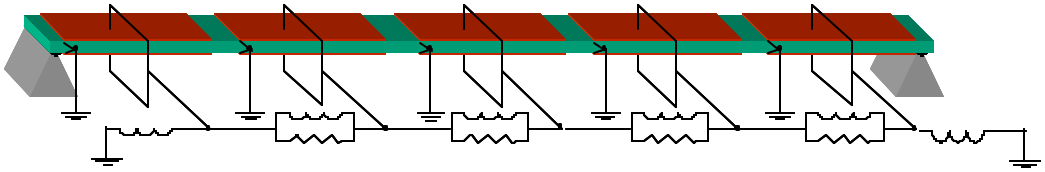

3. a beam coupled with the lumped version of an electric transmission line with line inductances and ground resistances

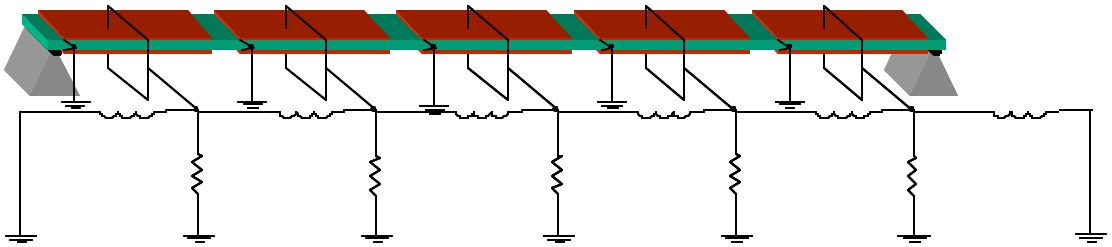

Their performances in the suppression of mechanical vibrations must be investigated as a function of the values of the electrical parameters to validate the theoretical and numerical results obtained in the previous chapters. To this aim the mechanical forced response can be found with the experimental setup in figure 7-13.

Since it will be necessary to vary simultaneously all the inductances and resistances, it will be auspicious to realize resistances[8] whose value can be imposed by means of a potential difference.

[7] The electrical boundary conditions have been designed by analogy to the mechanical ones.
[8] The values of the inductances are indirectly controlled by resistors since they will be realized by the GIC.

Indeed, their value could be imposed directly by the personal computer through the digital\analog converter, avoiding time-wasting and boring manual adjustments. A single analog output of the board could control all the resistance, another all the inductances.

7.6 Conclusions

In this experimental work a preparatory activity to a complex and original experimental project has been carried on. The components needed for the planned experiments have been assembled and tested. A complete experimental procedure for the extraction of the modal parameters of mechanical and electrical systems has been designed and tested with excellent results. Moreover a classical experience on shunted PZT has been reproduced with success. These results will be used as a benchmark for the validation of the analytical results obtained about the effectiveness of a distributed piezoelectric coupling of a structure with an electric network for broadband passive control of mechanical vibrations. To this aim a set of experiments has been planned.

Appendix A

Physical Dimensions

In the following table are resumed the physical dimensions of all the quantities introduced in Chapter 2. In the notation the subscripts are omitted.

Table A.1: Piezoelastic variables and characteristics: physical dimensions

Name	S.I.	S.I. base	Name	S.I.	S.I. base
T	$\frac{\mathrm{N}}{\mathrm{m}^2}$	$\frac{\mathrm{kg}}{(\mathrm{m})\,\mathrm{s}^2}$	ϵ	$\frac{\mathrm{F}}{\mathrm{m}}$	$\mathrm{A}^2\,\frac{\mathrm{s}^4}{(\mathrm{kg})\,\mathrm{m}^3}$
S	1	1	β	$\frac{\mathrm{m}}{\mathrm{F}}$	$\frac{\mathrm{m}^3}{\mathrm{A}^2\,\mathrm{s}^4}\,\mathrm{kg}$
E	$\frac{\mathrm{V}}{\mathrm{m}}$	$(\mathrm{kg})\,\frac{\mathrm{m}}{(\mathrm{A})\,\mathrm{s}^3}$	g	$\frac{\mathrm{m\,V}}{\mathrm{N}}$	$\frac{\mathrm{m}^2}{\mathrm{A\,s}}$
D	$\frac{\mathrm{C}}{\mathrm{m}^2}$	$(\mathrm{A})\,\frac{\mathrm{s}}{\mathrm{m}^2}$	d	$\frac{\mathrm{C}}{\mathrm{N}}$	$(\mathrm{A})\,\frac{\mathrm{s}^3}{\mathrm{kg\,m}}$
J	$\frac{\mathrm{C}}{\mathrm{m}^2\,\mathrm{s}}$	$\frac{\mathrm{A}}{\mathrm{m}^2}$	h	$\frac{\mathrm{N}}{\mathrm{C}}$	$(\mathrm{kg})\,\frac{\mathrm{m}}{\mathrm{s}^3\,\mathrm{A}}$
$\dot{\phi}$	V	$(\mathrm{kg})\,\frac{\mathrm{m}^2}{(\mathrm{A})\,\mathrm{s}^3}$	e	$\frac{\mathrm{C}}{\mathrm{m}^2}$	$(\mathrm{A})\,\frac{\mathrm{s}}{\mathrm{m}^2}$
ϕ	V s	$(\mathrm{kg})\,\frac{\mathrm{m}^2}{(\mathrm{A})\,\mathrm{s}^2}$	c	$\frac{\mathrm{N}}{\mathrm{m}^2}$	$\frac{\mathrm{kg}}{(\mathrm{m})\,\mathrm{s}^2}$
			s	$\frac{\mathrm{m}^2}{\mathrm{N}}$	$\frac{\mathrm{m}}{\mathrm{kg}}\,\mathrm{s}^2$

Appendix B

Material Properties and External Actions

In this Appendix the expressions of material properties appearing in the constitutive relations of the unidimensional model of the PEM beam studied in Chapter 3 will be furnished explicitly. They will be given for the beam in figures 4-1, 4-2 as a function of its material characteristics as a Cauchy Continuum and of its geometrical dimensions. Also the expressions of the external actions will be specified as a function of those defined for a Chauchy Continuum model.

B.1 Material Properties

- Mechanical properties
  - Stiffness

$$\begin{aligned} K_f &= K_f^{(b)} + K_f^{(p)} \\ K_l &= K_l^{(b)} + K_l^{(p)} \end{aligned}$$

$$\begin{array}{ll} K_f^{(b)} = \int_{\mathcal{S}_b} c_{11} p_3^2 & K_f^{(p)} = \left(\frac{t_h}{2}\right)^2 \int_{\mathcal{S}_{pu}} c_{11}^E + \left(\frac{t_h}{2}\right)^2 \int_{\mathcal{S}_{pl}} c_{11}^E \\ K_l^{(b)} = \int_{\mathcal{S}_b} c_{11} & K_l^{(p)} = \int_{\mathcal{S}_{pu}} c_{11}^E + \int_{\mathcal{S}_{pl}} c_{11}^E \end{array}$$

  - Density per unit of length

$$\lambda = \lambda^{(b)} + \lambda^{(p)}$$

$$\lambda^{(b)} = \left(\int_{\mathcal{S}_b} \rho\right) \quad \lambda^{(p)} = \left(\int_{\mathcal{S}_p} \rho\right)$$

– Inertia per unit of length

$$\alpha = \alpha^{(b)} + \alpha^{(p)}$$

$$\alpha^{(b)} = \left(\int_{\mathcal{S}_b} \rho p_3^2\right) \quad \alpha^{(p)} = \left(\frac{t_b^2}{4}\int_{\mathcal{S}_{pu}} \rho + \frac{t_b^2}{4}\int_{\mathcal{S}_{pl}} \rho\right)$$

- Electrical properties

  – Capacitance per unit of length

$$H = \frac{1}{t_p^2}\int_{\mathcal{S}_{pu}} \epsilon_{33}^S = H^{(u)} = H^{(l)}$$

- Coupling properties

$$\begin{aligned} G_l &= \frac{1}{t_p}\int_{\mathcal{S}_{pu}} e_{31} = \frac{1}{t_p}\int_{\mathcal{S}_{pL}} e_{31} \\ G_f &= \frac{t_b}{2t_p}\int_{\mathcal{S}_{pu}} e_{31} = \frac{t_b}{2t_p}\int_{\mathcal{S}_{pl}} e_{31} \end{aligned}$$

B.2 External Actions

- Horizontal force per unit of length

$$R_1 = B_1 + P_1$$

where

$$\begin{aligned} P_1 &= \int_{\partial\mathcal{S}} f_1 \\ B_1 &= B_1^{(b)} + B_1^{(p)} = \left(\int_{\mathcal{S}_p} b_1\right) + \left(\int_{\mathcal{S}_p} b_1\right) \end{aligned}$$

- Vertical force per unit of length

$$R_3 = B_3 + P_3$$

Table B.1: External actions: expressions and physical dimensions

Name	Expression	S.I. units,base
$B_1 = B_1^{(b)} + B_1^{(p)}$	$\left(\int_{\mathcal{S}_p} b_1\right) + \left(\int_{\mathcal{S}_p} b_1\right)$	$\frac{\mathrm{N}}{\mathrm{m}}, \frac{\mathrm{kg}}{\mathrm{s}^2}$
$P_1 = \int_{\partial\mathcal{S}} f_1$	$\int_{\partial\mathcal{S}} f_1$	$\frac{\mathrm{N}}{\mathrm{m}}, \frac{\mathrm{kg}}{\mathrm{s}^2}$
R_1	$B_1 + P_1$	$\frac{\mathrm{N}}{\mathrm{m}}, \frac{\mathrm{kg}}{\mathrm{s}^2}$
$B_3 = B_3^{(b)} + B_3^{(p)}$	$\left(\int_{\mathcal{S}_b} b_3\right) + \left(\int_{\mathcal{S}_p} b_3\right)$	$\frac{\mathrm{N}}{\mathrm{m}}, \frac{\mathrm{kg}}{\mathrm{s}^2}$
P_3	$\int_{\partial\mathcal{S}} f_3$	$\frac{\mathrm{N}}{\mathrm{m}}, \frac{\mathrm{kg}}{\mathrm{s}^2}$
R_3	$B_3 + P_3$	$\frac{\mathrm{N}}{\mathrm{m}}, \frac{\mathrm{kg}}{\mathrm{s}^2}$
$B_\theta = B_\theta^{(b)} + B_\theta^{(p)}$	$\left(\begin{array}{c}\int_{\mathcal{S}_b} p_3 b_1 + \\ + \frac{t_b}{2}\left(\int_{\mathcal{S}_{pu}} b_1 - \int_{\mathcal{S}_{pl}} b_1\right)\end{array}\right)$	$\mathrm{N}, (\mathrm{kg})\,\frac{\mathrm{m}}{\mathrm{s}^2}$
P_θ	$\int_{\partial\mathcal{S}} f_1 p_3$	$\mathrm{N}, (\mathrm{kg})\,\frac{\mathrm{m}}{\mathrm{s}^2}$
R_θ	$B_\theta + P_\theta$	$\mathrm{N}, (\mathrm{kg})\,\frac{\mathrm{m}}{\mathrm{s}^2}$

where

$$\begin{aligned} P_3 &= \int_{\partial\mathcal{S}} f_3 \\ B_3 &= B_3^{(b)} + B_3^{(p)} = \left(\int_{\mathcal{S}_b} b_3\right) + \left(\int_{\mathcal{S}_p} b_3\right) \end{aligned}$$

- Moment per unit of length

$$R_\theta = B_\theta + P_\theta$$

where

$$\begin{aligned} P_\theta &= \int_{\partial\mathcal{S}} f_1 p_3 \\ B_\theta &= B_\theta^{(b)} + B_\theta^{(p)} = \int_{\mathcal{S}_b} p_3 b_1 + \frac{t_b}{2}\left(\int_{\mathcal{S}_{pu}} b_1 - \int_{\mathcal{S}_{pl}} b_1\right) \end{aligned}$$

B.3 Physical Dimensions

In the tables the definitions of all the quantities are resumed with the respective physical dimensions in the SI units

Table B.2: Material characteristics: expressions and physical dimensions

Name	Expression	S.I. units
$\alpha = \alpha^{(b)} + \alpha^{(p)}$	$\left(\int_{\mathcal{S}_b} \rho p_3^2\right) + 2\frac{t_p^2}{4} \int_{\mathcal{S}_{pu}} \rho$	$\mathrm{kg\,m}$
$\lambda = \lambda^{(b)} + \lambda^{(p)}$	$\int_{\mathcal{S}_b} \rho + \int_{\mathcal{S}_p} \rho$	$\frac{\mathrm{kg}}{\mathrm{m}}$
$K_f = K_f^{(b)} + K_f^{(p)}$	$\left(\begin{array}{c} \int_{\mathcal{S}_b} c_{11} p_3^2 + \\ 2\left(\frac{t_b}{2}\right)^2 \int_{\mathcal{S}_{pu}} c_{11}^E \end{array}\right)$	$\mathrm{N\,m^2}, (\mathrm{kg})\,\frac{\mathrm{m}^3}{\mathrm{s}^2}$
$K_l = K_l^{(b)} + K_l^{(p)}$	$\int_{\mathcal{S}_b} c_{11} + 2\int_{\mathcal{S}_{pu}} c_{11}^E$	$\mathrm{N}, (\mathrm{kg})\,\frac{\mathrm{m}}{\mathrm{s}^2}$
G_l	$\frac{1}{t_p} \int_{\mathcal{S}_{pu}} e_{31}$	$\frac{\mathrm{C}}{\mathrm{m}}, (\mathrm{A})\,\frac{\mathrm{s}}{\mathrm{m}}$
G_f	$\frac{t_b}{2t_p} \int_{\mathcal{S}_{pu}} e_{31}$	$\mathrm{C}, \mathrm{A\,s}$
H	$\frac{1}{t_p^2} \int_{\mathcal{S}_{pu}} \epsilon_{33}^S$	$\frac{\mathrm{F}}{\mathrm{m}}, \mathrm{A}^2\,\frac{\mathrm{s}^4}{(\mathrm{kg})\,\mathrm{m}^3}$

Appendix C

Numerical Values

Here the numerical values of all the relevant quantities defined throughout the present work will be given explicitly for the material and geometrical characteristics of the simply supported PEM that was experimentally realized as described in Chapter 7.

C.1 Geometric and Local Material Characteristics

The experimentally realized beam can be thought as composed of five modules such as that in figures C-1 and C-2

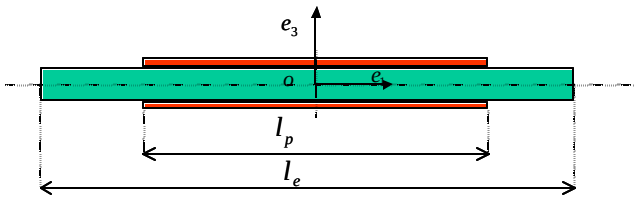

Figure C-1: Elementary cell of the electromechanical beam: lateral view.

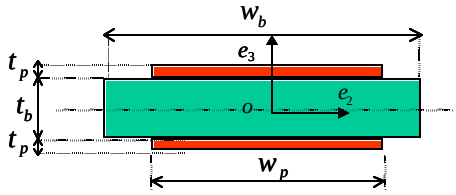

Figure C-2: Elementary cell of the electromechanical beam: cross section

The central elastic layer is constituted of aluminum, while the two piezoelastic layers are composed of the PZT *material PSI-5H4E Ceramic.* The material characteristics are [1]

$$\begin{array}{lll} c_{11} = 70 * 10^9 \,\mathrm{Pa} & \rho_a = 2700 \frac{\mathrm{kg}}{\mathrm{m}^3} & \rho_p = 7800 \frac{\mathrm{kg}}{\mathrm{m}^3} \\ c_{11}^E = 62 * 10^9 \,\mathrm{Pa} & \epsilon_{33}^s = 2.797 * 10^{-8} \frac{\mathrm{F}}{\mathrm{m}} & e_{31} = -19.84 \frac{\mathrm{N}}{\mathrm{m\,V}} \end{array} \tag{C.1a}$$

The geometrical dimensions of the basic cell are

$$\begin{array}{ll} w_b = 40 * 10^{-3} \,\mathrm{m} & w_p = 36.2 * 10^{-3} \,\mathrm{m} \\ t_b = 4 * 10^{-3} \,\mathrm{m} & t_p = 0.267 * 10^{-3} \,\mathrm{m} \end{array} \tag{C.2}$$

The length of an element is left as a parameter, however the following ratio between the length of the element l_e and the length of the PZT layers is assumed when necessary

$$f_l = \frac{l_p}{l_e} = 0.743$$

All the values above refer to those of the experimental setup that was realized.

C.2 Sectional Material Characteristics

Assuming a rectangular cross section beam as described before the integrated material characteristics presented in the *Appendix B* can be written explicitly. The results presented in table C.1 have been found[2]

C.3 Homogenized Material Characteristics

If the ratios

$$f_l = \frac{l_p}{l_e} \quad f_w = \frac{w_p}{w_b}$$

are left as parameters the homogenized material characteristics can be rewritten explicitly by the expressions given in *Chapter 5.*

[1] The notation is referred to that given when the constitutive relations have been introduced

[2] The coupling coefficients are relative to an out- of-phase parallel electric connection of the PZT layers for the bending case, to an in-phase parallel electric connection for the longitudianl-electric case.

Table C.1: Material characteristics:Expression and Numerical Values

Constant	Expression	Numerical Value
$\alpha^{(b)}$	$\rho_b \frac{t_b^3 w_b}{12}$	$5.76 * 10^{-7}\,\mathrm{kg\,m}$
$\alpha^{(p)}$	$\rho_p \frac{t_b^2 t_p w_p}{2}$	$6.03 * 10^{-7}\,\mathrm{kg\,m}$
$\lambda^{(b)}$	$\rho_b t_b w_b$	$4.32 * 10^{-1}\,\frac{\mathrm{kg}}{\mathrm{m}}$
$\lambda^{(p)}$	$2\rho_p t_b w_b$	$1.51 * 10^{-1}\,\frac{\mathrm{kg}}{\mathrm{m}}$
$K_f^{(b)}$	$c_{11} \frac{t_b^3 w_b}{12}$	$14.93\,\mathrm{N\,m^2}$
$K_f^{(p)}$	$c_{11}^E \frac{t_b^2 t_p w_p}{2}$	$4.79\,\mathrm{N\,m^2}$
$K_l^{(b)}$	$c_{11} t_b w_b$	$1.12 * 10^7\,\mathrm{N}$
$K_l^{(p)}$	$2c_{11}^E t_p w_p$	$1.20 * 10^6\,\mathrm{N}$
G_l	$\epsilon_{31} w_p$	$7.18 * 10^{-2}\,\frac{\mathrm{C}}{\mathrm{m}}$
G_f	$\frac{\epsilon_{31} w_p t_p}{2}$	$1.436 * 10^{-3}\,\frac{\mathrm{C}}{\mathrm{m}}$
H	$\frac{\epsilon_{33}^S w_p}{t_p}$	$3.70 * 10^{-6}\,\frac{\mathrm{F}}{\mathrm{m}}$

Table C.2: Homogenized Material Characteristics:Expression and Numerical Values

Name	Expression	Numerical Value[3]
$\bar{\alpha}$	$\alpha^{(b)} + f_l \alpha^{(p)}$	$1.02 * 10^{-6}\,\mathrm{kg\,m}$
$\bar{\lambda}$	$\lambda^{(b)} + f_l \lambda^{(p)}$	$5.44 * 10^{-1}\,\frac{\mathrm{kg}}{\mathrm{m}}$
$\bar{K}_f$	$K_f^{(b)} + f_l K_f^{(p)}$	$18.5\,\mathrm{N\,m^2}$
$\bar{K}_l$	$K_l^{(b)} + f_l K_l^{(p)}$	$1.21 * 10^7\,\mathrm{N}$
$\bar{G}_l$	$2 f_l G_l$	$1.07\,\frac{\mathrm{C}}{\mathrm{m}}$
$\bar{G}_f$	$2 f_l G_f$	$2.13 * 10^{-3}\,\mathrm{C}$
$\bar{C}_g$	$\frac{C_g}{l_e} + 2H f_l$	$5.50 * 10^{-6}\,\frac{\mathrm{F}}{\mathrm{m}}$

C.4 Dimensionless Parameters

C.4.1 Bending Coupling

The dimensionless parameters for the numerical values assumed are

$$\beta_l = \sqrt{\frac{\bar{\lambda}}{\bar{K}_f \bar{C}_g \bar{L}_l}}\, x_0 = 73.1\sqrt{\frac{x_0^3}{L_l n_e}} \qquad \delta_l = \frac{1}{2R_l C_g}\sqrt{\frac{\lambda}{K_f}} = 1.56\times 10^4 \frac{x_0}{R_l n_e}$$
$$\beta_g = \sqrt{\frac{\bar{\lambda}}{\bar{K}_f \bar{C}_g \bar{L}_g}}\, x_0^2 = 73.1\sqrt{\frac{n_e x_0^3}{L_g}} \quad \delta_g = \frac{x_0^2}{2R_g C_g}\sqrt{\frac{\lambda}{K_f}} = 1.56\times 10^4 \sqrt{n_e^3 x_0}\frac{1}{R_g}$$
$$\gamma = \frac{\bar{G}_f}{\sqrt{\bar{K}_f \bar{C}_g}} = 0.212 \qquad \kappa = \frac{\bar{C}_l}{\bar{C}_g x_0^2} = 1.82\times 10^5 \frac{C_l}{n_e x_0}$$

where the numerical values of the quantities left free must be inserted in the SI units.

C.4.2 Longitudinal Coupling

The dimensionless parameters for the numerical values assumed are

$$\beta_l = \sqrt{\frac{\bar{\lambda}}{\bar{C}_g \bar{L}_l \bar{K}_l}} = 9.04\times 10^{-2}\sqrt{\frac{x_0^3}{L_l n_e}} \qquad \delta_l = \frac{1}{2x_0 \bar{R}_l \bar{C}_g}\sqrt{\frac{\bar{\lambda}}{\bar{K}_l}} = 19.3\frac{1}{R_l}\frac{x_0}{n_e}$$
$$\beta_g = \sqrt{\frac{\bar{\lambda}}{\bar{K}_l \bar{C}_g \bar{L}_g}}\, x_0 = 9.04\times 10^{-2}\sqrt{\frac{n_e x_0^3}{L_g}} \quad \delta_g = \frac{1}{2\bar{R}_g \bar{C}_g}\sqrt{\frac{\bar{\lambda}}{\bar{K}_l}}\, x_0 = \frac{19.3}{R_g} n_e x_0$$
$$\gamma = \frac{\bar{G}_l}{\sqrt{\bar{C}_g \bar{K}_l}} = 0.131 \qquad \kappa = \frac{\bar{C}_l}{\bar{C}_g x_0^2} = 1.82\times 10^5 \frac{C_l}{n_e x_0}$$

where the numerical values of the quantities left free must be inserted in the SI units.

Bibliography

[1] M.E.Gurtin, *An Introduction to Continuum Mechanics*, Academic Press, 1981

[2] G.A.Maugin, *Continuum Mechanics of Electromagnetic Solids*, North Holland Series in Applied Mathematics and Mechanics, 1998.

[3] G.A.Maugin, *The Method of Virtual Power in Continuum Mechanics: Application to Coupled Field*, Acta Mechanica 3, 1980, pg. 1-70.

[4] B.A.Auld, *Acoustic Fields and Waves in Solid,* Vol. I-II, Krieger, 1989.

[5] B.D.Reddy, *Introductory Functional Analysis with Application to Boundary Value Problems and Finite Elements*, Springer, 1998.

[6] M.Reed, B.Simon, *Methods of Mathematical Physics*, Academic Press, 1972.

[7] T.Ikeda, *Fundamentals of Piezoelectricity*, Oxford University Press, 1990

[8] F.R.Gantmacher, *Lezioni di Meccanica Analitica*, Editori Riuniti, Edizioni Mir, 1980

[9] L.Brillouin, *Wave Propagation in Periodic Structures*, McGraw-Hill, 1946

[10] S.Timoshenko, D.H.Young and W.Weaver Jr, *Vibration Problem in Engineering* (fourth edition), New York, John Wiley, 1974.

[11] R.L.Clark, W.R.Saunders, G.P.Gibbs, *Adaptive Structures: Dynamics and Controls*, J.Wiley & Sons, 1998

[12] D.J.Ewins, *Modal Testing: Theory and Practice*, Research Studies Press LTD., England, 1986

[13] A.Sestieri, *Dispense del corso di Meccanica delle Vibrazioni*, 1998

[14] E.Dankowicz, *Lecture Notes of Advanced Vibrations,* Virginia Polytechnic Institute and State University, 2001

[15] V.I.Arnol'd, *Ordinary Differential Equations,* Springer-Verlag, 1992

[16] L.Perko, *Differential Equations and Dynamical Systems,* Springer-Verlag, Text in Applied Mathematics, 1991

[17] M.W.Hirsh and S.Smale, *Differential Equations*, John Wiley and Sons, New Jork, 1974

[18] D.J.Inman and H.H.Cudney, *Final Report to NASA Langley Research Center*, April 30 2000.

[19] R.Scozzafava, *Probabilità Soggettiva: Significato Valutazione, Applicazioni*, Masson, Milano, 1997

[20] F.dell'Isola, S.Vidoli, *Continuum Modeling of Electro-mechanical Truss Beams*, Archive Applied Mechanics 68 (1998)

[21] F.dell'Isola, S.Vidoli, *Bending-Waves Damping in Truss Beams by Electrical Transmission Line with PZT Actuators*, Archive Applied Mechanics 68 (1998)

[22] S.Vidoli, F.dell'Isola, *Modal Coupling in One-Dimensional Electro-Mechanical Structured Continua*, Acta Mechanica 141, 1-2 (2000)

[23] S.Alessandroni, *Electrical analogs for plate equations and their applications in mechanical vibration suppression by PZT. actuators*, Master Thesis at Virginia Polytechnic Institute and State University, 2000

[24] S. Alessandroni, F. dell'Isola, F. Frezza, *Optimal Piezo-Mechanical Coupling to Control Plate Vibrations*, Proceedings ISEM, Tokyo 2001

[25] F. dell'Isola, E.G. Henneke, M. Porfiri, *Synthesis of Electrical Networks Interconnecting PZT Actuators to Damp Mechanical Vibrations*, Proceedings ISEM, Tokyo 2001

[26] M.Porfiri, *Synthesis of Electric Networks Interconnecting, PZT Actuators to Efficiently Damp Mechanical Vibrations*, Master Thesis at Virginia Polytechnic Institute and State University, 2000

[27] R.Senani, *Alternative Modification of the Classical GIC Structure*, Electronics Letters, 18th July 1996 Vol.32 No.15

[28] Bisegna P., Caruso G., Del Vescovo D., Landini S., 1999, *Simulation of Vibrations Passive Damping of a Piezoactuated Cantilever Plate*, Annual Conference of Italian Society for Computer Simulations-ISCS, June.

[29] Bisegna P., Caruso G., Del Vescovo D., 1999, *Smorzamento Passivo Ottimale di Vibrazioni tramite Piezoelettrici: Risultati Numerici e Sperimentali,* Atti del XXVIII Congresso Nazionale dell'Associazione Italiana per l'Analisi delle Sollecitazioni, Vicenza 8-11 Settembre, pg. 959-567.

[30] Hagood W. and A. von Flotow, *Damping of Structural Vibrations with Piezoelectric Materials and Passive Electrical Networks*, Journal of Sound and Vibrations, 146(2):243-268, 1991.

[31] George A. Lesieutre, *Vibration Damping and Control Using Shunted Piezoelectric Materials*, The Shock and Vibrations Digest, Vol. 30, No.3, May 1998, 187-195

[32] V.Steffen Jr. and D.J.Inman, *Optimal design of a Piezoelectric Material for Vibration Damping in Mechanical Systems*, Journal of Intelligent Material Systems and Structures, Vol. 10-December 1999

[33] V.Steffen Jr, D.A. Rade, D.J.Inman, *Using Passive Techniques for Vibration Damping in Mechanical Systems*, Journal of Braz. So. Mechanical Sciences, Vol XXII, No 3,pp. 411-421, 2000

[34] X.Zouh, A.Chattopadhyay and R.Thornburgh, *Analysis of Piezoelectric Smart Composites Using a Coupled Piezoelectric-Mechanical Model*, Journal of Intelligent Material Systems and Structures, Vol. 11-March 2000.

[35] E.F.Crawley and J.de Luis, *Use of Piezoelectric Actuator as Elements of Intelligent Structures*, AIAA Journal, 25(10): 1373-1385.

[36] E.F.Crawley and E.H.Anderson, *Detailed Models of Piezoceramic Actuation of Beams*, Journal of Intelligent Materials and Structures, Vol I - January 1990.

[37] J.Sirohi and I.Chopra, *Fundamental Understanding of Piezoelectric Strain Sensor*, Journal of Intelligent Material Systems and Structures, Vol. 11-April 2000

[38] J.Duparre , P.Buker, B.Gotz, T.Martin, *Theoretical and Experimental Investigation of Significant Characteristic Parameters of Piezoelectrical Actuators*, Smart Structures and Materials 2000: Smart Structures and Integrated Systems, Norman M. Werely editor, Proceedings of SPIE Vol.3985 (2000).

[39] J.J.Hollkamp, *Multimodal Passive Vibration Suppression with Piezoelectric Materials and Resonant Shunts*, Journal of Intelligent Material Systems and Structures, Vol. 5-March 1994.

[40] J.J.Dosh, D.J. Inman, E.Garcia, *A Self Sensing Piezoelectric Actuator for Collocated Control*, Journal of Intelligent Material Systems and Structures, Vol.3-No.1,pp166-185, 1992.

[41] J.L.Fanson, T.K.Caughey, *Positive Position Feedback Control for Large Space Structures*, Prooceedings 28th AIAA/ASME/ASC/AHS Structures Structural Dyanmics and Materials Conference, Monterey, California. AIAA Paper No.87-0902, pp 588-598.

[42] J.J.Hollkamp, T.F.Starchville, *A Self-Tuning Piezoelectric Vibration Absorber*, Journal of Intelligent Material Systems and Structures, Vol.5-July 1994.

[43] K.W.Wang, *Structural Vibration Suppression via Parametric Control Actions - Piezoelectric Materials with Real-time Semi-Active Networks*, Wave Motion, Intelligent Structures and Nonlinear Mechanics, pp 112-134, edited by A.Guran and D.J.Inman, Series on Stability Vibration and Control of Structures: Vol.I, Word Scientific Publishing Company.

Vita

Corrado Maurini was born to Giorgio Maurini and Maria Antonietta Guidi on July 15, 1976 in Terni, Italy. He graduated from high school in 1995 at Liceo Classico G.C.Tacito, Terni.

Upon graduation from high school, he enrolled at University of Rome "La Sapienza". He received a Laurea in Mechanical Engineering in July 2001 at the University of Rome "La Sapienza". In November, 2001 he enrolled to a Ph.D. program in Theoretical and Applied Mechanics at the University of Rome "La Sapienza".